

Comparative and translational analysis of immune signaling pathways in *Arabidopsis* and *Solanaceae*

Dissertation

zur Erlangung des

Doktorgrades der Naturwissenschaften (Dr. rer. nat.)

der

Naturwissenschaftlichen Fakultät I - Biowissenschaften -

der Martin-Luther-Universität

Halle-Wittenberg

vorgelegt

von Herrn Johannes Gantner

geb. am 07.05.1986 in Darmstadt

Gutachter:

1. Prof. Dr. Ulla Bonas

2. Prof. Dr. Christian Eckmann

3. Prof. Dr. Jens Boch

Verteidigungstermin: 24.06.2020

Freitag, 26. Juni 2020

List of Publications

- Adlung, N, Prochaska, H, Thieme, S, Banik, A, Blucher, D, John, P, Nagel, O, Schulze, S, Gantner, J, Delker, C, Stuttmann, J, Bonas, U.** (2016). Non-host resistance induced by the *Xanthomonas* effector XopQ is widespread within the genus *Nicotiana* and functionally depends on EDS1. *Front Plant Sci* **7**, 1796
- Ordon, J, Gantner, J, Kemna, J, Schwalgun, L, Reschke, M, Streubel, J, Boch, J, Stuttmann, J.** (2017). Generation of chromosomal deletions in dicotyledonous plants employing a user-friendly genome editing toolkit. *Plant J* **89**, 155-68.
- Gantner, J, Ordon, J, Ilse, T, Kretschmer, C, Gruetzner, R, Loeffke, C, Dagdas, Y, Bürstenbinder, K, Marillonnet, S, Stuttmann, J.** (2018). Peripheral infrastructure vectors and an extended set of plant parts for the Modular Cloning system. *PLoS ONE* **13**, e0197185.
- Gantner, J, Ordon, J, Kretschmer, C, Guerois, R, and Stuttmann, J.** (2019). An EDS1-SAG101 complex is essential for TNL-mediated immunity in *Nicotiana benthamiana*. *Plant Cell*, tpc.00099.2019.

Zusammenfassung

Pflanzen verfügen nicht über ein adaptives Immunsystem, welches sich auf stetig ändernde Pathogene anpassen könnte. Jede pflanzliche Zelle besitzt ein genetisch kodiertes, angeborenes Repertoire an Proteinen, welche eine Infektion durch Pathogene detektieren und unterdrücken können. Das Repertoire an immun-assoziierten Proteinen unterscheidet sich signifikant in der Pflanzenwelt, abhängig von Spezies und Isolat. Generell wird eine zweistufige pflanzliche Immunabwehr beschrieben. Ein erster Mechanismus ist für die basale, allgemeine Erkennung von Pathogenen verantwortlich: Membranständige Rezeptoren (*pattern recognition receptors*, PRRs) erkennen bestimmte Muster an der Zelloberfläche und lösen eine Immunantwort aus. Durch sogenannte Effektoren, welche von angepassten Pathogenen in die Wirtszelle transloziert werden, kann diese Immunantwort jedoch unterdrückt werden. Resistente Isolate der Wirtspflanze hingegen können Effektoren durch Resistenzproteine/-gene (R) detektieren, wodurch eine weitere, starke Immunantwort ausgelöst wird. Pflanzliche Resistenzproteine werden, abhängig von ihren N-terminalen *Coiled-Coil* oder Toll/Interleukin Rezeptor 1-ähnlichen (TIR) Domänen, in zwei Gruppen unterteilt. Interessanterweise benötigen R Proteine mit einer N-terminalen TIR Domäne des Weiteren das in der Pflanzenwelt hoch konservierte Protein *Enhanced Disease Susceptibility 1* (EDS1), was eine Funktion dieses Proteins in der Signalweiterleitung vermuten lässt. EDS1 bildet heterodimere Komplexe mit zwei sequenzverwandten Proteinen, *Senescence Associated Gene 101* (SAG101) und *Phytoalexin Deficient 4* (PAD4). EDS1 Komplexe wurden zuvor intensiv in *Arabidopsis thaliana* untersucht, jedoch blieben molekulare Funktionen soweit ungeklärt.

Ein Hauptziel dieser Arbeit bestand in der funktionalen Analyse von EDS1 Komplexen in der Familie der Nachtschattengewächse (*Solanaceae*). So wurden einerseits potentielle Interaktoren in einem Hefe-Drei-Hybrid *screen* identifiziert und weiter charakterisiert. Andererseits wurden verschiedene Linien mit Mutationen in den Genen der *EDS1* Familie durch CRISPR/Cas in *Nicotiana benthamiana* generiert. Diese Linien wurden hinsichtlich ihrer Immunkapazitäten charakterisiert und für Struktur-Funktionsanalysen verwendet. Dabei wurden funktional wichtige Merkmale von EDS1 Komplexen identifiziert, und auch grundlegende Unterschiede zu EDS1 Funktionen in *Arabidopsis* aufgedeckt. Unter anderem durch den Transfer von Genen der *EDS1* Familie zwischen den Pflanzenfamilien wurde die Hypothese entwickelt, dass Signalweiterleitungsprozesse von R Proteinen zu EDS1 Komplexen konserviert sind, die folgenden Schritte in diesen Spezies aber unterschiedlich ablaufen. Dabei beruhen EDS1 Immunfunktionen vermutlich auf der Koevolution dieser Komplexe mit weiteren Proteinen des Immunnetzwerks in individuellen Spezies.

Summary

Plants do not possess an adaptive immune system which would allow them to adapt to continuously modifying pathogens. All cells of a plant possess a genetically encoded, innate repertoire of proteins enabling for detection of invading pathogenic microbes, suppression of their multiplication and a simultaneous priming of the whole plant for secondary infections. This repertoire of immune-associated proteins significantly differs among plants, depending on species and isolate. In general, plants possess a two-layered immune system. The first layer is responsible for basal pathogen detection. Membrane-associated receptors (pattern recognition receptors, PRRs) detect conserved pathogen-derived molecules on the outside of the cell and elicit an immune response. Adapted pathogens can overcome this immune response by delivering so-called effectors directly into host cells, which suppress PAMP-triggered immunity. However, in resistant isolates of the host plants, effectors can become detected by intracellular (R) resistance proteins or genes, thus initiating a rapid and efficient immune response. R proteins are subdivided in two major groups based on their N-terminal domains; either a coiled-coil (CC) or Toll/interleukin 1-like receptor (TIR) domain. Interestingly, TIR domain-containing R proteins additionally require the highly conserved, plant-specific Enhanced Disease Susceptibility 1 (EDS1) protein to initiate immune responses, suggesting a role in signal transduction. EDS1 engages into heterodimeric complexes with two sequence-related proteins, Phytoalexin Deficient 4 (PAD4) and Senescence Associated Gene 101 (SAG101). These EDS1 complexes were intensively analyzed in *Arabidopsis thaliana*, but precise molecular functions remain unclear.

One major objective of this work consisted in functional analysis of EDS1 complexes in *Solanaceae*. On the one hand, potential interactors were identified in a yeast-three-hybrid screen, and further characterized. On the other hand, different mutant lines deficient in genes of the *EDS1* family were generated in *Nicotiana benthamiana* by CRISPR/Cas9 genome editing technology. These mutant lines were characterized in respect to their immune capacities and used for structure-function studies. These analyses revealed first functionally important features of EDS1 complexes and also distinct differences for EDS1 functions in *Solanaceae* in comparison to *Arabidopsis*. Among other lines of evidence, especially the transfer of the *EDS1* family genes between the two studied plant families led to the hypothesis that the process of signal transduction from R proteins to EDS1 complexes follows a conserved mechanism in dicot plants, but different mechanisms evolved for the subsequent induction of immune responses. In this context, immune functions and downstream signaling of EDS1 presumably depend on the co-evolution of these complexes with other proteins of the immune network of individual species.

Index

| | |
|---|-----|
| Zusammenfassung..... | I |
| Summary..... | II |
| List of abbreviations | vii |
| List of tables, figures and supplemental data..... | xii |
| Opening remarks..... | 1 |
| Part I: Plant synthetic biology - resources and modules for efficient molecular cloning and assembly of multigene constructs..... | 2 |
| Introduction | 2 |
| 1.1. Cloning strategies – the long way to standardized assemblies of multigene constructs | 2 |
| 1.1. Aims, achievements and conclusions..... | 7 |
| 1.2. Peripheral infrastructure vectors and an extended set of plant parts of the Modular Cloning system | 8 |
| 1.2.1. Publication Gantner <i>et al.</i> , 2018 | 8 |
| 1.2.2. Supplemental material to publication Gantner <i>et al.</i> , 2018..... | 25 |
| 1.2.3. Summary of publication Gantner <i>et al.</i> , 2018..... | 29 |
| Part II – Toolkits for plant genome editing..... | 30 |
| Introduction | 30 |
| 2.1. Adaptive immunity of microbes – the CRISPR-Cas system..... | 30 |
| Aims, achievements and conclusions | 32 |
| 2.2. Generation of chromosomal deletions in dicotyledonous plants employing a user-friendly genome editing kit | 34 |
| 2.2.1. Publication Ordon <i>et al.</i> , 2016 | 34 |
| 2.2.2. Supplemental material to publication Ordon <i>et al.</i> , 2016..... | 48 |
| 2.2.3. Summary of publication Ordon <i>et al.</i> , 2016..... | 54 |
| Part III: Plant innate immune signaling in <i>Solanaceae</i> | 55 |
| Introduction | 55 |
| 3.1. The immune system of plants..... | 55 |

| | | |
|----------|--|-----|
| 3.1.1. | PTI – a first immune layer protects against non-adapted microbes | 55 |
| 3.1.2. | ETS versus ETI – a second immune layer rescues in case of effector-perception | 56 |
| 3.2. | NLR-type immune receptors – detection of a pathogen effector | 57 |
| 3.2.1. | NLRs – a defense strategy that developed twice? | 57 |
| 3.2.2. | Plant NLRs – modular architecture enables effector perception and downstream signaling | 58 |
| 3.2.2.1. | The coiled-coil domain | 59 |
| 3.2.2.2. | The Toll/interleukin-1-like receptor domain | 59 |
| 3.2.2.3. | The nucleotide-binding domain | 60 |
| 3.2.2.4. | The leucine-rich-repeat domain | 61 |
| 3.2.3. | NLR-occurrence in plant genomes | 61 |
| 3.2.4. | Structural re-organization of NLRs leads to activation | 63 |
| 3.2.5. | Effector Recognition | 65 |
| 3.2.6. | Integrated domains – a sophisticated strategy of NLRs | 66 |
| 3.3. | Signaling Downstream of NLRs | 67 |
| 3.3.1. | EDS1-family proteins are essential for at least TNL-mediated resistance | 68 |
| 3.3.2. | Helper NLRs – a common feature of TNLs? | 71 |
| 3.3.3. | Salicylic acid and systemic required resistance – staying alive <i>versus</i> apoptosis | 72 |
| 3.4. | Aims, achievements and conclusions | 74 |
| 3.5. | An EDS1-SAG101b complex functions is essential for TNL-mediated immunity in <i>Nicotiana benthamiana</i> | 76 |
| 3.5.1. | Publication Gantner <i>et al.</i> , 2019 | 76 |
| 3.5.2. | Supplemental material to publication Gantner <i>et al.</i> , 2019 | 96 |
| 3.5.3. | Summary of publication Gantner <i>et al.</i> , 2019 | 112 |
| 3.6. | Additional results to publication Gantner <i>et al.</i> , 2019: Identification of candidate interactors of S/EDS1-based heterocomplexes by Y3H screening | 114 |

| | | |
|----------|--|-----|
| 3.6.1. | Modified Y2H library screen considers EDS1-based heterocomplex formation..... | 116 |
| 3.6.2. | Identification, full length cloning and validation of corresponding genes of <i>Solanum lycopersicum</i> | 118 |
| 3.6.3. | Virus-induced gene silencing of candidate interactors..... | 121 |
| 3.6.3.1. | In planta growth assay of plants treated with VIGS..... | 124 |
| 3.6.4. | FRET-APB of candidate interactors..... | 125 |
| 3.6.5. | Summary and Conclusion | 128 |
| 4. | Discussion | 130 |
| 4.1. | <i>N. benthamiana</i> as a model system for analysis of TNL-mediated immunity | 130 |
| 4.2. | Different EDS1 complexes operate in plant immunity in Arabidopsis and <i>Solanaceae</i> : Co-evolution within species-specific signaling networks..... | 131 |
| 4.3. | Identification of candidate interaction partners of EDS1- heterocomplexes in <i>Solanaceae</i> | 133 |
| 4.3.1. | A Y3H library screen employing the tomato EDS1-PAD4 complex as bait | 133 |
| 4.3.2. | Knock-down of candidate interactor genes by virus-induced gene silencing | 134 |
| 4.3.3. | <i>In planta</i> localization and interaction studies of candidate interactors using FRET-acceptor photobleaching | 135 |
| 4.4. | Rapid structure-function studies in <i>N. benthamiana</i> identified EDS1 features required for immune signaling..... | 137 |
| 4.5. | Integration of EDS1 in immunity and hormonal networks – a central regulator of immunity and development? | 138 |
| 4.6. | Activation of EDS1 in plant immune signaling most likely relies on conserved mechanisms, possibly a small molecule messenger | 141 |
| 4.7. | EDS1-dependent immunity depends on plant family-specific helper-NLRs of the RPW8-type – positioning of EDS1 in networks of helper and sensor NLRs..... | 143 |
| 4.7.1. | EDS1-based heterocomplexes might rely on different hNLRs, depend on the heterocomplex partner | 143 |
| 4.7.2. | Different plant species, different positioning of hNLRs within TNL-mediated defense pathways? | 144 |

| | | |
|--------|--|-----|
| 4.7.3. | Localization and activation of hNLRs and EDS1-based heterocomplexes | 145 |
| 4.7.4. | Occurrence of CNL <i>versus</i> TNLs – detecting pathogens in the most efficient way | 147 |
| 4.8. | An updated model for EDS1 functions in immune signaling..... | 148 |
| | References..... | 152 |
| | Lebenslauf..... | 163 |
| | Danksagung | 164 |
| | Eidesstattliche Erklärung | 165 |

List of abbreviations

| | |
|------------------|---|
| aa | Amino acid |
| AD | Activation Domain |
| Ade | L-Adenine hemisulfate |
| ADP | Adenosine diphosphate |
| ADPR | Adenosine diphosphate ribose |
| ADR1 | Activated disease resistance 1 |
| AIM | <i>Agrobacterium</i> infiltration medium |
| APB | Acceptor photo bleaching |
| ARC | Present in Apaf1 (Apoptotic protease-activating factor 1) |
| ARF | Auxin response factor |
| <i>At</i> | <i>Arabidopsis thaliana</i> |
| ATP | Adenosine triphosphate |
| ATPase | Adenosine triphosphatase |
| ATR1 | <i>At</i> recognized 1 |
| Avr | Avirulence |
| BAK1 | Brassinosteroid insensitive 1-associated kinase1 |
| BD | Binding domain |
| BLAST | Basic local alignment search tool |
| bp | Base pairs |
| Ca ²⁺ | Calcium |
| Cas | CRISPR-associated |
| CC | Coiled-coil |
| CDS | Coding sequence |
| CED4 | Cell death protein 4 |
| CHS1 | Chilling sensitive 1 |
| CHS3 | Chilling sensitive 3 |
| CNL | CC-NB-LRR |
| Col-0 | <i>At</i> accession Columbia |
| CRISPR | Clustered regularly interspaced short palindromic repeats |
| CUL | Cullin |
| DDR | DNA damage response |
| <i>DM2</i> | <i>Dangerous Mix2</i> |
| DSB | Double strand break |
| dTALE | Designer transcription activator-like effector |

| | |
|-------------|--|
| EDR1 | Enhanced disease resistance 1 |
| EDS1 | Enhanced disease susceptibility 1 |
| EF-Tu | Elongation factor thermo unstable |
| EP | EDS1-PAD4 |
| <i>eps</i> | <i>eds1 pad4</i> and <i>sag101</i> |
| <i>epss</i> | <i>eds1a-1 pad4 sag101a-1 sag101b-1</i> |
| ETI | Effector-triggered immunity |
| ETS | Effector-triggered susceptibility |
| FLS2 | Flagellin sensing 2 |
| FRET | Förster resonance energy transfer |
| FRET E | FRET efficiency |
| GA | Gibberellin acid |
| GG | Golden gate |
| GID1 | Gibberellin insensitive dwarf 1 |
| GST | Glutathione S-transferase |
| H | L-Histidine |
| HDR | Homology directed repair |
| HMA | Heavy metal associated |
| hNLR | Helper NLR |
| HopQ1 | Hrp outer protein Q1 |
| <i>Hpa</i> | <i>Hyaloperonospora arabidopsidis</i> |
| hpi | Hours post infection |
| HR | Hypersensitive response |
| ICS1 | Isochorismate sythetase 1 |
| ID | Integrated domain |
| JA | Jasmonic acid |
| kb | Kilo base |
| L | Leucine |
| <i>Ler</i> | Landsberg <i>erecta</i> |
| LOF | Loss-of-function |
| LRR | Leucine-rich-repeat |
| Lys-M | Lysin-motif |
| MAMP | Microbe-associated pattern |
| mCherry | Monomeric red fluorescent protein |
| mEGFP | Monomeric enhanced green fluorescent protein |
| MoClo | Modular cloning |

| | |
|------------|--|
| NACHT | NAIP, CIITA, HET-E, and TP1 |
| NAD | Nicotinamide adenine dinucleotide |
| <i>Nb</i> | <i>Nicotiana benthamiana</i> |
| NB | Nucleotide binding |
| NBD | Nucleotide binding domain |
| NDR1 | Non-race specific disease resistance 1 |
| NHEJ | Non-homologues end-joining |
| NLR | NB-LRR |
| NLS | Nuclear localization signal |
| NOMAD | Nucleic acid ordered module assembly with directionality |
| NPR1 | Nonexpressor of PR genes 1 |
| NRG1 | N requirement gene 1 |
| OE | Overexpression |
| PAD4 | Phytoalexin deficient 4 |
| PAM | Protospacer adjacent motive |
| PAMP | Pathogen associated molecular patterns |
| PBL2 | PBS-1 like protein 2 |
| PCD | Programmed cell death |
| <i>Pfl</i> | <i>Pseudomonas fluorescens</i> |
| PGN | Peptidoglycan |
| PM | Plasma membrane |
| PR | Pathogenesis related |
| pre-crRNA | Precursor CRISPR RNA |
| PRR | Pattern recognition receptor |
| <i>pss</i> | <i>pad4 sag101a-1 sag101b-1</i> |
| <i>Pst</i> | <i>Pseudomonas syringae tomato</i> DC3000 |
| PTI | PAMP-triggered immunity |
| R | Resistance |
| RBA1 | Response HopBA1 |
| RE | Restriction endonucleases |
| RGL3 | Repressor of ga1-3-like 3 |
| RGN | RNA-guided nucleases |
| RIN4 | RPM1 interacting protein 4 |
| RKS1 | Resistance-related kinase 1 |
| RLCK | Receptor-like cytoplasmic kinase |
| RLK | Receptor-like kinase |

| | |
|------------|---|
| RLP | Transmembrane receptor-like protein |
| RNL | RPW8-NB-LRR |
| Roq1 | Recognition of XopQ 1 |
| ROS | Reactive oxygen species |
| RPM1 | Resistance to <i>Pseudomonas syringae</i> pv. <i>maculicola</i> 1 |
| RPP1 | Recognition of <i>Peronospera parasitica</i> 1 |
| RPS4 | Resistance to <i>Pseudomonas syringae</i> 4 |
| RPW8 | Resistance to powdery mildew 8 |
| RRS1 | Resistance to <i>Ralstonia solanacearum</i> 1 |
| S | Serine |
| SA | Salicylic acid |
| SAG101 | Senescence associated gene 101 |
| SAR | Systemic acquired resistance |
| SARM1 | Sterile alpha and TIR motif containing 1 |
| SCAF | Signaling by cooperative assembly formation |
| sgRNA | Single guide RNA |
| siRNA | Small interfering RNA |
| <i>Sl</i> | <i>Solanum lycopersicum</i> |
| SOC3 | Suppressors of chs1 3 |
| <i>Sp</i> | <i>Streptococcus pyogenes</i> |
| STAND | Signal transduction ATPases with numerous domains |
| T3E | Type III effectors |
| T3SS | Type III secretion system |
| T-DNA | Transfer DNA |
| TF | Transcription factor |
| TIR | Toll/interleukin 1 receptor |
| TNL | TIR-NB-LRR |
| tracrRNA | Transactivating CRISPR RNA |
| TRV | <i>Tobacco rattle virus</i> |
| v-cADPR | Cyclization variant of ADPR |
| VIGS | Virus induced gene silencing |
| W | Tryptophan |
| wt | Wild-type |
| <i>Xcv</i> | <i>Xanthomonas campestris</i> pv. <i>vesicatoria</i> |
| XopQ | Xanthomonas outer protein Q |
| Y2H | Yeast-two-hybrid |

| | |
|------|-----------------------------|
| Y3H | Yeast-three-hybrid |
| YFP | Yellow fluorescent protein |
| ZAR1 | HOPZ-activated resistance 1 |

List of tables, figures and supplemental data

Figures

| | |
|--|-----|
| Figure 1: Golden Gate Cloning: the hierarchical Modular Cloning (MoClo) system for standardized assemblies | 5 |
| Figure 2: Interaction between plants and pathogens: susceptibility <i>versus</i> resistance | 57 |
| Figure 3: Modular structure of NLR-type R proteins..... | 59 |
| Figure 4: Pathogenic effector detection by different types of NLRs..... | 67 |
| Figure 5: Role of EDS1-based heterocomplexes in TNL-mediated immunity and its localization | 70 |
| Figure 6: Communication of plant and pathogen | 73 |
| Figure 7: Flow sheet of the experimental setup to identify unknown interacting partners of the EDS1-based heterocomplex..... | 115 |
| Figure 8: Example of Y3H cDNA library screen | 117 |
| Figure 9: Phenotypic analysis of pathogen recognition in <i>Nb</i> after silencing of interacting candidate genes..... | 123 |
| Figure 10: <i>In planta</i> growth assay of silenced interactor candidates of the phenotypical VIGS-assay..... | 125 |
| Figure 11: subcellular localization and FRET-APB of interacting candidates | 127 |
| Figure 12: EDS1 recruits different interaction partners for immune signaling in <i>Nb</i> vs. <i>At</i> ... | 133 |
| Figure 13: Model of TNL-mediated defense signaling in <i>Nb</i> <i>versus</i> <i>At</i> | 145 |
| Figure 14: Model of effector activated TNL-signaling in <i>Solanaceae</i> | 149 |

Tables

| | |
|--|-----|
| Table 1: Properties of different cloning strategies | 6 |
| Table 2: Bait plasmids used for the interaction studies in yeast | 116 |
| Table 3: Potential interactors identified by BLASTn | 119 |
| Table 4: Candidates specifically interacting with the S ₁ EDS1-SPAD4 and S ₁ EDS1-SISAG101b heterocomplexes, their predicted localization, and interaction of the <i>At</i> -orthologs | 121 |
| Table 5: Targeted genes for VIGS approach | 122 |

Opening remarks

The laboratory work underlying this PhD thesis was conducted under the supervision of Dr. Johannes Stuttmann. He is an independent researcher and junior group leader at the Martin Luther University of Halle in the department of Plant Genetics, directed by Prof. Dr. Ulla Bonas. I was the first PhD student working in this young lab, and started my work in January of 2015. This was an exciting time in genetics and science in general, as Transcription Activator-like effectors had emerged as programmable DNA-binding modules and had also been employed for generation of designer nucleases for genome editing applications. At the same time, RNA-guided nucleases (RGNs) had just been discovered as an even simpler and potentially more versatile tool for genome editing, and initiated a yet ongoing revolution in the field. These breakthrough discoveries are able to overcome the limits between model and non-model organisms, and opened up a plethora of new perspectives in plant sciences.

Another breakthrough becomes feasible by advances in synthetic biology which now allow, for example, the synthesis of entire genomes with novel properties. One guiding idea in synthetic biology consists in the application of engineering principles, such as standardization and modularization, to DNA assembly and genome engineering. This can occur at the genome level, but similar principles can also be applied to basic molecular cloning or assembly of multigene constructs and gene clusters.

One aim of the group of Dr. Stuttmann was to implement the new technologies to decipher the role of an assumed signaling node in plant innate immune signaling. I participated shortly after initiation of these research lines and the implementation of the required technical infrastructure. To that end, the lab of Dr. Stuttmann developed tools for plant genome editing and resources for plant synthetic biology that build the basis for my work on plant immunity.

As a consequence, a significant fraction of my PhD work was more technical- or resource-oriented. For a coherent presentation, I decided to divide my thesis in three parts, dealing with i) plant synthetic biology, ii) genome editing and iii) innate immunity. The first two parts are rather a prerequisite for conducting work presented in the final part, and will not be discussed beyond what is stated in respective publications. For the last part, which represents the core of my thesis work, further unpublished results are presented, and the work is discussed in detail.

Part I: Plant synthetic biology - resources and modules for efficient molecular cloning and assembly of multigene constructs

Introduction

1.1. Cloning strategies – the long way to standardized assemblies of multigene constructs

Synthetic biology can revolutionize biology by designing microorganisms with desired features not existing in nature. These microorganisms might be able to produce, for instance, biofuels, chemical precursors or novel antibiotics. Another prospect could be the creation of synthetic, mitigated viruses to develop new vaccines or the generation of minimal living cells (Konig *et al.*, 2013). For all these applications, a key challenge is to assemble complex DNA modules in the right orientation and order to generate a synthetic gene string or even entire genomes. This can be considered as a technical limitation or engineering challenge. Indeed, the transfer of technical know-how from engineering to the field of molecular biology has led to major breakthroughs in synthetic biology in the past decade (Konig *et al.*, 2013). Application of engineering principles to DNA assembly includes standardization and automation of processes, and generally allows construction of many variations of a sequence to test and improve specific properties. This may be required for assembly and benchmarking of an entire synthetic genome, but underlying principles can also be exploited for cloning and manipulation of a single or a few genes of interest.

In the last 20 years, most cloning strategies relied on standard DNA construction techniques using REs (restriction endonucleases) and a DNA ligase, which often included multiple cloning steps. Alternatively, the commercial Gateway system was used (Casini *et al.*, 2015). Gateway cloning is highly efficient for regular cloning, however, the most important advantage is that only the initial creation of an entry clone, a PCR-based step, is critical and requires thorough verification. The mobilization of a DNA insert from an *entry* into a *destination* vector is highly efficient and basically failsafe. Another advantage is the reusability of entry clones, from which an insert can be shuttled into destination vectors for nearly any biological system and experimental setup (Lampropoulos *et al.*, 2013). The classical Gateway system represents a binary approach, in which one element (often a coding sequence) is mobilized to another sequence context. This limitation was overcome by the MultiSite Gateway technology (Sasaki *et al.*, 2004) allowing the combination of up to four

DNA fragments in a suitable Gateway destination vector, but this technology was not extensively used.

Today, a versatile cloning system should allow generation of multiple combinations of coding sequences with collections or variants of regulatory sequences, such as promoters and terminators, and epitope tags, as well as the assembly of multigene constructs (Weber *et al.*, 2011). The first system meeting these expectations was termed NOMAD (Nucleic acid Ordered Module Assembly with Directionality) (Rebatchouk *et al.*, 1996). NOMAD modules (i.e. promoters, epitope tags, coding sequences etc.) are flanked by recognition sites of the restriction enzyme *Syl*I, making them compatible with a specific destination vector (Rebatchouk *et al.*, 1996). However, NOMAD requires multiple cloning steps to assemble a transcription unit, as modules are cloned sequentially into the destination vector to generate a composite module. The next innovation, the BioBricks standard, described for the first time standardized basic biological parts like promoters, ribosome binding sites and terminators (Knight, 2003), flanked by standard prefix and suffix sequence overhangs that contain defined restriction sites. The ligation of two BioBrick parts produces a new, larger construct containing the same overhang sequences at the new pre- and suffix (Knight, 2003; Casini *et al.*, 2015). But BioBricks are limited in their ability to assemble multiple DNA fragments in a single step and generate a fusion site of 8 bp (base pairs), termed "scar" sequence, between two BioBricks (Sleight *et al.*, 2010).

Methods that do not rely on endonucleases have also been developed. For example, the USER-fusion enables to clone multiple DNA fragments, generated by PCR, simultaneously in a destination vector (Geu-Flores *et al.*, 2007). This method relies on the use of specific oligonucleotides containing a single deoxyuridine residue near the 5' end. Treatment of the PCR products with a deoxyuridine-excision reagent generates long 3' overhangs, designed to be complementary to the following part. However, a commercial USER-Mix has to be used, which makes this technique more expensive. Furthermore, PCR amplification may, despite the high fidelity of modern DNA Polymerases, induce sequence errors, and the complete insert has to be verified, i.e. by sequencing (Geu-Flores *et al.*, 2007). Moreover, the produced PCR fragments can generally not be reused in other applications.

Another PCR-based strategy is Gibson assembly (Gibson *et al.*, 2009). Here, linear DNA fragments, amplified by PCR and sharing identical sequence stretches of 20-30 bp at their ends, are stitched together in a single reaction. In Gibson assembly, 5' ends are first degraded by an exonuclease to create single strand 3' overhangs. By identical sequence ends, the complementary stretches of fragments anneal, and are fused by a ligase. With this technology, it is possible to assemble large sequences up to several 100 kb (kilo base) which can be assembled scar-free and without the use of restriction enzymes. Nevertheless,

Gibson assembly relies on oligonucleotides and PCR amplification and can, therefore, be error-prone. Additionally, the amplified parts cannot be used in multiple, different assemblies (Gibson *et al.*, 2009).

A major advance towards systematic DNA assembly was the invention of GG (Golden Gate) cloning based on use of Type IIS REs (Engler *et al.*, 2008). Type IIS REs differ from classical Type II REs, because they cleave DNA adjacent to their recognition site and produce sticky ends (Szybalski *et al.*, 1991). This provides the freedom to choose the produced sticky ends generated upon restriction of a DNA fragment. The design of inserts that have different sticky ends allows to generate a string of inserts with compatible overhangs, which can be assembled in a defined order into a single molecule by the use of a T4-ligase in a single tube reaction (Engler *et al.*, 2008). The produced DNA fragment has lost the RE-specific recognition sites, a re-opening of the produced fragment is not possible. Many “genetic toolkits” have been developed in the last years which underlie the principles of the GG cloning standard (Casini *et al.*, 2015). Recently, designers of GG cloning toolkits, at least in the plant field, agreed on using a common syntax. This standard defines twelve Type IIS overhangs that should form boundaries between the genetic elements commonly found within a eukaryotic gene (Patron *et al.*, 2015). This syntax ensures a sophisticated potential: the systems accumulate a continuously increasing common library of standardized bricks, which can be shared between the public research communities.

One GG-based standard for DNA assembly is the MoClo (Modular Cloning) system for hierarchical DNA assembly (Weber *et al.*, 2011). MoClo relies on different tiers/levels, whereby the destination vector of (for instance) level 1 will be an entry vector of the following level 2. As depicted in Figure 1, the top of this hierarchy are level 0 modules, so called phytobricks, the genetic elements building a eukaryotic gene. Different sticky ends in level 0 modules characterize the kind of genetic element, such as promoters, epitope tags, coding sequences etc., which can be ligated together in a defined order and orientation in the next higher level, level 1. In most cases, level 1 constructs will represent a single transcriptional unit, as shown in Figure 1. To build a following level 2 multigene construct, it is important to choose between seven different level 1 destination-vectors, defining the position in the next higher order multigene assembly. A maximum of six level 1 constructs can be combined in a level 2 recipient within one reaction. In a next step, these level 2 constructs can be assembled into multi-multi-gene constructs (Weber *et al.*, 2011).

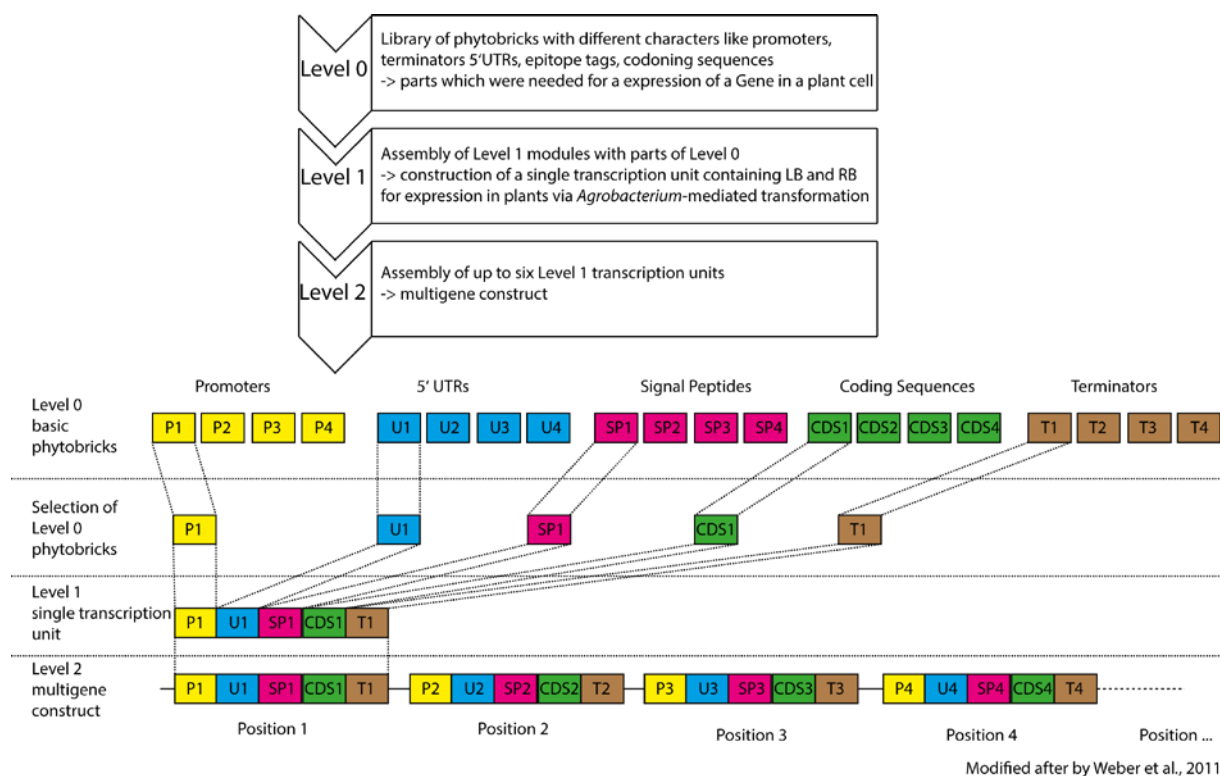


Figure 1: Golden Gate Cloning: the hierarchical Modular Cloning (MoClo) system for standardized assemblies

Description of different levels within the MoClo system. On top of the hierarchical system the phytobricks are located. These modules represent different parts needed to construct a transcriptional unit. The different types of phytobricks have to be chosen as well as the Level 1 destination vector, which determine the position within a hypothetical Level 2 assembly. Level 1 constructs are usable for expression *in planta* via *Agrobacterium*-mediated transient transformation, because left- and right borders are flanking the transcription unit. In the following Level 2, single transcription units can be subsequently fused to a multigene construct (Position.... indicates that up to six Level 1 transcription units can be fused to a Level 2 multigene construct) (Weber *et al.*, 2011).

A similar cloning standard, termed GoldenBraid, relies on the same fusion sites as MoClo, but reduces the number of level 1 destination vectors (Sarrion-Perdigones *et al.*, 2011; Sarrion-Perdigones *et al.*, 2013; Patron *et al.*, 2015; Vazquez-Vilar *et al.*, 2017). On the one hand, this leads to a lower number of vectors belonging to the toolkit and a simpler nomenclature. On the other hand, this reduction has the consequence that only two transcriptional units can be combined in one assembly step. In a next cloning step, two of these vectors could be combined, resulting in four transcriptional units combined in one vector. This approach, therefore, simplifies some aspects, but also increases the number of cloning steps necessary to generate a multigene construct of more than two transcriptional units (Casini *et al.*, 2015).

Yet another recently described method is termed Loop assembly (Pollak *et al.*, 2018). It promises to combine all the benefits of GG assembly, but only requires a set of eight plasmids to build constructs with theoretically unlimited length (Pollak *et al.*, 2018). This way, GG assemblies are made through repetitive loops, enabling alternating assembly cycles that rely on two sets of four plasmids. Here, the common level 0 bricks are used to create single

transcriptional units in each of four odd-numbered plasmids. In a second step, four level 1 modules can then be assembled into a level 2 construct in each of the four even-numbered vectors. Next, level 2 constructs can be assembled by cloning back into odd-numbered vectors to create level 3, which now possesses up to 16 transcriptional units. Theoretically, this can be continued without limit. Because of the recursive construction of this system, a mixture of parts from different levels of the same parity can be combined at any step (Pollak *et al.*, 2018).

Hierarchical GG assembly is probably best suited for applications where multiple genes or gene fragments have to be expressed. It is, therefore, reasonable, that it is used in kits for multiplex genome editing approaches by CRISPR/Cas9 (Casini *et al.*, 2015; Ordon *et al.*, 2017). The absolute requirement of domestication, the elimination of internal recognition sites of respective REs, most likely represents the most severe limitation (Weber *et al.*, 2011). The common standards (MoClo, GoldenBraid) use the Type IIS REs *BsaI*, *BpiI* and *BsmBI* that have a relatively long recognition site of six bp, and are therefore not frequent on average (frequency of 4^6 , it will occur every 4 kbp). To reduce domestication requirements, programmed DNA methylation is used in some standards like GreenGate, MASTER, and MetClo ligation methods (Chen *et al.*, 2013; Lampropoulos *et al.*, 2013; Lin&O'Callaghan, 2018) to guide digestion to desired sites allowing hierarchical assembly using a single Type IIS enzyme. Advantages, disadvantages, and characteristics of the different described cloning strategies are summarized in Table 1.

Table 1: Properties of different cloning strategies

| Cloning Method | Scar-free Assembly | Multigene Constructs | Domestication Required | Reuse of Constructs | Commercial application |
|--------------------------|---------------------------|-----------------------------|-------------------------------|----------------------------|-------------------------------|
| Gateway® ¹ | no | (yes) | no | yes | yes |
| NOMAD ² | yes | (no) | yes | yes | no |
| BioBricks ³ | no | yes | yes | yes | no |
| USER® ⁴ | yes | yes | no | no | yes |
| Gibson ⁵ | yes | yes | no | no | both |
| Golden Gate ⁶ | no | yes | yes | yes | no |

¹(Hartley *et al.*, 2000) ²(Rebatchouk *et al.*, 1996) ³(Knight, 2003) ⁴(Geu-Flores *et al.*, 2007) ⁵(Gibson *et al.*, 2009) ⁶(Weber *et al.*, 2011)

1.1. Aims, achievements and conclusions

At the beginning of this work, mainly Gateway cloning was used. It was decided to switch to the GG-based MoClo system, which required implementation of new standards and a new infrastructure. We generated multiple novel MoClo modules (e.g. promoters, epitope tags, terminators) to enhance versatility of the MoClo standard. Furthermore, multiple vectors were converted, e.g., for yeast-two-hybrid analysis or bacteria-to-plant protein translocation, and DNA modules were constructed allowing a toggling between the Gateway and the MoClo system. This resource was published in PLoS One (Gantner *et al.*, 2018), and respective material was shared *via* the non-profit organization Addgene. By now, hundreds of these vectors were requested through Addgene, demonstrating the value of modules generated in this work for the plant research community. Furthermore, this resource was essential for analyses presented in the following parts of this thesis, and contributed to assembly of >1000 vectors.

1.2. Peripheral infrastructure vectors and an extended set of plant parts of the Modular Cloning system

1.2.1. Publication Gantner *et al.*, 2018



RESEARCH ARTICLE

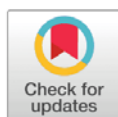
Peripheral infrastructure vectors and an extended set of plant parts for the Modular Cloning system

Johannes Gantner¹✉, Jana Ordon¹✉, Theresa Ilse¹✉, Carola Kretschmer¹, Ramona Gruetzner², Christian Löffke³, Yasin Dagdas³, Katharina Bürstenbinder⁴, Sylvestre Marillonnet², Johannes Stüttmann¹*

1 Institute for Biology, Department of Plant Genetics, Martin Luther University Halle (Saale), Halle, Germany, **2** Department of Cell and Metabolic Biology, Leibniz Institute of Plant Biochemistry, Halle (Saale), Germany, **3** Gregor Mendel Institute (GMI), Austrian Academy of Sciences, Vienna BioCenter (VBC), Vienna, Austria, **4** Department of Molecular Signal Processing, Leibniz Institute of Plant Biochemistry, Halle (Saale), Germany

✉ These authors contributed equally to this work.

* johannes.stuttmann@genetik.uni-halle.de



OPEN ACCESS

Citation: Gantner J, Ordon J, Ilse T, Kretschmer C, Gruetzner R, Löffke C, et al. (2018) Peripheral infrastructure vectors and an extended set of plant parts for the Modular Cloning system. *PLoS ONE* 13(5): e0197185. <https://doi.org/10.1371/journal.pone.0197185>

Editor: Alvaro Galli, CNR, ITALY

Received: February 21, 2018

Accepted: April 27, 2018

Published: May 30, 2018

Copyright: © 2018 Gantner et al. This is an open access article distributed under the terms of the [Creative Commons Attribution License](https://creativecommons.org/licenses/by/4.0/), which permits unrestricted use, distribution, and reproduction in any medium, provided the original author and source are credited.

Data Availability Statement: All relevant data are within the paper and its Supporting Information files.

Funding: This work was funded by GRC grant STU 642-1/1 (Deutsche Forschungsgemeinschaft, DFG) and seed funding by the CRC 648 (DFG) to Johannes Stüttmann. Ulla Bonas is acknowledged for generous support. The funder had no role in study design, data collection and analysis, decision to publish, or preparation of the manuscript.

Competing interests: The authors have declared that no competing interests exist.

Abstract

Standardized DNA assembly strategies facilitate the generation of multigene constructs from collections of building blocks in plant synthetic biology. A common syntax for hierarchical DNA assembly following the Golden Gate principle employing Type IIs restriction endonucleases was recently developed, and underlies the Modular Cloning and GoldenBraid systems. In these systems, transcriptional units and/or multigene constructs are assembled from libraries of standardized building blocks, also referred to as phytobricks, in several hierarchical levels and by iterative Golden Gate reactions. Here, a toolkit containing further modules for the novel DNA assembly standards was developed. Intended for use with Modular Cloning, most modules are also compatible with GoldenBraid. Firstly, a collection of approximately 80 additional phytobricks is provided, comprising e.g. modules for inducible expression systems, promoters or epitope tags. Furthermore, DNA modules were developed for connecting Modular Cloning and Gateway cloning, either for toggling between systems or for standardized Gateway destination vector assembly. Finally, first instances of a “peripheral infrastructure” around Modular Cloning are presented: While available toolkits are designed for the assembly of plant transformation constructs, vectors were created to also use coding sequence-containing phytobricks directly in yeast two hybrid interaction or bacterial infection assays. The presented material will further enhance versatility of hierarchical DNA assembly strategies.

Introduction

Molecular cloning belongs to the unbeloved, yet inevitable everyday tasks of many wet lab molecular biologists. In the past two decades, most labs either relied on classical ligation of restriction fragments or PCR products into a vector of interest, or used the Gateway system,

which is based on the recombination reactions taking place for integration and excision of the genome of phage lambda during bacterial infection [1]. Gateway cloning proved to be extraordinarily efficient for regular cloning, and also for high-throughput applications such as library generation. One striking advantage of Gateway cloning is that only the initial creation of entry clones represents a critical step. Subsequently, inserts may be mobilized from entry clones into a wide array of destination vectors by basically failsafe, highly efficient and unified recombination reactions. This is also facilitated by the availability of destination vectors for virtually any biological system and experimental setup [e.g. 2, 3]. However, Gateway cloning is relatively costly, as it relies on use of the proprietary BP/LR enzyme blends, and also represents a rather binary approach to molecular cloning where a single insert is mobilized into a new sequence context. To some extent, this was overcome by the invention of multisite Gateway systems [4]. The current MultiSite GatewayTM Pro technology allows combination of up to four DNA fragments in any (attR1/R2 site-containing) destination plasmid. Multisite Gateway was also combined with other cloning techniques in Golden GATEway cloning for further flexibility and generation of multigene constructs [5]. However, the multisite Gateway technology found only limited use in the scientific community, as novel DNA assembly strategies concomitantly emerged. Most popular strategies for combinatorial DNA assembly now rely on enzymatic reaction assembly (Gibson assembly, In-FusionTM Cloning [6–8]) or Golden Gate cloning.

In Gibson assembly [6], linear DNA fragments sharing identical sequence stretches of e.g. 20–30 base pairs at their ends are stitched together in a single tube reaction. First, 5' ends of DNA fragments are chewed back to create single strand 3' overhangs by an exonuclease. By the identical sequence ends, complementary fragments anneal. The annealed fragments are then covalently fused by a polymerase filling up gaps and a ligase removing nicks. Overlapping ends between fragments are also required for In-Fusion cloning. The In-Fusion enzyme generates 15-nucleotide single-stranded 5' overhangs. Fragments anneal by complementarity, and are covalently joined after transformation in *E. coli*. Thus, fusion sites from enzymatic reaction assembly are scarless, no particular sequence motifs such as restriction sites are required, and large sequences up to several hundred kilobases can be assembled [6–8]. However, Gibson assembly and In-Fusion cloning rely on the engineering of identical ends on sequence fragments (by PCR), and do therefore not provide a theoretical framework for re-utilization of DNA modules in multiple and diverse DNA assemblies. This was recently achieved by the invention of hierarchical DNA assembly strategies based on Golden Gate cloning [9]. Three major standards, GreenGate [10], GoldenBraid [11] and Modular Cloning [12] were developed in parallel and are commonly used in the plant research community. All systems are based on the same principles: Standardized four base pair (bp) overhangs (generated by Type II restriction endonucleases) are defined as fusion sites between building blocks of transcriptional units, such as promoters, untranslated regions, signal peptides, coding sequences, or terminators. Building blocks are cloned as Level 0 modules, which are flanked by these four bp overhangs and recognition sites for a given Type II endonuclease. These units are also referred to as phytobricks. In a second hierarchical level (Level 1), phytobricks are assembled into transcriptional units by highly efficient Golden Gate cloning. Multigene constructs are assembled with another Golden Gate reaction and a yet further hierarchical level (Level 2 or Level M). The drawback of Golden Gate-based DNA assembly is the requirement for “sequence domestication”, the removal of internal recognition sites for respective Type II endonucleases from sequences of interest. Efficient strategies were previously described [9, 13], but domestication of multiple internal recognition sites may render the generation of novel phytobricks cumbersome. Also, while internal recognition sites may be eliminated through silent mutations in protein-coding sequences, consequences of domestication are hardly predictable for non-coding sequences, as e.g. promoters. Each of the Golden Gate-based assembly systems

comes with its individual advantages and constraints. In GreenGate cloning, only the Type II enzyme *BsaI* is used. Thus, internal recognition sites of solely this enzyme have to be removed from phytobricks during domestication. However, Level 1 vectors of the GreenGate system are not plant transformation vectors, and an additional assembly step in a Level 2 “destination” vector is thus required prior to functional verification. Furthermore, multigene construct assembly is carried out by iterative rounds where additional transcriptional units (Level 1) are added to an existing (Level 2) construct. Both GoldenBraid and Modular Cloning rely on cloning steps of different hierarchical levels being carried out by iterative use of two different Type II enzymes—*BsaI* and *BpiI* in Modular Cloning, and *BsaI* and *BsmBI* for GoldenBraid. This obviously increases the requirement for sequence modifications during domestication, but streamlines cloning procedures and increases flexibility. The developers of GoldenBraid and Modular Cloning also agreed on a common set of fusion sites between building blocks, a common “grammar” or syntax, making these systems at least partially compatible [13, 14]. The main difference between systems consists in the approach for multigene construct assembly: Being a combinatorial process in GoldenBraid (combination of Level α and Ω), up to six Level 1 modules may be assembled in a Level 2 construct in a single step by Modular Cloning. This strategy facilitates and/or accelerates the assembly of multigene constructs, but comes at the expense of a more complex nomenclature and vector toolkit. GoldenBraid developers also provide online databases and software suites for end-users [15], and similar tools are yet unavailable for Modular Cloning. A number of research laboratories recently agreed on the use of the common molecular syntax underlying both Modular Cloning and GoldenBraid to foster re-utilization and sharing of DNA modules for bioengineering [16].

The previously released Modular Cloning Toolkit provides DNA modules facilitating domestication of novel sequences and assembly of multigene constructs following the Modular Cloning standard [13]. A simultaneously released collection of Plant Parts contains 95 modules coding for commonly used promoters, transcriptional terminators, epitope tags and reporter genes [13]. Together, these toolkits allow for a jump start into hierarchical DNA assembly for end users. In principle, the cloning of *your favorite gene (YFG)* in the Modular Cloning format (as a CDS1 or CDS1ns module: *YFG* flanked by *BsaI* restriction sites producing respective overhangs) will be sufficient for assembly of *YFG* together with different Plant Parts in various simple or complex plant transformation constructs. However, a peripheral infrastructure which allows re-using the Modular Cloning *YFG* modules (CDS1 or CDS1ns Level 0 modules) in other experimental setups, such as e.g. bacterial or yeast expression, and also an interface to Gateway cloning strategies, were so far missing. Here, we present molecular tools for connecting the Modular Cloning system with Gateway cloning, either for toggling between Modular Cloning and Gateway cloning, the cost-efficient generation of Gateway entry clones, or simple, hierarchical assembly of Gateway destination vectors. Furthermore, vectors were developed for re-utilization of Modular Cloning *YFG* modules for yeast two hybrid assays or bacterial translocation into plant cells. Finally, an extended collection of Plant Parts consisting of 82 Level 0 modules, or phytobricks, is provided for the sake of efficient bioengineering through shared resources.

Material and methods

Plant material, growth conditions, bacterial infection assays and virus induced gene silencing

Nicotiana benthamiana wildtype, *eds1a-1* mutant plants [17] and *pBs3:Bs3* transgenic plants [18] were cultivated in a greenhouse with 16 h light period, 60% relative humidity at 24/20°C (day/night). For transient *Agrobacterium*-mediated expression, plate-grown bacteria were

resuspended in *Agrobacterium* infiltration medium (AIM; 10 mM MES pH 5.7, 10 mM MgCl_2) to an $\text{OD}_{600} = 0.4$ or as indicated, and infiltrated with a needleless syringe. For imaging of IQD8 and Calmodulin2, *Agrobacterium* strains were mixed in a 1:1 ratio with a strain for expression of p19. Plasmids were mobilized into a *Pseudomonas fluorescens* strain containing a chromosomally-encoded *Pseudomonas syringae* type III secretion system ["EtHAn"; 19] by tri-parental mating, and plate-grown bacteria were resuspended in 10 mM MgCl_2 prior to infiltration. For virus induced gene silencing, *Agrobacterium* solutions were infiltrated in the bottom leaves of three week-old plants. Photo-bleaching was documented 14 d later, or plants were used for challenge inoculations.

Yeast two hybrid assays, immunoblotting and live cell imaging

Derivatives of pGAD and pGBK vectors (pJOG417-418 and pCK011-pCK012) were co-transformed into frozen competent yeast cells of strain PJ69-4a as previously described [20]. Single colonies were cultivated in liquid SD media for 48 h, and dilution series prepared. Yeast cell solutions were plated on selective media using a multichannel pipette, and plates were grown for 3–4 days prior to documentation. For immunoblot detection from yeast, proteins were extracted as previously described [21]. For extraction of plant proteins, leaf discs were ground in Laemmli buffer and boiled at 92°C for 5 minutes. Proteins were separated on SDS-PAGE gels, transferred to nitrocellulose membranes, and detected via HRP-conjugated secondary antibodies (GE Healthcare) using Supersignal West Pico and Femto substrates (Pierce; supplied by Thermo Scientific). Primary antibodies used were α -GFP (mouse monoclonal), α -HA (rat monoclonal; both from Roche and now distributed by Sigma), α -AD (GAL4 activation domain) and α -BD (GAL4 DNA-binding domain; both mouse monoclonal; Takara). Imaging was performed either on a Zeiss LSM 700 inverted microscope using a 40x water immersion objective, or a Zeiss LSM780 system. For imaging of IQD8 and Calmodulin2, mCherry was excited with a 555 nm laser, and emission was detected between 560 and 620 nm. Images are maximum intensity projections of z stacks. For simultaneous imaging of mTRQ, mEGFP and mCherry, fluorophores were excited with 458, 488 and 561 nm lasers, and emission was detected between 463–482, 499–543 and 587–630nm. For simultaneous imaging of mEGFP and chlorophyll A, 488 and 633 nm lasers were used for excitation, and emission was detected between 490–517 and 656–682 nm.

Molecular cloning

Vectors for generation of Gateway entry vectors (pJOG130-131) were generated by ligating a PCR amplicon encoding for a *ccdB* cassette and flanked by *BsaI* sites cutting respective 4 bp overhangs into the *AscI/NotI* sites of a pENTR/D derivative. Gateway modules (pJOG267, 387, 947, 956) were generated by ligation of an attR1-*ccdB*/cat-attR2 PCR amplicon into pAGM1287, pICH41308 or pAGM9121 [13], respectively, or into the *EcoRV* site of a custom cloning vector (pJOG397) for generation of pJOG562. For generation of GAL4-based yeast two hybrid vectors (pJOG417-418), *BsaI* sites in the backbones of pGAD and pGBK vectors (Clontech) were eliminated by mutagenesis, and a *lacZ* cassette was subsequently ligated into the *EcoRI/XhoI* sites. The pCK011-12 vectors were derived from these by replacing the *lacZ* cassette by a *ccdB* cassette with respective adaptors. The bacterial secretion vectors are based on a Golden Gate-compatible pBRM derivative [22], and secretion signals and *ccdB* cassette were ligated into the *BsaI/EcoRI* sites. To generate pRNA2-GG, PCR amplicons of the 5' and 3' fragments of TRV2 and a *ccdB* cassette were cloned between 35S promoter and terminator sequences in pVM_BGW [23]. All Level 0 modules (S3 Table) were constructed as described [13], and internal restriction sites eliminated. For ligations or Golden Gate reactions, generally

20 fmole of all components were used, and reactions performed as previously described [12]. Primer sequences are provided in S1 Table, and additional details are available upon request.

Results and discussion

Golden Gate cloning vectors for Gateway entry clone generation or shuttling from Modular Cloning to Gateway cloning

The Gateway cloning system is widely used, and will co-exist in most labs implementing hierarchical DNA assembly strategies (in the following Modular Cloning) at least for a transitional period. For Gateway cloning, no sequence domestication is required, which might also make it the preferable system when large numbers of candidate genes are handled. Vectors were developed to ensure gene flow between cloning platforms, and also to apply the principles and nomenclature of Modular Cloning for cost-efficient Gateway entry clone generation (Fig 1). The vectors pJOG130 and pJOG131 are based on a common backbone (Kanamycin resistance, M13fwd/rev priming sites), and contain a *ccdB* negative selection cassette flanked by Golden Gate cloning sites (*Bsa*I) and attL1/2 sites. The two vectors differ in overhangs generated by *Bsa*I digestion: pJOG130 uses overhangs of CDS1 modules of Modular Cloning, while pJOG131 uses those of CDS1ns modules (Fig 1A and 1B) [12, 13]. Vectors may thus be used to convert respective modules from Modular Cloning to Gateway cloning (Level 0 → GW entry) by simultaneous restriction and ligation using *Bsa*I (Fig 1A and 1B; in the following referred to as “*Bsa*I Golden Gate reaction”). Alternatively, PCR products carrying suitable adaptors (S1 Fig) may be cloned. While both vectors can theoretically receive PCR products containing or

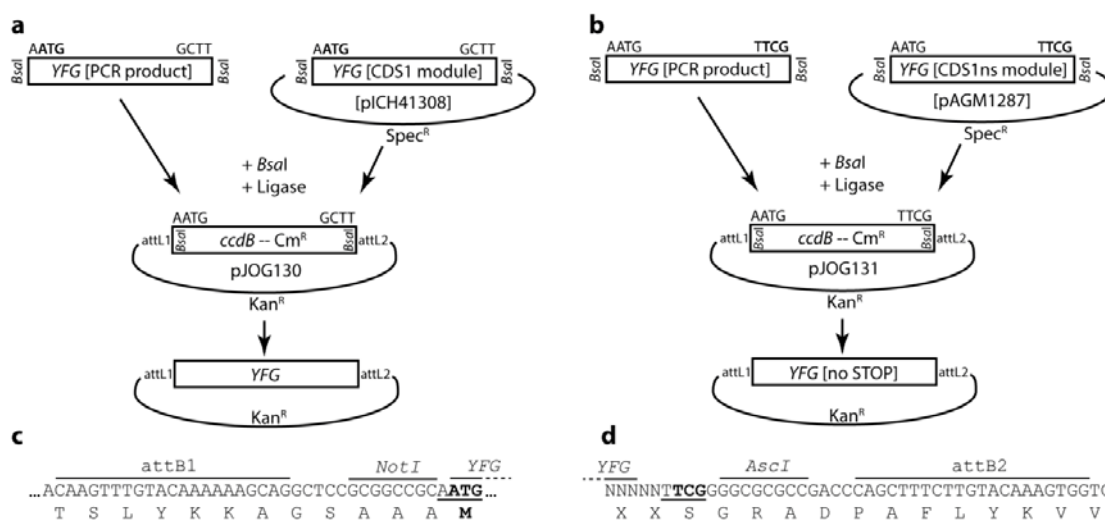


Fig 1. Generation of Gateway entry vectors by Golden Gate cloning. (a) Scheme of entry clone generation in pJOG130. Either PCR products flanked by *Bsa*I restriction sites and suitable 4 bp overhangs or CDS1 Level 0 modules of the Modular Cloning system may be cloned into pJOG130 by *Bsa*I cut/ligation in exchange for a *ccdB* cassette. (b) as in (a), but when using vector pJOG131 for PCR products with suitable adaptors or CDS1ns modules of the Modular Cloning system. (c) Amino acid sequence encoded by att1 sites / adaptor sequences in pJOG130. The sequence created from using a pJOG130 derivative in a LR recombination reaction is shown. Translation will either initiate at an upstream START codon of an N-terminal epitope tag, or at the ATG codon depicted in bold if no N-terminal tag is fused during LR recombination. (d) as in (c), but when using a pJOG131 derivative during LR recombination. Amino acid sequences encoded at 5' fusion sites (attB1) are equivalent as in (c) upon fusion of an N-terminal tag. The 3' fusion site and respective linker sequences are shown. Sequences preceding the TCG (Ser) triplet depicted in bold, which is part of the Golden Gate overhang, will depend on design of PCR product or Level 0 module.

<https://doi.org/10.1371/journal.pone.0197185.g001>

not a STOP codon, we intended to use pJOG130 for cloning of coding sequences with, and pJOG131 for sequences without a STOP codon to follow the Modular Cloning nomenclature. Fusion sites resulting from recombination of inserts from pJOG130 and 131 into Gateway expression vectors are depicted in Fig 1C and 1D. *Att* site-flanking *AscI* and *NotI* sites present in most entry plasmids are maintained, and fusion sites from Golden Gate cloning translate into serine or alanine residues commonly employed as linkers.

The described vectors, pJOG130/131, were used to convert Modular Cloning Level 0 modules to Gateway entry clones, and also for cloning of ~ 60 cDNAs encoding candidate interactors obtained in a yeast three hybrid screen (to avoid sequence domestication prior to further confirmation of interactions). Toggling from Modular Cloning to the Gateways system by a *BsaI* Golden Gate reaction was highly efficient, as previously described [9], and background free due to *ccdB* counter-selection. The efficiency of cloning PCR products depended on the quality of the PCR product and the number of internal *BsaI* sites. Amplicons without internal *BsaI* sites could be cloned with high efficiencies (> 80% correct clones), and also low abundance PCR products yielded reasonable efficiencies (> 20%). For cloning of amplicons with internal *BsaI* sites, a second ligation step is required subsequent to the Golden Gate reaction [9]. Even with two internal *BsaI* sites, cloning efficiencies from 20–80% were regularly obtained when using high-quality PCR products. It should be noted that, in rare cases, overhangs created by *BsaI* restriction at internal sites may match vector overhangs of pJOG130/131. In these cases, and also with inserts containing >2 internal *BsaI* sites, alternative methods for entry clone generation, such as BP reaction or TOPO cloning [1], will be preferable. Summarizing, next to shuttling inserts from Modular Cloning (or GoldenBraid) to Gateway cloning, pJOG130/131 are intended for generation of novel Gateway entry clones from PCR amplicons (containing ≤ 2 internal *BsaI* sites) with a generalized and cost-efficient cloning strategy (< 1 € per reaction).

Standardized assembly of simple or multipartite Gateway destination vectors by Modular Cloning

Most labs relying on the Gateway cloning strategy dispose of a rich collection of destination vectors, and many different vector series are available to the community [e.g. 2, 24, 25]. Nonetheless, e.g. the integration of improved fluorophores or specialized demands eventually necessitate the generation of novel destination vectors, which is often carried out by cumbersome and inefficient cloning strategies. However, Gateway destination vectors may also be generated by hierarchical DNA assembly from phytobricks [14].

In Modular Cloning, Level 0 modules (phytobricks) are combined to a transcriptional unit in a respective Level 1 recipient [12, 13]. Five different Level 0 modules (pJOG267/387/562/947/956) containing the Gateway cassette (*attR1*-*cat*/*ccdB*-*attR2*) were constructed, and are sufficient for assembly of Gateway destination vectors for virtually any application following the standardized Modular Cloning grammar (Fig 2). It should be noted that the 5' overhang of the Level 0 CDS1 and CDS1ns modules (A|ATG) encompasses a translation initiation codon. Thus, use of Gateway cassette-containing phytobricks of these types (pJOG267/387) in assemblies without an N-terminal tag module (NT1) will lead to a modified N-terminus in final expression products. Therefore, modules containing the NT1 5' overhang (CCAT) and either CDS1 (pJOG956) or CDS1ns (pJOG947) 3' overhangs were generated for assembly of Gateway destination vectors without epitope tag-encoding sequences or for C-terminal tagging, respectively (Fig 2A and 2B). pJOG387 and pJOG267 replace CDS1 and CDS1ns modules in Level 1 assemblies, and are designed for the generation of destination vectors for N-terminal or N- and C-terminal tagging of proteins (Fig 2C and 2D). Finally, pJOG562 carries overhangs to

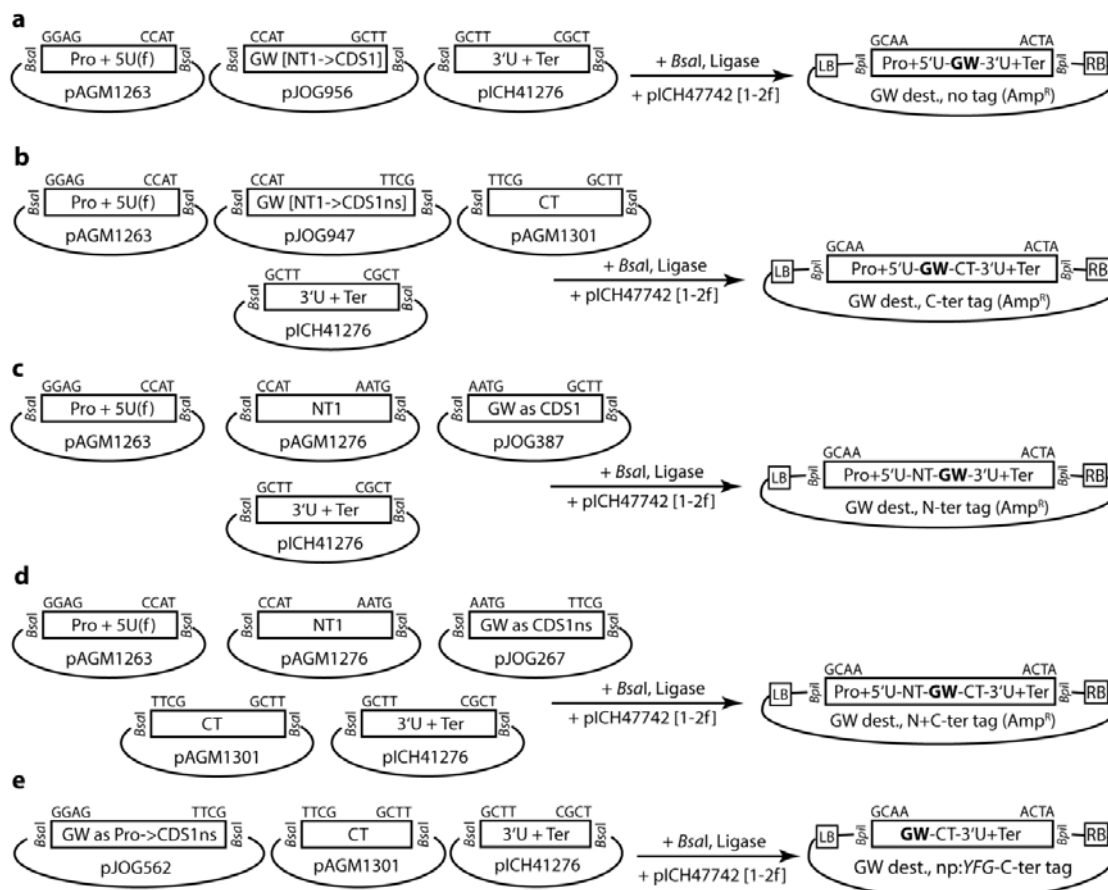


Fig 2. Assembly of simple Gateway (GW) destination vectors by Modular Cloning. (a) Assembly of Gateway destination vectors not encoding for epitope tags. (b) Assembly of Gateway destination vectors for C-terminal tagging of proteins of interest. (c) Assembly of Gateway destination vectors for N-terminal tagging of proteins of interest. (d) Assembly of Gateway destination vectors for N- and C-terminal tagging of proteins of interest. (e) Assembly of Gateway destination vectors for recombination of entry fragments containing both upstream regulatory sequences and a gene of interest, and for expression of C-terminally tagged proteins.

<https://doi.org/10.1371/journal.pone.0197185.g002>

replace promoter, 5'UTR and a CDS1ns module in assembly reactions (Fig 2E). Here, assembly yields Gateway destination vectors without promoter, designed for recombination of fragments encompassing promoter and coding sequence from a respective entry clone by LR reaction.

A Level 1 assembly of the Gateway cassette-containing Level 0 modules (pJOG267/387/562/947/956) with additional phytobricks yields simple Gateway destination plasmids lacking a plant-selectable marker, which may be used e.g. for *Agrobacterium*-mediated transient expression ("Agroinfiltration"). Multipartite Gateway destination plasmids integrating a plant-selectable marker and/or additional expression cassettes are obtained by an additional assembly step (Fig 3A; Level M assembly is preferable to avoid identical resistances between entry (often Kanamycin) and destination vectors). To test efficiency and functionality of assemblies,

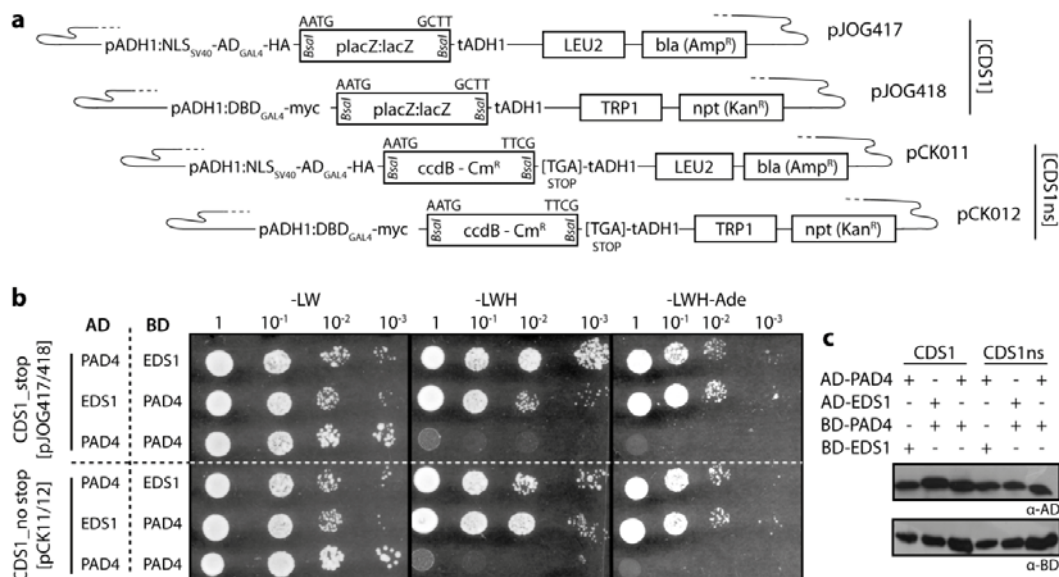


Fig 4. Modular Cloning-compatible vectors for a GAL4-based yeast two hybrid system. (a) Schematic depiction of yeast two hybrid vectors with most important features. (b) Functional verification of vectors shown in (a). Tomato *EDS1* and *PAD4* were mobilized into vectors shown in (a), resulting constructs co-transformed into yeast cells in the indicated combinations, and co-transformants grown in dilution series on media lacking leucine and tryptophan (-LW), or additionally lacking histidine (-LWH) and adenine (-LWH-Ade). (c) Immunoblot-detection of fusion proteins expressed in yeast cells in (b).

<https://doi.org/10.1371/journal.pone.0197185.g004>

strongly induced in presence of DEX, and N- and C-terminal fragments were detected by respective antibodies, confirming functionality of the newly constructed inducible expression vector (Fig 4D). Thus, the presented modules and strategy allows the assembly of simple or multipartite Gateway destination vectors in a highly efficient manner and following the standardized Modular Cloning grammar.

Yeast two hybrid vectors for use with Level 0 CDS modules of the Modular Cloning standard

The Modular Cloning system is dedicated to assembly of plant transformation constructs, and hierarchical DNA assembly resources available for e.g. yeast or bacteria do unfortunately not rely on the common plant synthetic biology syntax [16, 33, 34]. Thus, additional vector modules are required to allow seamless re-utilization of CDS1 and CDS1ns modules (encoding *your favorite gene*) in different experimental systems. As first instances of such peripheral infrastructure to the Modular Cloning system, the popular pGAD and pGBK vectors (Clontech) for GAL4-based yeast two hybrid interaction assays were converted to the Modular Cloning standard (Fig 4A). Bait and prey vectors pJOG417/418 can accommodate CDS1 modules. The analogous vectors (pCK011/012) designed to receive CDS1ns modules contain a STOP codon directly following the 3' Golden Gate cloning overhang (T|TCG). Thus, yeast fusions proteins will contain as few as 1–2 additional amino acids (depending on the design of the respective Level 0 module), and will terminate with a serine residue encoded by the TCG within the overhang. Minimal C-terminal extensions will allow (at least in most cases) use of identical CDS1ns modules e.g. for *in planta* expression with a C-terminal epitope tag and for

Y2H assays. Vectors may also be used for Golden Gate cloning of PCR products carrying *Bsa*I adapters, and are partially compatible with CDS modules of GoldenBraid (identical bacterial selection markers in pJOG417/pCK011 and pUPD).

Vectors were tested using EDS1 and PAD4 from tomato. Arabidopsis EDS1 and PAD4 strongly interact to form a heterodimeric complex [35]. We had previously confirmed that tomato EDS1 and PAD4 also interacted in Y2H using Gateway-compatible pGAD/pGBK derivatives. CDS1 and CDS1ns Level 0 modules of tomato EDS1 and PAD4 were used for *Bsa*I Golden Gate reactions with the Y2H vectors, and all tested clones were positive in restriction digests. Resulting constructs were co-transformed into yeast, and primary transformants replica-plated on reporter media in dilution series (Fig 4B). All yeast strains grew on–LW media selecting for presence of both plasmids in co-transformants. Growth on–LWH and–LWH–Ade media, indicative of interaction of bait and prey proteins, was observed upon co-expression of AD/BD fusions of EDS1 and PAD4 in either orientation, but not if PAD4 was tested for self-interaction (Fig 4B), as previously observed. All fusion proteins were detected by immunoblotting (Fig 4C), confirming full functionality of the presented Y2H vectors.

Bacterial type III secretion vectors for the Modular Cloning standard

Plant pathogenic bacteria often rely on the secretion of proteins (effectors) directly into the cytoplasm of host cells via a type III secretion system [36]. Substrates for type III secretion are recognized by a yet enigmatic N-terminal secretion signal, and proteins can be targeted for type III secretion by appending a respective signal. This has been extensively used to analyze e.g. the function of oomycete effectors in the “effector detector system” [37, 38]. Four different vectors for bacterial type III secretion and compatible with Modular Cloning (and GoldenBraid) were generated (Fig 5A). Vectors contain either amino acids 1–134 of AvrRps4 and are thus very similar to the previously described pEDV vectors [37], or amino acids 1–100 of the AvrRpt2 effector [39]. With each of these secretion signals, a vector for CDS1 modules and for

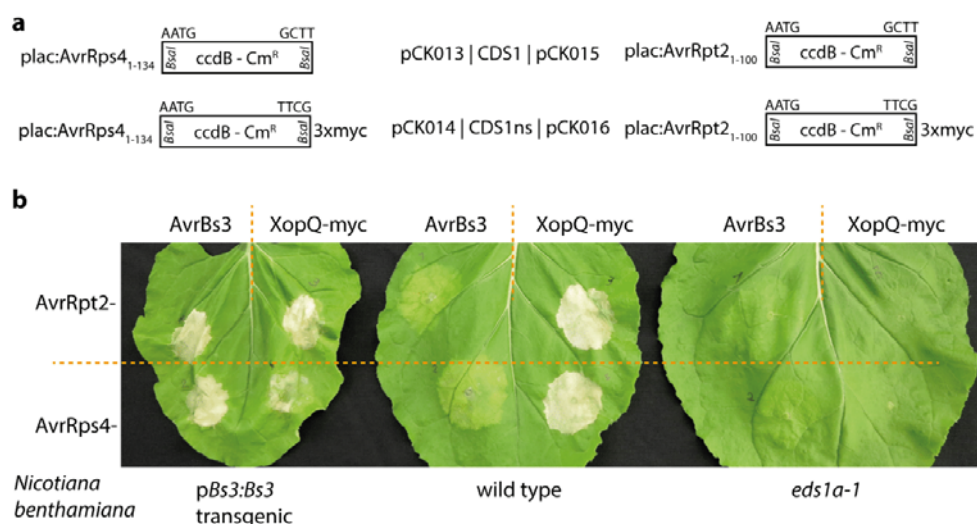


Fig 5. Bacterial type III-delivery of proteins into *N. benthamiana* cells. (a) Schematic depiction of vectors for type III-delivery of proteins. (b) Hypersensitive response induction assays for functional verification of vectors shown in (a). Either AvrBs3 or XopQ were cloned in vectors shown in (a), as indicated. Resulting constructs were mobilized into *Pseudomonas fluorescens*, strains inoculated at an $OD_{600} = 0.4$ on indicated *N. benthamiana* genotypes and symptoms documented 3 dpi.

<https://doi.org/10.1371/journal.pone.0197185.g005>

CDS1ns modules was generated, and ligation of CDS1ns modules results in a C-terminal 3xmyc epitope in final fusion proteins. The *Xanthomonas euvesicatoria* genes encoding the AvrBs3 and XopQ effectors were mobilized into CDS1 and CDS1ns vectors, respectively, for functional verification. AvrBs3 is a Transcription Activator-Like Effector (TALE), and AvrBs3-mediated induction of the *Bs3* resistance gene provokes a strong and rapid cell death reaction [40, 41]. XopQ is recognized in the non-host plant *Nbenth*, and induces a mild cell death reaction [42], which is abolished on an *eds1a-1* mutant *Nbenth* line [17]. Derivatives of the bacterial secretion vectors containing AvrBs3 or XopQ were mobilized into a *Pseudomonas fluorescence* strain carrying a chromosomal integration of the type III secretion system from *Pseudomonas syringae* ["EtHAN"; 19]. Resulting strains were infiltrated into wild type, *Bs3* transgenic, and *eds1a-1* mutant *Nbenth* plants (Fig 5B). AvrBs3-expressing strains provoked strong cell death on *Bs3* transgenic plants, as expected. This confirmed that both the AvrRps4- and AvrRpt2-derived secretion signals were functional. Similarly, XopQ-expressing strains provoked cell death reactions on wild type and *Bs3* plants, but not on *eds1a-1* plants (Fig 5B). Notably, cell death reactions upon infiltration of AvrRpt2-XopQ strains were substantially and reproducibly stronger than those of AvrRps4-XopQ strains (Fig 5B and S2 Fig), suggesting that either the AvrRpt2 signal might confer higher levels of protein translocation or the respective fusion protein might be more stable or active. This demonstrates the utility of testing several different signals for bacterial translocation of a protein of interest into plant cells.

An AvrRps4₁₋₁₃₆ protein fragment was previously used to mediate bacterial translocation of cargo proteins, and fusions were partially processed in plant cells due to AvrRps4 cleavage by a plant protease [37]. *In planta* processing of proteins expressed from AvrRps4₁₋₁₃₄ fusion vectors presented here was not tested. Irrespective of *in planta* processing, final proteins will carry non-native N-termini and might also lack e.g. post-translational modifications, potentially impairing protein functions. Thus, we do not consider the likelihood for functionality of delivered proteins to increase through cleavage of secretion signals. Indeed, high cell death-inducing activity of AvrRpt2-XopQ, for which no cleavage is expected, demonstrates that secretion signals may have minimal and different effects on cargo functionality. To possibly avoid negative effects of the fused translocation signal on the delivered cargo moiety, the two fragments are fused by a Gly-Gly-Ser linker in pCK13-16 vectors presented here.

Agrobacterium-mediated expression of XopQ in wild type *Nbenth* plants induces mild chlorosis to mild necrosis [42, 43]. In contrast, bacterial translocation of XopQ here induced a strong cell death response (Fig 5B). Although XopQ recognition negatively impacts on accumulation of proteins transiently expressed by *Agrobacterium* [44], the protein accumulates to high levels in plant tissues. Also, it is generally assumed that protein levels inside the plant cell obtained by *Agrobacterium*-mediated expression largely exceed those of bacterial translocation. Increased abundance of XopQ inside plant cells upon bacterial secretion is thus not a likely explanation for the phenotypic differences. As an alternative to protein dosage, we propose that a negative effect of *Agrobacterium* strain GV3101 on HR development [45] or other constraints during transient, *Agrobacterium*-based assays [46] might be at the basis of the observed differences in XopQ-induced HR development.

A Golden Gate-cloning vector for Tobacco Rattle Virus-induced gene silencing

Virus-induced gene silencing is an attractive and convenient method for the rapid knock-down of a gene of interest without the need for transformation or gene knockout. A Tobacco Rattle Virus (TRV)-based system is most commonly used, and functional in a number of different plant species including tomato and *Nbenth* [47, 48]. A fragment of the gene of interest is

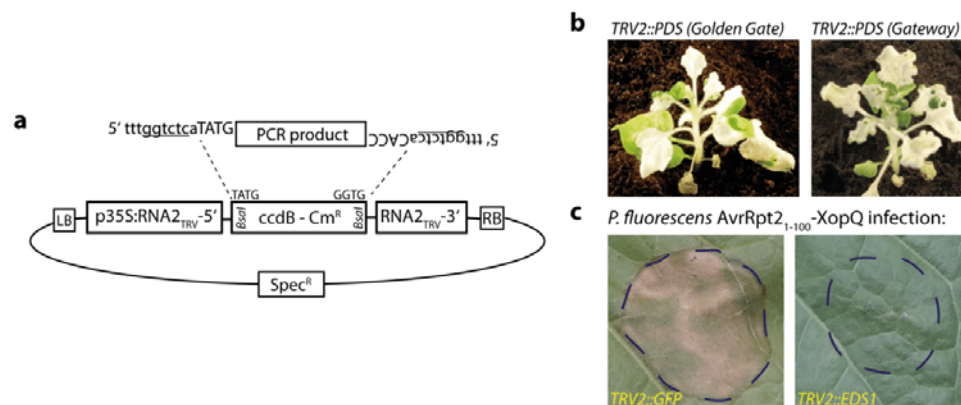


Fig 6. A Golden Gate cloning-compatible TRV2 vector for virus-induced gene silencing. (a) Schematic depiction of pTRV2-GG. The adaptors required for introduction of PCR products are indicated. (b) Functional verification of pTRV2-GG by silencing of *PDS*. pTRV2-GG and a commonly used Gateway-compatible TRV2 vector containing identical *PDS* fragments were compared for silencing efficiencies. (c) Silencing of *NbEDS1* using a pTRV2-GG derivative. *Pseudomonas fluorescens* bacteria expressing an AvrRpt2₁₋₁₀₀-XopQ fusion protein (OD₆₀₀ = 0.2) were inoculated 14 days after inoculation of pTRV strains, and plant reactions were documented 3 dpi.

<https://doi.org/10.1371/journal.pone.0197185.g006>

inserted into the RNA2 of the bipartite genome of TRV, and viral RNAs are reconstituted in the plant by expression from *Agrobacterium*-delivered T-DNAs. To facilitate rapid and cost-efficient cloning into a TRV RNA2 vector, an existing vector system [47] was adapted to Golden Gate cloning, and the cloning site was replaced by a *BsaI*-excised *ccdB* cassette as negative selection marker (Fig 6A). For functional verification, a fragment of the *Nbenth PDS* gene was inserted into a previously used, Gateway-compatible TRV2 vector and the newly generated Golden Gate-compatible vector. *PDS* encodes for Phytoene Desaturase essential for the production of carotenoids, and knock-down induces strong photo-bleaching of leaves. *Agrobacterium* strains carrying the respective TRV2 vectors were side-by-side co-inoculated with TRV1-containing strains into the lower leaves of *Nbenth* plants, and leaf bleaching documented 14 days later (Fig 6B). Both TRV vectors induced leaf bleaching to similar extents, confirming functionality of the Golden Gate-compatible derivative. The pTRV2-GG vector was also used for silencing of the *Nbenth EDS1* gene, and the XopQ-induced HR was consistently abolished on *EDS1* knock-down plants in several independent biological replicates (Fig 6C).

All vectors presented in this and previous sections are summarized in S2 Table. Annotated sequence files are provided in S1 File.

An extended set of plant parts, or phytobricks, for the Modular Cloning system

Level 0 modules, or phytobricks, are the building blocks and thus the limiting component for assemblies following the Modular Cloning grammar. As an extension to the previously released Plant Parts [13], we here provide ~ 80 additional Level 0 modules, summarized in S3 Table. These modules were experimentally verified as part of our ongoing projects if not indicated otherwise (S3 Table), and functional data is presented for a few selected modules. The provided new phytobricks comprise a variety of module types, e.g. modules for inducible gene expression (Fig 3), promoters for constitutive and tissue-specific gene expression in Arabidopsis (S3 Fig), transactivation (S4 Fig), additional fluorophores for (co-) localization and FRET analyses [49], signals for modifying subcellular localization, or epitope tags. In addition to the

Modular Cloning and Plant Parts toolkits, these modules will further enhance the versatility of this hierarchical DNA assembly system and facilitate its implementation in the plant research community. Most provided phytobricks (~ 60) are also directly compatible with GoldenBraid (S3 Table). Described vectors (S2 and S3 Tables) will be distributed as a collection via Addgene (Kit # 100000135), and selected vectors are also available directly through us. Annotated nucleotide sequences (GenBank format) are contained in S1 File.

Conclusions

Novel Golden Gate-based hierarchical cloning strategies, such as Modular Cloning, allow the rapid and cost-efficient assembly of simple transcriptional units or multigene constructs from basic building blocks (phytobricks). The underlying assembly standard, or molecular grammar, ensures efficient bioengineering by re-utilization and sharing of phytobricks. Accordingly, ~ 80 novel phytobricks are provided here to foster this idea of shared resources. Furthermore, we show how the Modular Cloning assembly standard may, by integrating just a few modules, also be used for inexpensive generation of Gateway entry clones, toggling between cloning systems, or standardized assembly of Gateway destination vectors. These alternative applications of Modular Cloning may be particularly helpful to avoid the eventually laborious domestication of sequences at early stages of a project, as e.g. a first screening of candidate genes, or to connect resources available for different cloning systems.

One major advantage of Gateway cloning consists in the availability of destination vectors for virtually any biological system or experimental setup. In contrast, Modular Cloning and GoldenBraid were so far mainly designated for the generation of plant expression/transformation constructs. Similar hierarchical DNA assembly systems were developed for e.g. yeast or prokaryotes [33, 34], but only some rely on the same fusion sites between building blocks for assembly [50]. Here, we present vectors for direct use of Modular Cloning Level 0 CDS modules in yeast interaction assays or for bacterial translocation into plant cells. Similarly, new vectors need to be adapted to this cloning standard in the future, e.g. for protein production in *Escherichia coli*. This will ensure seamless and efficient integration of synthetic biology standards and novel DNA assembly strategies, and will streamline laboratory workflows by reducing molecular cloning workloads.

Supporting information

S1 Fig. Primer design for cloning into Golden Gate-compatible entry vectors pJOG130/131. (a) The *ccdB* cassette contained in pJOG130 with *BsaI* restriction sites underlined is shown. The adaptors required for PCR amplification of suitable fragments are depicted below. Underlined sequences represent the 4 bp overhangs utilized for Golden Gate cloning, and Ns represent the gene specific portion of respective PCR primers. (b) as in (a), but for pJOG131. (PDF)

S2 Fig. Enhanced hypersensitive response induction by AvrRpt2-XopQ fusions. *Pseudomonas fluorescens* strains translocating either AvrRpt2₁₋₁₀₀-XopQ or AvrRps4₁₋₁₃₄-XopQ fusions were inoculated into wild type *N. benthamiana* plants, and symptom formation was documented 3 dpi. Four different bacterial densities, ranging from OD₆₀₀ = 0.4–0.05 were used, and were infiltrated descendingly in the indicated leaf sections. (PDF)

S3 Fig. Promoter fragments for tissue-specific gene expression in Arabidopsis leaves. Transgenic Arabidopsis plants expressing GUS-GFP under control of the indicated promoter fragments were generated, and three-week-old T₁ plants analyzed by confocal laser scanning

microscopy. Maximum intensity projections of z-stacks are shown. Three independent T₁ plants were analyzed for each construct with similar results.

(PDF)

S4 Fig. Utilization of TALEs for tightly regulated, high-level transactivation. (a) Schematic drawing of transactivation constructs used for transient expression. (b) Strong and specific transactivation of TALE-controlled genes. *Agrobacterium* strains containing constructs depicted in (a) were infiltrated into *N. benthamiana*. Leaf tissues were analyzed by confocal laser-scanning microscopy 3 dpi. (c) Immunoblot analysis of protein extracts prepared from leaf tissues analyzed in (b).

(PDF)

S1 File. Archive containing annotated sequence files (GenBank format) for all provided DNA modules.

(ZIP)

S1 Table. Oligonucleotides used in this study.

(PDF)

S2 Table. Modular Cloning-compatible vectors for specialized applications.

(PDF)

S3 Table. Modular Cloning Level 0 modules.

(PDF)

Acknowledgments

We thank Christopher Grefen for providing 2in1 FRET vectors, Annett Richter for providing a pZmUbi-containing plasmid, Tom Schreiber for providing AvrBs3 modules, Jens Boch for providing AvrRps4 and AvrRpt2-containing plasmids, all of which were used as PCR templates. Christine Wagner, Lennart Schwalgun and Samuel Grimm are acknowledged for technical assistance, and Jessica Erickson for assistance with CLSM imaging. We also thank Bianca Rosinsky for excellent plant growth conditions. Ulla Bonas is acknowledged for generous support.

Author Contributions

Conceptualization: Johannes Gantner, Johannes Stuttmann.

Funding acquisition: Johannes Stuttmann.

Investigation: Johannes Gantner, Jana Ordon, Theresa Ilse, Carola Kretschmer, Ramona Gruetzner, Christian Löffke, Katharina Bürstenbinder, Johannes Stuttmann.

Resources: Yasin Dagdas, Sylvestre Marillonnet, Johannes Stuttmann.

Supervision: Yasin Dagdas, Sylvestre Marillonnet, Johannes Stuttmann.

Writing – original draft: Johannes Stuttmann.

Writing – review & editing: Johannes Gantner, Jana Ordon, Theresa Ilse, Yasin Dagdas, Katharina Bürstenbinder, Sylvestre Marillonnet, Johannes Stuttmann.

References

1. Katzen F. Gateway(®) recombinational cloning: a biological operating system. *Expert Opin Drug Discov.* 2007; 2(4):571–89. <https://doi.org/10.1517/17460441.2.4.571> PMID: 23484762.

2. Nakagawa T, Kurose T, Hino T, Tanaka K, Kawamukai M, Niwa Y, et al. Development of series of gateway binary vectors, pGWBs, for realizing efficient construction of fusion genes for plant transformation. *J Biosci Bioeng*. 2007; 104(1):34–41. <https://doi.org/10.1263/jbb.104.34> PMID: 17697981.
3. Earley KW, Haag JR, Pontes O, Opper K, Juehne T, Song K, et al. Gateway-compatible vectors for plant functional genomics and proteomics. *Plant J*. 2006; 45(4):616–29. <https://doi.org/10.1111/j.1365-313X.2005.02617.x> PMID: 16441352.
4. Cheo DL, Titus SA, Byrd DR, Hartley JL, Temple GF, Brasch MA. Concerted assembly and cloning of multiple DNA segments using in vitro site-specific recombination: functional analysis of multi-segment expression clones. *Genome Research*. 2004; 14(10B):2111–20. <https://doi.org/10.1101/gr.2512204> PMID: 15489333.
5. Kirchmaier S, Lust K, Wittbrodt J. Golden GATEway cloning—a combinatorial approach to generate fusion and recombination constructs. *PLoS ONE*. 2013; 8(10):e76117. <https://doi.org/10.1371/journal.pone.0076117> PMID: 24116091.
6. Gibson DG, Young L, Chuang RY, Venter JC, Hutchison CA, 3rd, Smith HO. Enzymatic assembly of DNA molecules up to several hundred kilobases. *Nat Methods*. 2009; 6(5):343–5. <https://doi.org/10.1038/nmeth.1318> PMID: 19363495.
7. Sleight SC, Bartley BA, Lieviant JA, Sauro HM. In-Fusion BioBrick assembly and re-engineering. *Nucleic Acids Res*. 2010; 38(8):2624–36. <https://doi.org/10.1093/nar/gkq179> PMID: 20385581.
8. Zhu B, Cai G, Hall EO, Freeman GJ. In-fusion assembly: seamless engineering of multidomain fusion proteins, modular vectors, and mutations. *Biotechniques*. 2007; 43(3):354–9. PMID: 17907578.
9. Engler C, Kandzia R, Marillonnet S. A one pot, one step, precision cloning method with high throughput capability. *PLoS ONE*. 2008; 3(11):e3647. Epub 2008/11/06. <https://doi.org/10.1371/journal.pone.0003647> PMID: 18985154.
10. Lampropoulos A, Sutikovic Z, Wenzl C, Maegele I, Lohmann JU, Forner J. GreenGate—a novel, versatile, and efficient cloning system for plant transgenesis. *PLoS ONE*. 2013; 8(12):e83043. <https://doi.org/10.1371/journal.pone.0083043> PMID: 24376629.
11. Sarrion-Perdigones A, Falconi EE, Zandalinas SI, Juarez P, Fernandez-del-Carmen A, Granell A, et al. GoldenBraid: an iterative cloning system for standardized genetic assembly of reusable genetic modules. *PLoS ONE*. 2011; 6(7):e21622. <https://doi.org/10.1371/journal.pone.0021622> PMID: 21750718.
12. Weber E, Engler C, Gruetzner R, Werner S, Marillonnet S. A modular cloning system for standardized assembly of multigene constructs. *PLoS ONE*. 2011; 6(2):e16765. <https://doi.org/10.1371/journal.pone.0016765> PMID: 21364738.
13. Engler C, Youles M, Gruetzner R, Ehnert TM, Werner S, Jones JD, et al. A Golden Gate Modular Cloning Toolbox for Plants. *ACS Synthetic Biology*. 2014. <https://doi.org/10.1021/sb4001504> PMID: 24933124.
14. Sarrion-Perdigones A, Vazquez-Vilar M, Palaci J, Castelijnns B, Forment J, Ziarsolo P, et al. GoldenBraid 2.0: a comprehensive DNA assembly framework for plant synthetic biology. *Plant Phys*. 2013; 162(3):1618–31. <https://doi.org/10.1104/pp.113.217661> PMID: 23669743.
15. Vazquez-Vilar M, Quijano-Rubio A, Fernandez-Del-Carmen A, Sarrion-Perdigones A, Ochoa-Fernandez R, Ziarsolo P, et al. GB3.0: a platform for plant bio-design that connects functional DNA elements with associated biological data. *Nucleic Acids Res*. 2017; 45(4):2196–209. <https://doi.org/10.1093/nar/gkw1326> PMID: 28053117.
16. Patron NJ, Orzaez D, Marillonnet S, Warzecha H, Matthewman C, Youles M, et al. Standards for plant synthetic biology: a common syntax for exchange of DNA parts. *New Phytol*. 2015; 208(1):13–9. <https://doi.org/10.1111/nph.13532> PMID: 26171760.
17. Ordon J, Gantner J, Kemna J, Schwalgun L, Reschke M, Streubel J, et al. Generation of chromosomal deletions in dicotyledonous plants employing a user-friendly genome editing toolkit. *Plant J*. 2017; 89(1):155–68. <https://doi.org/10.1111/tpj.13319> PMID: 27579989.
18. Schreiber T, Sorgatz A, List F, Blüher D, Thieme S, Wilmanns M, et al. Refined requirements for protein regions important for activity of the TALE AvrBs3. *PLoS ONE*. 2015; 10(3):e0120214. <https://doi.org/10.1371/journal.pone.0120214> PMID: 25781334.
19. Thomas WJ, Thireault CA, Kimbrel JA, Chang JH. Recombineering and stable integration of the *Pseudomonas syringae* pv. *syringae* 61 *hrp/hrc* cluster into the genome of the soil bacterium *Pseudomonas fluorescens* Pf0-1. *Plant J*. 2009; 60(5):919–28. <https://doi.org/10.1111/j.1365-313X.2009.03998.x> WOS:000272188900014. PMID: 19682294
20. Gietz RD, Schiestl RH. Frozen competent yeast cells that can be transformed with high efficiency using the LiAc/SS carrier DNA/PEG method. *Nat Protoc*. 2007; 2(1):1–4. <https://doi.org/10.1038/nprot.2007.17> PMID: 17401330.

21. Kushnirov VV. Rapid and reliable protein extraction from yeast. *Yeast*. 2000; 16(9):857–60. [https://doi.org/10.1002/1097-0061\(20000630\)16:9<857::AID-YEA561>3.0.CO;2-B](https://doi.org/10.1002/1097-0061(20000630)16:9<857::AID-YEA561>3.0.CO;2-B) PMID: 10861908.
22. Szczesny R, Jordan M, Schramm C, Schulz S, Coge V, Bonas U, et al. Functional characterization of the Xcs and Xps type II secretion systems from the plant pathogenic bacterium *Xanthomonas campestris* pv *vesicatoria*. *New Phytol*. 2010; 187(4):983–1002. <https://doi.org/10.1111/j.1469-8137.2012.04210.x> PMID: 22738163. <https://doi.org/10.1111/j.1469-8137.2010.03312.x> PMID: 20524995.
23. Schulze S, Kay S, Büttner D, Egler M, Eschen-Lippold L, Hause G, et al. Analysis of new type III effectors from *Xanthomonas* uncovers XopB and XopS as suppressors of plant immunity. *New Phytol*. 2012; 195(4):894–911. <https://doi.org/10.1111/j.1469-8137.2012.04210.x> PMID: 22738163.
24. Grefen C, Donald N, Hashimoto K, Kudla J, Schumacher K, Blatt MR. A ubiquitin-10 promoter-based vector set for fluorescent protein tagging facilitates temporal stability and native protein distribution in transient and stable expression studies. *Plant J*. 2010; 64(2):355–65. <https://doi.org/10.1111/j.1365-3113.2010.04322.x> PMID: 20735773.
25. Schlucking K, Edel KH, Koster P, Drerup MM, Eckert C, Steinhilber L, et al. A new beta-estradiol-inducible vector set that facilitates easy construction and efficient expression of transgenes reveals CBL3-dependent cytoplasm to tonoplast translocation of CIPK5. *Mol Plant*. 2013; 6(6):1814–29. <https://doi.org/10.1093/mp/sst065> PMID: 23713076.
26. Shaner NC, Campbell RE, Steinbach PA, Giepmans BN, Palmer AE, Tsien RY. Improved monomeric red, orange and yellow fluorescent proteins derived from *Discosoma* sp. red fluorescent protein. *Nature Biotech*. 2004; 22(12):1567–72. <https://doi.org/10.1038/nbt1037> PMID: 15558047.
27. Aoyama T, Chua NH. A glucocorticoid-mediated transcriptional induction system in transgenic plants. *Plant J*. 1997; 11(3):605–12. PMID: 9107046.
28. Picard D. Steroid-binding domains for regulating the functions of heterologous proteins in cis. *Trends Cell Biol*. 1993; 3(8):278–80. PMID: 14731747.
29. Shaner NC, Lin MZ, McKeown MR, Steinbach PA, Hazelwood KL, Davidson MW, et al. Improving the photostability of bright monomeric orange and red fluorescent proteins. *Nat Methods*. 2008; 5(6):545–51. <https://doi.org/10.1038/nmeth.1209> PMID: 18454154.
30. Bürstenbinder K, Moller B, Plötner R, Stamm G, Hause G, Mitra D, et al. The IQD Family of Calmodulin-Binding Proteins Links Calcium Signaling to Microtubules, Membrane Subdomains, and the Nucleus. *Plant Phys*. 2017; 173(3):1692–708. <https://doi.org/10.1104/pp.16.01743> PMID: 28115582.
31. Hinsch M, Staskawicz B. Identification of a new *Arabidopsis* disease resistance locus, *RPS4*, and cloning of the corresponding avirulence gene, *avrRps4*, from *Pseudomonas syringae* pv. *psis*. *Mol Plant Microbe Interact*. 1996; 9(1):55–61. PMID: 8589423.
32. Sohn KH, Zhang Y, Jones JDG. The *Pseudomonas syringae* effector protein, AvrRPS4, requires *in planta* processing and the KRKY domain to function. *Plant J*. 2009; 57(6):1079–91. <https://doi.org/10.1111/j.1365-3113.2008.03751.x> WOS:000264088100010. PMID: 19054367
33. Lee ME, DeLoache WC, Cervantes B, Dueber JE. A Highly Characterized Yeast Toolkit for Modular, Multipart Assembly. *ACS Synthetic Biology*. 2015; 4(9):975–86. <https://doi.org/10.1021/sb500366v> PMID: 25871405.
34. Moore SJ, Lai HE, Kelwick RJ, Chee SM, Bell DJ, Polizzi KM, et al. EcoFlex: A Multifunctional MoClo Kit for *E. coli* Synthetic Biology. *ACS Synthetic Biology*. 2016; 5(10):1059–69. <https://doi.org/10.1021/acssynbio.6b00031> PMID: 27096716.
35. Wagner S, Stuttmann J, Rietz S, Guerois R, Brunstein E, Bautor J, et al. Structural basis for signaling by exclusive EDS1 heteromeric complexes with SAG101 or PAD4 in plant innate immunity. *Cell Host Microbe*. 2013; 14(6):619–30. <https://doi.org/10.1016/j.chom.2013.11.006> PMID: 24331460.
36. Büttner D. Behind the lines—actions of bacterial type III effector proteins in plant cells. *FEMS Microbiol Rev*. 2016. <https://doi.org/10.1093/femsre/fuw026> PMID: 27526699.
37. Sohn KH, Lei R, Nemri A, Jones JD. The downy mildew effector proteins ATR1 and ATR13 promote disease susceptibility in *Arabidopsis thaliana*. *Plant Cell*. 2007; 19(12):4077–90. <https://doi.org/10.1105/tpc.107.054262> PMID: 18165328.
38. Fabro G, Steinbrenner J, Coates M, Ishaque N, Baxter L, Studholme DJ, et al. Multiple candidate effectors from the oomycete pathogen *Hyaloperonospora arabidopsidis* suppress host plant immunity. *PLoS Pathog*. 2011; 7(11):e1002348. <https://doi.org/10.1371/journal.ppat.1002348> PMID: 22072967.
39. Innes RW, Bent AF, Kunkel BN, Bisgrove SR, Staskawicz BJ. Molecular analysis of avirulence gene *avrRpt2* and identification of a putative regulatory sequence common to all known *Pseudomonas syringae* avirulence genes. *J Bacteriol*. 1993; 175(15):4859–69. PMID: 8335641.
40. Römer P, Hahn S, Jordan T, Strauss T, Bonas U, Lahaye T. Plant pathogen recognition mediated by promoter activation of the pepper *Bs3* resistance gene. *Science*. 2007; 318(5850):645–8. <https://doi.org/10.1126/science.1144958> PMID: 17962564.

41. Boch J, Bonas U. Xanthomonas AvrBs3 family-type III effectors: discovery and function. *Annu Rev Phytopathol.* 2010; 48:419–36. Epub 2009/04/30. <https://doi.org/10.1146/annurev-phyto-080508-081936> PMID: 19400638.
42. Adlung N, Prochaska H, Thieme S, Banik A, Blüher D, John P, et al. Non-host Resistance Induced by the Xanthomonas Effector XopQ Is Widespread within the Genus *Nicotiana* and Functionally Depends on EDS1. *Front Plant Sci.* 2016; 7:1796. <https://doi.org/10.3389/fpls.2016.01796> PMID: 27965697.
43. Schultink A, Qi T, Lee A, Steinbrenner AD, Staskawicz B. Roq1 mediates recognition of the Xanthomonas and Pseudomonas effector proteins XopQ and HopQ1. *Plant J.* 2017. <https://doi.org/10.1111/tpj.13715> PMID: 28891100.
44. Adlung N, Bonas U. Dissecting virulence function from recognition: cell death suppression in *Nicotiana benthamiana* by XopQ/HopQ1-family effectors relies on EDS1-dependent immunity. *Plant J.* 2017; 91(3):430–42. <https://doi.org/10.1111/tpj.13578> PMID: 28423458.
45. Li W, Cao JY, Xu YP, Cai XZ. Artificial *Agrobacterium tumefaciens* strains exhibit diverse mechanisms to repress *Xanthomonas oryzae* pv. *oryzae*-induced hypersensitive response and non-host resistance in *Nicotiana benthamiana*. *Mol Plant Pathol.* 2017; 18(4):489–502. <https://doi.org/10.1111/mpp.12411> PMID: 27061769.
46. Erickson JL, Ziegler J, Guevara D, Abel S, Klosgen RB, Mathur J, et al. Agrobacterium-derived cytokinin influences plastid morphology and starch accumulation in *Nicotiana benthamiana* during transient assays. *BMC Plant Biology.* 2014; 14:127. <https://doi.org/10.1186/1471-2229-14-127> PMID: 24886417.
47. Liu Y, Schiff M, Dinesh-Kumar SP. Virus-induced gene silencing in tomato. *Plant J.* 2002; 31(6):777–86. PMID: 12220268.
48. Ratcliff F, Martin-Hernandez AM, Baulcombe DC. Tobacco rattle virus as a vector for analysis of gene function by silencing. *Plant J.* 2001; 25(2):237–45. PMID: 11169199.
49. Hecker A, Wallmeroth N, Peter S, Blatt MR, Harter K, Grefen C. Binary 2in1 Vectors Improve in Planta (Co)localization and Dynamic Protein Interaction Studies. *Plant Phys.* 2015; 168(3):776–87. <https://doi.org/10.1104/pp.15.00533> PMID: 25971551.
50. Perez-Gonzalez A, Kniewel R, Veldhuizen M, Verma HK, Navarro-Rodriguez M, Rubio LM, et al. Adaptation of the GoldenBraid modular cloning system and creation of a toolkit for the expression of heterologous proteins in yeast mitochondria. *BMC Biotechnol.* 2017; 17(1):80. <https://doi.org/10.1186/s12896-017-0393-y> PMID: 29132331.

1.2.2. Supplemental material to publication Gantner *et al.*, 2018

- Supplemental Figures S1 – S4 are shown below
- Additional files Tables S1 –S3 are available online:
(<https://journals.plos.org/plosone/article?id=10.1371/journal.pone.0197185>)

Figure S1 Gantner et al.

a pJOG130

```

--GCGGCCGCAATGTGAGACC---cat--ccdB---GGTCTCAGCTTGGCGCGCC--
--CGCCGGCGTTACACTCTGG---CCAGAGTCGAACCCGCGCGG--
          BsaI
          BsaI

```

Primer design (for cloning of CDS from ATG to STOP):

Forward: 5' tttggtctcaATG (N)₁₆₋₂₀ 3'Reverse: 5' tttggtctcaaaagcCTA (N)₁₆₋₂₀ 3'
 TTA
 TCA**b** pJOG131

```

--GCGGCCGCAATGTGAGACC---cat--ccdB---GGTCTCATTCGGGGCGCGCC--
--CGCCGGCGTTACACTCTGG---CCAGAGTAAGCCCCGCGCGG--
          BsaI
          BsaI

```

Primer design (for cloning of CDS from ATG without STOP):

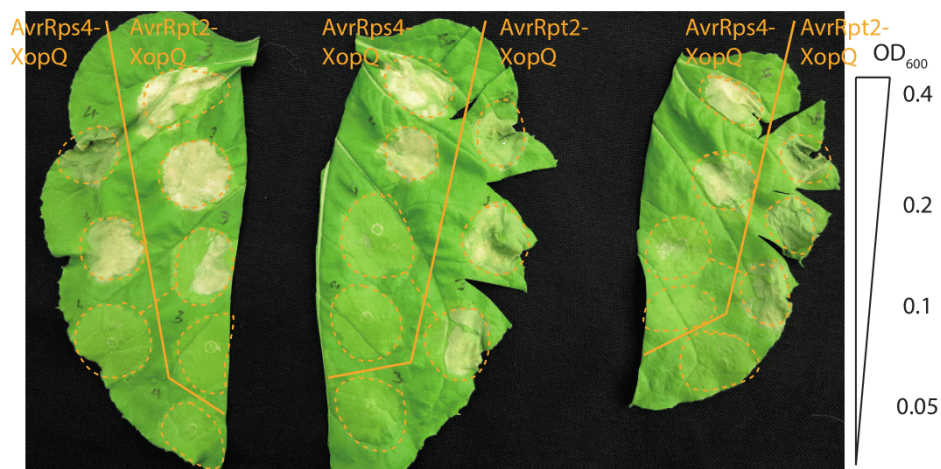
Forward: 5' tttggtctcaATG (N)₁₆₋₂₀ 3'Reverse: 5' tttggtctcacgaagc (N)₁₉₋₂₃ 3'
 | S | A |

Supplemental Figure S1: Primer design for cloning into Golden Gate-compatible entry vectors pJOG130/131.

(a) The *ccdB* cassette contained in pJOG130 with *BsaI* restriction sites underlined is shown. The adaptors required for PCR amplification of suitable fragments are depicted below. Underlined sequences represent the 4 bp overhangs utilized for Golden Gate cloning, and Ns represent the gene specific portion of respective PCR primers.

(b) as in (a), but for pJOG131.

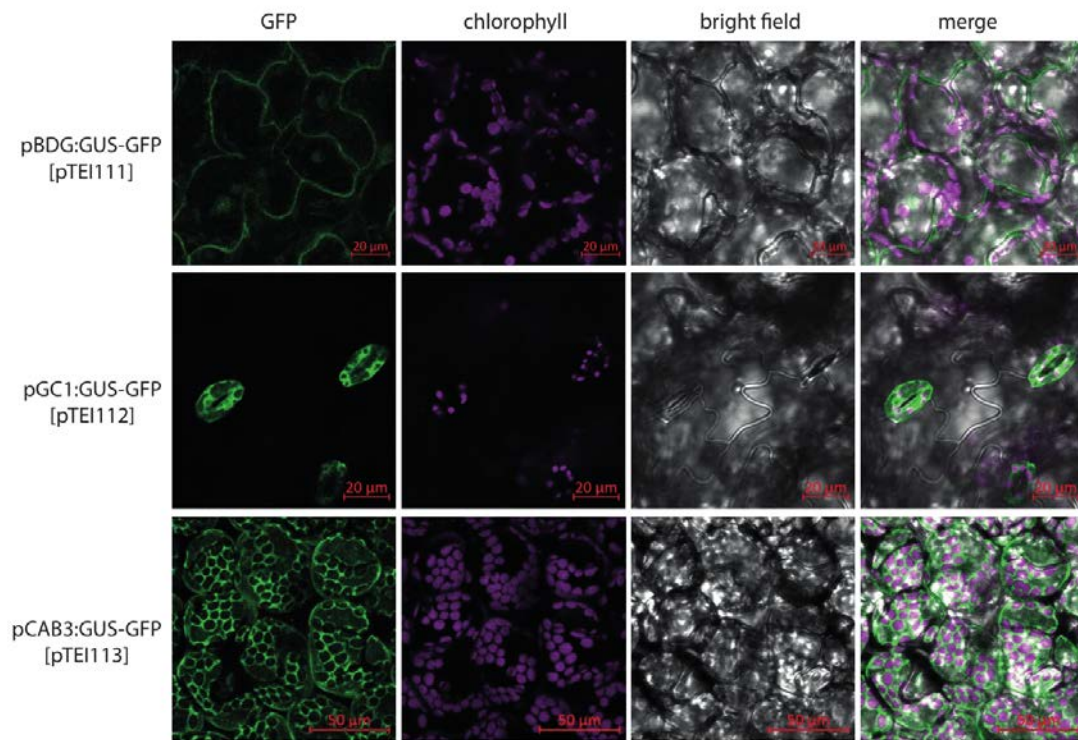
Figure S2 Gantner et al.



Supplemental Figure S2: Enhanced hypersensitive response induction by AvrRpt2-XopQ fusions.

Pseudomonas fluorescens strains translocating either AvrRpt2₁₋₁₀₀-XopQ or AvrRps4₁₋₁₃₄-XopQ fusions were inoculated into wild type *N. benthamiana* plants, and symptom formation was documented 3 dpi. Four different bacterial densities, ranging from OD₆₀₀=0.4-0.05 were used, and were infiltrated descendingly in the indicated leaf sections.

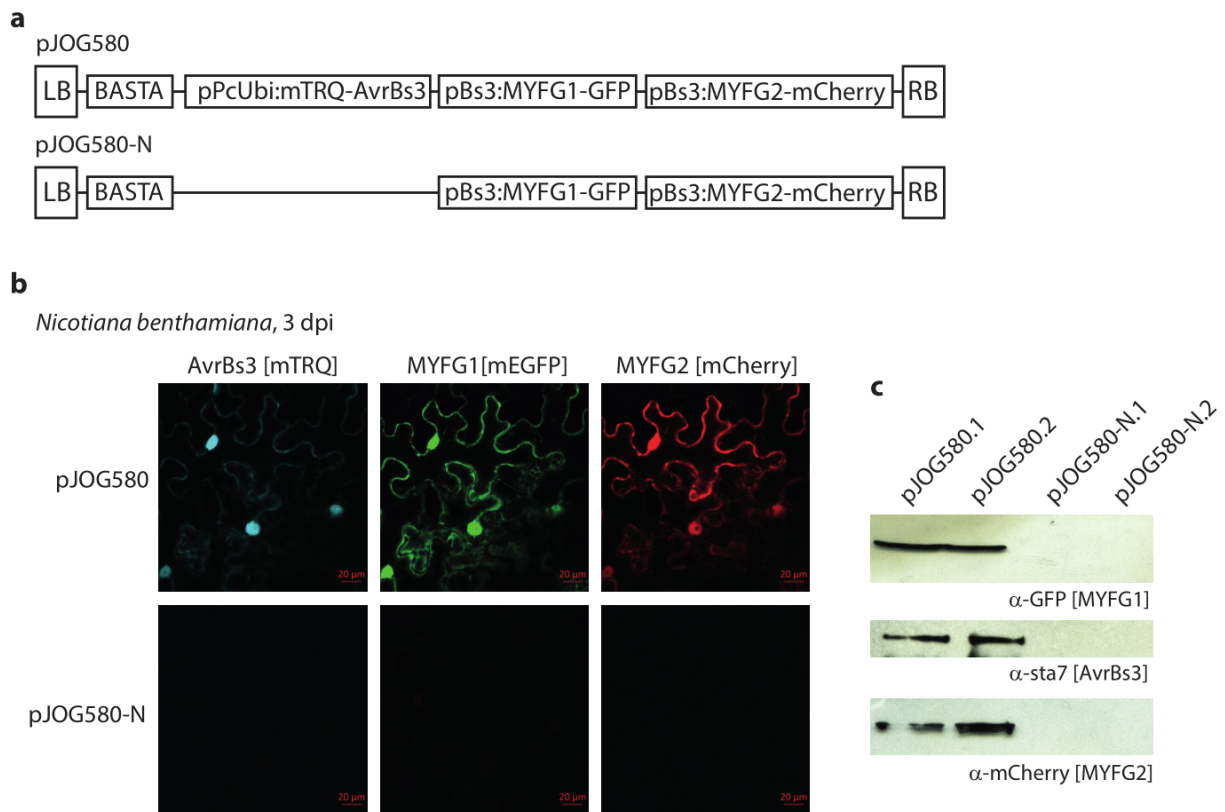
Supplemental Figure S3 Gantner et al.



Supplemental Figure S3: Promoter fragments for tissue-specific gene expression in Arabidopsis leaves

Transgenic Arabidopsis plants expressing GUS-GFP under control of the indicated promoter fragments were generated, and three-week-old T_1 plants analyzed by confocal laser scanning microscopy. Maximum intensity projections of z-stacks are shown. Three independent T_1 plants were analyzed for each construct with similar results.

Supplemental Figure S4 Gantner et al.



Supplemental Figure S4: Utilization of TALEs for tightly regulated, high-level transactivation

(a) Schematic drawing of transactivation constructs used for transient expression.

(b) Strong and specific transactivation of TALE-controlled genes. *Agrobacterium* strains containing constructs depicted in (a) were infiltrated into *N. benthamiana*. Leaf tissues were analyzed by confocal laser-scanning microscopy 3 dpi.

(c) Immunoblot analysis of protein extracts prepared from leaf tissues analyzed in (b).

1.2.3. Summary of publication Gantner *et al.*, 2018

Since the early days of molecular cloning, a constant effort was made to design new strategies to simplify the daily work of wet lab scientists. In the last two decades, mainly classical ligation of restriction fragments or PCR products into a vector of interest co-existed with the Gateway system as cloning procedures. However, there is one striking disadvantage in using these strategies: It is only possible to mobilize a single DNA fragment into a new sequence context. A few years ago, GG cloning was invented, a new cloning strategy relying on the use of Type IIs REs (Engler *et al.*, 2008). These enzymes generate 4 bp sticky ends next to their recognition site, which enable to design user-defined overhangs, and to ligate different fragments in a defined order. Cloning systems, like MoClo (Weber *et al.*, 2011) or GoldenBraid (Sarrion-Perdigones *et al.*, 2011) were invented, which define different hierarchical levels. The “library” level 0 defines all different genetic elements which are needed to construct a single expression cassette. These parts, called phytobricks, can be shared with the whole MoClo/GoldenBraid community, if the correct 4 bp sticky ends are respected, representing an immense advantage for end users.

However, the sparse amount of Phytobricks limits the applications of the two existing GG-based toolkits for plants and the destination vectors are made for T-DNA constructs, enabling for expression only in plants. It was not possible to re-use Phytobricks (mostly CDSs (coding sequences)) in Yeast-two-Hybrid applications or to toggle between the GG standards and other cloning strategies like Gateway.

This publication describes 96 vectors within the Modular Cloning standard. Most of the plasmids are Phytobricks, i.e. promoter elements (inducible/tissue specific), fluorophores, epitope tags, effectors, transcription factors etc. Moreover, we offered a solution to switch from Gateway to Modular Cloning by the ability to shuttle CDS modules directly to a Gateway-entry vector and to generate Gateway entry clones from PCR products. The hierarchical assembly of Gateway destination vectors is also possible. Additionally, we provided a set of vectors which will help to connect the Modular Cloning system, originally generated for applications only in plants, with Y2H and bacterial expression. With this publication, we aimed to share our resources with the plant community to increase the possibilities of Modular Cloning by an enhanced set of Phytobricks, the re-usability of coding sequences for bacterial and yeast expression as well as a link between Modular Cloning and Gateway.

Part II – Toolkits for plant genome editing

Introduction

2.1. Adaptive immunity of microbes – the CRISPR-Cas system

Prokaryotes are present in the whole environment and dominate many natural habitats including our gastrointestinal system as well as inhospitable milieus. They are under constant pressure to counteract invading viruses. The genetically diverse and rapidly altering viral population exceeds bacterial numbers by an order of magnitude (Fineran&Charpentier, 2012). It is not surprising that prokaryotes evolved ways to defend against invaders, including an adaptive immune system encoded at CRISPR (Clustered regulatory interspaced short palindromic repeats) loci and Cas (CRISPR-associated) genes. Respective gene products are together able to recognize and incoming, foreign genetic elements, to distinguish these from their own genome and to inactivate them (Fineran&Charpentier, 2012).

Cas immunization depends on the uptake of DNA from invading genetic elements like plasmids or viruses, and subsequent integration of parts of this foreign DNA into CRISPR loci. CRISPR loci commonly consist of short, partially palindromic DNA repeats that occur at regular intervals (CRISPR repeats), as well as stretches of variable sequence segments called spacers. The CRISPR spacers are sequences derived from invading DNA elements with a length of 23-55 nucleotides, which function as a molecular memory or database of previous invasion events (Jansen *et al.*, 2002; Bolotin *et al.*, 2005; Francisco JM Mojica *et al.*, 2005; Makarova *et al.*, 2006). One CRISPR array can possess > 500 repeats, but more commonly encompasses less than 50. Within the CRISPR array, each repeat is followed by a spacer segment (Horvath&Barrangou, 2010). CRISPR loci are flanked by *cas* genes which encode for a large and heterogeneous protein family carrying functional domains of nucleases, helicases, polymerases, and polynucleotide binding proteins, demonstrating that multiple biochemical functions are utilized in CRISPR-mediated immunity (Barrangou&Marraffini, 2014).

The CRISPR-Cas system functions in four different steps: adaptation, infection, interference, and targeting (Fineran&Charpentier, 2012). During adaptation, short fragments of the invading DNA (termed pre-spacers) are integrated into the CRISPR array. In the following infection-step, the complete repeat-spacer array is transcribed as a pre-crRNA (precursor CRISPR RNA). This pre-crRNA has to undergo one more step of maturation and will be processed into small interfering RNA segments called crRNAs. A crRNA consists of one

repeat and a spacer sequence, which functions as guide RNA for a nuclease. In the following phase of interference, a complex is formed with the Cas protein. In the last step, targeting of invading genetic elements takes place, the crRNA guides the Cas nuclease for specific cleavage of complementary sequences. In general, targeting is dependent on presence of a short DNA sequence known as the PAM (protospacer-adjacent-motif) at target sites. The interaction between the interference complex and the target is typically initiated by binding to the PAM, and the nuclease induces a DSB (double-strand break) in order to inactivate the foreign genetic elements (Fineran&Charpentier, 2012).

Analysis of the conserved Cas proteins led to a classification of CRISPR-Cas systems into two classes, five types and 16 different subtypes, based on *cas* gene content, *cas* operon architecture, and the specification of the corresponding proteins that underlie the four different stages of CRISPR-Cas activity. Class I represents multi-subunit crRNA-Cas complexes, whereas in class II, all functions of the crRNA-Cas complex are carried out by a single protein, such as the most famous *SpCas9*. *SpCas9*, derived from *Streptococcus pyogenes* (*Sp*), is a multi-domain protein contributing to adaptation as well as targeting and cleavage of DNA. Additionally, *SpCas9* requires a tracrRNA (transactivating CRISPR RNA) besides the crRNA to activate and guide the Cas9 nuclease (Makarova *et al.*, 2015).

CRISPR arrays were first identified in 1987 in *Escherichia coli*, but the biological function started to be unraveled only in 2005, when it was shown that the spacers are homologous to invading nucleic acids (Ishino *et al.*, 1987; Bolotin *et al.*, 2005; F. J. Mojica *et al.*, 2005; Pourcel *et al.*, 2005). In 2012, the idea was born to use the type II CRISPR-Cas9 system of *Sp* as a genome editing tool (Jinek *et al.*, 2012). It was shown that the target specificity of the *SpCas9* nuclease could be reprogrammed by simply changing 20 nucleotides of the spacer in the crRNA. Furthermore, it was shown that it is possible to fuse the crRNA (determining target specificity) with the tracrRNA (tethering the crRNA-tracrRNA complex to the Cas9 nuclease to form the functional ribonucleoprotein complex) to a chimeric sgRNA (single guide RNA). This finding results in a reduction from a three-component to a two-component system (Jinek *et al.*, 2012). Shortly afterwards, it was proven that the system is transferrable to eukaryotes to specifically target and introduce DNA-DSBs (Cho *et al.*, 2013; Cong *et al.*, 2013; Hwang *et al.*, 2013; Jinek *et al.*, 2013; Mali *et al.*, 2013). Furthermore it was discovered that multiple sgRNAs with different target-specificities could be combined in “multiplexing” applications to target more than one locus simultaneously (Cong *et al.*, 2013; Mali *et al.*, 2013).

A DSB in the genome of eukaryotes is normally repaired by NHEJ (non-homologous end-joining), which is a very fast DNA repair machinery. But NHEJ often produces small mutations which, in most cases, result in a frame shift and the disruption of the respective

gene, if the mutation occurs in a protein coding sequence. A second more accurate DNA-repair mechanism is HDR (homology-directed repair). However, HDR needs a homologous repair template in immediate proximity, which is often not available. HDR can be used to integrate new DNA segments with CRISPR/Cas9 by simultaneously delivering a nuclease provoking a DSB at a desired position, and a “repair” template with homology arms, including a DNA stretch or sequence alteration which should be integrated at the DSB (Bortesi&Fischer, 2015).

The sophisticated CRISPR/Cas-machinery, which functions in almost any organism, was quickly further developed. In 2015, genome editing facilitated by RGNs (RNA-guided nucleases) was termed the breakthrough of the year by *Science Magazine*. Ever since, there are many publications on mammals, animals as well as plants, and so called multiplexing toolkits have been established for many different organisms or biological systems. However, genome editing initiated *via* Cas9-based RGNs was mostly used for the induction of small deletions in plants and therefore it is complicated to identify or distinguish edited plants from wild-type individuals (Bortesi&Fischer, 2015). RGNs in plants were mostly expressed *via* a T-DNA, delivered by *Agrobacterium tumefaciens*. This delivery system requires a single T-DNA to encode multiple parts (i.e. transformation marker(s), Cas9-nuclease, and sgRNA(s)) (Ordon *et al.*, 2017), which may cause problems to potential users and necessitates well-designed cloning strategies.

Aims, achievements and conclusions

Genome editing mediated by RGNs was a new technology at the beginning of this thesis. Tools for plant genome editing were scarce or not existing for multiplexing applications. Therefore, we set out to create our own tools to use this technology for research with a new model plant (*Nicotiana benthamiana*). We created a simple and user-friendly toolkit, which allows the generation of multiplexing constructs containing up to eight sgRNAs with minimal effort and high fidelity (Ordon *et al.*, 2017). The toolkit is based on the Modular Cloning system (Part I), and both, the entire toolkit and single components were distributed to many different researchers in the plant community. We used this toolkit to generate numerous mutant lines, many of which were essential for further work (Part III).

In addition, we made an effort to further improve our vectors to overcome shortcomings of the first toolkit, e.g., low efficiency or difficulties to select genome-edited, but non-transgenic individuals in later generations. A first part of these optimization efforts was published

((Ordon *et al.*, 2019) without my contribution) and a further manuscript on which I will also be co-author is in preparation.

2.2. Generation of chromosomal deletions in dicotyledonous plants employing a user-friendly genome editing kit

2.2.1. Publication Ordon *et al.*, 2016

the plant journal

SEB
Society for
Experimental Biology

The Plant Journal (2016)

doi: 10.1111/tpj.13319

TECHNICAL ADVANCE

Generation of chromosomal deletions in dicotyledonous plants employing a user-friendly genome editing toolkit

Jana Ordon¹, Johannes Gantner¹, Jan Kemna¹, Lennart Schwalgun¹, Maik Reschke^{1,†}, Jana Streubel^{1,†}, Jens Boch^{1,†} and Johannes Stüttmann^{1,*}

¹Department of Genetics, Martin Luther University Halle (Saale), Weinbergweg 10, 06120 Halle, Germany

Received 5 July 2016; revised 23 August 2016; accepted 26 August 2016.

*For correspondence (e-mail johannes.stuttmann@genetik.uni-halle.de).

[†]Present address: Department of Plant Biotechnology, Leibniz University Hannover, Herrenhäuser Str. 2, 30419 Hannover, Germany.

SUMMARY

Genome editing facilitated by Cas9-based RNA-guided nucleases (RGNs) is becoming an increasingly important and popular technique for reverse genetics in both model and non-model species. So far, RGNs were mainly applied for the induction of point mutations, and one major challenge consists in the detection of genome-edited individuals from a mutagenized population. Also, point mutations are not appropriate for functional dissection of non-coding DNA. Here, the multiplexing capacity of a newly developed genome editing toolkit was exploited for the induction of inheritable chromosomal deletions at six different loci in *Nicotiana benthamiana* and *Arabidopsis*. In both species, the preferential formation of small deletions was observed, suggesting reduced efficiency with increasing deletion size. Importantly, small deletions (<100 bp) were detected at high frequencies in *N. benthamiana* T₀ and *Arabidopsis* T₂ populations. Thus, targeting of small deletions by paired nucleases represents a simple approach for the generation of mutant alleles segregating as size polymorphisms in subsequent generations. Phenotypically selected deletions of up to 120 kb occurred at low frequencies in *Arabidopsis*, suggesting larger population sizes for the discovery of valuable alleles from addressing gene clusters or non-coding DNA for deletion by programmable nucleases.

Keywords: CRISPR/Cas, chromosomal deletion, *Nicotiana benthamiana*, *Arabidopsis thaliana*, plant immunity, EDS1, technical advance.

INTRODUCTION

Genome editing refers to the targeted modification of defined positions within a genome using site-specific nucleases. Nuclease-generated double-strand breaks are repaired by non-homologous end-joining (NHEJ) or, in the presence of a repair template, by homology-directed repair (HDR). Error-prone NHEJ commonly creates small genomic deletions or insertions leading to the potential inactivation of a gene product (knockout), while HDR can mediate the introduction of specific sequences (knock-in). Zinc finger nucleases were initially used as programmable nucleases for genome editing applications (Kim *et al.*, 1996; Townsend *et al.*, 2009). A first genome editing revolution was then triggered by the invention of TALENs (Christian *et al.*, 2010). TALENs are fusions of the *FokI* nuclease domain to a DNA-binding domain derived from a TAL effector of plant pathogenic *Xanthomonas* bacteria. This DNA-binding

domain consists of 34-amino acid repeat modules, which bind to DNA in a one repeat-one nucleotide manner. Nucleotide-specificity is conferred by two hypervariable amino acids at positions 12 and 13 in each repeat (Boch *et al.*, 2009; Boch and Bonas, 2010). Due to the catalytic properties of *FokI*, two TALENs binding a target sequence in appropriate spacing have to be co-expressed to allow dimerization of the nuclease and to generate DSBs (Christian *et al.*, 2010). TALENs binding virtually any sequence with high specificity can be constructed with relative ease (e.g. Geissler *et al.*, 2011; Weber *et al.*, 2011b; Liang *et al.*, 2014), and TALENs were used for modification of both model and crop plant genomes (e.g. Christian *et al.*, 2013; Sosso *et al.*, 2015; Clasen *et al.*, 2016).

Genome editing was further simplified by harnessing RNA-guided nucleases (RGNs) derived from bacterial

© 2016 The Authors.

The Plant Journal published by Society for Experimental Biology and John Wiley & Sons Ltd.

This is an open access article under the terms of the Creative Commons Attribution-NonCommercial-NoDerivs License, which permits use and distribution in any medium, provided the original work is properly cited, the use is non-commercial and no modifications or adaptations are made.

1

2 Jana Ordon et al.

CRISPR/Cas systems for induction of DSBs (for review, see Wiedenheft *et al.*, 2012; Doudna and Charpentier, 2014). The Cas9 (CRISPR-associated Protein 9) from *Streptococcus pyogenes* is the most commonly used nuclease, and is in the natural system directed to target sites by a chimeric RNA consisting of crRNA and tracrRNA (Jinek *et al.*, 2012). This chimeric RNA species can be collapsed into one molecule, the single-guide RNA (sgRNA; Jinek *et al.*, 2012). Cas9 target specificity can thus be reprogrammed by co-expression of different sgRNAs. The sgRNA directs Cas9 to target sites by complementary base-pairing, but target sites have to be flanked by a protospacer-adjacent motif (PAM; NGG for *SpCas9*) in order to be cleaved.

The Cas9 system has been adapted for use in many different plants systems ranging from algae and mosses to monocotyledonous and dicotyledonous plants (Jiang *et al.*, 2014a; Belhaj *et al.*, 2015; Bortesi and Fischer, 2015). In most cases, Cas9-based nucleases are expressed in *planta* from an *Agrobacterium*-delivered T-DNA. This necessitates the construction of complex T-DNAs comprising multiple genes, which may represent a first challenge for potential users. Another challenge consists in the actual selection of mutants from a population of Cas9 and sgRNA (s)-expressing plants. So far, Cas9 was in plants mainly used for induction of point mutations at exemplary loci with associated mutant phenotypes (for review, see Belhaj *et al.*, 2015; Bortesi and Fischer, 2015). Here, a toolkit for extremely simple and efficient assembly of RGN-coding constructs was developed and employed for the generation of chromosomal deletions. Deletions of different sizes were induced at six independent loci in *Nicotiana benthamiana* and *Arabidopsis*, and mutant alleles were isolated either by associated phenotype or PCR screening. Our results show that large deletions up to 120 kb are feasible, but occur at low frequencies. In contrast, small deletions (<100 bp) can be induced with relatively high frequencies in both *Arabidopsis* and *N. benthamiana*, and provide a straightforward workflow for mutant identification.

RESULTS

Development of a streamlined toolkit for genome editing in dicotyledonous plants

The modular cloning principle and toolbox recently provided to the plant community as a synthetic biology 'starter kit' are at the basis of Dicot Genome Editting (pDGE) vectors developed here (Weber *et al.*, 2011a; Engler *et al.*, 2014). Different types of vectors were generated for streamlined assembly of RGN-encoding constructs (Figure 1a and Table S1). The *Agrobacterium*-mediated transformation-compatible 'one step, one nuclease' vectors pDGE62–65 are designated for expression of a single sgRNA together with Cas9 and plant selectable marker

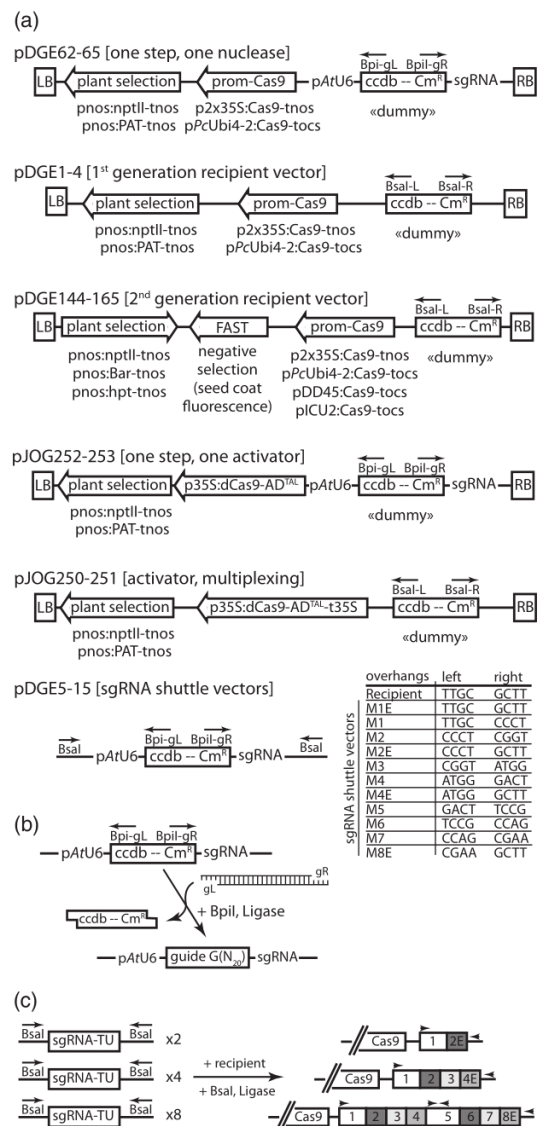


Figure 1. A toolkit for the simple and efficient assembly of RGN-coding constructs.

(a) Schemes of different types of pDGE vectors. Elements are not drawn to scale. sgRNA shuttle vectors differ in overhangs generated by restriction at flanking *Bsa*I sites, as shown in a table next to the vector scheme.

(b) Principle for generating sgRNA TUs in either sgRNA shuttle vectors or one step, one nuclease vectors.

(c) Assembly of sgRNA TU arrays from loaded derivatives of shuttle vectors. Arrows in sgRNA arrays mark unique sequences, which can be used for final sequence verification.

(BASTA or kanamycin resistance). Assembly of an sgRNA transcriptional unit (TU) in pDGE62–65 is achieved in a single step by exchanging a *ccdB* negative selection cassette for two hybridized oligonucleotides in a simultaneous

restriction/ligation reaction using *Bp*1 (*Bbs*I; Figure 1b). 'Recipient' vectors have a similar architecture as pDGE62–65, but are designated for multiplexing applications (Figure 1a). In a two-step assembly, sgRNA TUs are first assembled in 'sgRNA shuttle vectors,' and subsequently mobilized into recipient vectors. The generation of an sgRNA TU in shuttle vectors is carried out as described for the one step, one nuclease vectors (Figure 1b). Resulting sgRNA TUs are flanked by *Bsa*I restriction sites, and generated overhangs vary between shuttle vectors (Figure 1a). Arrays of two, four or eight sgRNA TUs can be assembled in any recipient plasmid by combining it with compatible derivatives of sgRNA shuttle vectors in a simultaneous restriction/ligation reaction using *Bsa*I (*Eco*31I, Figure 1c). For simplicity, shuttle vectors were named M1–M8 (for modules 1–8) according to their position in an sgRNA array, and modules closing the vector by ligation to the vector overhang received an additional 'E' (END; Figure 1b, c). Unique linker sequences were included in modules M1 and M5 to provide primer binding sites for sequence verification of sgRNA arrays (Figure 1c and Appendix S1). Based on the same principle, also nickase recipient (pDGE76–79; equivalent to pDGE1–4, but incorporating Cas9 D10A) and transcriptional activator vectors (Figure 1a; incorporating dCas9 fused to a TAL activation domain) were generated. These materials are made available, but will not be described in detail here.

sgRNA expression is driven by an Arabidopsis U6 promoter (pAtU6-26) in all vectors. The double 35S promoter (p35S) coupled with a *nos* terminator and the *Ubi4-2* promoter from parsley (pPcUbi) coupled with an *ocs* terminator were employed for Cas9 expression in one step, one nuclease vectors and first generation recipient vectors (Figure 1a). The 2 × 35S:Cas9 expression cassette and pPcUbi promoter were previously successfully used for genome editing in *N. benthamiana* and Arabidopsis, respectively (Belhaj *et al.*, 2013; Fauser *et al.*, 2014; Schiml *et al.*, 2014). The assembly of first generation recipient vectors integrated the Cas9 expression cassette as a level 1 module of the modular cloning system (Weber *et al.*, 2011a; Engler *et al.*, 2014), allowing simple modification of promoter/terminator sequences. However, this assembly strategy depended on custom modules for the introduction of plant selectable markers, and was of limited flexibility (Figure S1a). An improved assembly strategy (Figure S1b) was developed to accommodate additional modules in recipient vectors and achieve higher compatibility with the modular cloning system (Weber *et al.*, 2011a; Engler *et al.*, 2014). Based on this development, second generation recipient vectors providing additional promoters for Cas9 expression and selectable markers were generated (Figure 1a). The *DD45* (AT2G21740) and *INCURVATA2* (At5g67100) promoters were previously used for genome editing in Arabidopsis and might provide superior

efficiencies or avoid the generation of chimeric mutant plants (Hyun *et al.*, 2015; Wang *et al.*, 2015; Mao *et al.*, 2016). Additionally to kanamycin and BASTA selection, second generation recipients also allow for hygromycin selection, and contain a 'fluorescence-accumulating seed technology' (FAST, Shimada *et al.*, 2010) cassette in the T-DNA region. The FAST cassette mediates accumulation of RFP in the seed coat of various plant species, enabling for both positive and negative selection (Shimada *et al.*, 2010). Thus, non-transgenic seeds can be selected prior to screening (Gao *et al.*, 2016) or once an intended lesion has been obtained to further simplify the selection of stable mutant lines from genome editing approaches. Second generation recipient vectors were developed as a possible enhancement of the pDGE series subsequent to first application. In the following, mainly first generation vectors will be used.

Strategies and efficiencies for assembly of RGN-coding constructs

The exchange of the *ccdB* negative selection cassette in shuttle vectors and one step, one nuclease vectors for hybridized oligonucleotides by restriction/ligation (using *Bp*1, Figure 1b) takes place with high efficiency. Any negative clones obtained so far resulted from inaccuracies in oligonucleotide synthesis. Thus, vectors may also be used for screening applications in which libraries of unknown specificity nucleases are generated by cloning of degenerated guide sequences. Loaded shuttle vectors were used for the assembly of sgRNA arrays of different length in recipient vectors (Figure 1c). Efficiency of assembly reactions of two (M1 + M2E) or four (M1–M3, M4E) sgRNA TUs was consistently above 90%. The assembly efficiency of sgRNA arrays comprising eight TUs (M1–M7, M8E) was markedly decreased, but remained >50%. Following a conservative cloning scheme (Figure S2a), constructs for expression of at least four sgRNAs can thus be assembled without any PCR steps in 5 days.

The high efficiencies of the Golden Gate assembly reactions, and the background-free cloning due to *ccdB*-mediated counter selection at all stages, prompted us to test polyclonal plasmid preparations for assembly (Figure S2b). Restriction/ligation reactions from loading shuttle vectors with hybridized oligonucleotides were transformed in *E. coli* and directly used for liquid cultures and plasmid isolation. Polyclonal plasmid preparations were used to assemble a construct with four different sgRNA TUs. No decrease in efficiency in comparison to a conservative assembly was observed. The 'polyclonal' approach reduces time needed for the generation of a multiplexing construct by 1 day. More importantly, this strategy mitigates inaccuracies in oligonucleotide synthesis, as final assembly products will differ in incorporated oligonucleotide sequences. Furthermore, pooling of restriction/ligation reactions from loading sgRNA shuttle vectors prior

4 Jana Ordon et al.

to transformation into *E. coli* and polyclonal plasmid isolation was tested in a 'fast track' assembly approach (Figure S2c). More than 50% positive clones were obtained for assembly of an sgRNA array containing four TUs. However, the 'fast track' approach is of limited use, as individual sgRNA modules may not be reused in different assemblies.

Functional validation of nuclease constructs and effects of sgRNA and Cas9 dosage

A 'GUS-out-of-frame' recombination reporter was employed to test functionality of our genome editing toolkit. A spacer sequence was inserted in the coding sequence of a p35S-driven β -glucuronidase (GUS), shifting the GUS gene out of frame. Introduction of DSBs within the reporter's spacer and subsequent repair by NHEJ should, in some cases, re-establish the reading frame of the GUS gene (Figure S3a). Thus, GUS activity upon co-expression of reporter and a respective nuclease can be used as a quantitative readout for nuclease activity. *Agrobacterium*-mediated transient expression of the

GUS-out-of-frame reporter in *N. benthamiana* resulted in little to no GUS activity, as expected (Figure S3b). Enhanced GUS activity was detected upon co-expression of the reporter with paired TALENs targeting the reporter's spacer (Figure S3b), suggesting that the GUS-out-of-frame reporter is suitable to monitor *in planta* nuclease activity.

Derivatives of pDGE62–65 and pDGE144–165 containing sgRNA1 (Table 1) for targeting of the reporter were transiently expressed, alone or in combination with the GUS-out-of-frame reporter, in *N. benthamiana* leaf tissue. No or weak GUS activity was detected upon expression of RGNs or the reporter alone (Figure S4). Also, GUS activity did not exceed background level when Cas9 expression was driven by tissue-specific promoters (pDD45, pICU2). This suggests maintenance of expression patterns of these promoters in *N. benthamiana* transient assays. In contrast, strong GUS staining was obtained when Cas9 was expressed under control of the constitutive p35S and pPcUbi promoters in both vector sets (Figure S4). Thus, nucleases expressed from both one step, one nuclease and second generation recipient constructs are functional.

Table 1 Sequences of target sites selected for this study

| sgRNA# | Sequence [PAM] | Target | pDGE ^a | Score ^b |
|---------|----------------------------|--|-------------------|--------------------|
| sgRNA1 | TATATAAACCCCTCCAACC[AGG] | GUS Reporter | n/a | 0.13 |
| sgRNA2 | GAAATTGGTCTGTTGATGGT[TGG] | <i>NbEDS1a</i> + <i>NbEDS1b</i> (exon 1) | 30 | 0.35 |
| sgRNA3 | AGCAAATGCTTCATTAACCA[TGG] | | 30 | 0.33 |
| sgRNA4 | ATCCCGGAATTATCAGCACG[AGG] | <i>NbEDS1a</i> + <i>NbEDS1b</i> (exon 2) | 30 | 0.6 |
| sgRNA5 | TATGCTGCATGTAATCTGAA[AGG] | | 30 | 0.44 |
| sgRNA6 | CGAAACGTTGGCAGCTTTT[TGG] | <i>NbPAD4</i> (exon 2) | 38 | n/a ^c |
| sgRNA7 | CACCTCGCCGTGATTAAGT[TGG] | | 38 | 0.32 |
| sgRNA8 | TTCACCAAGTTCTAGCCTCG[AGG] | <i>NbPAD4</i> (exon 3) | 38 | 0.36 |
| sgRNA9 | TATAGAGATTAGAAGCTTCA[TGG] | | 38 | 0.05 |
| sgRNA10 | GTTTCGAGTCGAGCGAAACGT[TGG] | <i>NbPAD4</i> (exon 2) | 80 | 0.8 |
| sgRNA11 | GGCGAAGTGGCTATCCACCG[AGG] | | 80 | 0.3 |
| sgRNA12 | TCAGCTATCCGCGTTGTGT[TGG] | <i>NbPAD4</i> (exon 3/4) | 80 | 0.06 |
| sgRNA13 | CACCTATCTGTGCTCTTAG[TGG] | | 80 | 0.16 |
| sgRNA14 | AAATCTCACCGATACATGAA[AGG] | <i>DM2h</i> promoter to exon 2 | 143 | 0.1 |
| sgRNA15 | TGATTCTGCTAATTCATCA[AGG] | | 143 | 0.17 |
| sgRNA16 | ATTATACAGTTCAGTTACGA[TGG] | <i>DM2h</i> exon 3 | 143 | 0.21 |
| sgRNA17 | ATTATCAACCAAAGTGAAG[AGG] | | 143 | 0.23 |
| sgRNA18 | TAACGTCGCTCGGGTCCT[TGG] | <i>DM2^{er}</i> left | 89 & 90 | 0.01 |
| sgRNA19 | TGCGCCTTCGGATTCTCGGG[TGG] | | 89 & 90 | 0.57 |
| sgRNA20 | GTTAGTCTCTACGCAAGTAAC[TGG] | <i>DM2^{er}</i> right | 89 & 90 | 0.25 |
| sgRNA21 | CCACTGTTAGGCATGCATGA[TGG] | | 89 & 90 | 0.53 |
| sgRNA22 | CGGCTAAGCAATCTGATATG[TGG] | <i>DM2c</i> promoter to exon 1 | 142 | 0.11 |
| sgRNA23 | TCCATTAGAATGGTGAAGGA[TGG] | | 142 | 0.16 |
| sgRNA24 | GGACAAAAGCACCCAAATGA[TGG] | <i>DM2c</i> exon 2 | 142 | 0.33 |
| sgRNA25 | AGGGAAGTTACCTACCTTGC[TGG] | | 142 | 0.03 |
| sgRNA26 | TGTCATCAGAATAGAGCCTG[AGG] | <i>AtEDS1</i> (Col) left | 91 & 92 | 0.11 |
| sgRNA27 | GTATCCACGTGAGCGTATGA[TGG] | | 91 & 92 | 0.65 |
| sgRNA28 | CTCGAAACTCCAGTCATGT[CGG] | <i>AtEDS1</i> (Col) right | 91 & 92 | 0.31 |
| sgRNA29 | TTTGAGATGCTACTCTCGGT[TGG] | | 91 & 92 | 0.25 |

^apDGE construct containing respective sgRNA TUs.

^bOn-target efficacy score of sgRNA, from 0 to 1, with 1 being best (Doench et al., 2014).

^cConsecutive stretch of four Ts is not allowed by sgRNA designer tool.

In planta nuclease activity might be limited by availability of Cas9 protein and/or sgRNA. A possible sgRNA dosage effect was tested by increasing copy number of sgRNA1 in derivatives of pDGE1 (p35S:Cas9). As a control, a nuclease construct containing eight copies of sgRNA6 (Table 1) targeting an *N. benthamiana* endogenous locus was generated. In quantitative GUS measurements, low activity defining the background level was detected upon expression of either the nuclease containing eight sgRNA1 copies alone, the reporter alone, or the reporter together with the control nuclease containing sgRNA6 (Figure 2a). GUS activity was significantly enhanced upon co-expression of the reporter with a nuclease construct containing one copy of sgRNA1, as previously observed in qualitative GUS staining assays (Figures 2(a) and S4). With increasing sgRNA1 copy numbers, GUS activity was further enhanced (Figure 2a), suggesting that sgRNA abundance is one limiting factor for *in planta* nuclease activity at least in reporter-based assays. Furthermore, a respective sgRNA might be titrated out of the Cas9 complex by provision of additional sgRNAs in multiplexing applications. Nuclease constructs containing a single TU coding for sgRNA1, but additionally one, three or seven TUs coding for sgRNA6 were co-expressed with the GUS reporter (Figure 2a). GUS activity was not altered by expression of sgRNA6. The same constructs were tested in a reciprocal experiment using a GUS reporter for sgRNA6 activity (Figure 2a, inset). GUS activity was enhanced upon co-expression of Cas9 and sgRNA6, and activity increased with sgRNA6 copy number, confirming activity of sgRNA6. Taken together, these results suggest that eight or more loci can be targeted in multiplexing applications without reduction of nuclease activity at a given target site. The functionality of sgRNAs expressed from different positions in an sgRNA array was tested by placing the reporter-targeting sgRNA1 at any possible position, while all other positions were occupied by sgRNA6 TUs (Figure 2b). A similar enhancement of GUS activity was measured upon co-expression of all nuclease constructs with the GUS reporter, indicating that any position within an sgRNA TU array provides comparable genome editing activity. Finally, promoters for Cas9 expression were compared in quantitative nuclease activity assays (Figure 2c). Higher GUS activity and thus higher nuclease activity was obtained when using p2x35S in the *N. benthamiana* system. However, an amplification of nuclease activity by increasing sgRNA abundance was also detectable when using pPcUbi (Figure 2c). *In planta* nuclease activity is thus determined by both sgRNA and Cas9 abundance.

Generation of chromosomal deletions in *Nicotiana benthamiana*

Stable, inheritable chromosomal deletions of ~50–100 bp were previously generated in tomato, and ~1-kb deletions

© 2016 The Authors.
The Plant Journal published by Society for Experimental Biology and John Wiley & Sons Ltd.,
The Plant Journal, (2016), doi: 10.1111/tpj.13319

Cas9 for chromosomal deletions 5

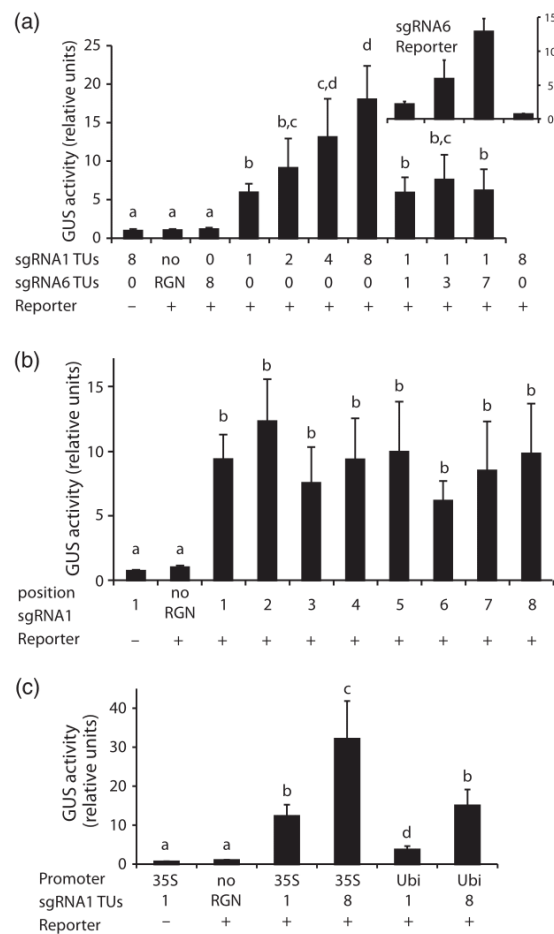


Figure 2. Functional characterization of pDGE recipient plasmids in transient, reporter-based nuclease activity assays.

(a) Effect of sgRNA dosage on *in planta* nuclease activity. Nuclease constructs containing varying copy numbers, as indicated, of reporter-targeting sgRNA1 or sgRNA6 (targeting an *N. benthamiana* endogenous locus) were co-expressed with the GUS-out-of-frame reporter in *N. benthamiana*. GUS activity was quantitatively determined at three dpi, normalized to total protein amounts, and expressed in relative units by arbitrarily setting GUS activity of the reporter alone to 1. Standard deviation of four biological replicates is shown, and letters indicate statistically significant differences (analysis of variance (ANOVA), Tukey's *Post-hoc* test, $P < 0.01$). The inset shows a reciprocal experiment, where the same constructs were co-expressed with a reporter targeted by sgRNA6.

(b) Functionality of sgRNA TUs within an sgRNA array. Nuclease constructs containing eight sgRNA TUs were expressed as in (a). Each construct contained seven copies of sgRNA6 and a single copy of sgRNA1. The position of sgRNA1 within the sgRNA array is indicated. Representation of GUS activity, replicates and statistics as in (a).

(c) Comparison of nuclease activity with different promoters driving Cas9 expression. Nuclease constructs with Cas9 expression driven by 2x35S or PcUbi4-2 promoters and containing either one or eight TUs for expression of the reporter-targeting sgRNA1 were expressed as in (a). Representation of GUS activity, replicates and statistics as in (a).

were induced at the *ABP1* locus in Arabidopsis using Cas9-based nucleases (Brooks *et al.*, 2014; Gao *et al.*, 2016). However, information for other species or about size

6 Jana Ordon et al.

biases for chromosomal deletions is to our knowledge so far missing. We made use of the simple and extensive multiplexing capacities of our genome editing toolkit to explore the generation of chromosomal deletions first in *N. benthamiana*. Three different nuclease constructs based on pDGE1 (p2x35S, nptII) and each containing four sgRNA TUs were generated. sgRNAs were designed for targeting of the immune regulatory genes *EDS1* and *PAD4*. *EDS1*-family genes additionally including *SAG101* encode essential regulators of plant innate immunity mediated by a subclass of nucleotide-binding/leucine-rich repeat- (NLR) type immune receptors containing an N-terminal Toll-Interleukin 1 receptor (TIR) domain (Feys *et al.*, 2001, 2005; Wagner *et al.*, 2013). The *N. benthamiana* genome contains two plausible *EDS1* orthologues, which we termed *NbEDS1a* and *NbEDS1b* (Table S2). In the following, only *NbEDS1a* will be analyzed. *NbPAD4* is encoded by a single gene (Table S2).

The four sgRNAs incorporated in each construct all targeted the same locus, and were designed two either generate small deletions (~100 bp) in pairs, or to generate larger deletions by cleavage of the outmost target sites (Figure 3a). Thus, the occurrence of small and large deletions can be analyzed in transformants originating from a single construct. pDGE30 (sgRNAs 2–5) targeted *NbEDS1*, while pDGE38 (sgRNAs 6–9) and pDGE80 (sgRNAs 10–13) targeted *NbPAD4* (Figure 3a and Table 1). Functionality of nucleases was first tested in transient expression experiments and using the amplified fragment length polymorphism (AFLP) assay (Belhaj *et al.*, 2013). The AFLP assay depends on detection of recombination products from paired nuclease activity by PCR using primers flanking the region targeted for deletion. Additional amplicons of the expected size were detected upon expression of pDGE30 and pDGE80 when querying for the generation of small deletions through cleavage of adjacent target sites (Figure 3b). On the same samples, no additional amplicons were detected when using outmost primers for detection. The activity of nucleases encoded by pDGE38 could not be detected.

Activity-confirmed nuclease constructs pDGE30 and pDGE80 were stably transformed into wild type *N. benthamiana*. Two independent plants transgenic for pDGE30 were genotyped for potential deletions. One plant apparently contained a deletion in exon 2 (Figure 3c), and band intensities suggested it was most likely heterozygous for the deletion. Sequencing of the smaller amplicon revealed that it corresponded to a 97-bp deletion in the second exon of *NbEDS1a* (*Nbeds1a-1*, Figure 3d). T₁ seedlings originating from the *Nbeds1a-1* candidate plant were genotyped, and the *Nbeds1a-1* deletion segregated as a Mendelian trait in this generation (Figure 3e). Upon transformation of pDGE80, 24 regenerated plants originating from 11 independent calli were obtained. None of the plants contained the deletion targeted by sgRNAs 12 and 13, but three

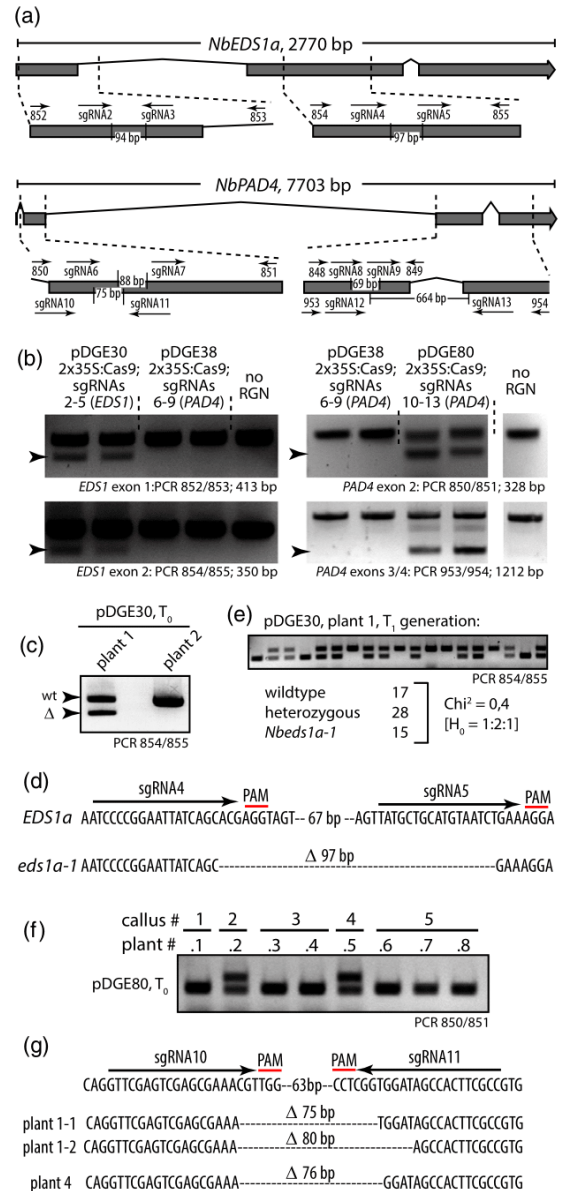


Figure 3. Generation of chromosomal deletions in *Nicotiana benthamiana*. (a) Schematic representations of the *NbEDS1a* and *NbPAD4* loci with oligonucleotides, sgRNA target sites and expected deletions indicated. (b) Recombination events from nuclease activity detected by AFLP assay. Indicated constructs were transiently expressed in *N. benthamiana*, DNA extracted at three dpi and used as template for PCRs as indicated. Arrowheads mark additional PCR products from target site cleavage and recombination. Additional lanes were spliced in the right panel. (c) Genotyping of two independent transgenic lines from stable transformation of pDGE30. (d) Molecular lesion in the *Nbeds1a-1* deletion allele from (c). (e) Segregation of the *Nbeds1a-1* deletion allele in T₁. A representative image from genotyping 20 T₁ individuals is shown with chi-squared statistics. (f) Genotyping of T₀ individuals from stable transformation of pDGE80. A representative image from genotyping in total 24 plants originating from 11 independent calli is shown. (g) Molecular lesion in two *Nbpad4* deletion alleles from (f).

independent transgenics homozygously carried a deletion in exon 2 of *NbPAD4* targeted by sgRNAs 10 and 11 (Figure 3f). Sequencing of amplicons revealed a bi-allelic deletion in plant 1 and a mono-allelic deletion in plant 4 (Figure 3g). T_1 seedlings were genotyped for two candidate homozygous deletion lines. The wild type *NbPAD4* allele could not be detected, demonstrating that mutations were germline-transmitted. Taking transformations of pDGE30 and pDGE80 together, 13 independent transgenic lines were genotyped. Although lines carrying small deletions could be recovered even in the homozygous state in T_0 , as previously described for tomato (Brooks *et al.*, 2014), no line carrying a larger deletion by cleavage of external sgRNA targets was recovered. Since the functionality of all

nucleases was shown via transient AFLP assays, this suggests reduced likelihood of larger deletions.

Genome editing at a complex resistance gene locus in Arabidopsis

The *DM2^{Le}* (*Dangerous Mix 2*; Alcazar *et al.*, 2009; Chae *et al.*, 2014) Resistance gene cluster from accession Landsberg (Ler) was chosen to exploit the generation of chromosomal deletions in Arabidopsis. *DM2^{Le}* contains eight complete or truncated genes (*DM2a-DM2h*; Figure 4a) most homologous to *RPP1* conferring resistance to different isolates of the oomycete pathogen *Hyaloperonospora arabidopsidis* (*Hpa*) (Botella *et al.*, 1998; Rehmany *et al.*, 2005). When combined in a single genetic background with

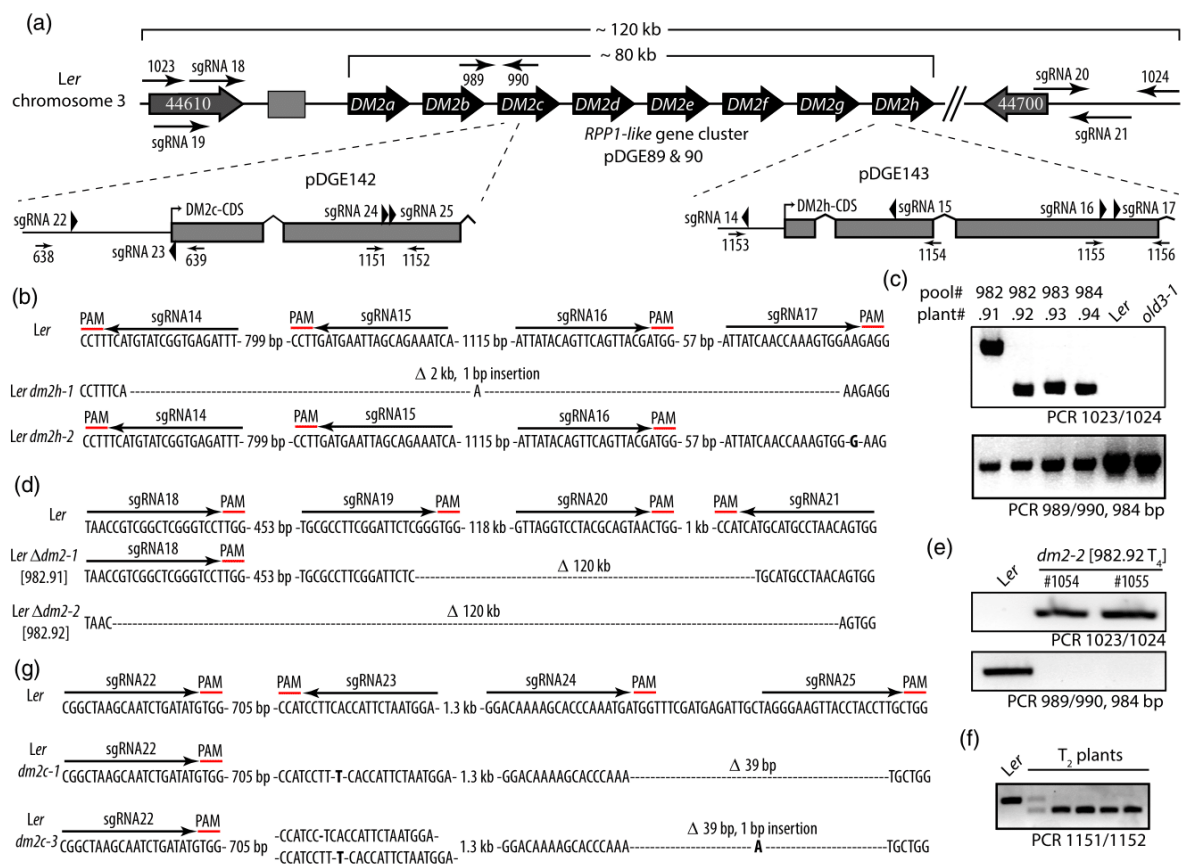


Figure 4. Generation of chromosomal deletions at the Arabidopsis *DM2* locus.

(a) Schematic representation of the *DM2^{er}* locus with oligonucleotides and sgRNA target sites indicated. *R*-gene encoding *DM2a-h* genes are represented as dark grey arrows. A transposable element is indicated as a light grey box. Grey arrows mark loci conserved between Arabidopsis accessions Col and Ler flanking the *DM2* locus, with numbers indicating Arabidopsis gene identifiers as At3gXXXXX.

(b) Molecular lesions detected in two phenotypically selected *dm2h* mutant lines (Figure S5a).

(c) Genotyping of phenotypically selected *Δdm2* mutant lines (Figure S5b).

(d) Molecular lesions in two *Δdm2* mutant lines.

(e) Genotyping of T_4 families for one *Δdm2* mutant line, *dm2-2*. T_4 seedlings were pooled for DNA extraction, and DNAs were used for PCR with the indicated oligonucleotides.

(f) Genotyping of plants selected from a primary screen of approximately 150 T_2 plants from pDGE142 transformation.

(g) Molecular lesions in two *dm2c* mutant lines, as detected in single, BASTA-sensitive T_3 plants.

© 2016 The Authors.

The Plant Journal published by Society for Experimental Biology and John Wiley & Sons Ltd.,
The Plant Journal, (2016), doi: 10.1111/tpj.13319

8 Jana Ordon et al.

alleles of *Strubbelig Receptor Family 3 (SRF3)* from accessions Kaschmir and Kondara, with a transgene encoding for nucleus-directed EDS1-YFP, or with an EMS-induced allele of the enzyme *O-acetylserine(thiol)lyase A1 (OLD3)*, *old3-1*, *DM2^{L^{er}}* mediates temperature-dependent induction of autoimmune response (Alcazar et al., 2010; Tahir et al., 2013; Stuttmann et al., 2016). *old3-1*-induced autoimmunity leads to seedling lethality at ambient temperature (22°C), but is suppressed under high temperature conditions (Shirzadian-Khorramabad et al., 2010; Tahir et al., 2013). *DM2^{L^{er}}* copy number strongly modulates *old3-1*-induced autoimmunity (our own observations, Shirzadian-Khorramabad et al., 2010): Plants homozygous for *old3-1*, but hemizygous for *DM2^{L^{er}}* are viable at 22°C, but further reduction of growth temperatures (18°C) induces strong autoimmunity. This allows for phenotypic differentiation of heterozygous and homozygous *dm2* mutant plants using different temperature regimes.

Four different genome editing constructs for targeting of the *DM2* cluster were generated. pDGE142 (sgRNAs 22–25) and pDGE143 (sgRNAs 14–17) were based on pDGE4 (pPcUbi, BASTA) and designed to target two deletions each in *DM2c* and *DM2h*, respectively (Figure 4a and Table 1). Two further constructs, pDGE89 and 90, were designed for deletion of the entire 120 kb region non-syntenic between *Arabidopsis* accessions Col and Ler and containing the *DM2* cluster (Figure 4a). Constructs contained the same sgRNAs (18–21; Table 1), but differed in promoters driving Cas9 expression (p35S in pDGE89 or pPcUbi in pDGE90). sgRNAs for directing Cas9 to two sites at each flank of the targeted region were incorporated to potentially increase the frequency of large deletions (Figure 4a). Constructs were transformed into Ler *old3-1* mutant plants, cultivated at 28°C to suppress *old3-1*-associated seedling lethality. T₁ transgenic plants were further BASTA-selected at 28°C, and propagated to obtain T₂ pools composed of five T₁ plants.

The *DM2h* locus necessary for mediating *old3-1*-induced autoimmunity (Stuttmann et al., 2016) was targeted in pDGE143-transgenic plants. When cultivated at 22°C, approximately 5–10% of T₂ seedlings were non-necrotic, representing candidate lines carrying at least one inactivating *dm2h* allele (Figure S5a). Further shifting plants to 18°C selected for homozygous *dm2h* mutant lines, which occurred at a frequency <10% among the *dm2h* candidate lines (Figure S5a). BASTA was brush-applied to rosette leaves of surviving, putative homozygous *dm2h* candidate lines, and six BASTA-sensitive (non-transgenic) lines were genotyped. Only one of these contained a PCR-detectable deletion (between sgRNA 14 and 17 target sites, Figure 4b). An additional point mutational allele was sequenced, revealing a single nucleotide insertion (Figure 4b). Both *dm2h* lines were mono-allelic, indicating that mutations were most likely present in the T₁ germline, and became homozygous in the T₂ generation.

Survival at ambient temperatures was also used to screen for mutant lines containing a deletion encompassing the entire *DM2* cluster from T₂ pools transgenic for pDGE89 and pDGE90. Rescued seedlings were obtained at a frequency of ~0.5% from pDGE90-derived, but not pDGE89-derived T₂ pools (Figure S5b). Four plants from different T₂ pools were randomly chosen for genotyping (Figure 4c). A PCR product corresponding to the deletion of the targeted 120 kb region was obtained in all cases, but differed in size. Sequencing revealed that size differences originated from either cleavage of the outer sgRNA18 and sgRNA21, or sgRNA19 and sgRNA21 targets (Figure 4d). Additional PCRs querying the presence of the wildtype *DM2^{L^{er}}* locus showed that lesions were heterozygous in deletion lines (Figure 4c, lower panel). Non-necrotic, putatively homozygous $\Delta dm2$ deletion lines were phenotypically isolated from segregating T₃ populations (Figure S5c), BASTA-sensitive individuals selected, and genotypes confirmed for two T₄ families (Figure 4e). Putative *dm2c* mutant lines were selected by PCR screening approximately 150 pDGE142-transgenic T₂ plants cultivated under permissive conditions (28°C). No deletions from cleavage of sgRNA22/23 targets were obtained. However, lines containing an ~40-bp deletion derived from cleavage of sgRNA24/25 target sites were obtained at a frequency of 2.7% in the homozygous state, and 8% in the heterozygous state (Figure 4f). Again, transgene-free homozygous deletion lines were successfully selected in T₃, and molecular lesions were analyzed for two independent lines (Figure 3g). Both lines contained the PCR-selected, ~40 bp deletion, and also additional point mutations from cleavage of the sgRNA23 target site. Taken together, these results suggest that in *Arabidopsis*: (i) point mutations occur with higher frequency than deletions targeted by paired nucleases, (ii) Cas9-induced deletions mainly occur in T₂ when using pPcUbi:Cas9, (iii) small deletions (here 40 bp) may occur at ~10% frequency among T₂ plants, (iv) relatively large chromosomal deletions (here 120 kb) are feasible, but occur at lower frequencies, and (v) *Ubiquitin* Promoter-driven Cas9 appears more suitable than p35S-driven Cas9.

Deletion of the tandem *EDS1* locus in *Arabidopsis* accession col

The performance of pPcUbi:Cas9 in comparison to p35S:Cas9 was again tested using the *EDS1* locus as target. Accession Col contains two functional *EDS1* copies encoded by At3g48080 and At3g48090 (Figure 5a), and a Col *eds1-2* line was generated by introgression of the *eds1-2* allele from accession Ler (Bartsch et al., 2006; Zhu et al., 2011). This line was instrumental for genetic analyses in the standard Col accession. However, it also contains the *DM2^{L^{er}}* cluster, which may produce unexpected interference upon reestablishment of *EDS1* activity in

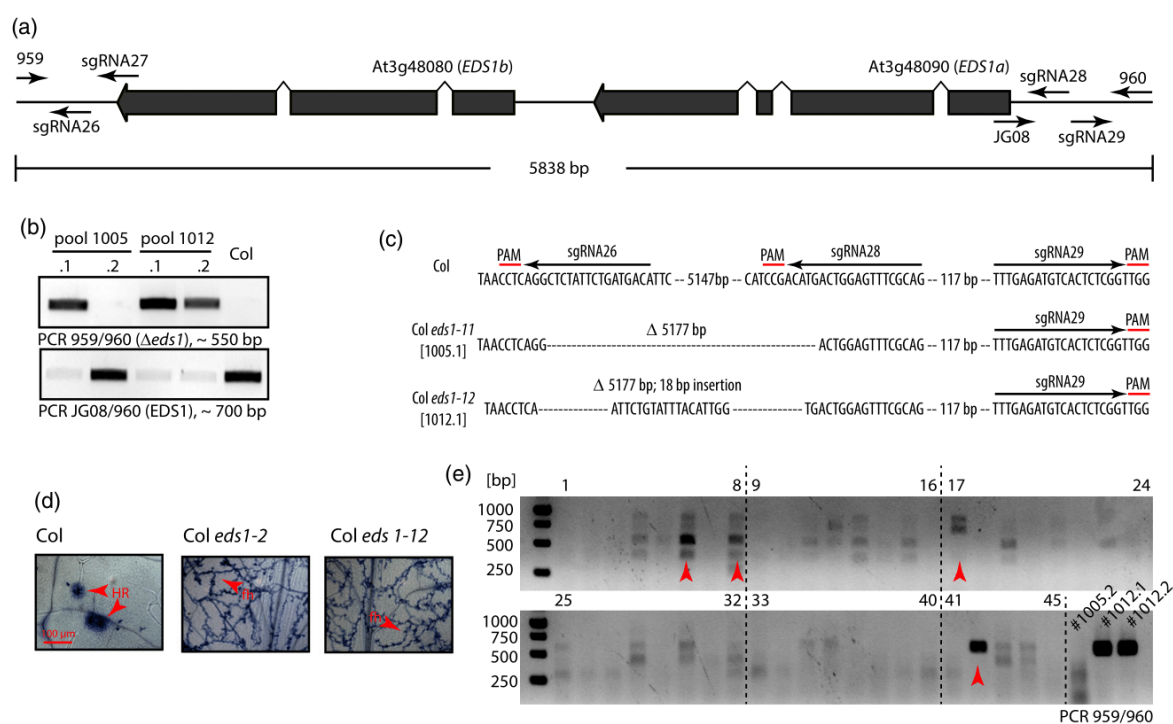


Figure 5. Deletion of the tandem *EDS1* locus in Arabidopsis accession Col.

(a) Schematic representation of the *EDS1* locus with oligonucleotides and sgRNA targets indicated.

(b) Genotyping of phenotypically selected putative *eds1* deletion alleles. T_2 seedlings from transformation of pDGE92 into wild type Columbia plants were subjected to infection with incompatible *Hpa* isolate Cala2. Putatively *Hpa* susceptible, *eds1* candidate lines were used for DNA extraction and genotyping with indicated oligonucleotides.

(c) Molecular lesions obtained in *eds1* deletion alleles.

(d) Infection phenotype of the newly selected *eds1-12* mutant line and controls. Representative micrographs from infection with *Hpa* isolate Cala2 and staining of first true leaves with Trypan Blue (six dpi) are shown. HR – hypersensitive response, fh – free hyphae.

(e) PCR screening of T_2 plants as in (b) for *eds1* deletion mutants. Arrowheads mark signals interpreted as putative deletion lines.

transgenic plants (Stuttman *et al.*, 2016). The Col *EDS1* locus was targeted for deletion by two constructs containing sgRNAs 26–29 (Table 1), and either p35S-driven (pDGE91) or pCubi-driven (pDGE92) Cas9. Constructs were transformed into Col wild type plants, primary transformants selected by BASTA resistance, and 15 T_2 pools corresponding to ~130 T_1 plants composed for each transformation. From T_2 pools, 60–70 seedlings were screened for putative *eds1* mutant plants by infection with *Hpa* isolate Cala2. Resistance to *Hpa* Cala2 in Col is *EDS1*-dependent, and mediated by the TIR domain-containing immune receptors RPP2a/b (Sinapidou *et al.*, 2004). None of the seedlings from transformation of pDGE91 (p35S:Cas9) was scored as *Hpa* Cala2 susceptible, but four plants from two independent pDGE92 T_2 pools were selected as potential *eds1* mutants. The expected ~5-kb deletion was detected in three *eds1* candidate lines (Figure 5b, upper panel). The wild type *EDS1* locus was not detected in lines containing the deletion, suggesting they were homozygous (Figure 5b, lower panel). Sequencing of deletion alleles from

two *eds1* candidate lines revealed mono-allelic deletions encompassing the region flanked by sgRNA 26 and 28 target sites, while the sgRNA 29 target site remained intact in both lines (Figure 5c). A Col *eds1-12* mutant line not containing the pDGE92 transgene was selected in the T_3 generation, and seedlings were infected with *Hpa* Cala2 (Figure 5d). Col *eds1-12* seedlings were fully susceptible, and indistinguishable from the previously characterized Col *eds1-2* introgression line, confirming germline transmission of the deletion allele. With *eds1* being fully recessive, phenotypic screening for *Hpa* (Cala2) susceptibility fails to detect heterozygous deletion lines. From PCR screening 230 individuals originating from six pDGE92 transformation-derived pools, either homo- or heterozygous deletion alleles were estimated to occur in ~10% of T_2 (Figure 5e). However, actual frequencies might be lower, as stable, germline-transduced alleles may be confounded with somatic genome editing events occurring in leaf tissues used for DNA preparation. Taking deletions of the *DM2^{er}* cluster and the tandem *EDS1* locus together,

10 Jana Ordon et al.

chromosomal deletions were obtained at two independent loci when using pPcUbi-driven Cas9, but not p35S-driven Cas9. Deletions apparently occurred at low frequencies in the T₁ generation, and became more frequent in T₂. Overall, the generation of chromosomal deletions not only provides a scheme for simple, PCR-based mutation identification, but also represents a feasible approach to overcome genetic redundancy or for functional dissection of non-coding DNA.

DISCUSSION

Strategies for assembly of RGN-coding constructs may include several PCR steps, combine different cloning strategies or rely on additional DNA modules such as destination vectors, thus adding variability and complexity (e.g. Lowder et al., 2015; Ma et al., 2015; Zhang et al., 2015; Mao et al., 2016). The presented pDGE toolkit sacrifices some flexibility, but enables for extremely simple and fast assembly of RGN-coding constructs by Golden Gate cloning. Only hybridized oligonucleotides are required as 'external' components, while all other DNA modules are part of the toolkit (Figure 1). Construction of second generation recipients showed how novel components and functionalities can be adapted for the 'preassembled recipient' strategy (Figures 1 and S1). Arrays of two, four or eight sgRNA TUs may be assembled using sgRNA shuttle vectors. Arrays of different length can be constructed by providing suitable end-linkers in assembly reactions (Weber et al., 2011a). A detailed manual for the assembly of RGN constructs is provided (Appendix S1), and plasmids can be obtained via Addgene (www.addgene.org) (kit # 1000000084) or through us. Currently, functionality was only tested in *N. benthamiana* and Arabidopsis. However, functionality of pAtU6 (for driving sgRNA expressions) as well as pPcUbi and p35S (for driving Cas9 expression) in many dicotyledonous plant species can be assumed.

We made use of the simple and efficient multiplexing capacity of our system to assemble multiple constructs incorporating four sgRNA TUs for the generation of chromosomal deletions. sgRNA target sites addressed by individual constructs were mostly chosen for the generation of either two small deletions by cleavage of nearby target sites, or larger deletions by cleavage of more distant target sites at the same locus (e.g. Figure 3a). In both *N. benthamiana* and Arabidopsis, mainly occurrence of small deletions (<100 bp) was observed, and in only one case, more distant sites were cleaved to generate a large deletion (*dm2h-1*, Figure 4b). Also, phenotypically selected deletions of 5 kb (*AtEDS1*) and 120 kb (*AtDM2*) occurred at low frequencies (below 1%), while small deletions were obtained at frequencies around 10% (*AtDM2c*) by PCR screening. Taken together, this suggests a reduction in the efficiency of deletion induction with increasing deletion size. However, a correlation between deletion size and

frequency was not consistently observed in animal cells (Xiao et al., 2013; Canver et al., 2014; He et al., 2015), and frequencies might strongly depend on sgRNA activity rather than deletion size also in plant systems. In either case, the applied strategy of incorporating multiple sgRNAs in constructs for targeting of a single locus proved extremely valuable, as in most cases, only one of several possible deletions was obtained. Negative effects were not observed among Cas9-transgenic lines, indicating that unspecific cleavage at off-target sites is most likely not a major problem in plants. Thus, extensive multiplexing may not only be used for generation of higher order mutants, but also to increase mutation frequencies at single loci to reduce transformation and screening efforts.

Mainly point mutational alleles were obtained when phenotypically screening for inactivating alleles at the *DM2h* locus, corroborating lower frequencies of deletions in comparison to cleavage and repair events at single target sites. However, phenotypical selection is generally neither possible nor desired. In these cases, the induction especially of small chromosomal deletions provides a simple and straightforward workflow for the selection of mutant lines in genome editing approaches. Minor differences between wild type and deletion allele, as induced here at *NbEDS1a*, *NbPAD4* and *AtDM2c*, should generally not perturb PCR stoichiometry, and allow faithful selection of hetero- or homozygous deletion lines from simple PCR screening. Confounding of recombination events occurring in populations of somatic cells with germline-transmitted alleles present in all cells only becomes problematic when targeting larger regions for deletion (Figure 5e). Deletion alleles are also convenient for downstream genetic analyses. Although high resolution melting analysis or dCAPS markers can be used to detect virtually any SNP (single nucleotide polymorphism) in segregating populations, for example identification of an *N. benthamiana eds1 pad4* double mutant line, which was obtained at a frequency of 1/192 only, was simplified by the availability of size polymorphism markers for mutant alleles.

The RNA polymerase III (RNAP III)-transcribed U6/U3 promoter systems are most commonly used for the expression of sgRNAs in both animal and plant cells, as U6/U3 transcripts are not capped or polyA-tailed, are not exported from nuclei, transcription start sites are clearly defined, and a simple T stretch (≥ 6 Ts, Nielsen et al., 2013) is sufficient as termination signal. Our strategy for the expression of multiple sgRNAs consisted in repeated U6-driven TUs identical to each other with the exception of the specificity-determining, variable guide sequence (Figure 1). Transient, recombination reporter-based assays indicated strong dependency of nuclease activity on sgRNA abundance, limited by the expression level of U6-driven sgRNAs (Figure 2a). However, it remains unclear whether nuclease activity at endogenous loci is similarly

affected by sgRNA abundance. Also, limited nuclease activity might enhance Cas9-specificity (Fu *et al.*, 2013; Hsu *et al.*, 2013). Importantly, repetitive sgRNA expression units were not prone to silencing, as constructs were successfully used for the generation of multiple mutant lines, and mutations most likely occurred mainly in the T₂ generation in Arabidopsis. Thus, technically more demanding sgRNA expression systems bear valuable alternatives for specific applications as e.g. tissue-specific sgRNA expression (Gao and Zhao, 2014; Nissim *et al.*, 2014; Xie *et al.*, 2015), but efficient multiplexing is also achieved by clustering sgRNA TUs. In reporter-based assays, eight sgRNAs could be expressed without detectable reduction of nuclease activity at a given target site (Figure 2a), suggesting extensive multiplexing capacities also for the targeting of endogenous loci.

Various RNAP II promoters were previously reported as functional for driving Cas9 expression in genome editing applications (e.g. Gao *et al.*, 2015; Hyun *et al.*, 2015; Wang *et al.*, 2015; Mao *et al.*, 2016) (see Bortesi and Fischer, 2015 for review). The 2x35S promoter was highly efficient in transient, reporter-based assays in comparison to the *PcUbi* promoter, and was also highly efficient for the generation of stable deletion mutants in *N. benthamiana* (Figures 2 and 3). However, in two independent cases, deletion mutants could here be generated in Arabidopsis when using *pPcUbi*-driven, but not *p35S*-driven Cas9 in otherwise identical constructs. 35S:Cas9-mediated genome editing in Arabidopsis was previously reported (e.g. Feng *et al.*, 2013; Jiang *et al.*, 2014b), but direct comparison suggests reduced efficiency of this promoter. The egg cell-specific *DD45* promoter for driving Cas9 expression was recently reported to induce homozygous mutants at high frequency in the T₁ generation (Wang *et al.*, 2015), and was therefore incorporated in Cas9 units of second generation recipient vectors (Figure 1a). However, systematic comparison of promoters for Cas9 expression with unified target loci and selection schemes will be necessary to identify optimal Cas9 expression systems for genome editing in Arabidopsis in the future.

Besides sgRNA and Cas9 expression systems, choice of target sites and design of sgRNAs in perspective to the selection of mutant lines represent critical parameters for genome editing approaches. Among the 29 sgRNAs used in this study, we clearly observed differences in activity, with for example sgRNAs 10/11 efficiently inducing recombination events at the *NbPAD4* locus, but sgRNAs 6–9 not at all (Figure 3b). To date, no sgRNA design rules for plant systems are available, but predictive models for sgRNA on-target efficiency were deduced in an animal system (Doench *et al.*, 2014, 2016). Although with a limited dataset at hand, we considered whether design rules for highly efficient sgRNAs might explain variable nuclease activities observed here. Indeed, sgRNA pairs 6/7 and 8/9, for which

no activity was detected, both contained an unfavorable target site (Table 1), and target sites for highly active sgRNAs 10/11 scored ≥ 0.3 . However, sgRNA pair 2/3 and 4/5 targets also consistently obtained scores ≥ 0.3 , but sgRNAs did not induce recombination with efficiencies comparable to sgRNA 10/11 (Table 1 and Figure 3b). Also, sgRNA 28/29 target site scores were highly similar, but only cleavage of sgRNA28 was observed (Figure 5c). Thus, there is no strict correlation between high *in planta* activity and predicted activity. Future studies will help to confirm or define sgRNA design guidelines for plant systems, facilitating more informed target site selection.

EXPERIMENTAL PROCEDURES

Construction of pDGE1–4 vectors

Full lists of plasmids and oligonucleotides used in this study are provided in Tables S1 and S3. Annotated vector sequences are provided as multi-record GenBank file in Appendix S2. If not further indicated, all pCH/pAGM/pICSL plasmids originate from the Plant Modular Cloning Toolbox (Engler *et al.*, 2014). *PAT* and *nptII* plant selectable marker cassettes were amplified from pAM-PAT (Genbank: AY436765.1) and pGWB5 (Nakagawa *et al.*, 2007), respectively, using oligonucleotides JS584/688, and fragments cloned into pUC57-*Bsal* by an *SmaI* cut/ligation, yielding pJOG32 (*PAT*) and pJOG33 (*nptII*). A *Bsal* recognition site within the *ccdB* gene of pDON207 (www.thermofisher.com) was eliminated using JS691/692. The resulting derivative, pDON207-*Bsal*, was used as template to amplify a *ccdB*-Cm^R (Cm^R – chloramphenicol resistance, *cat*) cassette using JS694/695. The resulting PCR product was cloned into pUC57-*Bsal* by *EcoRV* cut/ligation, yielding pJOG34. Golden Gate modules encompassing the Cas9 CDS (pICH41308::hCas9, Addgene #49770) as well as a 2xp35S:Cas9-tnos (pICH47742::2x35S-5'UTR-hCas9(STOP)-NOST, Addgene #49771) (Belhaj *et al.*, 2013) were obtained from Addgene. The parsley *Ubi4-2* promoter, *pPcUbi* (Fauser *et al.*, 2014), was amplified from parsley genomic DNA using JS834/835, and cloned into pICH41295 by *Bpil* cut/ligation, yielding pJOG20. *pPcUbi* (pJOG20), Cas9 (pICH41308::Cas9) and the *ocs* terminator (*tocs*, pICH41432) were combined in pICH47742 by *Bsal* cut/ligation, yielding pJOG30. pICH47742::2x35S-5'UTR-hCas9(STOP)-NOST, pJOG34 and either pJOG33 or pJOG32, and pJOG30, pJOG34 and either pJOG33 or pJOG32 were assembled in the pVM_BGW vector backbone (Schulze *et al.*, 2012), a derivative of pBGWFS7 (Karimi *et al.*, 2002), to create pDGE1–4, respectively. Assembly was carried out by *Bsal/Bpil* cut/ligation, followed by a cycle of ligation (Figure S1a), and a final digestion of the ligation reaction using *XbaI* to digest unincorporated pJOG34.

Construction of sgRNA shuttle vectors

A fragment encompassing the *AtU6* promoter, a guide sequence and the sgRNA scaffold was synthesized (Integrated DNA Technologies, Leuven, Belgium) and used for amplification *AtU6* promoter and sgRNA scaffold using oligonucleotides JS775/776 and JS779/780. A *ccdB*-Cm^R cassette was amplified using JS777/778 and pDON207-*Bsal* as template. The three PCR fragments were diluted, mixed and used as template for SOE PCRs for individual shuttle vectors using oligonucleotides indicated in Table S3. PCR products were cloned into pUC57-*Bsal* by *EcoRV* cut/ligation. To generate pDGE012 (M5), PCR fragments generated as previously using JS793/794 and generated with JS791/792 on Arabidopsis

12 Jana Ordon et al.

genomic DNA were fused by *Bsal* cut/ligation and used as template for PCR with JS791/794. The amplicon was cloned into pUC57-*Bsal* by *EcoRV* cut/ligation. To generate pDGE005 (M1), a linker sequence was amplified from Arabidopsis genomic DNA using JS781/782, the *AtU6* promoter was amplified using JS783/776, PCR fragments were diluted, mixed as previously, used as template for PCR with JS781/784, and the amplicon was cloned into pUC57-*Bsal* by *EcoRV* cut/ligation.

Construction of pDGE62–65 vectors

A *Bpil* recognition site in pVM_BGW was mutagenized by amplification with JS704/705, followed by *Bpil* cut/ligation. The resulting pVM_BGW-*Bpil* backbone was used for assembly of pDGE62–65 from pCH47742::2x35S-5'UTR-hCas9(STOP)-NOST, pDGE006 and pJOG33 or pJOG32, and pJOG30, pDGE006 and either pJOG33 or pJOG32, respectively, by *Bsal/Bpil* cut/ligation, followed by a cycle of ligation and a final restriction with *XbaI*.

Construction of pDGE144–165

pJOG292 was constructed by combining the vector backbone (PCR JS1028/1029 on pVM_BGW-*Bpil*) and a *lacZ* fragment (PCR JS1030/1031 on pCH41264) in a *Bsal* cut/ligation reaction. A *ccdB* negative selection cassette (PCR JS1032/1033 on pDGE1) was subcloned into pUC57-*Bsal* by *EcoRV* cut/ligation. Promoter fragments were amplified from Arabidopsis DNA (DD45-JS1074/1075; ICU2-JS1055/1056) and cloned into pCH41295 by *Bpil* cut/ligation to yield pJOG301 and pJOG298, respectively. The Pro+5U modules were used for assembly of pJOG323 and pJOG326 in pCH47742. The FAST cassette from the Modular Cloning Plant Parts (Engler et al., 2014) was used as level 1-3f module (pJOG304). pDGE144–165 were assembled by *Bpil* cut/ligation (Figure S1b).

Construction of pDGE76–79

Annealed oligonucleotides JS910/911 were used in a *Bsal/EcoRV* cut/ligation reaction with pCH41308::Cas9. After denaturing, the reaction was supplemented with fresh ATP, DTT, Ligase and *EcoRV* to obtain pJOG58. pJOG69 (2x35S:Cas9 (D10A)-tnos) and pJOG70 (pPcUbi:Cas9(D10A)-tocs) were assembled in pCH47742 with pJOG58, pCH51288, pCH41421, pJOG20 and pCH41432 by *Bpil* cut/ligation. pDGE76–79 were assembled from pJOG69/70 and pJOG32, pJOG33 and pJOG34 as described for pDGE1–4.

Construction of pJOG250–253

An N863A mutation was introduced into the Cas9 CDS in pJOG58, the insert amplified (JS912/913) and cloned into pAGM1287 by *Bpil* cut/ligation to yield pJOG60. A fragment coding for the C-terminus of Hax3 (AY993938) was amplified (oligonucleotides CTH3-GG-Jo-F/R) and subcloned into pPCR-Blunt, yielding pJOG241. pJOG242 was assembled from pJOG60, a Ser-Gly linker (oligonucleotides JS914/915 subcloned in pPCR-Blunt), pJOG241, pCH51277 and pCH41414 in pCH47742. pJOG250–251 and pJOG252–253 were constructed from pJOG242, pJOG32, pJOG33, pJOG34 and pDGE6 as described for pDGE1–4 and pDGE62–65, respectively.

Assembly of nuclease constructs

sgRNAs as indicated in Table 1 were cloned into sgRNA shuttle vectors, and derivatives were subsequently used for assembly of nuclease constructs (pDGE30, 38, 80, 89–92, 142–143) as described in Appendix S1.

Construction of the GUS-out-of-frame recombination reporter and TALENs

The β -glucuronidase coding sequence was amplified from pGWB3 (Nakagawa et al., 2007) using oligonucleotides GUS_TALE-N_Ax7LR-F and pTALENgus-R, and the resulting PCR product was cloned into pENTR/D TOPO (www.thermofisher.com) as according to the manufacturer. The GUS-out-of-frame insert was subsequently mobilized into pGWB2 (Nakagawa et al., 2007) by LR reaction, yielding pMR006. TALENs were assembled as previously described (Richter et al., 2014).

Agrobacterium-mediated expression, AFLP and GUS assay

Constructs were electroporated into *Agrobacterium* strain GV3101 pMP90 and grown on YEB medium. For transient expression, plate-grown bacteria were resuspended ($OD_{600} = -0.6$) in Agro infiltration medium (AIM; 10 mM MES pH 5.7, 10 mM $MgCl_2$). Solutions were syringe-infiltrated. DNA was extracted by CTAB method at three dpi for AFLP assays. For qualitative GUS staining, leaf discs were collected three dpi, stained in GUS staining solution, destained with Ethanol, briefly rehydrated and dried in cellophane. For quantitative GUS assays, two leaf discs (9 mm diameter) were harvested per replicate, frozen in liquid nitrogen and lysed in a mixer mill. Tissue powder was resuspended in 300 μ l GUS extraction buffer (50 mM NaH_2PO_4/Na_2HPO_4 pH7, 10 mM EDTA, 0.1% SDS, 0.1% Triton X-100) and samples cleared by centrifugation. 10 μ l were mixed with 90 μ l extraction buffer containing 5 mM 4-methylumbelliferyl-beta-D-glucuronide (4MUG), incubated for 1 h, reactions stopped adding Na_2CO_3 , and 4MU production measured on a Tecan Plate Reader against a series of 4MU standards. 4MU production was normalized against total protein amounts of the same samples determined by Bradford assay (Roti-Quant, www.carlroth.com) as according to the manufacturer.

Plant growth conditions and infection assays

N. benthamiana plants were cultivated in a greenhouse with 16 h light period, 60% relative humidity at 24/20°C (day/night). *A. thaliana* wild type accessions Columbia and Landsberg *erecta*, and the previously published *Ler old3-1* (Tahir et al., 2013) and *Col eds1-2* (Bartsch et al., 2006) mutants were used. Arabidopsis plants were grown under short day conditions at 23/21°C and with 60% relative humidity or in a greenhouse under long day conditions. For suppression of autoimmunity, plants germinated under short day conditions (7 days) before transfer to 28/26°C (day/night). *Hpa* infection assays were done as previously described (Wagner et al., 2013).

sgRNA design

CRISPR-P (Lei et al., 2014), CasOT (Xiao et al., 2014) and the sgRNA designer tool (Doench et al., 2014) were used for selection of sgRNAs.

ACKNOWLEDGEMENTS

We thank Sylvestre Marillonnet, Nicola Patron and Vladimir Nekrasov and Sophien Kamoun for providing the Modular Cloning Toolkit (Addgene #1000000044), the Modular Cloning Plant Parts (Addgene #1000000047) and hCas9 modules (Addgene #49771 and #49770), respectively. Christine Wagner, Hannelore Espenhahn and Samuel Grimm are acknowledged for excellent technical assistance. This work and JO and JG were funded by a grant from the Deutsche Forschungsgemeinschaft to the Collaborative

Research Centre (CRC) SFB 648. MR and JStr were supported by a grant from the Deutsche Forschungsgemeinschaft (BO 1496/8-1 to JB), a grant from the European Regional Development Fund of the European Commission to JB, and by the COST action FA1208 'SUSTAIN'. The authors do not declare any conflict of interest.

SUPPORTING INFORMATION

Additional Supporting Information may be found in the online version of this article.

Figure S1. Scheme for assembly of first and second generation recipient vectors.

Figure S2. Strategies and use of polyclonal DNA preparations for the assembly RGN-coding constructs.

Figure S3. Design and functionality of the GUS-out-of-frame recombination reporter.

Figure S4. Functional validation of one step, one nuclease and second generation recipient plasmids in transient reporter assays.

Figure S5. Phenotypic isolation of candidate *dm2h* and *dm2* mutant plants.

Table S1. Plasmids used in this study.

Table S2. Sequences of *N. benthamiana* *EDS1* and *PAD4* orthologues.

Table S3. Oligonucleotides used in this study.

Appendix S1. Manual for assembly of RGN-coding constructs using pDGE vectors.

Appendix S2. Annotated vector sequences of pDGE vectors (multi-record GenBank file).

REFERENCES

- Alcazar, R., Garcia, A.V., Parker, J.E. and Reymond, M. (2009) Incremental steps toward incompatibility revealed by Arabidopsis epistatic interactions modulating salicylic acid pathway activation. *Proc. Natl Acad. Sci. USA* **106**, 334–339.
- Alcazar, R., Garcia, A.V., Kronholm, I., de Meaux, J., Koornneef, M., Parker, J.E. and Reymond, M. (2010) Natural variation at Strubbelig Receptor Kinase 3 drives immune-triggered incompatibilities between Arabidopsis thaliana accessions. *Nat. Genet.* **42**, 1135–1139.
- Bartsch, M., Gobbato, E., Bednarek, P., Debey, S., Schultze, J.L., Bautor, J. and Parker, J.E. (2006) Salicylic acid-independent ENHANCED DISEASE SUSCEPTIBILITY1 signaling in Arabidopsis immunity and cell death is regulated by the monooxygenase FMO1 and the Nudix hydrolase NUDT7. *Plant Cell*, **18**, 1038–1051.
- Belhaj, K., Chaparro-Garcia, A., Kamoun, S. and Nekrasov, V. (2013) Plant genome editing made easy: targeted mutagenesis in model and crop plants using the CRISPR/Cas system. *Plant Methods*, **9**, 39.
- Belhaj, K., Chaparro-Garcia, A., Kamoun, S., Patron, N.J. and Nekrasov, V. (2015) Editing plant genomes with CRISPR/Cas9. *Curr. Opin. Biotechnol.* **32**, 76–84.
- Boch, J. and Bonas, U. (2010) Xanthomonas AvrBs3 family-type III effectors: discovery and function. *Annu. Rev. Phytopathol.* **48**, 419–436.
- Boch, J., Scholze, H., Schornack, S., Landgraf, A., Hahn, S., Kay, S., Lahaye, T., Nickstadt, A. and Bonas, U. (2009) Breaking the code of DNA binding specificity of TAL-type III effectors. *Science (New York, NY)*, **326**, 1509–1512.
- Bortesi, L. and Fischer, R. (2015) The CRISPR/Cas9 system for plant genome editing and beyond. *Biotechnol. Adv.* **33**, 41–52.
- Botella, M.A., Parker, J.E., Frost, L.N., Bittner-Eddy, P.D., Beynon, J.L., Daniels, M.J., Holub, E.B. and Jones, J.D. (1998) Three genes of the Arabidopsis RPP1 complex resistance locus recognize distinct Peronospora parasitica avirulence determinants. *Plant Cell*, **10**, 1847–1860.
- Brooks, C., Nekrasov, V., Lippman, Z.B. and Van Eck, J. (2014) Efficient gene editing in tomato in the first generation using the clustered regularly interspaced short palindromic repeats/CRISPR-associated9 system. *Plant Physiol.* **166**, 1292–1297.
- Canver, M.C., Bauer, D.E., Dass, A., Yien, Y.Y., Chung, J., Masuda, T., Maeda, T., Paw, B.H. and Orkin, S.H. (2014) Characterization of genomic deletion efficiency mediated by clustered regularly interspaced palindromic repeats (CRISPR)/Cas9 nuclease system in mammalian cells. *J. Biol. Chem.* **289**, 21312–21324.
- Chae, E., Bombliès, K., Kim, S.T. et al. (2014) Species-wide genetic incompatibility analysis identifies immune genes as hot spots of deleterious epistasis. *Cell*, **159**, 1341–1351.
- Christian, M., Cermak, T., Doyle, E.L., Schmidt, C., Zhang, F., Hummel, A., Bogdanove, A.J. and Voytas, D.F. (2010) Targeting DNA double-strand breaks with TAL effector nucleases. *Genetics*, **186**, 757–761.
- Christian, M., Qi, Y., Zhang, Y. and Voytas, D.F. (2013) Targeted mutagenesis of Arabidopsis thaliana using engineered TAL effector nucleases. *G3: Genes - Genomes - Genetics* **3**, 1697–1705.
- Clasen, B.M., Stoddard, T.J., Luo, S. et al. (2016) Improving cold storage and processing traits in potato through targeted gene knockout. *Plant Biotechnol. J.* **14**, 169–176.
- Doench, J.G., Hartenian, E., Graham, D.B., Tothova, Z., Hegde, M., Smith, I., Sullender, M., Ebert, B.L., Xavier, R.J. and Root, D.E. (2014) Rational design of highly active sgRNAs for CRISPR-Cas9-mediated gene inactivation. *Nat. Biotechnol.* **32**, 1262–1267.
- Doench, J.G., Fusi, N., Sullender, M. et al. (2016) Optimized sgRNA design to maximize activity and minimize off-target effects of CRISPR-Cas9. *Nat. Biotechnol.* **34**, 184–191.
- Doudna, J.A. and Charpentier, E. (2014) Genome editing. The new frontier of genome engineering with CRISPR-Cas9. *Science (New York, NY)*, **346**, 1258096.
- Engler, C., Youles, M., Gruetznert, R., Ehrert, T.M., Werner, S., Jones, J.D., Patron, N.J. and Marillonnet, S. (2014) A golden gate modular cloning toolbox for plants. *ACS Synth. Biol.* **3**, 839–843.
- Fausser, F., Schiml, S. and Puchta, H. (2014) Both CRISPR/Cas-based nucleases and nickases can be used efficiently for genome engineering in Arabidopsis thaliana. *Plant J.* **79**, 348–359.
- Feng, Z., Zhang, B., Ding, W. et al. (2013) Efficient genome editing in plants using a CRISPR/Cas system. *Cell Res.* **23**, 1229–1232.
- Feys, B.J., Moisan, L.J., Newman, M.A. and Parker, J.E. (2001) Direct interaction between the Arabidopsis disease resistance signaling proteins, EDS1 and PAD4. *EMBO J.* **20**, 5400–5411.
- Feys, B.J., Wiermer, M., Bhat, R.A., Moisan, L.J., Medina-Escobar, N., Neu, C., Cabral, A. and Parker, J.E. (2005) Arabidopsis SENESCENCE-ASSOCIATED GENE101 stabilizes and signals within an ENHANCED DISEASE SUSCEPTIBILITY1 complex in plant innate immunity. *Plant Cell*, **17**, 2601–2613.
- Fu, Y., Foden, J.A., Khayter, C., Maeder, M.L., Reyon, D., Joung, J.K. and Sander, J.D. (2013) High-frequency off-target mutagenesis induced by CRISPR-Cas nucleases in human cells. *Nat. Biotechnol.* **31**, 822–826.
- Gao, Y. and Zhao, Y. (2014) Self-processing of ribozyme-flanked RNAs into guide RNAs in vitro and in vivo for CRISPR-mediated genome editing. *J. Integr. Plant Biol.* **56**, 343–349.
- Gao, Y., Zhang, Y., Zhang, D., Dai, X., Estelle, M. and Zhao, Y. (2015) Auxin binding protein 1 (ABP1) is not required for either auxin signaling or Arabidopsis development. *Proc. Natl Acad. Sci. USA* **112**, 2275–2280.
- Gao, X., Chen, J., Dai, X., Zhang, D. and Zhao, Y. (2016) An effective strategy for reliably isolating heritable and Cas9-free Arabidopsis mutants generated by CRISPR/Cas9-mediated genome editing. *Plant Physiol.* **171**, 1794–1800.
- Geissler, R., Scholze, H., Hahn, S., Streubel, J., Bonas, U., Behrens, S.E. and Boch, J. (2011) Transcriptional activators of human genes with programmable DNA-specificity. *PLoS ONE*, **6**, e19509.
- He, Z., Proudfoot, C., Mileham, A.J., McLaren, D.G., Whitelaw, C.B. and Lillico, S.G. (2015) Highly efficient targeted chromosome deletions using CRISPR/Cas9. *Biotechnol. Bioeng.* **112**, 1060–1064.
- Hsu, P.D., Scott, D.A., Weinstein, J.A. et al. (2013) DNA targeting specificity of RNA-guided Cas9 nucleases. *Nat. Biotechnol.* **31**, 827–832.
- Hyun, Y., Kim, J., Cho, S.W., Choi, Y., Kim, J.S. and Coupland, G. (2015) Site-directed mutagenesis in Arabidopsis thaliana using dividing tissue-targeted RGEN of the CRISPR/Cas system to generate heritable null alleles. *Planta*, **241**, 271–284.
- Jiang, W., Brueggeman, A.J., Horken, K.M., Plucinak, T.M. and Weeks, D.P. (2014a) Successful transient expression of Cas9 and single guide RNA genes in Chlamydomonas reinhardtii. *Eukaryot. Cell*, **13**, 1465–1469.

© 2016 The Authors.

The Plant Journal published by Society for Experimental Biology and John Wiley & Sons Ltd., The Plant Journal, (2016), doi: 10.1111/tpj.13319

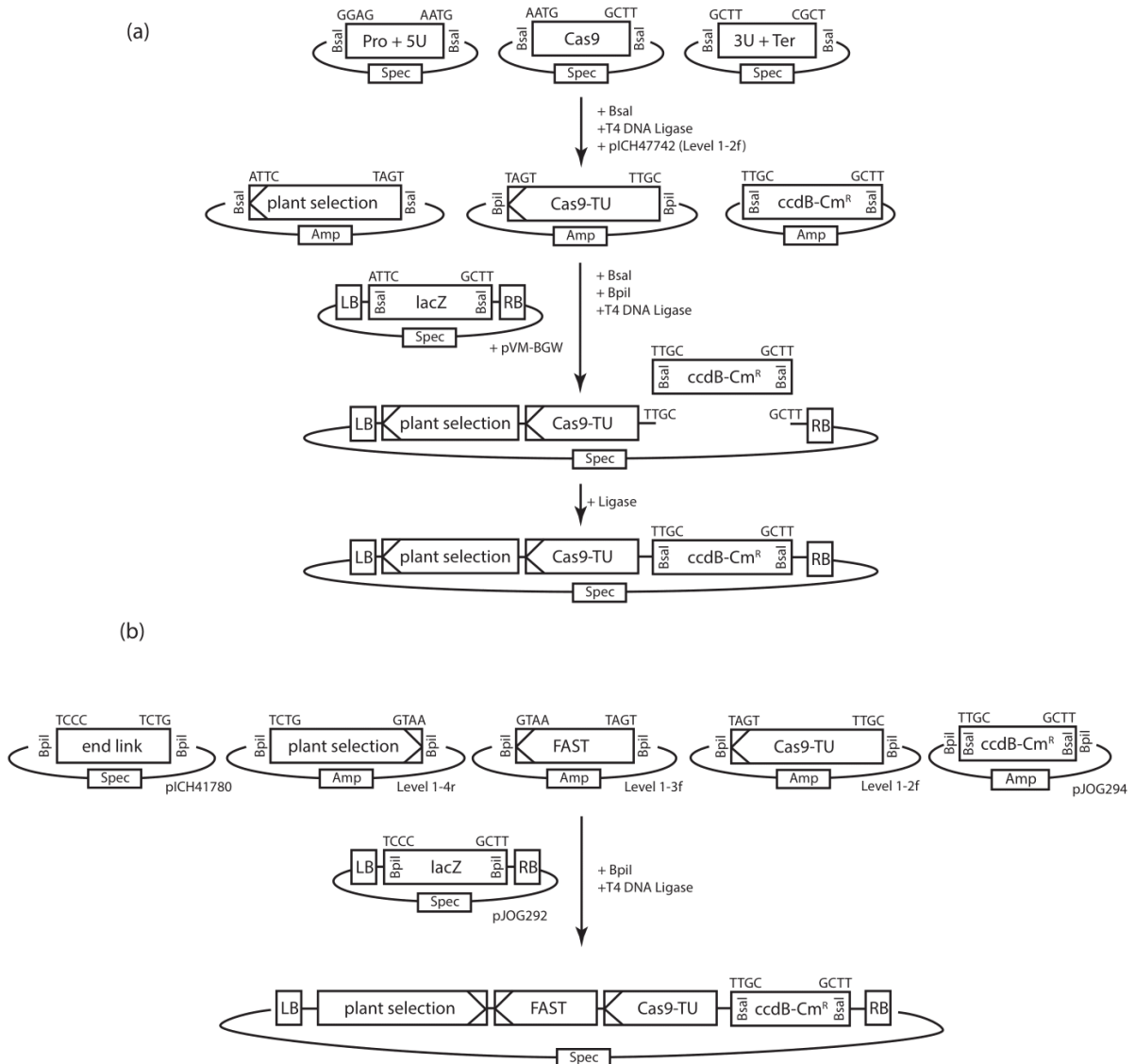
14 *Jana Ordon et al.*

- Jiang, W., Yang, B. and Weeks, D.P. (2014b) Efficient CRISPR/Cas9-mediated gene editing in *Arabidopsis thaliana* and inheritance of modified genes in the T2 and T3 generations. *PLoS ONE*, **9**, e99225.
- Jinek, M., Chylinski, K., Fonfara, I., Hauer, M., Doudna, J.A. and Charpentier, E. (2012) A programmable dual-RNA-guided DNA endonuclease in adaptive bacterial immunity. *Science (New York, NY)*, **337**, 816–821.
- Karimi, M., Inze, D. and Depicker, A. (2002) GATEWAY vectors for Agrobacterium-mediated plant transformation. *Trends Plant Sci.* **7**, 193–195.
- Kim, Y.G., Cha, J. and Chandrasegaran, S. (1996) Hybrid restriction enzymes: zinc finger fusions to Fok I cleavage domain. *Proc. Natl Acad. Sci. USA* **93**, 1156–1160.
- Lei, Y., Lu, L., Liu, H.Y., Li, S., Xing, F. and Chen, L.L. (2014) CRISPR-P: a web tool for synthetic single-guide RNA design of CRISPR-system in plants. *Mol. Plant* **7**, 1494–1496.
- Liang, J., Chao, R., Abil, Z., Bao, Z. and Zhao, H. (2014) FairyTALE: a high-throughput TAL effector synthesis platform. *ACS Synth. Biol.* **3**, 67–73.
- Lowder, L.G., Zhang, D., Baltus, N.J., Paul, J.W. 3rd, Tang, X., Zheng, X., Voytas, D.F., Hsieh, T.F., Zhang, Y. and Qi, Y. (2015) A CRISPR/Cas9 toolbox for multiplexed plant genome editing and transcriptional regulation. *Plant Physiol.* **169**, 971–985.
- Ma, X., Zhang, Q., Zhu, Q. *et al.* (2015) A robust CRISPR/Cas9 system for convenient, high-efficiency multiplex genome editing in monocot and dicot plants. *Mol. Plant* **8**, 1274–1284.
- Mao, Y., Zhang, Z., Feng, Z., Wei, P., Zhang, H., Botella, J.R. and Zhu, J.K. (2016) Development of germ-line-specific CRISPR-Cas9 systems to improve the production of heritable gene modifications in *Arabidopsis*. *Plant Biotechnol. J.* **14**, 519–532.
- Nakagawa, T., Kurose, T., Hino, T., Tanaka, K., Kawamukai, M., Niwa, Y., Toyooka, K., Matsuoka, K., Jinbo, T. and Kimura, T. (2007) Development of series of gateway binary vectors, pGWBs, for realizing efficient construction of fusion genes for plant transformation. *J. Biosci. Bioeng.* **104**, 34–41.
- Nielsen, S., Yuzenkova, Y. and Zenkin, N. (2013) Mechanism of eukaryotic RNA polymerase III transcription termination. *Science (New York, NY)* **340**, 1577–1580.
- Nissim, L., Perli, S.D., Fridkin, A., Perez-Pinera, P. and Lu, T.K. (2014) Multiplexed and programmable regulation of gene networks with an integrated RNA and CRISPR/Cas toolkit in human cells. *Mol. Cell* **54**, 698–710.
- Rehmany, A.P., Gordon, A., Rose, L.E., Allen, R.L., Armstrong, M.R., Whisson, S.C., Kamoun, S., Tyler, B.M., Birch, P.R.J. and Beynon, J.L. (2005) Differential recognition of highly divergent downy mildew avirulence gene alleles by RPP1 resistance genes from two *Arabidopsis* lines. *Plant Cell*, **17**, 1839–1850.
- Richter, A., Streubel, J., Blucher, C., Szurek, B., Reschke, M., Grau, J. and Boch, J. (2014) A TAL effector repeat architecture for frameshift binding. *Nat. Commun.* **5**, 3447.
- Schimi, S., Fauser, F. and Puchta, H. (2014) The CRISPR/Cas system can be used as nuclease for in planta gene targeting and as paired nickases for directed mutagenesis in *Arabidopsis* resulting in heritable progeny. *Plant J.* **80**, 1139–1150.
- Schulze, S., Kay, S., Buttner, D. *et al.* (2012) Analysis of new type III effectors from *Xanthomonas* uncovers XopB and XopS as suppressors of plant immunity. *New Phytol.* **195**, 894–911.
- Shimada, T.L., Shimada, T. and Hara-Nishimura, I. (2010) A rapid and non-destructive screenable marker, FAST, for identifying transformed seeds of *Arabidopsis thaliana*. *Plant J.* **61**, 519–528.
- Shirzadian-Khorramabad, R., Jing, H.C., Everts, G.E., Schippers, J.H., Hille, J. and Dijkwel, P.P. (2010) A mutation in the cytosolic O-acetylserine (thiol) lyase induces a genome-dependent early leaf death phenotype in *Arabidopsis*. *BMC Plant Biol.* **10**, 80.
- Sinapidou, E., Williams, K., Nott, L., Bahkt, S., Tor, M., Crute, I., Bittner-Eddy, P. and Beynon, J. (2004) Two TIR:NB:LRR genes are required to specify resistance to *Peronospora parasitica* isolate Cala2 in *Arabidopsis*. *Plant J.* **38**, 898–909.
- Sosso, D., Luo, D., Li, Q.B. *et al.* (2015) Seed filling in domesticated maize and rice depends on SWEET-mediated hexose transport. *Nat. Genet.* **47**, 1489–1493.
- Stuttman, J., Peine, N., Garcia, A.V. *et al.* (2016) *Arabidopsis thaliana* DM2h (R8) within the Landsberg RPP1-like resistance locus underlies three different cases of EDS1-conditioned autoimmunity. *PLoS Genet.* **12**, e1005990.
- Tahir, J., Watanabe, M., Jing, H.C., Hunter, D.A., Tohge, T., Nunes-Nesi, A., Brotman, Y., Fernie, A.R., Hoefgen, R. and Dijkwel, P.P. (2013) Activation of R-mediated innate immunity and disease susceptibility is affected by mutations in a cytosolic O-acetylserine (thiol) lyase in *Arabidopsis*. *Plant J.* **73**, 118–130.
- Townsend, J.A., Wright, D.A., Winfrey, R.J., Fu, F., Maeder, M.L., Joung, J.K. and Voytas, D.F. (2009) High-frequency modification of plant genes using engineered zinc-finger nucleases. *Nature*, **459**, 442–445.
- Wagner, S., Stuttman, J., Rietz, S., Guerois, R., Brunstein, E., Bautor, J., Niefind, K. and Parker, J.E. (2013) Structural basis for signaling by exclusive EDS1 heteromeric complexes with SAG101 or PAD4 in plant innate immunity. *Cell Host Microbe*, **14**, 619–630.
- Wang, Z.P., Xing, H.L., Dong, L., Zhang, H.Y., Han, C.Y., Wang, X.C. and Chen, Q.J. (2015) Egg cell-specific promoter-controlled CRISPR/Cas9 efficiently generates homozygous mutants for multiple target genes in *Arabidopsis* in a single generation. *Genome Biol.* **16**, 144.
- Weber, E., Engler, C., Gruetzner, R., Werner, S. and Marillonnet, S. (2011a) A modular cloning system for standardized assembly of multigene constructs. *PLoS ONE*, **6**, e16765.
- Weber, E., Gruetzner, R., Werner, S., Engler, C. and Marillonnet, S. (2011b) Assembly of designer TAL effectors by Golden Gate cloning. *PLoS ONE*, **6**, e19722.
- Wiedenheft, B., Sternberg, S.H. and Doudna, J.A. (2012) RNA-guided genetic silencing systems in bacteria and archaea. *Nature*, **482**, 331–338.
- Xiao, A., Wang, Z., Hu, Y. *et al.* (2013) Chromosomal deletions and inversions mediated by TALENs and CRISPR/Cas in zebrafish. *Nucleic Acids Res.* **41**, e141.
- Xiao, A., Cheng, Z., Kong, L., Zhu, Z., Lin, S., Gao, G. and Zhang, B. (2014) CasOT: a genome-wide Cas9/gRNA off-target searching tool. *Bioinformatics*, **30**, 1180–1182.
- Xie, K., Minkenberg, B. and Yang, Y. (2015) Boosting CRISPR/Cas9 multiplex editing capability with the endogenous tRNA-processing system. *Proc. Natl Acad. Sci. USA* **112**, 3570–3575.
- Zhang, Z., Mao, Y., Ha, S., Liu, W., Botella, J.R. and Zhu, J.K. (2015) A multiplex CRISPR/Cas9 platform for fast and efficient editing of multiple genes in *Arabidopsis*. *Plant Cell Rep.* **35**, 1519–1533.
- Zhu, S., Jeong, R.D., Venugopal, S.C., Lapchik, L., Navarre, D., Kachroo, A. and Kachroo, P. (2011) SAG101 forms a ternary complex with EDS1 and PAD4 and is required for resistance signaling against turnip crinkle virus. *PLoS Pathog.* **7**, e1002318.

2.2.2. Supplemental material to publication Ordon *et al.*, 2016

- Supplemental Figures S1 – S5 are shown below
- Additional supporting information are available online:
<https://onlinelibrary.wiley.com/doi/full/10.1111/tpj.13319>

Supplemental Figure S1 Ordon et al.

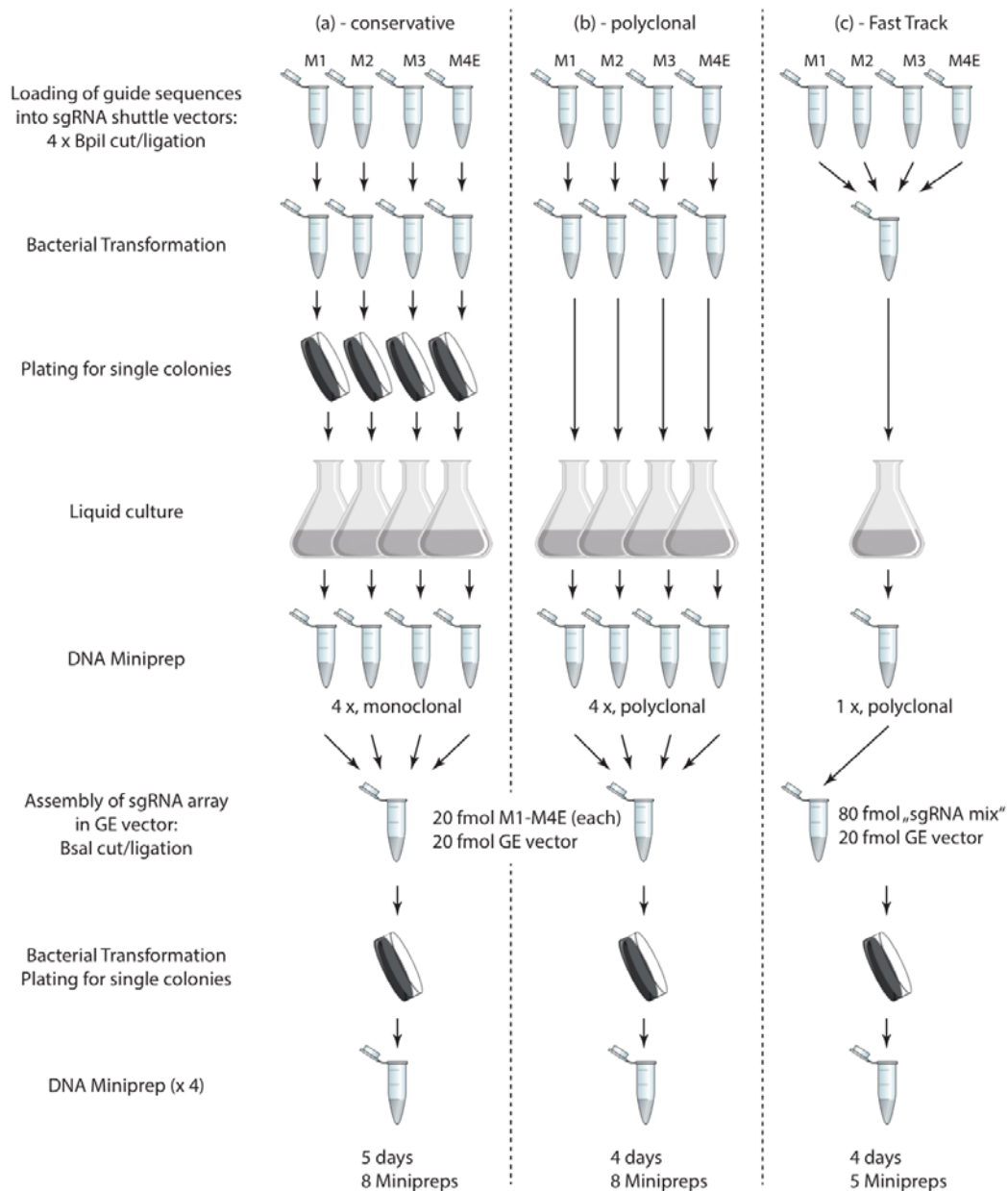


Supplemental Figure S1: Scheme for assembly of first and second generation recipient vectors

(a) Assembly of first generation recipient vectors. A Cas9 TU is assembled as a level 1-2 module according to the modular cloning standard (Weber et al. 2011). Plant-selectable markers are introduced as custom modules. Final assembly is achieved by *Bsal/Bpil* restriction and ligation, followed by a cycle of ligation. A final cycle of digestion with *XbaI* was used to reduce background.

(b) Assembly of second generation recipient plasmids. Expression cassettes for Cas9, plant-selectable marker and potentially additional modules are prepared as level 1-2, 1-3 and 1-4 modules according to the modular cloning standard. Final assembly is conducted by *Bpil* restriction/ligation of modules together with pJOG292 (vector backbone) and pJOG294 ("dummy"). A suitable end-linker (Engler et al. 2014) has to be used according to the number of level 1 modules incorporated.

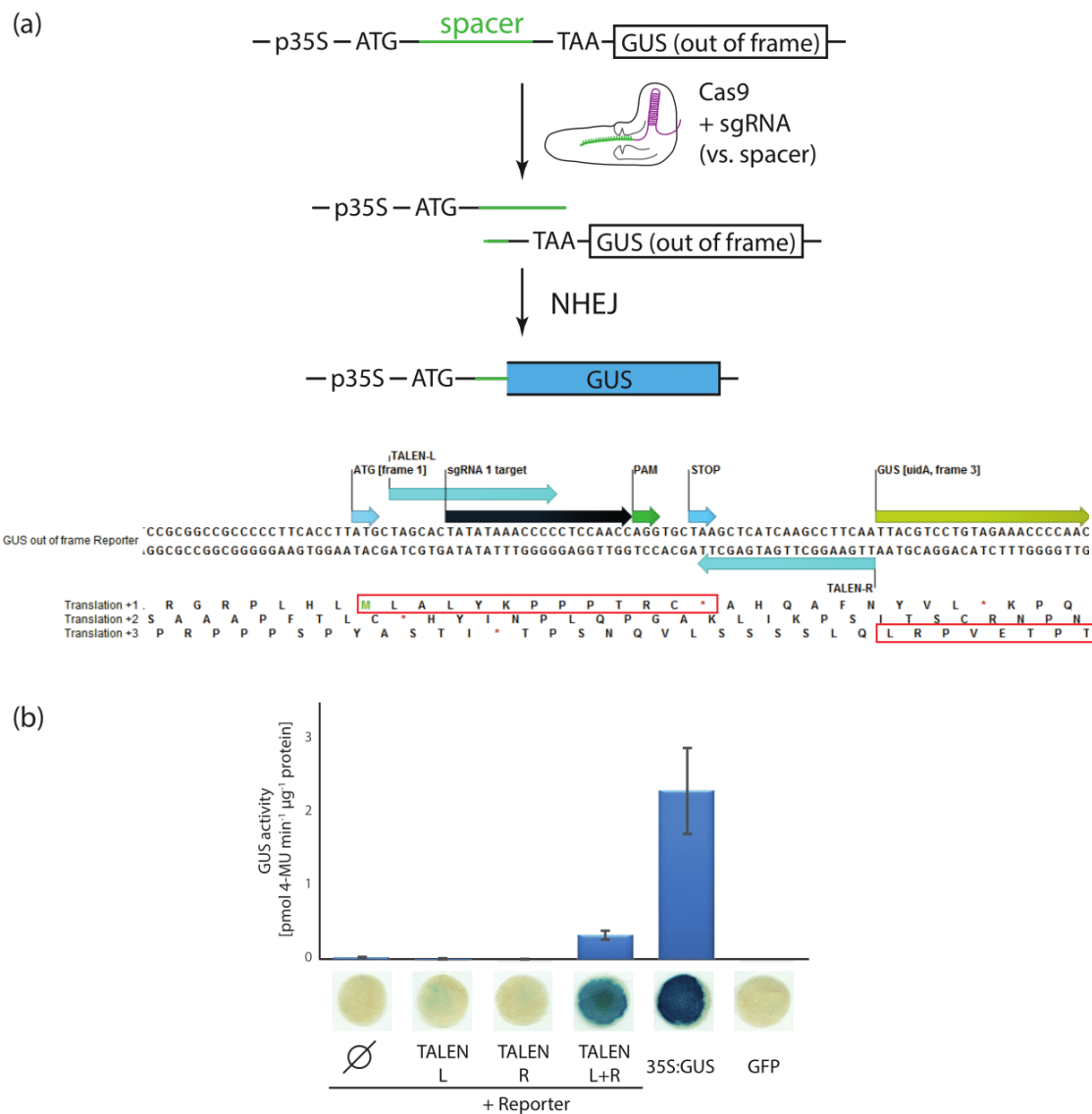
Supplemental Figure S2 Ordon et al.



Supplemental Figure S2: Strategies and use of polyclonal DNA preparations for the assembly RGN-coding constructs

In a conservative strategy, guide sequences are loaded into sgRNA shuttle vectors, and monoclonal plasmid preparations are used for the second cloning step after plating and picking of single colonies. In the polyclonal strategy, polyclonal plasmid preparations are used for subsequent cloning steps by directly inoculating liquid cultures after loading of guide sequences into shuttle vectors. Using this strategy, inconsistencies in primer synthesis are mitigated, as final assembly products are not uniform. Thus, sequencing of 2-3 final assembly products will always identify an error-free clone. Additionally, the whole cloning procedure is reduced from 5d to 4d. The Fast Track assembly scheme implies a further reduction of material expenses by combining loaded shuttle vectors in a single polyclonal culture. This approach does not allow further use of single sgRNA shuttle modules in different assemblies.

Supplemental Figure S3 Ordon et al.

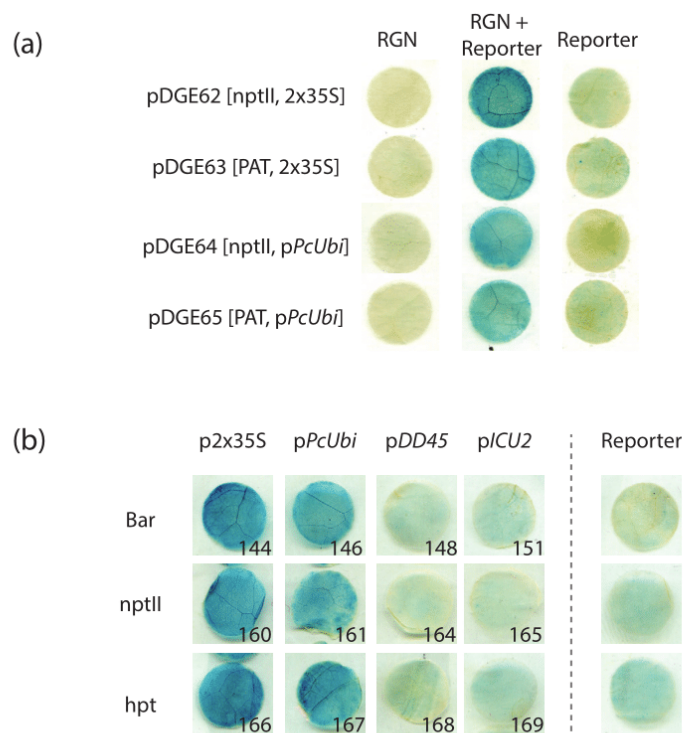


Supplemental Figure S3: Design and functionality of the GUS-out-of-frame recombination reporter

(a) General principle and sequence details of the GUS-out-of-frame reporter. A p35S-driven β-glucuronidase is shifted out of frame due to insertion of a spacer. Introduction of DSBs within the spacer sequence by RGNs or paired TALENs and its repair by NHEJ eventually reconstitutes a functional *GUS* gene. Sequence details with TALEN binding sites and the sgRNA1 target site are provided.

(b) Functionality of the GUS-out-of-frame recombination reporter. Reporter and reporter-targeting TALENs were, alone or in combination, transiently expressed in *N. benthamiana*. Leaf discs were collected at 2 dpi and used for qualitative and quantitative GUS assays. 35S:GUS and 35S:GFP were carried along as controls. Standard deviation of three biological replicates is shown.

Supplemental Figure S4 Ordon et al.

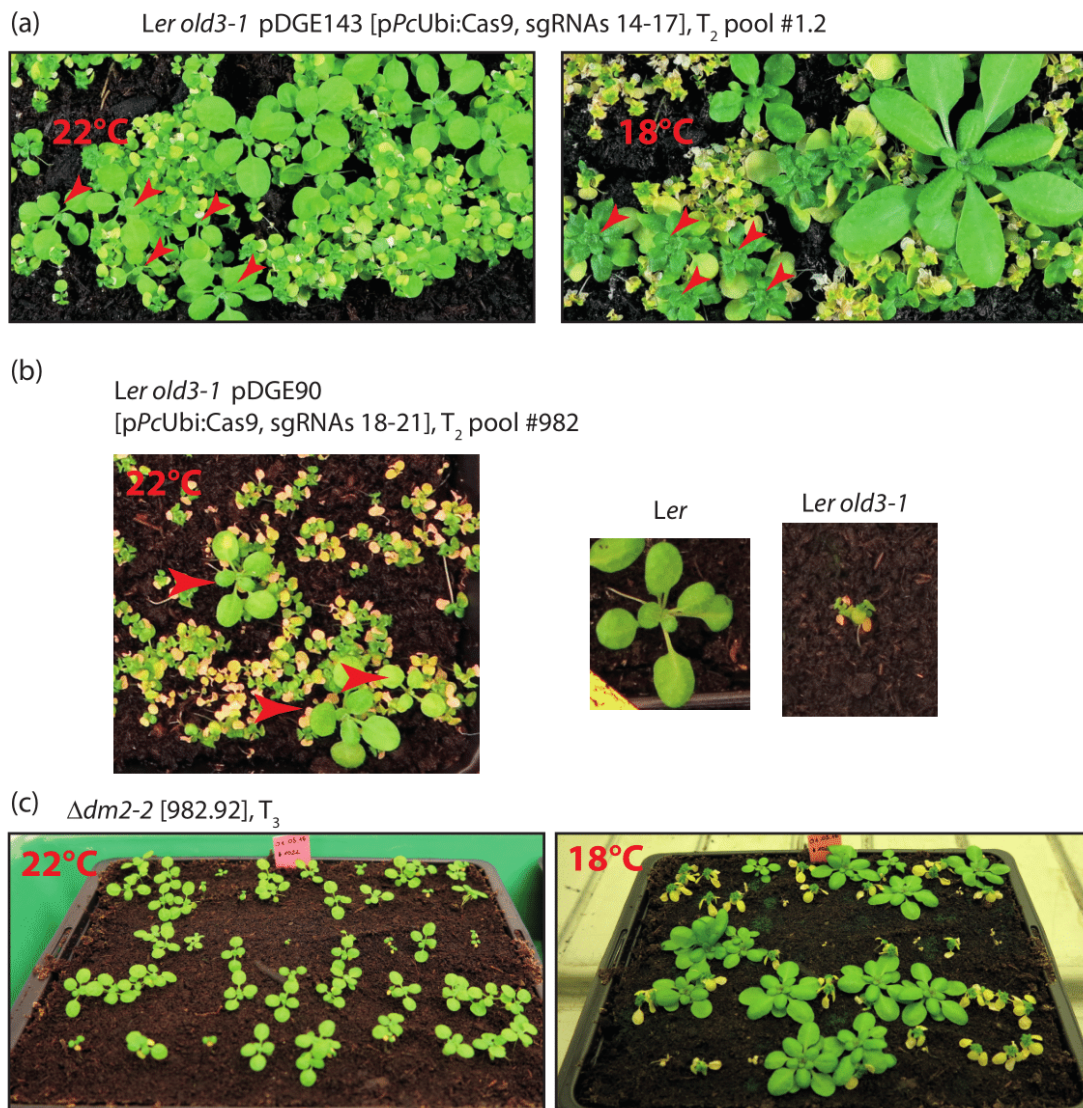


Supplemental Figure S4: Functional validation of one step, one nuclease and second generation recipient plasmids in transient reporter assays

(a) pDGE62-65 were loaded with sgRNA1 for targeting of the GUS recombination reporter. Derivatives and reporter were transiently expressed in *N. benthamiana*. Leaf discs were collected 3 dpi and subjected to qualitative GUS staining.

(b) As in (a), but derivatives of second generation recipient vectors pDGE144-169 were used, as indicated.

Supplemental Figure S5 Ordon et al.

Supplemental Figure S5: Phenotypic isolation of candidate *dm2h* and *dm2* mutant plants

(a) T₂ plants from transformation of pDGE143 (targeting *DM2h*) into the *Ler old3-1* background were cultivated for 3.5 weeks at 22°C (left panel). Non-necrotic plants obtained under these conditions represent candidate *dm2h* mutant lines containing at least one inactivating allele at the *DM2h* locus. Plants were subsequently shifted to 18°C and cultivated for additional 2 weeks (right panel), allowing survival of only plants homozygously carrying inactivating alleles at the *DM2h* locus. One putative homozygous *dm2h* mutant is visible. Arrowheads mark individuals surviving at 22°C, but with necrosis induced at 18°C.

(b) As in (a), but pDGE90 (targeting the *DM2* cluster) was used for transformation. *Ler* and *Ler old3-1* were grown alongside as controls. A representative image of pool #982 is shown.

(c) Segregation of the $\Delta dm2$ phenotype in the T₃ generation. Plants were first cultivated at 22°C for 3.5 weeks (left panel), and subsequently shifted to 18°C (right panel). Plants non-necrotic at 18°C were tested for BASTA-sensitivity by brush application of the herbicide to single rosette leaves, and re-genotyped in the T₄ generation (Figure 4e).

2.2.3. Summary of publication Ordon *et al.*, 2016

Genome editing using Cas9-based RGNs came into the spotlight in the last years. RGNs were mainly used for the induction of point mutations, which make it difficult to differentiate between edited (mutant) and wild-type individuals. Furthermore, point mutations are mostly not sufficient to disrupt functions of non-coding DNA.

We developed a genome editing toolkit with high multiplexing capacity, and used this to induce chromosomal deletions at six independent loci in *Nb* and *Arabidopsis*. Our toolkit relies on *Sp*Cas9, and the nuclease is guided to target sites by sgRNAs, representing a fusion of crRNA and tracrRNA naturally executing this activity in *Sp*. The toolkit is based on preassembled vectors containing all components on a T-DNA, except the sequence specific sgRNAs. Assembly of these “recipient” vectors is carried out following the modular cloning system. The specific sgRNA units are prepared by first ligating hybridized oligonucleotides into one out of a set of “shuttle vectors”, and are subsequently mobilized from the shuttle vectors into a recipient vector of choice. This procedure allows generating a final genome editing construct containing up to eight sgRNA transcriptional units PCR-free in only four days with maximal variability and minimal effort.

Chromosomal deletions were generated, on one hand, by targeting Cas9 to four sites within a single gene, and target sites were chosen for the generation of either two small or one large deletion within the same locus. On the other hand, certain regions within the genome were targeted for deletion by directing Cas9 to two sites flanking at either end the targeted region (four target sites in total). Analysis of mutant plants and editing events revealed that increasing the size of deletions apparently reduces their occurrence in both tested plant species, *Nb* (with mainly deletions < 100 bp observed) and *Arabidopsis thaliana* (*At*) (deletions up to 120 kb isolated, but with low frequency). Furthermore, at least in *At*, the most frequent event was the generation of independent point mutations at target sites, rather than the loss of sequence stretches flanked by target sites. In this work, *eds1* and *pad4* single mutant lines in *Nb* and *eds1* deletion mutants in *At* accession Columbia, which contains two tandemly arranged EDS1-coding genes, were generated. Furthermore, multiple lines with mutations in a complex resistance gene cluster, the *DANGEROUS MIX 2* cluster (Stuttman *et al.*, 2016), were generated.

Besides providing a comprehensive toolkit to the community and generating novel mutant lines of interest for people working on plant-pathogen interactions, we also reported on factors influencing genome editing efficiencies in plants and on workflows for the isolation of desired mutant alleles.

Part III: Plant innate immune signaling in *Solanaceae*

Introduction

3.1. The immune system of plants

Plants do not possess mobile immune cells or an adaptive immune system. Each plant cell has a repertoire of innate immune factors, and plants are further protected by systemic signals emanating from invaded tissues or nearby neighboring plants (Dangl&Jones, 2001; Ausubel, 2005). Plants evolved a two-layered immune system to protect themselves against invaders and to ensure their integrity (Jones&Dangl, 2006). Plant-pathogens have evolved diverse strategies to invade their hosts or suppress plant immunity. While many bacterial pathogens proliferate in intercellular spaces, the apoplast, fungi and oomycetes are able to build so-called haustoria to collect nutrients from the plant (Jones&Dangl, 2006). Other pathogens, like nematodes, are able to breach host cells with a stylet. Many microbial plant pathogens and also nematodes translocate effector molecules into plant cells thus increasing microbial fitness and suppressing recognition by the plant immune system. Effectors, in turn, can be recognized by the plant by so-called corresponding R (resistance) genes or proteins (Jones&Dangl, 2006). Domestication of crop plants interferes with the natural adaptation and selection to steadily diversifying pathogens, which, as a consequence, are responsible for yield losses up to 30 % in crops worldwide (Jones *et al.*, 2016).

3.1.1. PTI – a first immune layer protects against non-adapted microbes

The first immune layer provides a relatively basal or low level disease resistance. PM (plasma membrane)-localized PRRs (pattern recognition receptors) are able to detect extracellular, microbial molecules, so-called (PAMPs/MAMPs (pathogen/microbe associated molecular patterns, hereafter referred to as PAMPs) (Jones&Dangl, 2006). PRRs are divided in two classes, transmembrane RLKs (receptor-like kinases) and RLPs (transmembrane receptor-like proteins). RLPs lack an apparent intracellular signaling domain, and therefore are dependent on signaling partners (Creagh&O'Neill, 2006). The extracellular domain of PRRs often consists of a LRR (leucine-rich-repeat) domain, which detects PAMPs by direct binding (Dodds&Rathjen, 2010; Faulkner&Robatzek, 2012). PAMPs are, in most cases, molecules which are conserved across pathogenic and commensal microbes, like lipopolysaccharides, chitin, or peptides derived from the EF-Tu (elongation factor thermo

unstable) or flagellin (Macho&Zipfel, 2014; Yu *et al.*, 2017). A well-studied PAMP is flg22, which is a 22 aa (amino acid) peptide derived from flagellin. flg22 is detected by the Arabidopsis PRR FLS2 (Flagellin sensing 2) (Boller&Felix, 2009). Once flg22 is recognized, FLS2 builds an active signaling complex with the co-receptor of most PRRs, the LRR-RLK BAK1 (Brassinosteroid Insensitive 1-Associated Kinase1) (Chinchilla *et al.*, 2007). Another well-known PAMP is the cell wall component chitin. In Arabidopsis, chitin is recognized by the Lys-M (lysine-motif) domain proteins LYM1 and LYM3, which activate the Lys-M receptor-like kinase CERK1 (Miya *et al.*, 2007). The following intracellular signal transduction pathways end in a variety of immune response programs, which are qualitatively similar and independent of the PAMP/PRR combination (Bigeard *et al.*, 2015). Plant reactions are characterized by an increase of cytosolic Ca²⁺ (calcium), production of ROS (reactive oxygen species), activation of Ca²⁺-dependent and mitogen-activated protein kinases and reprogramming of gene transcription (Boller&Felix, 2009).

As shown in Figure 2A, this immune layer is called PTI (PAMP-triggered Immunity), which is a multifaceted immune response efficient against a broad spectrum of pathogenic or non-pathogenic, non-adapted microbes.

3.1.2. ETS versus ETI – a second immune layer rescues in case of effector-perception

Adapted microbes can overcome PTI by delivering so-called effector molecules (called effectors) directly into the cytosol of the host cell. One major function of pathogen effectors is the suppression of plant immune reactions. It is not known that bacterial effectors are able to passively diffuse across the plant membrane, they therefore depend on delivery systems (Büttner, 2016). One example is the T3SS (type III secretion system) present in many plant-pathogenic Gram-negative bacteria, which directly translocates T3Es (type III effectors) into the plant cytosol of the host, and effector translocation enables the pathogen to manipulate plant cellular pathways to its benefit (Büttner, 2016). The T3SS consists of an extracellular pilus-like structure. The translocon mediates the translocation by building a pore-forming complex that is able to integrate into the PM of the plant cell (Matteï *et al.*, 2011). One T3E from *Pseudomonas syringae* is AvrPtoB which acts as an E3 ubiquitin ligase and targets the flagellin receptor FLS2 for degradation through the 26S proteasome. As a consequence, *Pseudomonas* is no longer recognized by the infected plant cell (Göhre *et al.*, 2008). The suppression of recognition is called ETS (effector-triggered susceptibility), the plant cell is susceptible as shown in Figure 2B.

Plants are able to counter this virulence strategy if they possess specialized *R* (resistance) genes or proteins which are able to detect effectors. This detection enables the plant cell to

initiate a fast and effective immune reaction called ETI (effector-triggered immunity), often accompanied by programmed cell death at infection sites, the HR (hypersensitive response) (Jones&Dangl, 2006). Because most R proteins possess a central NB domain and a C-terminal LRR domain they are termed NB-LRRs, otherwise referred to as the NLR-superfamily. Effectors eliciting an ETI response are named Avr (avirulence) proteins. It has often been speculated that PTI and ETI do not necessarily function as independent, parallel systems, but rather share signaling pathways and pathogen targets (Knepper *et al.*, 2011).

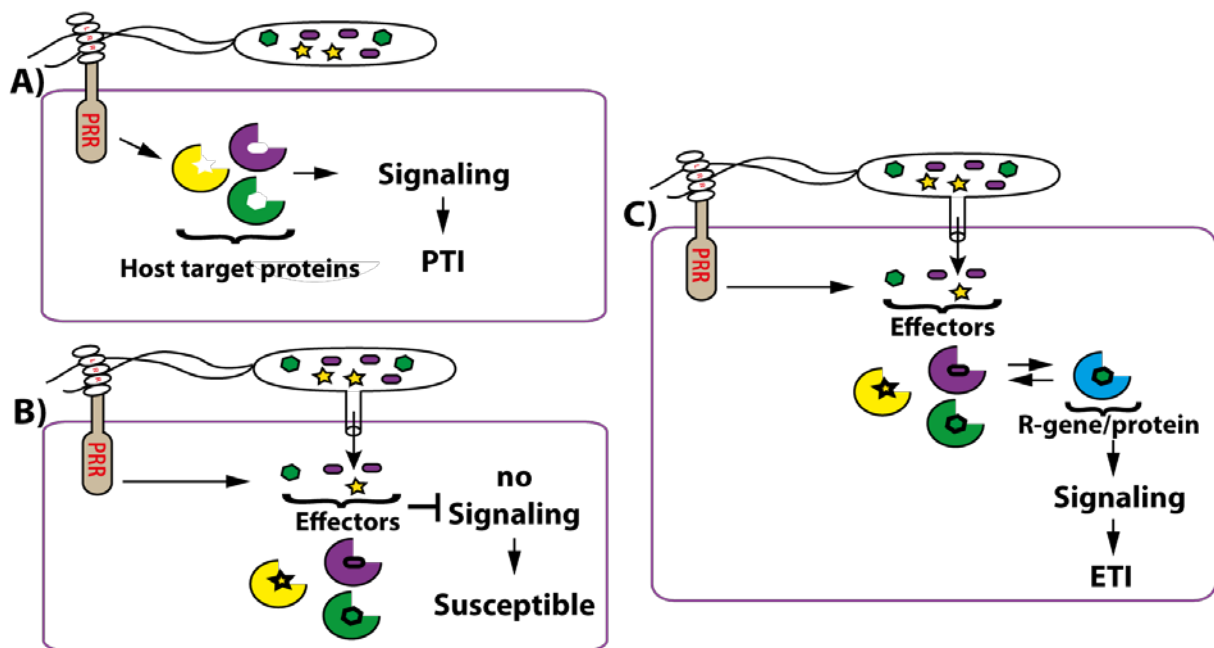


Figure 2: Interaction between plants and pathogens: susceptibility versus resistance

A) PRRs (Pattern recognition receptors) of the plant cell detect a pathogen *via* so-called PAMPs (pathogen associated molecular patterns). Defense signaling of the plant cell leads to a response reaction called PTI (PAMP-triggered immunity). **B)** Additionally to the first scheme, the pathogen is able to translocate effector molecules directly into the cytosol of the infected plant cell. Effectors interact with intracellular host target proteins and inhibit the PTI; the plant is susceptible. **C)** Additionally to B), plants possess a repertoire of R (resistance) proteins recognizing specific effectors. In case of recognition, the plant cell initiates an immune reaction called ETI (effector-triggered immunity).

3.2. NLR-type immune receptors – detection of a pathogen effector

3.2.1. NLRs – a defense strategy that developed twice?

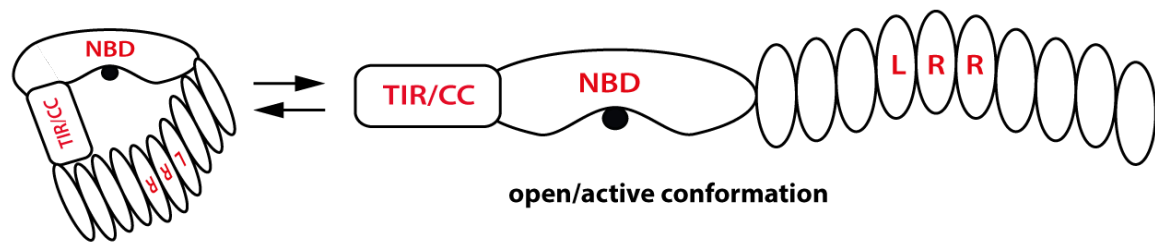
Intriguingly, both plants and animals use NLRs for innate immune reactions, but there is a debate whether the NLRs evolved from the same or distinct ancestral origins (Urbach&Ausubel, 2017; Adachi *et al.*, 2019). The prevalent hypothesis over the last decades assumed that animal and plant NLRs derived from different ancestral prokaryotic adenosine triphosphatases (ATPases) (Jones *et al.*, 2016).

Plant and animal NLRs share a similar modular domain architecture including the core NB domain and a C-terminal LRR domain, but there are critical differences at the outside N- and C-terminal domains (Jones *et al.*, 2016). The NB is part of the STAND (signal transduction ATPases with numerous domains) AAA⁺ ATPase superfamily. Typically, Walker A (p-loop) and Walker B motifs are included, which are both involved in ADP (adenosine diphosphate) binding and hydrolysis (Walker *et al.*, 1982; Leipe *et al.*, 2004). The modular architecture of the STAND proteins allows them to simultaneously act as a sensor, switch, and response factor. Plant proteins of the STAND superfamily contain either a nucleotide-binding site as well as the ARC (present in Apaf1 (Apoptotic protease-activating factor 1), R proteins, and CED4 (cell death protein 4))-domain, which is associated with two α -helical domains (Baggs *et al.*, 2017). In contrast, animal NLRs possess a different central NBD subtype, the NACHT (NAIP, CIITA, HET-E, and TP1) domain, which is associated with three α -helical domains (Koonin&Aravind, 2000). NB-ARC and NACHT are also present in fungal proteins, with various C- and N-terminal domains, but not associated with LRR domains (Dyrka *et al.*, 2014).

All NLRs or NLR-like proteins seem to have a switch-like mechanism from a suppressed to an active state, mediated by their central NB domain. Interestingly, the exchange of bound ADP to ATP (adenosine triphosphate) leads to a conformational change of the NB domain which, at least in some cases, results in an oligomerization of NLRs (Maekawa *et al.*, 2011a; Williams *et al.*, 2011). NLRs are able to hydrolyze ATP to ADP, which probably plays an important role in the regulation of NLRs into the inactive/resting state (Williams *et al.*, 2011; Jones *et al.*, 2016). In animals, NLRs can function by ligand-dependent oligomerization, which leads to an active recruitment of signaling adapters initiated by the N-terminal domain (Bentham *et al.*, 2016). NLR pathways in animals are better understood in contrast to those of plants. The structural and biochemical understanding of plant NLRs mostly originates from studies of the animal NLRs Apaf-1, as well as CED4 (Riedl *et al.*, 2005; Yan *et al.*, 2005). In plants, the C-terminal, diverse LRR domain appears to be responsible for effector detection, the central NB domain for a switch from a resting to an active state and the N-terminal domain initiates downstream signaling (Takken&Goverse, 2012).

3.2.2. Plant NLRs – modular architecture enables effector perception and downstream signaling

Plant NLRs are further divided in two subgroups either possessing a Coiled-Coil (CC) or Toll/interleukin-1 receptor (TIR) domain at the N-terminus; CC-NB-LRRs (CNLs) or TIR-NB-LRRs (TNLs) as depicted in Figure 3 and described below.



closed/inactive conformation

Figure 3: Modular structure of NLR-type R proteins

NLRs have a modular structure containing a C-terminal LRR (leucine-rich-repeat)-domain, a central NBD (nucleotide-binding domain) and a N-terminal domain either formed by a CC (coiled-coil) or a TIR (Toll/interleukin-1 receptor) domain. The central NBD comprises a pocket to bind either ADP (adenosine diphosphate) (closed conformation) or ATP (adenosine triphosphate) (open/active conformation), both imaged with a dot below the NBD.

3.2.2.1. The coiled-coil domain

The crystal structure of the CC-domain of the barley R protein Mla10 has been solved (Maekawa *et al.*, 2011a). This structure shows two CC-protomers, each with a helix-loop-helix structure, revealing a rod-shaped homodimer with autonomous folding capacities. A comparison with RPM1 (Resistance to *Pseudomonas syringae* pv. *maculicola* 1) from *Arabidopsis* which is a highly similar CNL, suggests that the CC-domain might form a dimer as well. Other CNLs, such as Lr10 from Emmer wheat, are predicted to form a helix-loop-helix structure (Takken&Goverse, 2012). Further, it has been shown that the expression of only the CC-domain of Mla10 is sufficient to trigger ETI. It is assumed that the CC-domain dimerizes in its active conformation. Dimerization, therefore, needs to be regulated, since an overexpression of only the CC-domain is able to induce a cell death reaction (Maekawa *et al.*, 2011a).

3.2.2.2. The Toll/interleukin-1-like receptor domain

The crystal structure of the TIR-domain from the TNL L6 (flax), as well as the structure of the single TIR protein AtTIR (*At* = *Arabidopsis thaliana*) (Chan *et al.*, 2010; Bernoux *et al.*, 2011), and a number of bacterial and animal TIR-domains expose two monomeric parts, building a asymmetric structure (Adamian *et al.*, 2011). Research on the flax NLR protein L6 revealed that a self-association of the TIR-domain is crucial for defense signaling. In the case of the paired NLRs AtRPS4 (Resistance to *Pseudomonas syringae* 4) and AtRRS1 (Resistance to *Ralstonia solanacearum* 1), a TIR:TIR heterodimer formation is necessary for the activation of a downstream signaling (Williams *et al.*, 2014). Furthermore, the TIR-domain alone of L6 and numerous other TNLs was shown to be sufficient to trigger HR-like cell death as described for the CC-domain (Brikos&O'Neill, 2008; Monie *et al.*, 2009; Swiderski *et al.*, 2009; Tapping, 2009; Chan *et al.*, 2010; Bernoux *et al.*, 2011).

Recently published data showed that TIR-domains in plants and animals may possess enzyme activity. NAD⁺-depletion and a NADase-activity could be shown for the mammalian TIR domain-containing protein SARM1 (sterile alpha and TIR motif containing 1) (Essuman *et al.*, 2017). For the TIR-domains of *AtRPS4* and *AtRPP1* a depletion of NAD⁺ was only observed in an *in vitro* approach, but no NAD⁺-depletion could be measured *in planta* (Horsefield *et al.*, 2019; Wan *et al.*, 2019). Based on a crystal structure of SARM1-TIR, a putative active site harboring a central glutamate residue was identified. More than 140 TIR-domains of *At* were analyzed and most of those showed this conserved active site, but this site is absent in sensor NLRs like RRS1 (Wan *et al.*, 2019). In a transient expression assay in *Nb* it was shown that the enzymatic activity is essential for TNL-mediated defense signaling as auto-active TIR-domains from *AtRPS4*, *AtRPP1* as well as an auto-active fragment of SARM1 are no longer able to induce a cell death reaction *in planta* if the respective glutamic acid residues are substituted to alanine. Nevertheless, the mechanism in plants and animals might not be the same as only the TIR-fragment of SARM1 was able to deplete NAD⁺ *in planta*. It is postulated that plants catalyze another molecule or that the depletion rate is much lower than in animals (Wan *et al.*, 2019).

3.2.2.3. The nucleotide-binding domain

The central nucleotide-binding (NB) domain of plant NLR-proteins consists of three subunits, the NB, ARC1 and ARC2 (van der Biezen&Jones, 1998). It has been shown that this domain possesses nucleotide binding and ATP hydrolysis activity (Tameling *et al.*, 2002; Tameling *et al.*, 2006; Maekawa *et al.*, 2011b). Until recently, the structurally related Apaf1, CED4 and other STAND ATPases have been consulted for homology modelling (Riedl *et al.*, 2005; Yan *et al.*, 2005; Qi *et al.*, 2010). The crystal structure of Apaf1 shows that the p-loop motif of NB-ARC is critical for ADP-binding, which is bound to the protein in a closed/inactive stage. This flexible, glycine-rich loop contains a highly conserved lysine, which is responsible for an electrostatic interaction with the β -phosphate and essential for binding to ADP (Riedl *et al.*, 2005). In plant NLRs, binding to the γ -phosphate of ATP seems to be crucial. This was shown by substitution of the highly conserved lysine, resulting in a loss of function in numerous plant NLRs (Dinesh-Kumar *et al.*, 2000; Bendahmane *et al.*, 2002; Tameling *et al.*, 2002; Bernoux *et al.*, 2011).

Another motif downstream of the p-loop, the so-called RNBSB/sensor1 motif, was proposed to be important in the differentiation of bound nucleotides *via* interaction with γ -phosphate of ATP (Ogura&Wilkinson, 2001; Takken *et al.*, 2006). Furthermore, the GxP/GLPL (aa glycine, proline, leucine) motif in the ARC1 sub-domain is assumed to act as a hinge between a

closed/inactive and a more open/active conformation of the whole protein. Structure models of the NB-ARC domain, again based on crystal structures of Apaf1 and CED4, imply that the GLPL motif stabilizes the adenosine and ribose backbone. Many LOF (loss-of-function) mutations of this motif are described, suggesting that the structural changes triggered by nucleotide exchange are essential for auto-inhibition and activation (Sueldo *et al.*, 2015).

3.2.2.4. The leucine-rich-repeat domain

In comparison to the NB, the C-terminal LRR of NLRs is assumed to vary much in structure. Several NLRs were analyzed, and based on a crystal structure of a ribonuclease inhibitor, it is assumed that the LRR-domain resembles a horseshoe-shaped structure (Takken&Goverse, 2012). Keeping in mind that this part of the protein is commonly responsible for effector detection, it is not surprising that the variations in LRR-domains are immense. These domains are highly irregular, with different repeat length and non-canonical LRR-motifs, which make it challenging to construct a high confidence, comprehensive structural model. However, such a model is available for CNL Lr10 of emmer wheat, showing a compact horseshoe-like structure which is separated in two domains. The N-terminal part contains a cluster of positively charged residues. An enrichment of aromatic amino acids, possibly involved in hydrophobic interactions, is present at the C-terminal part (Sela *et al.*, 2012). The removal or substitution of the LRR-domain can lead to a loss of sensitivity towards the cognate effector. Furthermore, it has been shown that the removal of this domain can lead to cell death caused by auto-activation for some NLRs, indicating that the LRR-domain is involved in auto-inhibition (Bentham *et al.*, 2016). If the protein is in the resting state, the three subunits form a closed nucleotide binding pocket which could be recently shown by a cryo-EM-based structure of the CNL AtZAR1 (HOPZ-Activated Resistance 1) (Wang *et al.*, 2019b). In contrast to the flexible C-terminal part of NB-domain, the LRR-domain mediates an interaction between ZAR1 and RSK1 (Resistance-related Kinase 1) which is a preformed complex, needed to induce the switch between an inactive and active state of the protein (Wang *et al.*, 2019b).

3.2.3. NLR-occurrence in plant genomes

NLR-coding genes appeared early in plant evolution. They are present in plants from mosses to 'higher' plants, including all angiosperms. Immune-related genes of plants are associated with the copy number variable regions of the genome (Baggs *et al.*, 2017). NLR copy numbers vary across species. NLR-coding genes are often organized in complex gene

clusters which are distributed asymmetrically in the genome. The size of clusters is different; the largest clusters contain more than ten NLRs (Jacob *et al.*, 2013). In rice, for example, 25 % of all NLRs are encoded on chromosome 11, and 51 % of all NLRs are resident in 41 clusters (Baggs *et al.*, 2017). The clusters can be divided in two subtypes; (i) homogenous clusters, which usually contain only one NLR-subtype (TNL or CNL) and (ii) heterogeneous clusters, containing a mixture of TNLs and CNLs. Homogenous clusters are thought to be the result of tandem duplication, whereas the heterogeneous cluster subtype has probably evolved by ectopic duplications, transpositions or large scale duplications. Such clusters might be a reservoir of genetic variation of NLRs. The size of the clusters seems to positively correlate with the frequency of transposable elements on the same chromosome, which may be involved in the evolution of NLRs, possibly by increasing genomic instability (Ameline-Torregrosa *et al.*, 2008; Li *et al.*, 2010). All processes involved in the evolution of NLRs like duplication, unequal crossing over, ectopic recombination, or gene conversion lead to a fast diversification *via* the accumulation of mutations. Because of such processes, the *NLRs* represent the most variable gene family in plant genomes (Jacob *et al.*, 2013). Increased NLR-frequencies have been associated with woody plants that have longer lifespans, which leave them behind in the evolutionary arms race. Trees possess uncommon meiosis and could therefore cope with their pathogens. An elevated number of NLRs should lead to broader pathogen recognition and more frequent recombination events. In apples, for example, a whole genome duplication 5.5-21.5 million years ago has resulted in a rapid expansion of NLRs (Jia *et al.*, 2015). Experiments show that a disposition to mutations is variable between the different domains of an NLR, probably due to selective pressure. Non-synonymous mutations are enriched in the LRR-domain in comparison to the NB-ARC-domain (Mondragón-Palomino *et al.*, 2002; Baggs *et al.*, 2017). Indeed, experimental tests demonstrated that LRR-polymorphism lead to a detection of yet unrecognized pathogens (Baggs *et al.*, 2017).

Despite their early evolution within land plant lineages, TNLs are not found in monocotyledonous species, they are only present in all higher plants except the dicot *Aquilegia coerulea* and the dicotyledonous order *Lamiales*. TNLs were probably lost in monocotyledonous and the two mentioned dicot species (Bai *et al.*, 2002; Collier *et al.*, 2011).

3.2.4. Structural re-organization of NLRs leads to activation

NLR proteins switch between a resting and an active stage. Derived from a model by Takken&Goverse (2012), the central NB-ARC domain interacts with the N-terminal part of LRR, keeping the protein in a closed, resting conformation in absence of an Avr protein. A cluster of positively charged aa in the N-terminal LRR surface seems to build an electrostatic interface with the NB-ARC domain, which stabilizes the closed, inactive conformation (Sela *et al.*, 2012). The C-terminal part of LRR seems to be exposed like an antenna, recognizing electronic charge changes in the surroundings. Structural models of the rod-shaped CC-domain as well as the more complicatedly folded TIR-domain, predict that both domains are able to interact with the NB-ARC and the LRR-domain (Takken&Goverse, 2012). The N-terminal TIR/CC-domains seem to be in direct vicinity of the C-terminal LRR-part resulting in a compact structure in case of a resting state of NLRs. In the auto-inhibited state, the NB-ARC domain is bound to ADP, in contrast to the observations that an auto-active mutant of the NLR flax M, as well as many others, has a preference to ATP, whereas the wild-type protein prefers an ADP-bound, closed state (Williams *et al.*, 2011). The perception of an effector leads to dramatic structural re-organization of the protein. Especially, the N-terminal CC/TIR and the C-terminal LRR domain change their conformation, as they were tied to the NB or ARC2 subdomains, respectively. This conformational change is mostly triggered by the LRR-sensor domain. The resulting “uncommitted” NB-ARC domain allows an exchange from ADP to ATP, which initiate the adoption of the more open and active conformation (Takken&Goverse, 2012).

A model named SCAF (signaling by cooperative assembly formation) (Bentham *et al.*, 2016) assumed that the unchallenged NLR exists in equilibrium between the closed inactive conformation, which is stabilized by ADP-binding, and an active opened conformation, with the equilibrium strongly skewed in direction of the closed inactive form (Bernoux *et al.*, 2016). In case of pathogen detection, both, the elicitor and ATP-binding, stabilize the open, active conformation. Only when ATP and elicitor are bound to the NLR, the equilibrium shifts sufficiently towards the active conformation, enabling the activation of downstream pathways. The now active protein presents new interfaces because of the conformational switch to the open state. Analogous to the human NLR pair NAIP/NLRC4, a small amount of active NLRs might induce conformational transition of further inactive NLRs to an active conformation, allowing them to oligomerize (Zhang *et al.*, 2015). This cooperative activation may lead to a fast all-or-nothing response, which is necessary under pathogen attack. This might be a key component of signal proliferation, because multiple rounds of effector recognition would not be an efficient mechanism, and probably too slow to counteract a pathogen infestation (Bentham *et al.*, 2016).

Recently published results show for the first time the biomolecular mechanism and reconstitution after activation of the plant CC-NLR protein ZAR1 of *At* (Wang *et al.*, 2019a). It was known that ZAR1 built distinct preformed immune receptor complexes and interacts with various members of the subfamily XII of RLCKs (receptor-like cytoplasmic kinases). These complexes specifically detect bacterial effectors (Wang *et al.*, 2015). The authors described a stepwise activation. In an auto-inhibited resting state, ZAR1 is monomeric, ADP-bound and in complex with the RLCK RKS1 (Resistance related kinase 1). The corresponding elicitor of ZAR1, AvrAC, is indirectly recognized *via* the protein kinase PBL2 (PBS-1 like protein 2), which is uridylated by AvrAC. PBL2^{UMP} then binds to ZAR1-RKS1 and together they build an intermediate conformation which releases ADP. This release exposes the NB-site which will, together with dATP/ATP (d = deoxy), end in the oligomerization to a wheel-like pentameric complex containing ZAR1, RKS1 and PBL2^{UMP} (Wang *et al.*, 2019b), the so-called resistosome.

Furthermore, it was shown that after oligomerization the N-terminal α -helices of the CC-domain build a funnel-shaped structure that protrudes out of the wheel-defined pentameric plane. The conformational change after oligomerization to a funnel-shaped sequestered structure of the N-terminal CC-domains leads to an association with the PM. This association to the PM is essential to elicit an HR but is dispensable for the assembly of the oligomeric ZAR1 resistosome-complex (Wang *et al.*, 2019a). Most of the CC-domain is substantially buried, only the funnel-shaped structure sticks out which is formed by the oligomerized N-terminal amphipathic α 1 helix. Interestingly, the inner surface of the funnel-shaped structure contains several negatively charged residues. A substitution of two of these residues significantly reduces a ZAR1-mediated HR but did not affect the AvrAC-induced association with the PM, suggesting that PM-association might be required, but is not sufficient to trigger an immune response (Wang *et al.*, 2019a). Thus, the pore-like interior of the funnel-shaped structure appears essential for ZAR1-mediated immunity, and it was proposed that the resistosome may act as an ion channel to alter charge of the penetrated cell. This is a common phenomenon, observed after a recognized pathogen attack in plants. The Ca²⁺ concentration is rapidly elevated and is therefore an important second messenger in plant immunity (Zhang *et al.*, 2014). Interestingly, the fold-switch to the resistosome after activation is reminiscent of membrane pores and ion channels which are made during pathogen-induced cell death in animals and fungi (Cai *et al.*, 2014; Adachi *et al.*, 2019; Wang *et al.*, 2019a). The mechanistic and structural similarities between NLRs of animals, fungi, and plants argue more towards a mutual evolutionary origin of multi-domain ATPases, rather than the previously proposed independent evolutionary origin (Urbach&Ausubel, 2017; Adachi *et al.*, 2019).

3.2.5. Effector Recognition

Recognition of a pathogen effector is commonly mediated by the LRR domain of the NLR (Takken&Goverse, 2012). Plants are generally under high pressure to detect a large amount of different effectors while simultaneously maintaining their own integrity (Stavrinos *et al.*, 2008; Ravensdale *et al.*, 2011). Functional analysis reveals a diverse localization, activation, and signaling of plant NLRs to fulfill this task. The direct interaction between an effector and the NLR is possible, but might only occur less frequent (Dangl *et al.*, 2013). NLR responses can require a pair of NLR proteins, in which one senses an elicitor (sensor) whereas the other one is responsible for the activation of the downstream pathway (helper) (Peart *et al.*, 2005; Sarris *et al.*, 2016). One example is resistance to Tobacco Mosaic Virus in tobacco, which requires the sensor TNL protein N and the helper CNL NRG1 (N requirement gene 1) (Peart *et al.*, 2005). However, the reliance on NRG1 could be a general phenomenon of other TNLs as well. In absence of NRG1, the TNLs Roq1 (Recognition of XopQ 1) and RPP1 (Recognition of *Peronospera parasitica* 1) are also unable to induce a cell death reaction after effector recognition (Qi *et al.*, 2018), but downstream signaling is not affected in absence of NRG1, as long as the sensor NLR is classified to the CNL subclass (Wu *et al.*, 2019).

Direct interaction between effector and (sensor)-TNL is sufficient to trigger a defense reaction for several plant NLRs (Dodds *et al.*, 2004; Dodds *et al.*, 2006; Krasileva *et al.*, 2010), but exclusive reliance on direct detection of specific effectors by individual NLRs would represent an insurmountable challenge due to the large number and diversity of effectors. The NLRs, encoded only in the germline of plants, would not be able to diversify as fast as pathogens with their much shorter lifespan (Baggs *et al.*, 2017). It seems more parsimonious to 'guard' an effector target, rather than to evolve new, specific R proteins for each effector. Such scenario of indirect effector recognition has indeed been shown to exist frequently (Kourelis&van der Hoorn, 2018). If the NLR recognizes effector-mediated modifications of a host target protein (guardee), it is called a guard NLR. In another scenario, the NLR protein detects modifications of a decoy protein that mimics a true effector target protein. These decoy proteins only exist to enable indirect NLR detection of effectors, and have lost their initial biological function. Indirect recognition had evolved to enable the plant to detect a wide variety of effectors with only a limited repertoire of NLRs (ca. 200 in *Arabidopsis* and ca. 460 in rice). For instance, RIN4 (RPM1 interacting protein 4) gardeed protein is targeted by four bacterial effectors and is guarded by two independent NLRs (Cesari, 2018). The easiest way for pathogens to avoid detection in the host cell is altering the effector recognized directly by a NLR. However, in the guard/decoy model altering of the

effector would not be successful, as this alteration could interfere with the targeting of specific host proteins (Cesari, 2018).

3.2.6. Integrated domains – a sophisticated strategy of NLRs

The discovery of unusual domains integrated into NLRs revealed an additional degree of complexity in ETI defense mechanisms. Analyses of the so-called IDs (integrated domains) unraveled their essential function within the NLRs, which led to the development of the integrated decoy model (Cesari *et al.*, 2014). As classical decoy proteins, IDs originate from the duplication of effector target genes, which are then integrated into *NLR* genes, resulting in NLRs with an effector target site. In rice, for example, the integrated HMA (heavy metal associated) domain of the NLR Pik-1 interacts with a pathogen effector, thereby activating resistance programs (Cesari *et al.*, 2014; Maqbool *et al.*, 2015). Similarly, the HMA domain-containing protein Pi21 is necessary for the susceptibility to the rice blast fungus, supporting the hypothesis that the HMA domain integrated into Pik-1 represents a decoy derived from the original effector target. In a similar scenario, the effectors PopP2 and AvrRps4 target WRKY TFs (transcription factors) in Arabidopsis, and an integrated WRKY decoy domain found within the NLR RRS1 is required for detection of these effectors (Deslandes *et al.*, 2003; Le Roux *et al.*, 2015; Sarris *et al.*, 2015). Based on the integrated decoy model, higher plant- and moss-genomes were analyzed for the occurrence of IDs (Kroj *et al.*, 2016; Sarris *et al.*, 2016). The overall frequency of unusual domains integrated into NLRs was estimated to be 3.5 %. These unusual domains are present in all plant lineages and in all major groups of NLRs. The domains identified were extremely diverse in function and the integrated position within the NLRs differs. This phenomenon indicates that an integration of unusual domains has appeared frequently and repeatedly in plant evolution (Cesari *et al.*, 2014; Kroj *et al.*, 2016).

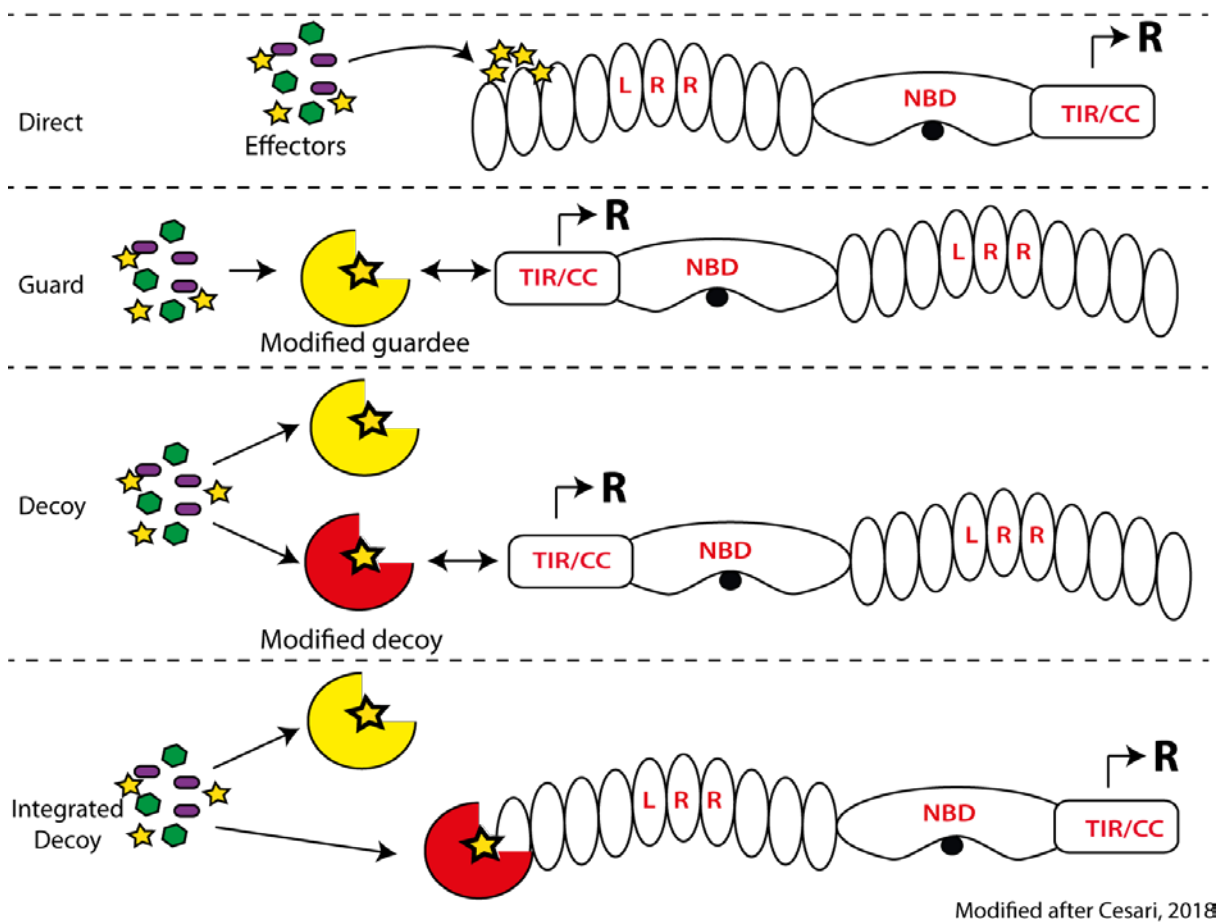


Figure 4: Pathogenic effector detection by different types of NLRs

Pathogenic effectors can be recognized directly as depicted in the upper part. The interaction induces a resistance (R). Indirect recognition of an effector occurs when target proteins of an effector are guarded by an NLR. The guarded protein is called guardee. Another possibility is a duplication of effector target genes which evolves into decoy proteins and are monitored by NLRs. In both cases, the NLRs are detecting modifications of the targets (guardee or decoy). However, decoys could be also integrated into the structure of the NLRs, enabling effector detection *via* direct binding.

3.3. Signaling Downstream of NLRs

The precise nature of events associated with defense outputs after perception of a pathogen molecule is not fully understood. Downstream of the activation of an NLR, one can observe two distinct signaling pathways, depending on the N-terminal domain of the NLR. While many CNLs require the plasma membrane-associated protein NDR1 (Non-race specific disease resistance 1) for downstream signaling, all tested TNLs are strictly dependent on the nucleocytoplasmic lipase-like protein EDS1 (Enhanced disease susceptibility 1) as shown in Figure 5 (Aarts *et al.*, 1998). As central regulators of NLR-mediated defense signaling, NDR1 and EDS1 represent critical nodes essential for the activation of plant resistance.

3.3.1. EDS1-family proteins are essential for at least TNL-mediated resistance

EDS1 was first identified in *At* in a screen for mutants defective in RPP1- and RPP5-specified resistance to isolates of the oomycete *Hpa* (*Hyaloperonospora arabidopsidis*) (Parker *et al.*, 1996). Further analysis of *eds1* mutant Arabidopsis plants revealed defects in basal immunity to virulent isolates of *Hpa* and *Erysiphe pisi* (obligate biotrophic fungus) (Wiermer *et al.*, 2005). Furthermore, susceptibility to *Pst* (*Pseudomonas syringae tomato* DC3000) and *P. syringae maculicola* was observed (Wiermer *et al.*, 2005). These observations indicated that EDS1 plays a central role in basal and TNL-dependent immunity in *Brassicaceae* (Wiermer *et al.*, 2005).

Interactor screens revealed that EDS1 builds heterocomplexes with PAD4 (Phytoalexin deficient 4) and SAG101 (Senescence-associated gene 101), respectively (Feys *et al.*, 2001; Feys *et al.*, 2005). Phylogenetic analyses revealed that *EDS1*, *PAD4*, and *SAG101* genes are present in the genomes of flowering plants, but not in the moss *Physcomitrella patens* or algae. Moreover, genes encoding SAG101 orthologous are missing in the genomes of monocots and in of *Aquilegia coerulea* or *Mimulus guttatus* eudicot genomes (Wagner *et al.*, 2013). Interestingly, the latter plants lack TNLs in general as well as members of the NRG1-family of NLRs with an atypical RPW8-CC domain (Collier *et al.*, 2011; Qi *et al.*, 2018). A wider presence of *EDS1* and *PAD4* is hypothesized to be linked to their role in basal immunity, and the co-occurrence of *SAG101* with TNL coding genes and *NRG1* in eudicot lineages implies a role in ETI immune signaling (Wagner *et al.*, 2013). Both proteins, PAD4 and SAG101, are similar in sequence to EDS1, and all three share an N-terminal homology to eukaryotic lipases (α/β -hydrolases). C-terminally, they all contain an EP (EDS1-PAD4) domain with no significant homology to non-plant proteins. The highly conserved EP domain occurs only in plants, and in combination with the lipase-like domain, these characteristics define the EDS1-protein family (Wagner *et al.*, 2013).

Furthermore, a motif with the typical appearance of a catalytic SDH triad including the characteristic GX SXG motif was observed within the lipase-like domain of EDS1 and PAD4, but is lost in SAG101. In spite of the conserved hydrolase domain in EDS1 and PAD4 orthologous, no enzymatic activity was observed for *At*EDS1. Neither full length *At*EDS1 nor the lipase-like domain alone (*At*EDS1¹⁻³⁸⁴) were able to hydrolyze p-nitrophenol esters *in vitro* when tested (Wagner *et al.*, 2013). Additionally, the catalytic activity is not required for the immune function of the proteins in *At*: substitution of the respective aa (SDH->AAA) of the catalytic triad in *At*EDS1 and simultaneous substitution of the critical S (serine) in *At*PAD4 (S118A) did not impair immune capacities of the respective proteins (Wagner *et al.*, 2013). This suggests a structural rather than an enzymatic role for the lipase-like domain (Wiermer *et al.*, 2005). However, binding of a metabolite to EDS1 and/or PAD4 may still occur, and a

similar mechanism was reported for several α/β -hydrolase-based hormone receptors, such as GID1 or KAI2 (Mindrebo *et al.*, 2016).

The crystal structure of the heterodimer *AtEDS1-AtSAG101* provided new insights to structure and function of EDS1-based heterocomplexes. Based on this crystal structure, a model of *AtEDS1-AtPAD4* complex was derived, and it was demonstrated that EDS1 builds mutually exclusive heterodimers with PAD4 and SAG101, respectively. These dimers differ in their ability to mediate both basal and TNL-mediated immune responses. Whereas a LOF of *AtSAG101* (*sag101* mutant plants) is largely recovered by the EDS1-PAD4 heterocomplex, a LOF of *pad4* leads to decreased defense reactions (Feys *et al.*, 2005; Wagner *et al.*, 2013). Furthermore, double mutants of the heterocomplex partners (*sag101 pad4*) as well as a single *eds1* mutant are indiscernible in their immune response, and are both fully defective for TNL-mediated immune responses (Feys *et al.*, 2005).

Localization studies of EDS1 and PAD4 in *Arabidopsis* show an equal distribution of proteins between the cytosol and the nucleus when expressed alone or during co-expression (Feys *et al.*, 2005). In contrast, SAG101 was solely detected in the nucleus, and in co-expression with EDS1, stronger nuclear EDS1-accumulation was observed, indicating that SAG101 draws EDS1 into the nucleus (Feys *et al.*, 2005). When all three EDS1-family members are co-expressed, PAD4 is able to disrupt the nuclear localization and retain some EDS1 in the cytosol as summarized in Figure 5B. Furthermore, it was shown that the expression level of *SAG101* is relatively low, even after a pathogen stimulus in comparison to *EDS1* and *PAD4* (Zhu *et al.*, 2011). This suggests that relative levels of PAD4 and SAG101 may drive the subcellular localization of EDS1 in response to active defense signaling (Zhu *et al.*, 2011).

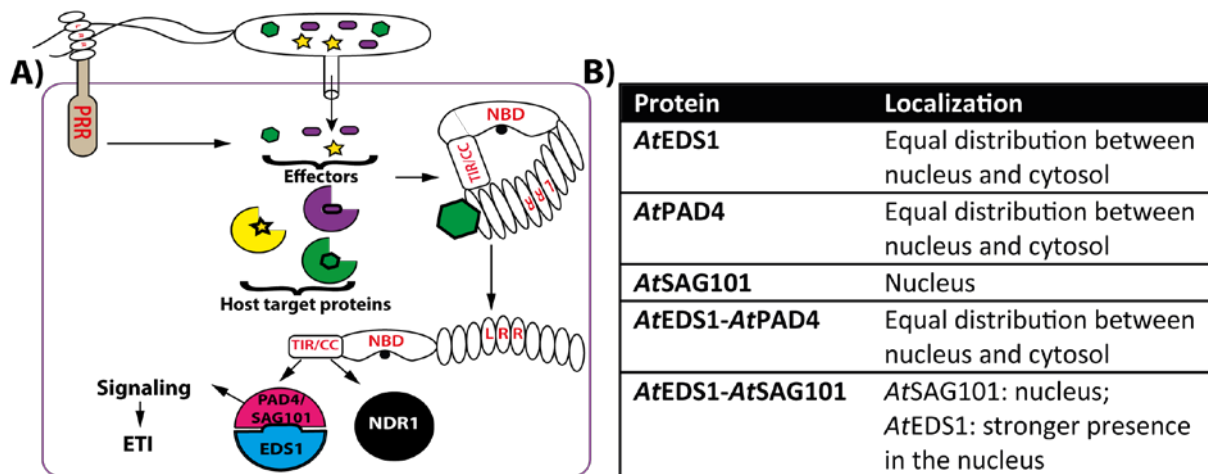


Figure 5: Role of EDS1-based heterocomplexes in TNL-mediated immunity and its localization

A) PAMPs (here falgellin) recognized by PRRs are not able to induce a PTI reaction, because the pathogen delivers effectors into the cytosol of the host cell which interact with host target proteins and thereby suppress PTI. A specific NLR R protein is able to detect one specific effector (green). The NLR changes its conformation to an open, and active state. An NLR containing a N-terminal CC-domain requires NDR1 (Non-race specific disease resistance 1), whereas an NLR with an N-terminal TIR domain are functionally dependent on EDS1 (Enhanced disease susceptibility 1)-based heterocomplexes. A induction of ETI will follow upon activation. **B)** Localization of EDS1-family proteins PAD4 (Phytoalexin deficient 4) and SAG101 (Senescence associated gene 101) of *At* (*Arabidopsis thaliana*) either singly or co-expressed *in planta*.

Additionally, it has been proposed that the inability of SAG101 to fully complement a missing PAD4 may be due to its nuclear localization (Feys *et al.*, 2005). EDS1-based complexes are probably also needed in the cytosol or the mobility between the compartments could be important, as was shown for another plant defense regulator, NPR1 (Nonexpressor of pathogenesis-related genes 1), which controls basal and systemic resistance (Mou *et al.*, 2003; Feys *et al.*, 2005). However, at least the nuclear accumulation of EDS1 is critical for defense-mediated transcriptional reprogramming during ETI, indicating an important EDS1 nuclear function in resistance (Garcia *et al.*, 2010). Interestingly, the OE (overexpression) of *AtEDS1* does not trigger an autoimmune phenotype even if this OE is solely directed to the nucleus *via* a NLS (nuclear localization signal). An exception is represented by the *Arabidopsis* accession *Ler* (*Landsberg erecta*). This line contains the TNL gene cluster *DM2^{Ler}* (*Dangerous Mix2*), and expression of an EDS1-YFP^{NLS} (yellow fluorescent protein fused with a NLS) fusion with enforced nuclear localization leads to autoimmunity in this genetic background (Stuttman *et al.*, 2016). Also, it was reported that OE of the complex *AtEDS1-AtPAD4* leads to autoimmunity resulting in a dwarf phenotype and amplified immunity in general, which is not the case for OE of only *AtEDS1* (Cui *et al.*, 2016). More importantly, minimal accumulation of EDS1 seems to be sufficient for a proper defense signaling (Garcia *et al.*, 2010; Heidrich *et al.*, 2011; Stuttmann *et al.*, 2016).

Interaction studies showed that EDS1, but not SAG101, co-immunoprecipitates with myc-PAD4 (as well as with myc-SAG101) (Feys *et al.*, 2005). However, a ternary

AtSAG101-AtEDS1-AtPAD4 nuclear complex was shown in a pulldown experiment as well (Zhu *et al.*, 2011). This ternary complex could potentially represent another active signaling form, but is not supported by structural data (Wagner *et al.*, 2013). *AtEDS1* is also able to self-associate at least in Y2H (yeast-two-hybrid) assays, but homodimerization does not play any role in basal or TNL-triggered immunity since the absence of the heterocomplex partners *PAD4* and *SAG101* leads to abolished resistance. Moreover, an *EDS1-EDS1* interaction *in planta* could not be proved (Feys *et al.*, 2005; Wagner *et al.*, 2013). This is supported by a GST (glutathione S-transferase) pulldown assay, which could not show any homodimerization of *AtEDS1 in vitro* (Li *et al.*, 2019). Recently, it was shown that the heterocomplex formation of *EDS1*-based complexes itself is essential for resistance signaling. The crystal structure of *AtEDS1-AtSAG101* and modelling of the *AtEDS1-AtPAD4* heterocomplex revealed a large interface including residues of the lipase-like and the EP domains. Mainly hydrophobic interactions between the α H-helix of *AtEDS1*, which fits neatly into a pocket of *AtSAG101* or *AtPAD4*, constitute the N-terminal complex interface, which is essential for driving heterocomplex formation (Wagner *et al.*, 2013). Quadruple aa exchanges to alanine of *AtEDS1* within this helix (in *AtEDS1-LLIF*) lead to a loss of heterocomplex formation, and abolish resistance signaling (Wagner *et al.*, 2013). The C-terminal interface formed by parallel aligned α -helices of the adjacent EP domains has little contribution to overall complex formation, and its importance remains yet to be revealed.

Physical interaction of *EDS1* with several TNLs was reported. The discovery that TNLs directly interact with *EDS1* led to the provoking hypothesis that *EDS1* might actually represent a guard of many, if not all, TNLs (Zhu *et al.*, 2010; Bhattacharjee *et al.*, 2011). In turn it may be that the intrinsic basal resistance signaling of *EDS1* was then co-opted for ETI (Heidrich *et al.*, 2011). This means that some TNLs guard *EDS1 via* the binding of effectors which normally interact with *EDS1* in order to block basal resistance. In turn the activated TNLs interact with *EDS1* and induce a boost to the PTI-associated defense pathway, now called ETI (Heidrich *et al.*, 2011).

3.3.2. Helper NLRs – a common feature of TNLs?

The different signaling branches of ETI, the CNL (dependent mostly on *NDR1*) and the TNL (*EDS1*-dependent) pathways, might work additively and therefore boost a defense response. As another possibility, *EDS1* might contribute to resistance mediated by some CNLs as well. CNLs with atypical CC-domains, carrying a *RPW8*-like (Resistance to Powdery Mildew 8) CC-domain are known to act as helper NLRs and therefore interwork with TNLs. For example, CNLs of the *ADR1* (Activated Disease Resistance)-family act downstream of some

CNL (RPS2) and TNL (RPP2, RPP4, SNC1, CHS2) immune receptors (Dong *et al.*, 2016). The same is true for the CNL NRG1 (N required resistance1) which is required for several TNL-mediated signaling pathways, like Roq1, RPP1 or N, but not for CNLs like RPS2 or Bs2 (Peart *et al.*, 2005; Collier *et al.*, 2011; Shao *et al.*, 2016; Qi *et al.*, 2018; Castel *et al.*, 2019; Wu *et al.*, 2019). This observation and the fact that NRG1 is only present in plants possessing TNLs leads to a hypothesis of the common requirement of NRG1 for TNL immune signaling (Qi *et al.*, 2018).

3.3.3. Salicylic acid and systemic required resistance – staying alive *versus* apoptosis

Resistance signaling is not generally associated with cell death, but can in some cases lead to restriction of pathogen growth without observable symptoms. Plants may therefore be able to tune subcellular defense pathways in order to attack a pathogen penetration in the most effective way and simultaneously preserve the integrity of the plant. Besides the initiation of PCD (programmed cell death), for instance triggered by an EDS1-dependent downregulation of DNA repair machinery and coincidentally an increase of damaged DNA (Rodriguez *et al.*, 2018), the plant cell is also able to induce SAR (Systemic Acquired Resistance) which is triggered by local and systemic accumulation of the phytohormone SA (salicylic acid) (Fu&Dong, 2013). SA is produced in the chloroplast *via* ICS1 (isochorismate sythetase 1) upon local infection (Wildermuth *et al.*, 2001). An accumulation of SA leads to cellular redox reactions and thus to a nuclear translocation of the normally cytosolic, homodimeric NPR1 (Mou *et al.*, 2003). High concentrations of SA close to the infection site promote NPR3/NPR4-dependent NPR1-degradation which in turn activate PCD (Fu *et al.*, 2012). In the neighboring areas the intermediate SA-concentration do not promote NPR1-NPR3 binding, resulting in an accumulation of NPR1 monomers in the nucleus. Nuclear NPR1 is able to interact with TFs to promote the activation of endoplasmatic-reticulum-genes, the expression of antimicrobial PR (pathogenesis related) genes, and the resistance to secondary infection (Fu *et al.*, 2012; Fu&Dong, 2013). Interestingly, beside NPR1 degradation, NPR3 and NPR4 negatively regulate the stability of EDS1 by functioning as a CUL3 (Cullin3)-based E3 ligase adaptors to mediate EDS1 degradation by the 26S proteasome (Chang *et al.*, 2019). In summary, the concentration of SA is crucial for choosing between staying alive or initiating HR which would result in apoptosis.

It was shown that *AtEDS1* and *AtPAD4* are able to facilitate *ICS1* gene expression leading to an accumulation of SA as a part of an amplifying loop in basal and TNL-immunity in *Arabidopsis* (Wiermer *et al.*, 2005). Intriguingly, besides the ability of *AtEDS1-AtPAD4* to bolster SA-concentration, the heterocomplex works with ICS1-generated SA in parallel (Cui

et al., 2016). A major *AtEDS1-AtPAD4* function seems to be independent of ICS1-generated SA. It is proposed that this additive mechanism is important to cover immune signaling in loss of one pathway, for instance by an inactivation of SA-signaling caused by an effector (Cui *et al.*, 2016).

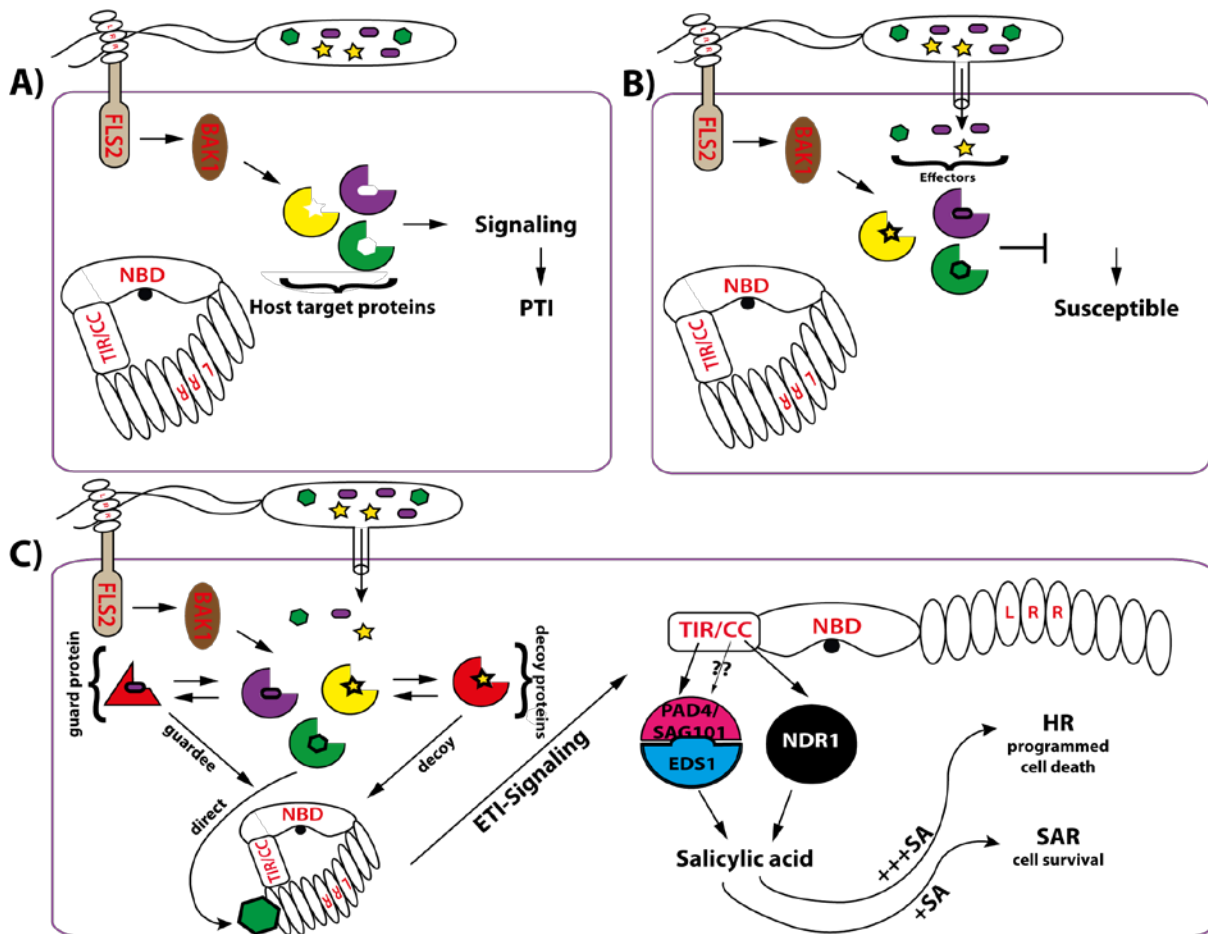


Figure 6: Communication of plant and pathogen

A) Example of perception of a non-adopted bacterial pathogen. The pattern recognition receptor (PRR) FLS2 recognizes flagellin of the flagellum of the pathogen. FLS2 is activated and interacts with BAK1 (Brassinosteroid Insensitive 1-associated kinase 1). A signaling cascade is activated, resulting in a defense reaction called PTI. **B)** Example of an adopted microbe without perception of an NLR. The same pathogen attack as in a), but the bacteria deliver effectors into the host cell. The effector(s) interact(s) with host target proteins which are involved in resistance signaling and therewith suppress the PTI. **C)** Example of a resistance plant cell isolat. The same pathogen attack as in B), but the effector(s) is/are recognized either directly (green) or indirectly with the help of a decoy (yellow/red) or a guardee (purple/red) which lead to an activation of the respective NLR. The NLR now activates downstream signaling, addicted to the subtype of the NLR (TNL = activation of EDS1-based heterocomplexes, either with PAD4 or SAG101 / CNL = activation of NDR1) which will both result in an accumulation of SA (salicylic acid). Dependent on the concentration of SA, it will be decided if the cell runs the SAR (systemic required resistance) or HR (hypersensitive response) program.

3.4. Aims, achievements and conclusions

EDS1 was discovered two decades ago as a central regulator of plant immune responses (Parker *et al.*, 1996; Falk *et al.*, 1999). It could be shown that EDS1 builds mutually exclusive complexes with SAG101, and PAD4 respectively. This heterocomplex formation is required for the TNL-mediated signaling cascade, and it is proposed that EDS1 is also involved in basal resistance at least in Arabidopsis (Aarts *et al.*, 1998; Feys *et al.*, 2001; Feys *et al.*, 2005; Wagner *et al.*, 2013). However, irrespective of 20 years of biochemical and genetic analyses, molecular function of EDS1 and features important for immune activity within the ETI-signaling pathway remain elusive.

EDS1 had so far mainly been analyzed in Arabidopsis. Although Arabidopsis is an excellent model system in particular when it comes to genetics, it also has its disadvantages. To that end, for example functional characterization of EDS1 variants includes the generation of stable transgenic lines and is thus time- and labor-intensive. Furthermore, it is questionable whether additional studies in the Arabidopsis model system are likely to provide novel key information required to understand EDS1 molecular functions considering the large number of preceding analyses.

Therefore, one major aim of this work was to transpose analysis of EDS1 functions into the model plant *Nb* (*Nicotiana benthamiana*; wild tobacco). The key advantage of *Nb* consists in highly efficient transient gene expression by *Agrobacterium* infiltration. Furthermore, *Nb* as a member of *Solanaceae* is only distantly related to Arabidopsis (an asterid). Thus, differences between the systems can be expected, and may facilitate acquisition of new key data or provide new perspectives. However, *Nb* has an allotetraploid genome, and only partial sequences and gene annotations are available, and *Nb* was so far not regularly used for genetic analyses. Thus a number of problems needed solving and steps had to be established to actually analyze EDS1 functions in *Nb*.

Genes of the EDS1 family were identified in different *Solanaceae* species, annotated for *Nb*, and first mutant lines generated by CRISPR/Cas (Ordon *et al.*, 2017). On the basis of a *Nb eds1* mutant line, XopQ from *Xcv* (*Xanthomonas campestris* pv. *vesicatoria*) could be identified as an inducer of EDS1-dependent defenses (Adlung *et al.*, 2016), and the respective immune receptor was in parallel identified by another group (Schultink *et al.*, 2017). Initial analysis of an *Nb pad4* mutant line suggested that PAD4 had no major contribution to immunity in *Nb*, and prompted us to further dissect the entire EDS1-family in this system.

In this work, we determined that EDS1 in complex with a SAG101 isoform, SAG101b, is necessary and sufficient for TNL-mediated immune responses in *Nb*. From co-occurrence of SAG101 with TNLs, we propose that this might be the case for most, if not all, plants that have TNLs except the *Brassicaceae*. Most importantly, we provide comprehensive data suggesting that EDS1 complexes, together with either PAD4 or SAG101, do not form a functional immune signaling module by themselves, but co-evolve with further cellular components, most likely protein interactors. Indeed, another concomitant study suggests that these components are most likely helper NLRs of the NRG1 class (Lapin *et al.*, 2019). Our work also identified important features of EDS1 heterocomplexes required for immunity. Together with the identification of NRG1 as a factor most likely acting downstream of EDS1 in *Nb* (Qi *et al.*, 2018), this has provided important new impulses and perspectives.

3.5. An EDS1-SAG101b complex functions is essential for TNL-mediated immunity in *Nicotiana benthamiana*

3.5.1. Publication Gantner *et al.*, 2019

The Plant Cell, Vol. 31: 2456–2474, October 2019, www.plantcell.org © 2019 ASPB.



An EDS1-SAG101 Complex Is Essential for TNL-Mediated Immunity in *Nicotiana benthamiana*^[OPEN]

Johannes Gantner,^a Jana Ordon,^{a,1} Carola Kretschmer,^a Raphaël Guerois,^b and Johannes Stüttmann^{a,2}

^a Institute for Biology, Department of Plant Genetics, Martin Luther University Halle-Wittenberg, Weinbergweg 10, 06120 Halle (Saale), Germany

^b Institute for Integrative Biology of the Cell (I2BC), IBITECS, CEA, CNRS, Univ Paris-Sud, Université Paris-Saclay, F-91198, Gif-sur-Yvette, France

ORCID IDs: 0000-0003-3961-8660 (J.G.); 0000-0001-8764-6418 (J.O.); 0000-0001-7315-7840 (C.K.); 0000-0001-5294-2858 (R.G.); 0000-0002-6207-094X (J.S.)

Heterodimeric complexes containing the lipase-like protein ENHANCED DISEASE SUSCEPTIBILITY1 (EDS1) are regarded as central regulators of plant innate immunity. In this context, a complex of EDS1 with PHYTOALEXIN DEFICIENT4 (PAD4) is required for basal resistance and signaling downstream of immune receptors containing an N-terminal Toll-interleukin-1 receptor-like domain (TNLs) in *Arabidopsis thaliana*. Here we analyze EDS1 functions in the model Solanaceous plant *Nicotiana benthamiana* (*Nb*). Stable *Nb* mutants deficient in EDS1 complexes are not impaired in basal resistance, a finding which contradicts a general role for EDS1 in immunity. In *Nb*, PAD4 demonstrated no detectable immune functions, but TNL-mediated resistance responses required EDS1 complexes incorporating a SENESCENCE ASSOCIATED GENE101 (SAG101) isoform. Intriguingly, SAG101 is restricted to those genomes also encoding TNL receptors, and we propose it may be required for TNL-mediated immune signaling in most plants, except the Brassicaceae. Transient complementation in *Nb* was used for accelerated mutational analyses while avoiding complex biotic interactions. We identify a large surface essential for EDS1-SAG101 immune functions that extends from the N-terminal lipase domains to the C-terminal EDS1-PAD4 domains and might mediate interaction partner recruitment. Furthermore, this work demonstrates the value of genetic resources in *Nb*, which will facilitate elucidation of EDS1 functions.

INTRODUCTION

Plants lack mobile immune cells but have evolved an elaborate innate immune system to defend against invading pathogens (Spoel and Dong, 2012; Jones *et al.*, 2016). Cell surface-resident pattern recognition receptors (PRRs) can detect pathogen-/microbe-associated molecular patterns (PAMPs/MAMPs). MAMP perception and PRR activation induces PRR-triggered immunity (PTI; also referred to as MAMP/PAMP-triggered immunity), a multifaceted, low-level immune response efficient against a broad spectrum of nonadapted pathogens (Macho and Zipfel, 2014; Yu *et al.*, 2017). However, many host-adapted pathogens use effector proteins, which are secreted directly into the host cell cytoplasm, to suppress PTI (Macho and Zipfel, 2015; Büttner, 2016). As a second layer of the plant immune system, effectors can become recognized by plant resistance proteins (R proteins) in resistant plant lines. Effector recognition induces a rapid and efficient immune response termed effector-triggered immunity (ETI; Jones *et al.*, 2016; Khan *et al.*, 2016). The ETI response

commonly culminates in programmed cell death at infection sites, the hypersensitive response (HR), which in most cases correlates with inhibition of plant colonization by the pathogen (Cui *et al.*, 2015; Büttner, 2016).

Most plant R proteins are nucleotide-binding domain–leucine-rich repeat (NLR)-type immune receptors. The canonical NLR architecture consists of a C-terminal leucine-rich repeat domain, a central nucleotide-binding domain, and a variable N-terminal domain (Monteiro and Nishimura, 2018). Structurally similar NLR receptors operate in animal innate immunity and often function by ligand-dependent oligomerization and recruitment of signaling adapters via oligomeric N-terminal domain assemblies (Bentham *et al.*, 2017; Shen *et al.*, 2019). Until recently, plant NLRs were less well understood than animal NLRs. However, according to a general working model, the leucine-rich repeat domain often defines specificity, the nucleotide-binding domain acts as an ATP-driven switch controlling the transition of the receptor from a resting to an active signaling state, and the N-terminal domain conveys downstream signaling (Bernoux *et al.*, 2011, 2016; Maekawa *et al.*, 2011a, 2011b; Takken and Govers, 2012). The N-terminal domains of most plant NLRs are Toll-interleukin-1 receptor (TIR) or coiled-coil (CC) domains. Beyond analogy to animal NLRs, a function in downstream signaling is supported by the induction of HR-like cell death upon expression of TIR or CC domains alone (Swiderski *et al.*, 2009; Bernoux *et al.*, 2011; Collier *et al.*, 2011; Maekawa *et al.*, 2011b).

Recent structural elucidation of the *Arabidopsis thaliana* immune receptor HOPZ-ACTIVATED RESISTANCE1 (ZAR1) provided groundbreaking new insights to our knowledge of

¹ Present address: Department of Plant Microbe Interactions, Max Planck Institute for Plant Breeding Research, Carl-von-Linné-Weg 10, 50829 Köln, Germany

² Address correspondence to: johannes.stuttmann@genetik.uni-halle.de. The author responsible for distribution of materials integral to the findings presented in this article in accordance with the policy described in the Instructions for Authors (www.plantcell.org) is: Johannes Stüttmann (johannes.stuttmann@genetik.uni-halle.de).

^[OPEN]Articles can be viewed without a subscription. www.plantcell.org/cgi/doi/10.1105/tpc.19.00099

IN A NUTSHELL

Background: Plant pathogenic bacteria inject effector proteins inside the plant cell during infection. In resistant plant lines, effectors can be recognized by intracellular immune receptors (“NLR receptors”), which prevents plant disease. NLRs are divided in two main classes. Those receptors containing a TIR (Toll-interleukin-1 receptor) domain require complexes based on the protein EDS1 (ENHANCED DISEASE SUSCEPTIBILITY 1) to confer resistance. EDS1 forms mutually exclusive complexes with two sequence-related proteins, PAD4 (PHYTOALEXIN-DEFICIENT 4) or SAG101 (SENESCENCE-ASSOCIATED GENE 101). EDS1 and PAD4 are highly conserved, and can be found within the genomes of all higher plants. In contrast, SAG101 is only found in those plants that also have TIR-type immune receptors. So far, EDS1 functions were mainly analyzed in the model Brassicaceae plant *Arabidopsis thaliana*, in which the EDS1-PAD4 complex is most important for immune functions. However, molecular functions of EDS1 complexes yet remain unknown.

Question: We set out to analyze functions of EDS1 complexes in a different model species, *Nicotiana benthamiana*. *N. benthamiana* is genetically more complex than *A. thaliana*, but has advantages for functional analyses.

Findings: By genome editing (CRISPR/Cas) of *EDS1*, *PAD4* and *SAG101* and infection assays, we discovered that EDS1 and a SAG101 isoform (but not PAD4) are required for immune responses in *N. benthamiana* (a Solanaceae plant). However, when we transferred genes between plant species, we were surprised to discover that Solanaceae EDS1-PAD4, but not EDS1-SAG101 can fulfil immune functions in *A. thaliana*. This unravels an unexpected complexity in immune signaling pathways in different plant species, and implies that EDS1 complexes co-evolve with other cellular components to execute immune functions. Furthermore, we used transient reconstitution assays, the prime advantage of the *N. benthamiana* system, to identify features of EDS1 complexes required for plant immunity.

Next steps: Other recent studies showed that “helper NLRs”, that do not contain a TIR domain and can most likely induce resistance responses by directly interfering with cell membrane integrity, are required downstream of EDS1 complexes. Transient reconstitution assays in the *N. benthamiana* system established here will be instrumental to answer the pressing question how EDS1 complexes connect TIR domain-containing immune receptors with helper NLRs to convey immunity.

CC-type plant NLRs (CNLs; Wang et al., 2019a, 2019b): ZAR1 persists as an ADP-bound monomer in the resting state and forms a pentameric “resistosome” upon effector-triggered nucleotide exchange. In the resistosome, the ZAR1 CC domain assembly forms a funnel-shaped structure that may directly insert into the plasma membrane to interfere with membrane integrity or to function as an ion channel. Thus, CNLs most likely initiate the HR directly, and indirectly regulate downstream immune signaling (Wang et al., 2019a). Although several lines of evidence suggest that additional CNLs form ZAR1-like resistosomes (Wang et al., 2019a), such a direct function in HR initiation is unlikely to apply to TIR-type NLRs (TNLs). First, TNLs were recently shown to require so-called helper NLRs of the CC-type to mediate immunity (Qi et al., 2018; Castel et al., 2019; Wu et al., 2019). Furthermore, all known responses mediated by TNLs are dependent on ENHANCED DISEASE SUSCEPTIBILITY1 (EDS1; Aarts et al., 1998; Wirthmueller et al., 2007).

EDS1 was identified in *Arabidopsis* in a screen for mutants impaired in resistance to the obligate biotrophic oomycete *Hyaloperonospora arabidopsidis* (*Hpa*; Parker et al., 1996; Falk et al., 1999). EDS1 interacts with two sequence-related proteins, PHYTOALEXIN DEFICIENT4 (PAD4) and SENESCENCE-ASSOCIATED GENE101 (SAG101; Feys et al., 2001, 2005). All three proteins share homology with eukaryotic lipases (α/β -hydrolases) in their N termini and contain a C-terminal EP (EDS1-PAD4) domain. Occurrence of the unique EP domain together with an N-terminal lipase-like domain defines the EDS1 family (Wagner et al., 2013). Although a catalytic triad (S-D-H including a GX SXG motif) is conserved in EDS1 and PAD4 orthologs, it is not required for immune functions of EDS1-PAD4 complexes in *Arabidopsis*, suggesting a noncatalytic mode of

action (Wagner et al., 2013). Elucidation of the EDS1-SAG101 heterodimer structure and modeling of the EDS1-PAD4 complex showed that EDS1 engages in mutually exclusive heterodimers with PAD4 or SAG101 (Wagner et al., 2013), which differentially contribute to immunity in *Arabidopsis*: Loss of EDS1-PAD4 complexes (in *pad4* mutant plants) severely impairs immune signaling, whereas loss of EDS1-SAG101 (in *sag101* mutant plants) is largely compensated by presence of EDS1-PAD4 (Feys et al., 2005; Wagner et al., 2013). Complete loss of EDS1-based complexes (in *eds1* single or *pad4 sag101* double mutant plants) abolishes TNL-mediated resistance signaling. In agreement with genetic data, structure-guided mutations untethering EDS1 from PAD4 and SAG101 provided strong evidence for heterodimeric assemblies executing immune functions (Wagner et al., 2013).

In addition to its strict requirement for TNL-mediated immune responses, EDS1 also contributes to resistance mediated by some CNLs and to basal resistance (Wiermer et al., 2005; Venugopal et al., 2009; Cui et al., 2017). Basal resistance is a somewhat promiscuously employed term, generally used to describe the residual resistance observed upon challenge of a wild-type plant with a virulent pathogen isolate. To that end, for example, *Pseudomonas syringae* (*Pst*) strain DC3000 bacteria grow significantly better in *eds1* mutants than in wild-type lines. Similarly, *Arabidopsis* accession Columbia-0 (Col-0) is resistant to *Pst* bacteria translocating AvrRpt2, recognized by the CNL RPS2 (Bent et al., 1994; Mindrinos et al., 1994), but resistance is impaired in plants lacking EDS1 and the defense-associated hormone salicylic acid (SA; Venugopal et al., 2009; Vlot et al., 2009; Cui et al., 2017). It remains unclear whether EDS1 has distinct functions in basal, TNL-, and CNL-mediated resistance. An alternative explanation is that abolishment of weak TNL signaling, provoked

by minor effector recognition in interactions termed “compatible,” is at the basis of enhanced pathogen growth in *eds1* plants (Jones and Dangl, 2006; Poland et al., 2009; Krasileva et al., 2011; Kushalappa et al., 2016; Wei et al., 2018). Similarly, combined loss of weak recognition mediated by TNLs (*eds1*) and SA-mediated bolstering of immune responses (*sid2*) may lower immune capacities in *eds1 sid2* plants below a critical threshold, allowing plant colonization by otherwise incompatible *Pst* AvrRpt2 bacteria without any direct contribution of EDS1 to CNL-mediated responses. This explanation is supported by the notion that EDS1 and SA function additively, and not redundantly, in RPS2-mediated resistance, and by induction of residual cell death by AvrRpt2 in the absence of EDS1 and SA (Cui et al., 2017). A general function for EDS1 complexes in plant immunity is suggested by the conservation of EDS1 and PAD4, but not SAG101, in plant lineages that lost TNLs in the course of evolution, such as monocotyledonous plants and the eudicots *Aequilegia courulea* and *Mimulus guttatus* (Collier et al., 2011; Jacob et al., 2013; Wagner et al., 2013). Accordingly, it was proposed that EDS1-PAD4 form an ancient module regulating basal resistance, which has been co-opted for TNL-mediated immunity in eudicots (Feys et al., 2005; Rietz et al., 2011), but EDS1 immune functions in the absence of TNLs remain largely unexplored (Chen et al., 2018). Indeed, EDS1 functions have mainly been analyzed in Arabidopsis.

We and others generated *eds1* mutant lines in the model Solanaceous plant *Nicotiana benthamiana* (Ordon et al., 2017; Schultink et al., 2017). In *N. benthamiana*, genetic analyses are hampered by allotetraploidy and incomplete genome sequences, but a key advantage is the efficient transient protein expression after agroinfiltration (Goodin et al., 2008; Bombarely et al., 2012; Naim et al., 2012). Stable *Nbeds1* mutant lines confirmed the conserved role of EDS1 in TNL signaling and revealed EDS1-dependent recognition of the effector protein XopQ from *Xanthomonas campestris* pv *vesicatoria* (*Xcv*; also *Xanthomonas euvesicatoria*) in this species (Peart et al., 2002; Hu et al., 2005; Adlung et al., 2016; Adlung and Bonas, 2017; Qi et al., 2018). *Xcv* is the causal agent of bacterial spot disease on pepper (*Capsicum annuum*) and tomato (*Solanum lycopersicum*) and is virulent in *N. benthamiana* after deletion of *xopQ* or in *Nbeds1* mutant plants. The corresponding TNL receptor, *Recognition of XopQ 1* (*Roq1*), was subsequently identified (Schultink et al., 2017), completing the signal transduction pathway from XopQ toward EDS1-conditioned immunity in the *Xcv* – *N. benthamiana* interaction. Also, *N requirement gene 1* (*NRG1*) was identified as a novel component in TNL signaling downstream of *Nbeds1* (Qi et al., 2018). However, the molecular role of EDS1 complexes in TNL signaling remains elusive.

In this study, we genetically dissected the *EDS1* family in *N. benthamiana*. Although major immune functions in Arabidopsis reside in EDS1-PAD4, we show that an EDS1-SAG101 complex is essential for TNL-mediated resistance responses in *N. benthamiana*. TNL activation and signaling can be uncoupled from complex biotic interactions in transient complementation assays in *N. benthamiana*, which facilitates straightforward and simplified gene functional analyses. This system will prove seminal for future functional analyses of EDS1 complexes toward a mechanistic understanding.

RESULTS

Duplication of SAG101 in Solanaceous Plants

We previously mined genomes of tomato and *N. benthamiana* for homologs of *EDS1* and *PAD4* (Ordon et al., 2017). Single genes were identified for *PAD4* in both species. For *EDS1*, a single copy was detected in tomato, whereas the *N. benthamiana* genome contains two loci with similarity to *EDS1* but one is a pseudogene (Adlung et al., 2016). *N. benthamiana* *EDS1* and *PAD4* loci were targeted by genome editing to generate *Nbeds1* and *Nbpad4* mutant plants (Ordon et al., 2017). Growth restriction of *Xcv* (strain 85-10) bacteria due to Roq1-mediated XopQ recognition was abolished in *Nbeds1* (Adlung et al., 2016; Schultink et al., 2017) but not in *Nbpad4* plants (see later sections).

We suspected that EDS1-PAD4 and EDS1-SAG101 complexes might function redundantly in Roq1 signaling and extended genome mining to *SAG101* orthologs from tomato and *N. benthamiana*. Two different *SAG101* isoforms, termed *SAG101a* and *SAG101b*, were identified in tomato and were further duplicated in *N. benthamiana* in agreement with its allotetraploid genome (Supplemental Figure 1; Supplemental Data Set 1). However, *NbSAG101a2* and *NbSAG101b2* are likely pseudogenes, as experimentally supported gene models encode for truncated proteins (Supplemental Figure 1), and were not further inspected.

To analyze the possible biological significance of the apparent duplication of *SAG101*, additional genomes from *Solanaceae* and other species were analyzed for *SAG101* orthologs. The genomes of the core eudicots *Coffea canephora* (*Cc*) and *Mimulus guttatus* (*Mg*), belonging like *Solanaceae* to the asterids, and of the rosid Arabidopsis were analyzed. *Musa accuminata* (*Ma*) was included as a monocotyledonous plant. A phylogeny was constructed using predicted EDS1 family proteins of these species (Figure 1). *SAG101* homologs were not detected in species lacking TNL receptors (here *Ma* and *Mg*), as previously described by Wagner et al. (2013). In agreement with the distant relationship, the rosid *AtSAG101* was clearly separated from *SAG101* orthologs of asterid plants. Genes encoding *SAG101a* and *SAG101b* isoforms were detected in all analyzed *Solanaceae* genomes except pepper (*Capsicum annuum*, *Ca*), and respective proteins formed two distinct groups within the *SAG101* branch (Figure 1A). The single copy *SAG101* from pepper grouped within the *SAG101b* branch. The asterid *CcSAG101* grouped more closely with *Solanaceae* *SAG101a* but with low branch-point support. This suggests that diversification of *SAG101a* and *SAG101b* most likely occurred at a time point similar to separation of the lineages leading to *Cc* and *Solanaceae*, and that *SAG101a* was lost in *Ca* relatively recently.

Retention of two *SAG101* isoforms in most *Solanaceae* genomes is indicative of functional diversification. To get an insight into expression of *SAG101* isoforms and *EDS1* family genes in general, we assessed a public RNA sequencing (RNA-seq) data set from tomato plants treated with different bacterial isolates or the MAMP flgII-28 (Rosli et al., 2013) using the TomExpress platform (Supplemental Figure 2; Zouine et al., 2017). All four genes were expressed in control (mock-treated) plants. Treatment with *Pseudomonas fluorescens* and *Pseudomonas putida* bacteria, inducing robust PTI responses in *Solanaceae* (Chakravarthy

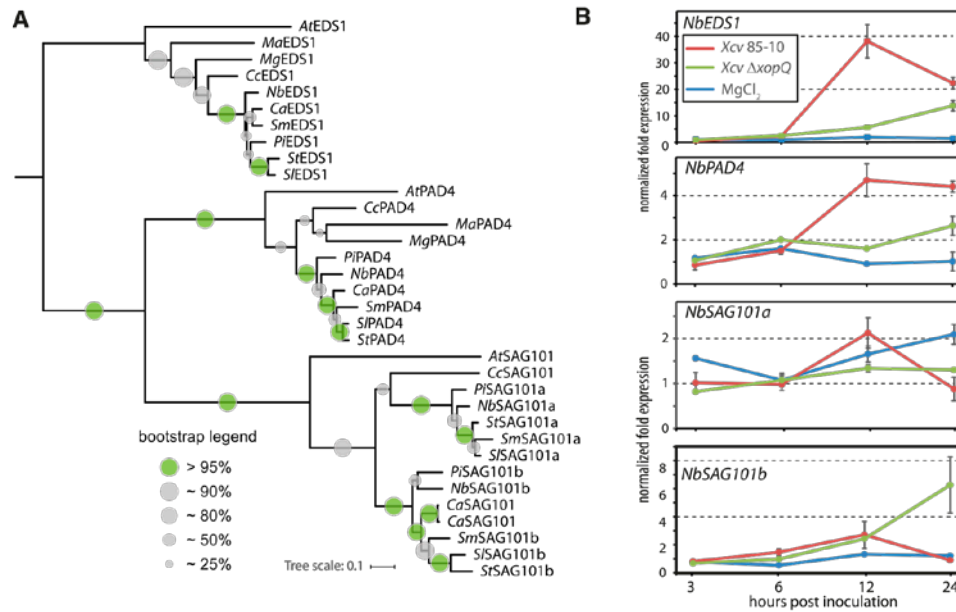


Figure 1. Occurrence and Expression of *EDS1* Family Genes in *Solanaceae*.

(A) Phylogenetic clustering of putative *EDS1* family proteins from *Solanaceae* and control species. The tree was midpoint rooted. *At*, *Arabidopsis thaliana*; *Ca*, *Capsicum annuum* (SAG101 orthologs from cultivars Zunla and CM334 shown); *Cc*, *Coffea canephora*; *Ma*, *Musa accuminata*; *Mg*, *Mimulus guttatus*; *Pi*, *Petunia inflata*; *Nb*, *Nicotiana benthamiana*; *Sl*, *Solanum lycopersicum*; *Sm*, *Solanum melongena*.

(B) Expression of *EDS1* family genes in *N. benthamiana*. Plants were challenged with virulent (*Xcv* Δ*xopQ*) or avirulent (*Xcv* 85-10) *Xanthomonas campestris* pv *vesicatoria* bacteria or mock treated (MgCl₂). RNA was extracted at indicated time points, and expression of *EDS1* family genes measured by quantitative RT-PCR. Displayed data originates from normalization to *PP2A* expression, and similar results were obtained when using *Elongation Factor 1-α* (*EF1α*) for normalization. Data points represent means of four biological replicates with *SE* shown.

et al., 2010; Rosli et al., 2013), moderately induced expression of *EDS1* family genes (6 h after treatment).

We also examined the expression of *EDS1* family genes in *N. benthamiana*. Plants were infected with avirulent (*Xcv* 85-10) or virulent (*Xcv* Δ*xopQ*) *Xcv* bacteria. Gene expression was analyzed by RT-qPCR in a time course experiment (Figure 1B). Expression of *NbEDS1* was strongly upregulated in response to avirulent *Xcv* 85-10 and, to a lesser extent, by the Δ*xopQ* mutant strain (Figure 1B). Expression peaked 12 h after infection and then declined. A similar expression profile was observed for *NbPAD4*, although its overall induction (~35-fold for *NbEDS1*, fivefold for *NbPAD4*; Figure 1B) was less pronounced. *NbSAG101a* and *NbSAG101b* were expressed but not regulated under infection conditions. These data indicate that two SAG101 isoforms are expressed in tomato and *N. benthamiana*, and they may form heterocomplexes with *EDS1* and thus contribute to immune signaling.

Localization and Complex Formation of tomato *EDS1* Family Proteins

EDS1 family proteins from tomato (*Solanum lycopersicum*, *Sl*) are very similar to those of *N. benthamiana* (percentage of identity and similarity, 79% and 86%, respectively [EDS1], 77% and 85% [PAD4], 81% and 87% [SAG101a], and 72% and 79% [SAG101b]; comparison of tomato proteins to Arabidopsis: 40% and 57%

[EDS1], 38% and 53% [PAD4], 33% and 45% [SAG101a], and 34% and 45% [SAG101b]), suggesting that they can likely functionally replace each other. For simplicity, we decided to first clone cDNAs of *EDS1* family genes from tomato for functional characterization, although we aimed at genetic dissection of functions of *EDS1* complexes in the *N. benthamiana* model system.

For subcellular localization studies, *SlEDS1* was fused to *mCherry*, and *SIPAD4*, *SISAG101a*, and *SISAG101b* were fused to *mEGFP*, respectively, in 35S promoter-controlled expression constructs. Fusion proteins were transiently expressed alone or in combination in *N. benthamiana*, and tissues were analyzed by live-cell imaging (Figure 2; Supplemental Figure 3). *SlEDS1* and *SIPAD4* were detected in both the cytoplasm and the nucleus, whereas *SISAG101a* was located exclusively in the nucleus. Similar subcellular localization patterns were described for Arabidopsis orthologs (Feys et al., 2005; García et al., 2010). In co-expression with *SISAG101a*, *SlEDS1* was detected exclusively in the nucleus (compared with Figure 2A and Supplemental Figure 3A). In contrast, *SISAG101b* was nucleocytoplasmically distributed both alone and in combination with *SlEDS1*. In summary, *SlEDS1* family proteins from tomato localize to cytoplasm and/or nucleus, although we cannot fully exclude cell wall or membrane association. All proteins were detected on immunoblots, and the GFP-tagged *SIPAD4*, *SISAG101a*, and *SISAG101b*

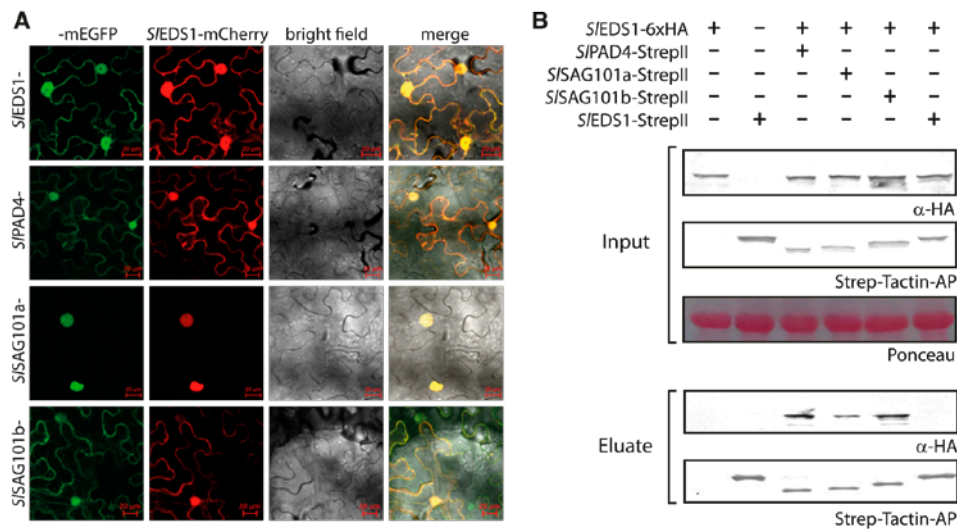


Figure 2. Complex Formation and Localization of Tomato EDS1 Family Proteins.

(A) Protein localization in living cells detected by confocal laser scanning microscopy. Indicated proteins (from tomato) were transiently coexpressed as GFP fusions together with S/EDS1 in *N. benthamiana* leaf tissues by agroinfiltration, and protein localization was analyzed 3 dpi. Localization of single proteins and integrity of fluorophore fusions is shown in Supplemental Figure 3. Scale bar = 20 μ m.

(B) Formation of complexes by tomato EDS1 proteins. Indicated proteins were transiently (co)expressed in *N. benthamiana* by agroinfiltration. At 3 dpi, extracts were used for StrepII purification, and total extracts and eluates analyzed by immunoblotting. Ponceau staining is shown as loading control.

appeared to be stabilized by coexpression of S/EDS1 (Supplemental Figure 3B).

Förster resonance energy transfer (FRET) and acceptor photobleaching (FRET-APB) was used to probe formation of S/EDS1-based complexes in living cells. mCherry and mEGFP-tagged proteins were expressed from a single T-DNA for reduced variation in coexpression rates for FRET analyses (Hecker et al., 2015). Robust FRET was detected upon coexpression of S/EDS1-mCherry and S/PAD4, S/SAG101a or S/SAG101b, but not S/EDS1, fused with mEGFP (Supplemental Fig. 3C). Complex formation was further analyzed by protein copurification (Figure 2B). In line with results obtained by FRET-APB, S/EDS1 (fused to a 6xHA tag) copurified with Strep-tagged S/PAD4, S/SAG101a and S/SAG101b, but not S/EDS1. We conclude that S/EDS1 engages in heterocomplexes containing S/PAD4, S/SAG101a or S/SAG101b, but does not form homodimers. Hence, considering the high similarity of NbEDS1 and S/EDS1 family proteins, three different heterocomplexes with NbEDS1 are most likely also established by the orthologous NbPAD4, NbSAG101a and NbSAG101b proteins.

Identification of EDS1 Complexes Functioning in XopQ Recognition

Gene expression analyses and interaction studies suggested that two different EDS1-SAG101 complexes exist in *N. benthamiana*. Furthermore, we could not exclude functionality of the SAG101a2 and SAG101b2 isoforms we considered pseudogenes. To reveal a potential role of SAG101 isoforms in TNL-mediated immunity, all four SAG101 genes were targeted for mutagenesis by SpCas9

(Supplemental Figure 4). A respective genome editing construct was transformed into the previously generated *Nbpad4-1* mutant line (Ordon et al., 2017), and primary transformants (T_0) were tested for recognition of XopQ. Plants were inoculated with a *P. fluorescens* derivative engineered for Type III system-dependent translocation (Thomas et al., 2009) and expressing the effector XopQ fused to a secretion signal of the *P. syringae* effector AvrRpt2. This *Pfo xopQ* strain induces a strong EDS1-dependent HR in wild-type *N. benthamiana* (Gantner et al., 2018) and the *Nbpad4-1* mutant line (Figure 3).

One T_0 plant failed to initiate the HR in response to XopQ and thus phenocopied the *Nbeds1* line. Sequencing revealed that the assumed pseudogenes SAG101a2 and SAG101b2 did not contain any mutations in this line and thus can be dismissed. Hereafter, only SAG101a1 and SAG101b1 will be considered, and they will be referred to as SAG101a and SAG101b for simplicity. The primary line nonresponsive to XopQ was homozygous for a *sag101a-1* mutation, and heterozygous for two different *sag101b* alleles (Supplemental Figure 4). From the resulting T_1 plants, a line lacking the genome editing transgene and homozygous for the *sag101b-1* allele (i.e., a *pad4-1 sag101a-1 sag101b-1* triple mutant; *pss*) was selected. An additional double mutant line containing the *pad4-1* and *sag101b-1* mutant alleles (*pSs*) was isolated from a cross (*pss* x wild type). We failed to isolate a *sag101b-1* single mutant line from the same cross. Allele identifiers of *N. benthamiana* lines will be omitted hereafter.

N. benthamiana mutant lines were tested alongside control plants for recognition of XopQ by inoculation with *Pfo xopQ* and Xcv bacteria (Figure 3A). Both bacterial strains induced the HR in

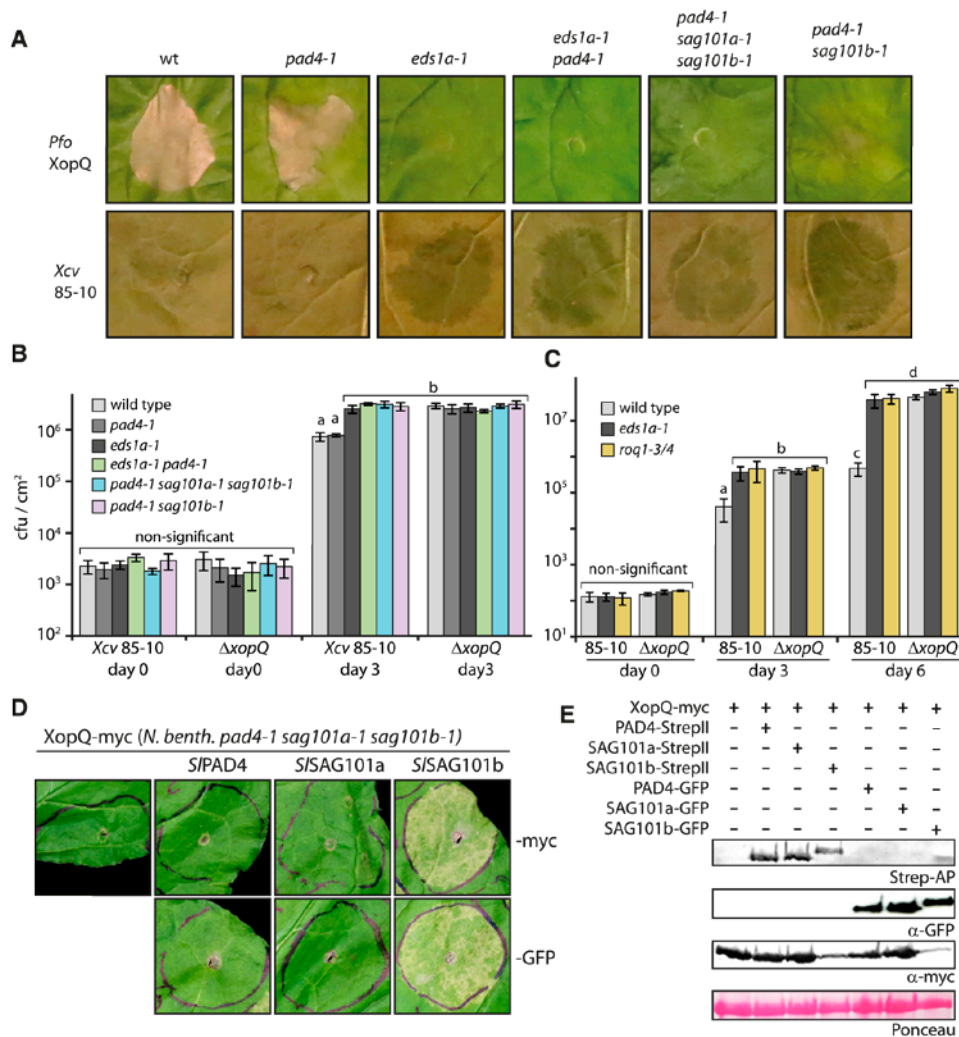


Figure 3. Immune Responses of *N. benthamiana* Mutant Lines Deficient in *EDS1* Family Genes or *Roq1*

(A) Recognition of XopQ in different mutant lines. Indicated *N. benthamiana* lines were challenged with XopQ-translocating *P. fluorescens* bacteria (top; infiltrated at $OD_{600} = 0.2$) or *Xcv* strain 85-10 bacteria (bottom; infiltrated at $OD_{600} = 0.4$). Phenotypes were documented at 4 dpi. Similar results were obtained in three independent experiments, and multiple plants of the indicated genotypes were infiltrated in each experiment.

(B) Bacterial growth of *Xcv* bacteria on mutant lines. Indicated lines were infected with *Xcv* strain 85-10 or a corresponding mutant strain lacking XopQ ($\Delta xopQ$). Means and SD of four biological replicates are shown. Letters indicate statistically significant differences as determined by one-way ANOVA and Fisher LSD post hoc test ($P < 0.01$).

(C) Bacterial growth in *eds1* and *roq1* mutant lines. As in **(B)**, but means and SD of eight biological replicates are shown for days 3 and 6. The *roq1* mutant line was a T_1 line segregating for two disruptive alleles at the *Roq1* locus (Supplemental Fig. 4F).

(D) Reconstitution of XopQ detection in the *pss* triple mutant line. By agroinfiltration, XopQ was expressed alone or in combination with PAD4, SAG101a, or SAG101b (from tomato and fused to a StrepII and $4 \times c$ -myc tag or GFP). Phenotypes were documented 5 dpi.

(E) Immunodetection of fusion proteins expressed in **(D)**. Samples were taken 3 dpi from a second infiltration on the same leaf shown in **(D)**. Ponceau staining of the membrane is shown as loading control.

leaves of wild-type and *pad4* plants. The remaining mutant lines (*eds1 pad4* (*ep*), *pss*, *pSs*) failed to initiate the HR and were indistinguishable from *eds1* mutant plants (Figure 3A). In addition, in planta bacterial titers of *Xcv* and *Xcv* $\Delta xopQ$ bacteria were determined for quantitative analysis of immune responses in

different *N. benthamiana* mutant lines (Figure 3B). The growth of *Xcv*, but not $\Delta xopQ$ bacteria, was restricted in wild-type and *pad4* plants. *Xcv* replication in leaves of *eds1* and any of the *pad4 sag101* mutant lines was similar, and not different from that of $\Delta xopQ$ bacteria on wild-type plants (Figure 3B). Therefore, the

SAG101a isoform present in the *pad4 sag101b* (*pSs*) double mutant does not contribute to immunity, and loss of *PAD4* and *SAG101b* phenocopies *eds1* mutants.

Notably, none of the mutant lines showed an enhanced susceptibility or basal resistance phenotype: bacterial titers of $\Delta xopQ$ (in any plant genotype) and *Xcv* in *eds1* or *pad4 sag101* mutant plants were identical. We also compared bacterial growth in *eds1* and *roq1* mutant plants (Supplemental Figure 4) up to 6 d (Figure 3C). Identical titers for *Xcv* were observed in *eds1* and *roq1* plants, and were similar to bacterial growth of $\Delta xopQ$ bacteria. This result further corroborates that *N. benthamiana* plants deficient in EDS1 complexes lack a basal resistance phenotype, and that XopQ is indeed the only *Xcv* effector inducing EDS1-dependent defenses (Adlung et al., 2016).

Full susceptibility of *Nbpad4 sag101b* mutant lines to the *Xcv* wild-type strain suggests that EDS1-PAD4 and EDS1-SAG101b complexes might function redundantly in immune signaling. Alternatively, only EDS1-SAG101b might have immune functions in *N. benthamiana*. To discriminate between these scenarios, XopQ and tomato *S/PAD4* or *S/SAG101* proteins were transiently expressed in the *pss* background. Coexpression of XopQ with *S/SAG101b*, but not *S/PAD4* or *S/SAG101a*, restored HR induction (Figure 3D). All proteins were detected on immunoblots using two different epitope tags (Figure 3E). The same complementation assay was performed expressing untagged proteins with identical results. We also compared *NbEDS1* and *NbSAG101b* with their respective tomato orthologs for restoration of XopQ recognition (Supplemental Figure 5). EDS1 or SAG101b orthologs from the two species were equally efficient for restoration of the XopQ-induced HR in respective mutant backgrounds (Supplemental Figures 5A and 5B), and *S/PAD4*, *S/SAG101a* and *S/SAG101b* engaged into complexes with *NbEDS1* (Supplemental Figure 5C). We concluded that tomato EDS1 family proteins can functionally replace *N. benthamiana* orthologs, as anticipated, and decided to use tomato proteins for further functional characterization.

Taking together the observations (1) that *pad4* mutant *N. benthamiana* lines are not impaired in XopQ-induced resistance (Figures 3A and 3B) and (2) that only expression of SAG101b can restore XopQ recognition in the *pss* background (Figure 3D), these results suggest that an EDS1-SAG101b complex is necessary and sufficient for resistance signaling downstream of XopQ in *N. benthamiana*. Despite its upregulation during infection (Figure 1B), *PAD4* appears to not contribute to Roq1-mediated immune signaling in *N. benthamiana*.

EDS1-SAG101b Functions in Diverse TNL-Mediated Responses

The finding that EDS1 and SAG101b are required for XopQ-induced resistance responses in *N. benthamiana* was surprising because major resistance-signaling functions reside in EDS1-PAD4 in Arabidopsis (Feys et al., 2005; Wagner et al., 2013; Cui et al., 2017, 2018). We tested additional inducers of presumed EDS1-dependent defense responses in our set of mutant lines to analyze whether EDS1-SAG101b are generally required for immune signaling in *N. benthamiana* or whether this is specific for the TNL Roq1 recognizing XopQ (Schultink et al., 2017). Expression of a TIR domain fragment of the TNL DM2h (Stuttman

et al., 2016), a variant of a TIR fragment of RPS4 (RPS4₁₋₂₃₄-E111K; Swiderski et al., 2009; Williams et al., 2014), and coexpression of the Tobacco mosaic virus helicase protein p50 together with the tobacco TNL receptor N (Burch-Smith et al., 2007) induced HR-like cell death on wild-type but not *eds1* or *pss* mutant plants (Figure 4). As with XopQ, cell-death induction could be restored in *pss* plants by coexpression of *S/SAG101b* but not *S/SAG101a* or *S/PAD4* (Figure 4A). These results indicate that EDS1-SAG101b are generally required for TNL-induced defenses in *N. benthamiana*, whereas *PAD4* and *SAG101a* cannot functionally replace *SAG101b*, even when expressed under control of the strong 35S promoter in transient assays.

In a complementary approach, the *Roq1* gene was transferred into Arabidopsis wild-type and *eds1*, *sag101*, and *pad4* mutant lines. *Roq1* was expressed under control of the Arabidopsis *RPS6* promoter and the octopine synthase terminator (*ocs*, *Agrobacterium tumefaciens*). *RPS6* encodes a TNL receptor recognizing HopA1 from *Pseudomonas syringae* pv *syringae* strain 61 (Kim et al., 2009), and its promoter was chosen for *Roq1* expression to potentially avoid dominant negative effects often arising from overexpression of immune receptors (e.g., Wirthmueller et al., 2007). T₁ transgenic seeds from transformation of the *Roq1* expression constructs into Col-0 wild type and *eds1-12*, *pad4-1* and *sag101-1* mutant lines were selected by FAST seed coat fluorescence (Shimada et al., 2010), respective plants grown in soil and infected with *Pst* DC3000 bacteria. Strain DC3000 contains the effector HopQ1 homologous to XopQ, which is also recognized by Roq1 (Adlung et al., 2016; Schultink et al., 2017; Zembek et al., 2018).

If Roq1 can function in Arabidopsis, we expected to generate resistance to *Pst* DC3000, which is an aggressive pathogen in accession Col-0. Indeed, severe tissue collapse was observed in Col-0 plants infected with DC3000 at 3 d post inoculation (dpi), whereas plants containing the *Roq1* transgene were mostly asymptomatic (Figure 4B). As a TNL receptor, we expected Roq1 to function in an EDS1-dependent manner in Arabidopsis. In agreement, tissue collapse similar to that of Col-0 plants was observed in *eds1-12 pRPS6:Roq1* plants. The *pad4-1* transgenics containing the *pRPS6:Roq1* transgene behaved similar to *eds1-12* transgenics and Col-0, whereas transgenic lines in the *sag101* background were as resistant as wild-type plants expressing Roq1 (Figure 4B). Similar results were obtained when Roq1 was expressed under the control of a *Ubiquitin 10* promoter fragment. Roq1 is thus functionally dependent on EDS1-SAG101b in *N. benthamiana* but requires EDS1-PAD4 to mediate resistance in Arabidopsis. We conclude that it is not the TNL receptors but rather the differences within the EDS1 protein family of respective plant species that determine which EDS1 heterocomplexes function in TNL signaling.

EDS1 Complexes Are Not Sufficient for TNL Signaling, but Additional Factors Divergent between Individual Species Are Required

Considering that EDS1-PAD4 and EDS1-SAG101b are required for immune signaling in Arabidopsis and *N. benthamiana*, respectively, these complexes might have identical functions, albeit different evolutionary origin. Alternatively, functional

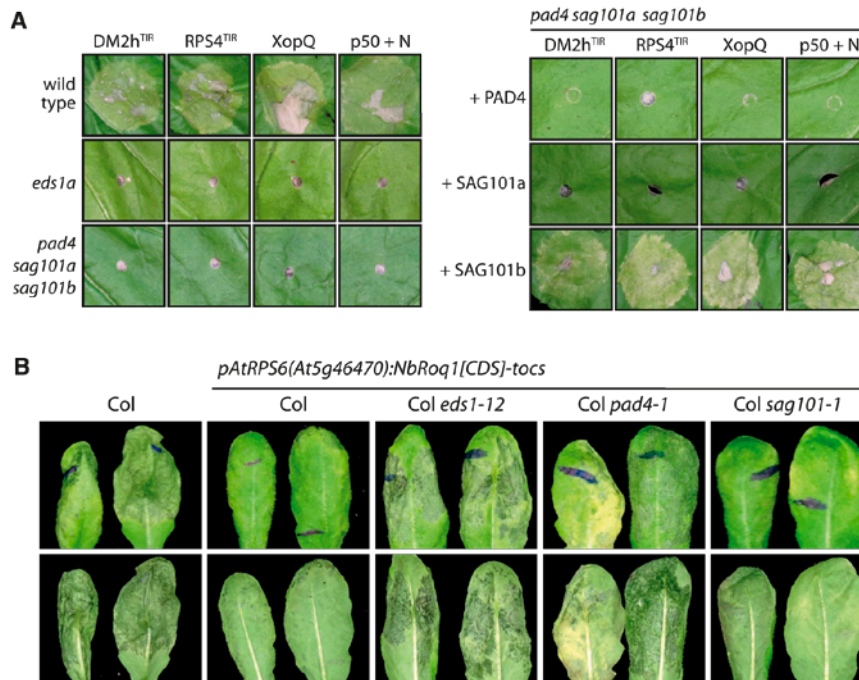


Figure 4. Genetic Dependencies of TNL-Type Immune Receptors in *N. benthamiana* and Arabidopsis.

(A) EDS1-dependent cell-death induction requires SAG101b in *N. benthamiana*. Inducers of presumably EDS1-dependent cell death (DM2h^{TIR}–DM2h₍₁₋₂₇₉₎; RPS4^{TIR}–RPS4₍₁₋₂₃₄₎–E111K [Swiderski et al., 2009]; XopQ–XopQ-myc; p50 + N–p50-Cerulean + N-Citrine [Burch-Smith et al., 2007]) were expressed in different *N. benthamiana* lines, as indicated (left), or coexpressed with PAD4, SAG101a or SAG101b (from tomato and fused to a 4xmyc-TwinStrep tag) in the *pss* mutant line (right). Phenotypes were documented 5 dpi.

(B) Functionality and genetic dependency of Roq1 in Arabidopsis. A T-DNA construct coding for Roq1 under control of an *RPS6* promoter fragment and an *ocs* terminator was transformed into the indicated Arabidopsis lines. Four-week-old control and T₁ plants were infected with *Pst* DC3000 bacteria (syringe infiltration, OD₆₀₀ = 0.001). Symptom development was documented 3 dpi. At least eight independent T₁ plants were tested for each genotype per replicate, and the experiment was conducted three times with similar results.

recruitment to immune signaling might occur by different mechanisms in these species. We sought to analyze these aspects by transferring *EDS1* family genes from Arabidopsis into *N. benthamiana* and vice versa. We first attempted to restore XopQ-induced cell death in *eds1* or *pss* mutant *N. benthamiana* plants (Figure 5; Supplemental Figure 6). Arabidopsis *EDS1* family genes were expressed, in different combinations and with or without an epitope tag, from a single T-DNA, and XopQ was coexpressed (Supplemental Figure 6A). As controls, *S/EDS1*-HA and *S/SAG101b*-myc were coexpressed with XopQ. Arabidopsis and tomato orthologs were expressed to similar levels (Supplemental Fig. 6B). However, XopQ-induced cell death was efficiently restored by coexpression of *S/EDS1* and *S/SAG101b* (in *eds1* and *pss* mutant plants, respectively), but not by coexpression of the Arabidopsis *EDS1* family proteins, in any given combination (Figure 5A). Thus, Arabidopsis *EDS1* complexes fail to function in Roq1 signaling in *N. benthamiana*.

Reciprocally, the Arabidopsis *eds1-2 pad4-1* double mutant line was transformed with constructs encoding *EDS1* and *PAD4* from Arabidopsis or tomato and under control of the corresponding native promoter elements from Arabidopsis (Supplemental

Figure 6C). For each transformation, several independent T₂ populations were tested for complementation of the *eds1-2 pad4-1* immunity defects by infection with *Hpa* isolate Cala2. Cala2 is recognized via the TNL RPP2 in Col-0 (Sinapidou et al., 2004) but is highly virulent on *eds1 pad4* plants (Figure 5B). Transformants expressing *EDS1*-*PAD4* from tomato were as resistant to *Hpa* Cala2 as transformants expressing the Arabidopsis homologs and indistinguishable from wild-type Col-0 (Figure 5B). In simultaneously generated transgenics expressing epitope-tagged variants, *EDS1* and *PAD4* from Arabidopsis and tomato accumulated to similar levels as assessed by immunodetection (Supplemental Figure 6D). An additional set of transgenic plants was generated in the *eds1-2 pad4-1 sag101-1* triple mutant background that expressed *S/EDS1* and different combinations of *S/PAD4* and/or *S/SAG101* isoforms (Supplemental Figure 6E). Transgenic plants expressing *S/EDS1* together with *S/PAD4* and *S/SAG101* isoforms were resistant to *Hpa* isolate Cala2, although HR-associated cell death appeared less confined than in Col-0 or control plants expressing Arabidopsis *EDS1*-*PAD4* (Supplemental Figure 6E). By contrast, transgenics expressing *S/EDS1* and a *S/SAG101* isoform, but not *S/PAD4*, were susceptible. Again, all proteins

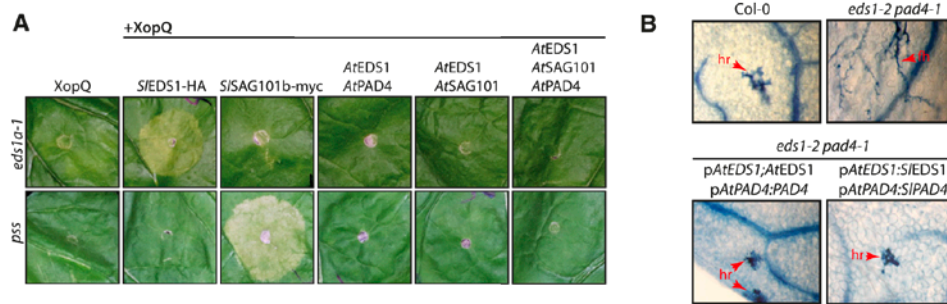


Figure 5. Cross-Species Transfer of *EDS1* Family Genes.

(A) Arabidopsis EDS1-PAD4-SAG101 proteins cannot functionally replace EDS1-SAG101b in *N. benthamiana*. Indicated proteins were expressed (by agroinfiltration) either in *eds1* or *pss* mutant lines, and phenotypes were documented 7 dpi. Arabidopsis proteins were expressed with or without an epitope tag, and images originate from untagged proteins (Supplemental Figure 6 shows details on T-DNA constructs and protein detection).

(B) Tomato EDS1-PAD4 can function in TNL signaling in Arabidopsis. Col *eds1-2 pad4-1* double mutant was transformed with constructs for expression of EDS1 and PAD4, either from Arabidopsis or tomato and with or without an epitope tag (Supplemental Figure 6C) and under control of Arabidopsis promoter fragments. Segregating T_2 populations were selected with BASTA, and 3-week-old plants infected with *H. arabidopsidis* isolate Cala2. True leaves were used for Trypan Blue staining 7 dpi. At least four independent T_2 populations were tested for each construct with similar results. Lines expressing untagged proteins were used for infection assays. Lines expressing epitope-tagged proteins were used for immunodetection (Supplemental Figure 6D). fh, free hyphae; hr, hypersensitive response.

were detected in transgenic plants expressing epitope-tagged variants (Supplemental Figure 6F).

Hence, *S/EDS1-S/SAG101b* are sufficient for all tested immune responses in *N. benthamiana* but fail to function in Arabidopsis. By contrast, *S/EDS1-S/PAD4* can function in RPP2-mediated resistance in Arabidopsis but not in any tested TNL-mediated response in *N. benthamiana*. Thus, proteins of the PAD4 phylogenetic clade appear to operate, together with EDS1, in TNL signaling in Arabidopsis, and these functions are executed by EDS1-SAG101 in *N. benthamiana*. Taken together with the observation that *AtEDS1-AtSAG101-AtPAD4* fail to mediate TNL signaling *N. benthamiana*, we conclude that EDS1 complexes do not form a complete functional module in TNL signaling by themselves. We propose that additional factors, divergent between species as a result of coevolution with EDS1 complexes, are required by these heterocomplexes to mediate immune responses.

Rapid Analyses of EDS1 Complexes in the *N. benthamiana* System

One rationale for genetic dissection of the *EDS1* gene family in *N. benthamiana* was the establishment of an experimental system that allows rapid analysis of EDS1 complexes and their immune competence. Previous experiments showed that XopQ-induced cell death can be restored in the *eds1* and *pss* mutant lines by *Agrobacterium*-mediated coexpression of EDS1 and SAG101b, respectively (Figure 4A; Adlung et al., 2016; Qi et al., 2018). The HR-like cell death provoked by XopQ expression is relatively mild in wild-type *N. benthamiana* plants and further delayed and dampened in transient complementation assays but highly reproducible under our conditions.

A crystal structure of the Arabidopsis EDS1-SAG101 complex and an experimentally validated homology model of the EDS1-PAD4

complex were reported (Wagner et al., 2013). Because Arabidopsis EDS1 complexes were not functional in *N. benthamiana*, homology models of EDS1-based heterodimers from tomato were generated (Figure 6). A structure similar to that of Arabidopsis EDS1-SAG101 was predicted for the immune-competent tomato EDS1-SAG101b complex, and most surface-exposed, conserved residues mapped to the heterocomplex interface (Figures 6A and 6B).

To validate the structural models and the *N. benthamiana* system, we decided to disrupt EDS1-SAG101b complex formation by mutagenesis of key amino acids within the N-terminal interaction interface (Wagner et al., 2013). The N-terminal interface is formed mainly by hydrophobic interactions between a protruding helix of EDS1 accommodated in a corresponding pocket on SAG101b (Figure 6A). Residues within the EDS1 helix were sequentially mutated: T264F and I268E (TI), followed by V265E (TIV), V269E (TIVV) and L261E (TIVVL). All variants accumulated to comparable levels in planta, and TIV or higher order mutants did not copurify in detectable amounts with StrepII-tagged SAG101b (Figure 6C). When tested by yeast two hybrid, interaction of the EDS1 variants with SAG101b and also PAD4 and SAG101a gradually declined and was still detectable for the TIVV quadruple mutant variant (Supplemental Figure 7). In accordance with complex formation being progressively impaired, *S/EDS1* variants also lost their activity for restoring XopQ-induced cell death when coexpressed in *eds1* mutant *N. benthamiana* plants (Figure 6D). Only the quintuple TIVVL variant was completely nonfunctional. Similarly, mutations were serially introduced into SAG101b: F17S and L22S (FL), L13S (FLL), L16S (FLLL) and L18S (FLLLL). In copurification assays, interaction with EDS1 was detectable only for wild-type SAG101b, and protein accumulation of SAG101 variants was mildly affected (Figure 6E). SAG101b variants were tested for functionality by appearance of HR-like cell death upon coexpression with XopQ in *pss* mutant plants (Figure 6F).

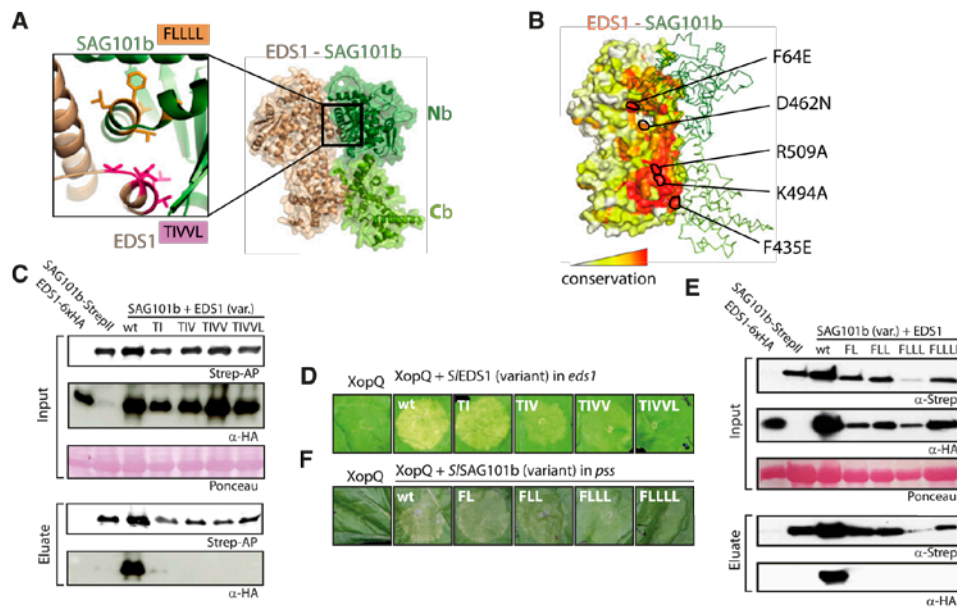


Figure 6. EDS1-SAG101b Heterocomplexes Are the Functional Modules in *N. benthamiana* TNL Signaling.

(A) Homology model of the tomato EDS1-SAG101b complex used for transient reconstitution of TNL-signaling in mutant *N. benthamiana* tissues. The N-terminal (Nb) and C-terminal (Cb) domains of SAG101b are depicted in dark and light green, respectively. The inset shows the symmetrically arranged helices of EDS1 and SAG101b forming the N-terminal interaction interface. Amino acids targeted by mutagenesis are shown as sticks and are highlighted in pink (EDS1) and orange (SAG101b), respectively.

(B) Conservation of surface-exposed amino acids in S/EDS1. S/SAG101b is shown in ribbon presentation (green). EDS1 residues functionally interrogated by mutagenesis are marked.

(C) Interaction of EDS1 variants with SAG101b. Indicated proteins were (co)expressed in *N. benthamiana* by agroinfiltration and tissues used for StrepII purification at 3 dpi.

(D) Functionality of EDS1 variants affected in heterocomplex formation. Indicated variants (as in [C], with C-terminal 6xHA) were coexpressed with XopQ-myc in *eds1* mutant plants, and plant reactions were documented 7 dpi.

(E) Interaction of SAG101b variants with EDS1. As in [C], but SAG101b-StrepII variants were coexpressed with EDS1.

(F) Functionality of SAG101b variants affected in heterocomplex formation. SAG101b-StrepII variants were coexpressed with XopQ-myc in *pss* mutant plants, and plant reactions were documented 7 dpi.

Cell death was reduced for SAG101b-FLL and abolished for the quadruple and quintuple mutant variants. These data suggest that heterocomplex formation is required for immune functions of EDS1 and SAG101b and thus support previous findings from analysis of EDS1 in the Arabidopsis system (Wagner et al., 2013).

Next, we set out to identify additional functionally relevant features of EDS1-SAG101b complexes (a summary of tested variants is shown in Supplemental Table 1). We first focused on several positively charged residues lining an assumed cavity on the heterodimer surface (Wagner et al., 2013) and recently reported as required for immune signaling in Arabidopsis (Bhandari et al., 2019). The residues within S/EDS1 (R509, K494), homologous to those reported in Arabidopsis (R493, K478), were targeted by mutagenesis, and respective variants tested for functionality (Supplemental Figure 8). All variants restored XopQ-induced HR-like cell death as efficiently as wild type S/EDS1. We propose that functional relevance of the positively charged residues might be masked by overexpression in the *N. benthamiana* system or might not be conserved across different species.

We also introduced F64E, F435E, and D462N exchanges into S/EDS1 (Figure 7). F64 is a single, conserved residue exposed on the N-terminal lipase-like domain of EDS1 and framing the assumed cavity (Figure 6B). F435 is exposed in the monomeric EDS1 but fully buried by the association with SAG101 and was used to probe the importance of the C-terminal interaction surface. D462 connects the N- and C-terminal domains and might mediate crosstalk at the domain interface. All variants retained interaction with SAG101b, as tested by copurification, although stability of D462N was impaired (Figure 7A). When coexpressed with XopQ in *eds1* plants, immune activities were reduced for F64E and D462N variants and fully abolished for F435E. We also tested F435D and F435A variants. While F435D failed to restore immune capacity in *eds1* plants, F435A was functional (Supplemental Figure 8). We assume that disruption of the apolar patch at the C-terminal interface and introduction of a charged residue in F435E/D dislocates the EP domains within the EDS1-SAG101b heterocomplex against each other without disturbing overall complex assembly mainly driven by the N-terminal

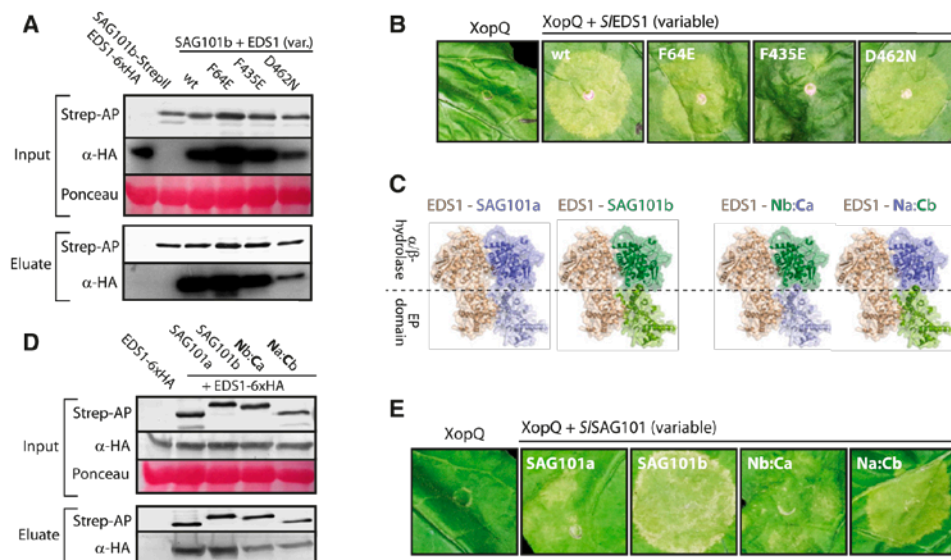


Figure 7. Identification of Nonfunctional EDS1-SAG101b Complex Variants.

(A) Interaction of EDS1 variants with SAG101b. Indicated proteins were (co)expressed in *N. benthamiana* by agroinfiltration. Tissues were used 3 dpi for StrepII purification.

(B) Immune activities of EDS1 variants. Indicated EDS1 variants (with C-terminal 6xHA tag) were transiently coexpressed with XopQ-myc in *eds1* mutant plants by agroinfiltration. Plant reactions were documented 7 dpi.

(C) Structural basis for S/SAG101a-S/SAG101b chimeric proteins. EDS1 and SAG101 both contain an N-terminal hydrolase-like and a C-terminal EP domain. In the heterodimer, an N-terminal interface is formed by the hydrolase-like domains, and a C-terminal interface is formed by the EP domains. For chimeras, the N terminus of SAG101b (aa 1-322) or SAG101a (aa 1-339) was fused with the C terminus of SAG101a (aa 340-581) or SAG101b (aa 323-567), respectively.

(D) Heterocomplex formation by SAG101 chimeric proteins. SAG101 chimeras and native SAG101 isoforms (with a C-terminal StrepII tag) were coexpressed with EDS1-6xHA by agroinfiltration. Tissues were used 3 dpi for StrepII-purification.

(E) Functionality of SAG101 chimeric proteins. Indicated proteins were expressed together with XopQ-myc in *pss* mutant plants by agroinfiltration. Plant reactions were documented 7 dpi.

interaction surface. This finding supports a role for the heterodimeric EP domain surface in TNL signaling.

We constructed chimeric proteins from nonfunctional SAG101a and functional SAG101b to further analyze this aspect (Figure 7C). Although differences between SAG101a and SAG101b isoforms remain unclear, we hypothesized that if the EP domain surface is crucial for immune functions, only the chimeric protein carrying the C terminus of SAG101b might be functional, whereas both chimeras should engage in heterocomplexes with EDS1. SAG101a/b chimeras accumulated to levels comparable with the native isoforms when expressed by agroinfiltration and also formed complexes with EDS1 (Figure 7D). Chimeras and native SAG101 isoforms were coexpressed with XopQ in *pss* mutant plants to test for functionality. SAG101a and the Nb:Ca chimeric protein did not show any activity. In contrast, the Na:Cb chimeric protein was able to restore XopQ-induced cell death, albeit to a lesser extent than SAG101b (Figure 7E). These results suggest that the main differences discriminating SAG101a and SAG101b and their immune competence reside in the C-terminal EP domain and further support the EP domain surface as crucial for the function of EDS1 heterodimers in TNL signaling (Wagner et al., 2013; Bhandari et al., 2019). As the most probable mode of action of EDS1 complexes in

immune signaling, we propose that further interaction partners might be recruited via the heterodimeric EP domain surface.

DISCUSSION

EDS1 is essential for signaling downstream of TNL-type immune receptors and forms mutually exclusive heterodimeric complexes with PAD4 and SAG101 (Hu et al., 2005; Rietz et al., 2011; Wagner et al., 2013; Schultink et al., 2017). Based on analyses in Arabidopsis, immune functions were so far mainly accounted to EDS1-PAD4 (Feys et al., 2005; Wagner et al., 2013; Cui et al., 2017, 2018). In this study, we show that an EDS1-SAG101 complex is necessary and sufficient for all tested TNL-dependent immune responses in *N. benthamiana*, whereas PAD4 does not appear to contribute to immunity (Figures 3 and 4). A role for *NbSAG101* in effector-triggered immunity was also reported in previous virus-induced gene-silencing-based analyses (Pombo et al., 2014).

Several lines of evidence suggest that EDS1-SAG101 complexes, rather than EDS1-PAD4, might also fulfill immune signaling functions in other species containing TNL-type immune receptors outside the *Brassicaceae* family. First, there is strict co-occurrence of *SAG101* and TNL-type immune receptors in

genomes, strongly suggesting a functional link (Figure 1A; Wagner et al., 2013). Second, *Brassicaceae* PAD4 orthologs lack an insertion within the lipase-like domain, which is present in non-*Brassicaceae* PAD4 orthologs and EDS1 orthologs but absent in SAG101 orthologs (Wagner et al., 2013). Therefore, PAD4 might have evolved by a unique path or mechanism in *Brassicaceae*, supporting the hypothesis that PAD4 immune-signaling functions in this family might represent a notable exception. It is interesting to note that *NbPAD4* is induced concomitantly with *NbEDS1* under infection conditions, although it does not contribute to immune signaling in our experiments. In contrast, only minor transcript changes were detected for the signaling-competent *NbSAG101b* (Figure 1B). A possible explanation might be that upregulation of *PAD4* serves to inactivate EDS1-SAG101b-mediated immune signaling, by titration of SAG101b from EDS1. Competition of interactors for the EDS1 moiety for complex formation is supported by enhanced XopQ-induced cell death observed in reconstitution assays in *pss* mutant plants in comparison to *eds1* mutant plants, but overexpression of *S/EDS1* together with *S/SAG101b* without XopQ was not sufficient for cell-death induction. Future reverse genetic studies are needed to clarify which EDS1-containing hetero-complexes function predominantly in TNL signaling. Furthermore, it remains to be determined which functions are exerted by EDS1 complexes that are not involved in immune signaling or EDS1 complexes (with PAD4) in organisms lacking TNLs.

Genome analysis revealed a duplication of *SAG101* in most *Solanaceae* (Figure 1B). Absence of the *SAG101a* isoform in *C. annuum* might indicate reduced selective forces toward its preservation. However, although both the *NbSAG101a2* and *NbSAG101b2* genes showed signs of pseudogenization in allotetraploid *N. benthamiana*, this was not observed for *SAG101a* in any of the remaining analyzed *Solanaceae* genomes. In addition, differential subcellular localization patterns were detected for *S/SAG101* isoforms (Figure 2; Supplemental Figure 3). This finding argues against *SAG101a* representing merely a duplicated gene but rather supports distinct functions of individual isoforms. An additional EDS1-SAG101 complex might provide fine-tuning of EDS1 activities in many *Solanaceae*, but no evidence shows a contribution to TNL-mediated immune responses. It is conceivable that *NbSAG101a* may participate in signaling downstream of yet uncharacterized *N. benthamiana* TNLs, as some Arabidopsis TNLs were also reported to depend on EDS1-SAG101 rather than EDS1-PAD4 (Zhu et al., 2011; Xu et al., 2015). We did not analyze functional relevance of EDS1 subcellular distribution in *N. benthamiana*, but nuclear-localized EDS1 was required and sufficient for several tested immune responses in Arabidopsis (García et al., 2010; Stuttmann et al., 2016). It is worth noting that both *AtEDS1-AtSAG101* and *S/EDS1-S/SAG101a* are confined to nuclei and have only minor or no functions in immunity, whereas complexes required for TNL signaling (*AtEDS1-AtPAD4*, *S/EDS1-S/SAG101b*) also distributed to the cytoplasm.

In interactions of Arabidopsis with *P. syringae* bacteria or filamentous pathogens *Hpa* and *Golovinomyces orontii*, *eds1* mutant plants are significantly impaired in basal resistance (Falk et al., 1999; Lipka et al., 2005; Rietz et al., 2011; Schön et al., 2013). Similarly, an *eds1* mutant tomato line (*sun1-1*) was more susceptible to several virulent pathogens, including *Xcv* (Hu et al.,

2005). By contrast, we did not observe any basal resistance phenotype when comparing in planta growth of avirulent (*Xcv* 85-10) and virulent (*Xcv* Δ xopQ) bacteria in wild-type, *eds1*, *pss*, and *roq1 N. benthamiana* lines (Figure 3; Adlung et al., 2016; Schultink et al., 2017; Qi et al., 2018). Moreover, basal resistance to several viral or other bacterial isolates was not impaired in *EDS1*-silenced *N. benthamiana* plants (Pearl et al., 2002). These results do not support a general role of EDS1 complexes in basal immunity. We therefore assume that any contribution of EDS1 to basal resistance results from loss of TNL-mediated ETI and thus does not represent an independent function. This is in line with expression of basal resistance by the term "PTI/MTI + weak ETI – effector-triggered susceptibility" (Jones and Dangl, 2006), and the TNL-mediated component of "weak ETI" being abolished in *eds1* lines. One explanation why TNL-mediated ETI may have less importance in *N. benthamiana* is the the relatively small complement of TNLs in this species. Automated *R* gene identification previously identified only 17 TIR domain-encoding genes in *N. benthamiana* (Hofberger et al., 2014). Although incomplete *N. benthamiana* genomes and flawed annotations likely lead to underestimation of TNL diversity, TNLs represent the predominant class of NLRs in Arabidopsis with ~70 to 100 TNLs per genome (Meyers et al., 2003; Peele et al., 2014; Van de Weyer et al., 2019). By contrast, CNLs appear to be the predominant NLR class present in *N. benthamiana*.

The *N. benthamiana* system features the key advantage of rapid and robust transient protein expression by agroinfiltration. This was exploited to design transient complementation assays for EDS1-SAG101b functional analyses based on induction of HR-like cell death by XopQ (Adlung et al., 2016; Schultink et al., 2017; Qi et al., 2018). We confirmed significance of results obtained in this highly simplified system by disrupting EDS1-SAG101b complex formation (Figure 6). We mutagenized key residues within the interface and showed that higher order mutants containing multiple amino acid exchanges fail to function in immune signaling. Notably, several EDS1 and SAG101 variants for which interaction was undetectable by copurification (e.g., EDS1-T1VV, SAG101-FLL) still functioned, at least partially, in cell-death induction, indicating that low-level complex formation is sufficient for immune responses. Similarly, a previously described Arabidopsis PAD4-MLF variant (Wagner et al., 2013) deficient in complex formation complemented immune deficiency of *apad4-1 sag101-3* double mutant line when tested (J. Stuttmann and J. Parker, unpublished data). Consequently, extension of the interface analysis from EDS1 to its interaction partner SAG101 lends important support to the previous notion that complex formation is a prerequisite for immune signaling.

Beyond the N-terminal interaction surface, five highly conserved positions distributed all along the surface of EDS1 in the vicinity of the interface with SAG101b were tested for functional significance in the *N. benthamiana* system (Figure 7). R509 and K494 are located in a large conserved cavity formed in EDS1 heterodimeric assemblies, and homologous positions are crucial for full EDS1 immune activities in Arabidopsis (Bhandari et al., 2019). However, we did not observe reduced immune functions for corresponding *S/EDS1* variants. D462 was targeted to probe potential domain crosstalk within EDS1. The *S/EDS1*^{D462N} variant was considerably less competent in restoration of XopQ-induced

HR, but this might also be explained by reduced stability (Figures 7A and 7B). In contrast, F64E and F435E/D, which delimit upper and lower boundaries of the assumed cavity, were not impaired in stability but had reduced or abolished immune activities, respectively. F64 might act as conserved gatekeeper, whereas perturbation of the C-terminal interface by F435E/D is expected to have more profound effects on overall topology of the EP domain assembly (Figure 7). The F435 variants suggest a crucial role of the C-terminal EP domains for immune signaling (Wagner et al., 2013; Bhandari et al., 2019), which is further supported by partial restoration of immune functions in SAG101a by grafting of the SAG101b C terminus in SAG101^{Na-Cb} protein chimeras (Figure 7). Nonetheless, functional impairment of S/EDS1^{F64E} shows that also the N-terminal α/β -hydrolase domain contributes to immune signaling, and roles are thus not limited to alignment of C-terminal EP domains in the heterodimer.

A most plausible hypothesis is that the large surface on S/EDS1 delimited by F435 and F64 is required for interactor recruitment to mediate immune signaling. Recruitment of protein interactors is also supported by results of our cross-species transfer of Roq1 and EDS1 family genes. In line with previous reports showing that even immune receptors from evolutionarily distant species maintain functionality when introduced into new plant lineages (Maekawa et al., 2012), transgenic expression of *NbRoq1* in *Arabidopsis* conferred resistance to *Pst* DC3000 bacteria, presumably through recognition of HopQ (Figure 4B). In contrast, AtEDS1-AtPAD4-AtSAG101 failed to restore immune signaling in *N. benthamiana* mutant plants (Figure 5A). Similarly, S/EDS1-S/PAD4 can fulfill immune functions in *Arabidopsis* but not *N. benthamiana*, whereas the opposite was observed for S/EDS1-S/SAG101b (Figure 5B; Supplemental Figure 6). Consequently, NLR functions are generally conserved, but EDS1 complexes functionally diverged in different species, which suggests co-evolution of signaling-competent heterodimeric assemblies with additional factors, most likely protein interactors. One expectation would be that mutant lines deficient in interactors required for EDS1 immune signaling are impaired in TNL-mediated resistance responses. Although a number of proteins were reported to interact with EDS1 complexes (*Arabidopsis* Interactome Mapping Consortium, 2011; Bhattacharjee et al., 2011; Heidrich et al., 2011; Kim et al., 2012; Cui et al., 2018), mutant lines deficient in respective genes are not generally TNL signaling deficient.

Importantly, the atypical CNL receptor NRG1 was recently identified as a key component required for signaling by TNL receptors (Brendolise et al., 2018; Qi et al., 2018; Castel et al., 2019; Wu et al., 2019). *N. benthamiana nrg1* mutant plants still retain some competence to detect XopQ (via Roq1), and it was hypothesized that residual TNL signaling in these plants might be mediated by the Activated Disease Resistance1 (ADR1) class of helper CNLs (Bonardi et al., 2011; Dong et al., 2016; Schultink et al., 2017; Qi et al., 2018). Indeed, differential requirement of TNLs for helper CNLs of the NRG1 and ADR1 classes and partial redundancy of helper functions were reported in *Arabidopsis*: NRG1 proteins are critical for function of most TNLs, but others require helpers of the ADR1 class or can signal via both pathways (Dong et al., 2016; Castel et al., 2019; Wu et al., 2019). CNLs of the NRG1 family are limited to those genomes containing TNLs (Collier et al., 2011), as also observed for SAG101, and physical

association of *NbNRG1* with *NbEDS1* was reported (Qi et al., 2018). Thus, proteins of the NRG1 class of helper CNLs may represent plausible candidate interaction partners, which might be recruited by EDS1 complexes to form a functional signaling module. Indeed, Lapin et al (2019) show that coexpression of AtNRG1 together with AtEDS1-AtSAG101 can restore XopQ-induced cell death and Roq1-mediated bacterial growth restriction in *N. benthamiana* plants deficient in EDS1 family genes, thus strongly supporting this hypothesis (Lapin et al., 2019). However, physical association of NRG1 proteins with EDS1, as reported by Qi et al. (2018), will require further analysis. A similar interaction between AtEDS1 and AtNRG1.1 could be detected by Wu et al. (2019) only when using EDS1 as bait in coimmunoprecipitation assays (co-IPs) but not in reciprocal experiments and might result from stickiness of EDS1 in co-IP experiments (Wu et al., 2019). It should be noted that co-IPs in the report by Qi et al. (2018) also show formation of *NbEDS1* homodimers. We could not detect homodimerization of the highly similar S/EDS1 in co-IPs, FRET-based interaction assays (Figure 2; Supplemental Figure 3), or by yeast two hybrid. The mechanisms underlying the functional relationships between TNLs, EDS1 complexes, and helper CNLs thus remain a major question to pursue in future analyses.

METHODS

Plant Material, Growth Conditions, Bacterial Strains and Infection Assays

Nicotiana benthamiana wild-type plants and the published *eds1a-1* and *pad4-1* single and *eds1a-1 pad4-1* double mutant lines were used (Ordon et al., 2017). *N. benthamiana* plants were cultivated in a greenhouse with a 16-h light period (sunlight and/or IP65 lamps (Philips) equipped with Agro 400 W bulbs (SON-T); 130–150 $\mu\text{E}/\text{m}^2 \cdot \text{s}$; switchpoint $\sim 100 \mu\text{E}/\text{m}^2 \cdot \text{s}$), 60% relative humidity at 24/20°C (day/night). *Arabidopsis* (*Arabidopsis thaliana*) wild-type accession Columbia and the previously published *eds1-2 pad4-1* double, *eds1-2 pad4-1 sag101-1* triple mutant (Feys et al., 2005; Wagner et al., 2013), and *eds1-12* single mutant (Ordon et al., 2017) lines were used. *Arabidopsis* plants were grown under short day conditions at 23/21°C and with 60% relative humidity or in a greenhouse under long day conditions for seed set.

For bacterial growth assays, the Xcv strain 85-10 (Thieme et al., 2005) and the ΔxopQ mutant (Amlung et al., 2016) were syringe-infiltrated at an $\text{OD}_{600} = 0.0004$, leaf discs were harvested with a cork borer at different time points and disrupted in 10 mM MgCl_2 using a bead mill, and bacterial titers were determined by plating dilution series. For each time point and strain, samples were taken from at least four independent leaves and treated as biological replicates. Bacterial growth assays were repeated at least three times with similar results.

For type III secretion system-dependent protein translocation via *Pseudomonas fluorescens*, a previously described derivative of the “ETHAn” strain (Thomas et al., 2009) containing a plasmid for translocation of XopQ fused to a secretion signal of AvrRpt2, was used (Gantner et al., 2018). *Hyaloperonospora arabidopsidis* isolate Cala2 was used for infection of *Arabidopsis* plants, and infections were done as described previously by Stuttmann et al., 2011. True leaves were stained with Trypan Blue 7 dpi, and representative micrographs are shown.

Phylogenetic Analyses

Genomes as indicated in Supplemental Data Set 1 were mined for EDS1 family genes by tBLASTn using tomato (*Solanum lycopersicum*) proteins as

query. Gene models were examined or assigned using fgenesh+ (Solovyev, 2007) and multiple sequence alignments. For the verification of *N. benthamiana* EDS1 family gene models, RNA-seq data (accession number GSE83618; Legay et al., 2016) was downloaded from the National Center for Biotechnology Information Gene Expression Omnibus website and mapped to the *N. benthamiana* genome (v1.01; Bombarely et al., 2012) using the CLC genomics workbench (version 7.5.5; Qiagen). Read mappings were inspected manually and supported gene models depicted in Supplemental Figure 1 for *NbEDS1*, *NbPAD4* and *NbSAG101a1*. For *NbSAG101a2* and *NbSAG101b2*, the Niben101Scf03969g06010 and Niben101Scf09577g01001 locus annotation (encoding for truncated SAG101 proteins), not the fgenesh+-predicted gene models, were supported by inspection of RNA-seq data. The *NbSAG101b1* gene model was verified by cloning of the cDNA. For phylogenetic tree construction, sequences as provided in Supplemental Data Set 1 were aligned using the MAFFT G-INS-I algorithm (Katoh and Standley, 2013). A phylogenetic tree was calculated using a procedure derived from the SeaView graphical user interface (Gouy et al., 2010). Site selection was performed using Gblocks (Castresana, 2000) to trim the alignments from highly gapped columns with options $-b4 = 5$, $-b5 = h$, $-b2 = 18$ (50% of number of species + 1) for less stringent selection. Then, the tree was computed with the PhyML program (version 3.1; Guindon et al., 2010) using the LG substitution model (with optimized across-site rate variation using four substitution rate categories), empirical amino acid equilibrium frequencies, and an optimized fraction of invariable sites. The tree topology search was performed using the best of NNI (Nearest Neighbor Interchange) and SPR (Subtree Pruning and Regrafting) strategy. Branch support for the final tree was computed with PhyML using 1,000 bootstrap replicates. The final tree was visualized with iTol (Letunic and Bork, 2019). The associated multiple sequence alignment was visualized with Jalview (Waterhouse et al., 2009) and is provided as Supplemental Data Set 2.

Agrobacterium-Mediated Expression, StrepII Purification, and Immunodetection

For transient *Agrobacterium*-mediated expression of proteins in *N. benthamiana* (agroinfiltration), plate-grown bacteria were resuspended in *Agrobacterium* infiltration medium (10 mM MES, pH 5.8, 10 mM MgCl₂). Single strains were infiltrated at an OD₆₀₀ = 0.6. For coexpression, OD₆₀₀ = 0.4 for each strain was used. All constructs for expression of proteins in *N. benthamiana* contained the 35S promoter. EDS1, PAD4, SAG101, or variants were coexpressed with XopQ-myc in reconstitution assays, and phenotypes were documented 5 to 7 dpi. Phenotypic assays were conducted at least 4 times, and representative results are shown. For immunodetection of proteins in support of reconstitution assays and for copurification, proteins were expressed without XopQ to avoid interference due to the negative effect of XopQ recognition on *Agrobacterium*-mediated protein expression (Adlung and Bonas, 2017) but using the same *N. benthamiana* genetic background as in respective reconstitution experiments. Leaf tissue was ground in liquid nitrogen, powder was resuspended in Laemmli buffer, and proteins were denatured by boiling before SDS-PAGE for immunodetection. For StrepII purifications, 1 g of leaf tissue was ground in liquid nitrogen, and the leaf powder was resuspended in 2.5 mL of extraction buffer (50 mM Tris pH 8, 150 mM NaCl, 5 mM EDTA, 5 mM EGTA, 10 mM DTT, 0.1% (v/v) Triton X-100). Suspensions were cleared by centrifugation and supernatants passed through a 0.45 μm syringe filter. 2 mL of cleared extracts were incubated with 120 μL of Strep-Tactin high-capacity matrix (IBA) for 20 min at 4°C on a rotary wheel. The matrix was washed several times with extraction buffer before elution of proteins by boiling with 100 μL of Laemmli buffer. Proteins were resolved by SDS-PAGE and transferred to a nitrocellulose membrane (GE Healthcare). StrepII-tagged proteins were detected using Strep-Tactin alkaline phosphatase conjugate (IBA)

or a mouse monoclonal StrepII antibody (Sigma-Aldrich). Further primary antibodies used were α-mCherry (Abcam, ab167453); mouse monoclonal α-GFP and α-c-myc, rat α-HA (all from Roche); and α-FLAG (Sigma-Aldrich). Secondary antibodies were coupled to horseradish peroxidase (GE Healthcare) or alkaline phosphatase (Sigma-Aldrich). Protein gel blots were used for verification of protein expression in support of reconstitution assays, and protein copurification assays were repeated at least three times with similar results.

Plant Transformation and Genome Editing

Arabidopsis plants were transformed as previously described (Logemann et al., 2006). For transformation of *N. benthamiana*, leaves of greenhouse-grown plants were surface sterilized, cut, and cocultivated with *Agrobacterium* containing Cas9/sgRNA constructs. Explants were surface-sterilized, and transgenic plants were regenerated. A detailed protocol is provided as an online resource (dx.doi.org/10.17504/protocols.io.sbaeai). Details on constructs, target sites for editing of *N. benthamiana* SAG101 isoforms and *Roq1*, and generated mutant alleles are provided in Supplemental Figure 4. T₀ plants were tested phenotypically by challenge inoculation with XopQ-translocating *P. fluorescens* bacteria and screened by PCR. A transgene-free *pad4-1 sag101a-1 sag101b-1* (*pss*) triple mutant was isolated from a segregating T₁ population by PCR screening and crossed to wild type for isolation of the *pad4-1 sag101b-1* double mutant line. Homozygous, nontransgenic seed lots were used for experiments. For the *roq1* mutant line, a T₁ population segregating for two different disruptive alleles (*roq1-3* and *roq1-4*; Supplemental Figure 4) was used for infection assays.

Live-Cell Imaging and Analysis by Förster Resonance Energy Transfer and Acceptor Photobleaching

Images were taken on a LSM780 laser scanning microscope (Zeiss). For imaging of GFP and mCherry, fluorophores were excited with 488 nm and 561 nm laser lines, and emission detected at 493-556 nm and 597-636 nm, respectively. For localization studies, at least three independent experiments were conducted, and multiple images were taken for each replicate and each construct. Similar results were obtained in all experiments. For intensity-based Förster resonance energy transfer (FRET; FRET and acceptor photobleaching), mCherry was bleached using the 561 nm laser at 100% intensity, and GFP fluorescence was measured before and after bleach. Nuclei were selected for measurements. FRET efficiency was calculated by the formula $E_{FD} = 1 - F_{D1}/F_{D2}$ (E_{FD} , FRET-efficiency donor; F_{D1} , intensity donor before bleach, F_{D2} , intensity donor after bleach) using the FRET module of ZEN software (Zeiss). At least 15 measurements per donor/acceptor combination were done per experiment, and data were reproduced in four independent repetitions.

Molecular Cloning and Yeast Two Hybrid Interaction Assays

Constructs were generated by Golden Gate (Engler et al., 2008) and Gateway (Thermo Fisher Scientific; according to manufacturer's instructions) cloning. Golden Gate reactions with either *BsaI* or *BpiI* were performed using 20 to 40 fmol of each DNA module and cycling between 37°C and 16°C, as described previously by Weber et al., 2011. DNA modules of the MoClo Plant Toolkit, Plant Parts I (Engler et al., 2014), and Plant Parts II (Gantner et al., 2018) collections were used. Novel level 0 modules were generated as described previously, and restriction sites were eliminated by site-directed mutagenesis or overlapping PCR products (Engler et al., 2008, 2014). Details on generated constructs and oligonucleotides used for cloning are provided in Supplemental Tables 2 and 3, respectively. Previously described (Gantner et al., 2018) Golden Gate-compatible or Gateway-converted derivatives of pGADT7 and pGBKT7

(Clontech) were used for yeast two hybrid assays. Respective constructs were transformed in yeast strain PJ69-4a by standard procedures (Gietz and Schiestl, 2007). Plate-selected cotransformants were cultivated in liquid Synthetic Drop-Out media for 48 h, and dilution series were prepared and plated on selective media using a multipipette. Extraction of proteins for immunodetection was performed as described previously by Kushnirov (2000).

Gene Expression Analysis

Tomato RNA sequencing data was accessed using the TomExpress portal (<http://tomexpress.toulouse.inra.fr/>; Zouine et al., 2017). Data was visualized as a normalized expression heatmap using Spearman representation. Expression values for different conditions were added manually. For gene expression analyses in *N. benthamiana*, plants were syringe infiltrated with *Xcv* bacteria at an $OD_{600} = 0.02$ in 10 mM $MgCl_2$ or mock infiltrated. RNA was extracted by a standard protocol using TRIzol reagent (ambion; Thermo Fisher Scientific). Briefly, two leaf discs (diameter 9 mm) were frozen in liquid nitrogen, and tissues were disrupted using Zirkonia beads (N039.1; Carl Roth) and a bead mill. RNA was extracted with 1 mL TRIzol; 100 μ L of bromochloropropane was added for phase separation; and RNA was precipitated, washed, dried, and resuspended in 40 μ L water. The Reverse Transcriptase Core Kit was used for cDNA synthesis, and the Takyon No ROX SYBR 2X MasterMix Blue dTTP qPCR Kit (both Eurogentech) was used for quantitative real-time PCR using a CFX96 detection system (Bio-Rad). The previously described reference genes *Protein Phosphatase 2A (PP2A)* and *Elongation Factor 1- α (EF1 α)* were used for data normalization (Liu et al., 2012) with similar results, and data from normalization to *PP2A* is shown. Primers used for quantitative real-time PCR are listed in Supplemental Table 4. All primers had efficiencies of 90% to 105%, as evaluated by dilution series.

Protein Modeling

Structural models of *S. lycopersicum* EDS1-SAG101a and EDS1-SAG101b complexes were modeled using the structure of the Arabidopsis EDS1-SAG101 complex as a template (PDB:4NFU; Wagner et al., 2013). Sequences of *S*/SAG101a and *S*/SAG101b share 38% and 36% sequence identity with *At*SAG101, respectively, whereas *S*/EDS1 and *At*EDS1 share 40%. All three sequence-template pairs could thus be confidently aligned using the hhpred algorithm (Zimmermann et al., 2018), and structural models were generated and relaxed based on these alignments using rosettaCM (Song et al., 2013) with limited need for manual realignment in the regions with insertions. Sequence conservation was calculated using the rate4site algorithm (Pupko et al., 2002) and mapped at the surface of structural models using PyMOL (PyMOL Molecular Graphics System, version 2.0; Schrödinger). Structural models and analysis are provided in Supplemental Data Set 3.

Accession Numbers

Sequence data from this article can be found in The Arabidopsis Information Resource, GenBank, and/or Solgenomics databases or the QUT *N. benthamiana* genome database (<http://benthgenome.qut.edu.au/>) under the following accession numbers: *AtEDS1-At3g48090* (Gene ID: 823964); *AtPAD4-At3g52430* (Gene ID: 824408); *AtSAG101-At5g14930* (Gene ID: 831345); *S*/EDS1-Solyc06g071280.2; *S*/PAD4-Solyc02g032850.2; *S*/SAG101a-Solyc02g069400.2; *S*/SAG101b-Solyc02g067660.2; *NbEDS1-Niben101Scf06720g01024.1* (QUT: Nbv6.1trP77101); *NbPAD4-Niben101Scf02544g01012.1* (QUT: Nbv6.1trP15293); *NbSAG101a-Niben101Scf00271g02011.1* (QUT: Nbv6.1trP10532); *NbSAG101b-Niben101Scf01300g01009.1* (QUT: Nbv6.1trP73488); *NbRcq1-GenBank: MF773579.1*. Additional sequence information is provided in Supplemental Data Set 1.

Supplemental Data

Supplemental Figure 1. EDS1 family gene models from Arabidopsis, *S. lycopersicum*, and *N. benthamiana*. Supports Figure 1.

Supplemental Figure 2. Expression of tomato EDS1 family genes. Supports Figure 1.

Supplemental Figure 3. Localization and complex formation of tomato EDS1 proteins. Supports Figure 2.

Supplemental Figure 4. Generation of mutant lines by genome editing. Supports Figure 3.

Supplemental Figure 5. Functional comparison of EDS1 and SAG101b from *N. benthamiana* and *S. lycopersicum* for XopQ-induced cell death. Supports Figure 3.

Supplemental Figure 6. Cross-species transfer of EDS1-family genes. Supports Figure 5.

Supplemental Figure 7. Heterocomplex formation by EDS1 variants in a yeast two hybrid system. Supports Figure 6.

Supplemental Figure 8. Immune competence of further EDS1 variants. Supports Figure 7.

Supplemental Table 1. *S*/EDS1 and *S*/SAG101 variants functionally interrogated in this study.

Supplemental Table 2. Plasmids used in this study.

Supplemental Table 3. Oligonucleotides used in this study.

Supplemental Table 4. Oligonucleotides used for quantitative RT-PCR.

Supplemental Data Set 1. Protein sequences used for phylogenetic analyses and associated gene models.

Supplemental Data Set 2. Multiple sequence alignment underlying phylogenetic analyses. Extended data supporting Figure 1.

Supplemental Data Set 3. Structural models and analysis of tomato EDS1, PAD4, SAG101a, and SAG101b.

ACKNOWLEDGMENTS

We thank Bianca Rosinsky for taking care of plant growth facilities and growing plants; Ulla Bonas for generous support, discussions, and critical reading of the article; Martin Schattat for assistance with FRET experiments; Magdalena Krzymowska for providing N and p50 expression constructs; and Jessica Andreani for assistance with phylogenetic analyses. This work was funded by the Deutsche Forschungsgemeinschaft (DFG) (GRC grant STU 642-1/1 to J.S.) and seed funding by the CRC 648 (DFG) to J.S., and by the French Infrastructure for Integrated Structural Biology (FRISBI) (grant ANR-10-INSB-05-01 to R.G.).

AUTHOR CONTRIBUTIONS

J.G. and J.O. performed most of the experiments and analyzed data. C.K. performed additional experiments. J.S. designed the study, supervised the research, and analyzed data. R.G. performed phylogenetic analyses and homology modeling and provided structural insights. J.S. wrote the article with contributions from J.G. and R.G.

Received February 15, 2019; revised May 31, 2019; accepted July 1, 2019; published July 2, 2019.

REFERENCES

- Aarts, N., Metz, M., Holub, E., Staskawicz, B.J., Daniels, M.J., and Parker, J.E. (1998). Different requirements for *EDS1* and *NDR1* by disease resistance genes define at least two *R* gene-mediated signaling pathways in *Arabidopsis*. *Proc. Natl. Acad. Sci. USA* **95**: 10306–10311.
- Adlung, N., and Bonas, U. (2017). Dissecting virulence function from recognition: Cell death suppression in *Nicotiana benthamiana* by XopQ/HopQ1-family effectors relies on EDS1-dependent immunity. *Plant J.* **91**: 430–442.
- Adlung, N., Prochaska, H., Thieme, S., Banik, A., Blüher, D., John, P., Nagel, O., Schulze, S., Gantner, J., Delker, C., Stuttmann, J., and Bonas, U. (2016). Non-host resistance induced by the *Xanthomonas* effector XopQ is widespread within the genus *Nicotiana* and functionally depends on EDS1. *Front. Plant Sci.* **7**: 1796.
- Arabidopsis Interactome Mapping Consortium. (2011). Evidence for network evolution in an Arabidopsis interactome map. *Science* **333**: 601–607.
- Bent, A.F., Kunkel, B.N., Dahlbeck, D., Brown, K.L., Schmidt, R., Giraudat, J., Leung, J., and Staskawicz, B.J. (1994). RPS2 of *Arabidopsis thaliana*: a leucine-rich repeat class of plant disease resistance genes. *Science* **265**: 1856–1860.
- Bentham, A., Burdett, H., Anderson, P.A., Williams, S.J., and Kobe, B. (2017). Animal NLRs provide structural insights into plant NLR function. *Ann. Bot.* **119**: 698–702.
- Bernoux, M., Ve, T., Williams, S., Warren, C., Hatters, D., Valkov, E., Zhang, X., Ellis, J.G., Kobe, B., and Dodds, P.N. (2011). Structural and functional analysis of a plant resistance protein TIR domain reveals interfaces for self-association, signaling, and autoregulation. *Cell Host Microbe* **9**: 200–211.
- Bernoux, M., Burdett, H., Williams, S.J., Zhang, X., Chen, C., Newell, K., Lawrence, G.J., Kobe, B., Ellis, J.G., Anderson, P.A., and Dodds, P.N. (2016). Comparative analysis of the flax immune receptors L6 and L7 suggests an equilibrium-based switch activation model. *Plant Cell* **28**: 146–159.
- Bhandari, D., Lapin, D., Kracher, B., vonBorn, P., Bautor, J., Niefind, K., and Parker, J. (2019). An EDS1 heterodimer signaling surface enforces timely reprogramming of immunity genes in *Arabidopsis*. *Nat. Commun.* **10**: 772.
- Bhattacharjee, S., Halane, M.K., Kim, S.H., and Gassmann, W. (2011). Pathogen effectors target *Arabidopsis* EDS1 and alter its interactions with immune regulators. *Science* **334**: 1405–1408.
- Bombarely, A., Rosli, H.G., Vrebalov, J., Moffett, P., Mueller, L.A., and Martin, G.B. (2012). A draft genome sequence of *Nicotiana benthamiana* to enhance molecular plant-microbe biology research. *Mol. Plant Microbe Interact.* **25**: 1523–1530.
- Bonardi, V., Tang, S., Stallmann, A., Roberts, M., Cherkis, K., and Dangl, J.L. (2011). Expanded functions for a family of plant intracellular immune receptors beyond specific recognition of pathogen effectors. *Proc. Natl. Acad. Sci. USA* **108**: 16463–16468.
- Brendolise, C., Martinez-Sanchez, M., Morel, A., Chen, R., Dinis, R., Deroles, S., Peeters, N., Rikkerink, E., and Montefiori, M. (2018). NRG1-mediated recognition of HopQ1 reveals a link between PAMP and effector-triggered immunity. <https://www.biorxiv.org/content/10.1101/293050v1>.
- Burch-Smith, T.M., Schiff, M., Caplan, J.L., Tsao, J., Czymmek, K., and Dinesh-Kumar, S.P. (2007). A novel role for the TIR domain in association with pathogen-derived elicitors. *PLoS Biol.* **5**: e68.
- Büttner, D. (2016). Behind the lines-actions of bacterial type III effector proteins in plant cells. *FEMS Microbiol. Rev.* **40**: 894–937.
- Castel, B., Ngou, P.M., Cevik, V., Redkar, A., Kim, D.S., Yang, Y., Ding, P., and Jones, J.D.G. (2019). Diverse NLR immune receptors activate defence via the RPW8-NLR NRG1. *New Phytol.* **222**: 966–980.
- Castresana, J. (2000). Selection of conserved blocks from multiple alignments for their use in phylogenetic analysis. *Mol. Biol. Evol.* **17**: 540–552.
- Chakravarthy, S., Velásquez, A.C., Ekengren, S.K., Collmer, A., and Martin, G.B. (2010). Identification of *Nicotiana benthamiana* genes involved in pathogen-associated molecular pattern-triggered immunity. *Mol. Plant Microbe Interact.* **23**: 715–726.
- Chen, G., Wei, B., Li, G., Gong, C., Fan, R., and Zhang, X. (2018). TaEDS1 genes positively regulate resistance to powdery mildew in wheat. *Plant Mol. Biol.* **96**: 607–625.
- Collier, S.M., Hamel, L.P., and Moffett, P. (2011). Cell death mediated by the N-terminal domains of a unique and highly conserved class of NB-LRR protein. *Mol. Plant Microbe Interact.* **24**: 918–931.
- Cui, H., Tsuda, K., and Parker, J.E. (2015). Effector-triggered immunity: From pathogen perception to robust defense. *Annu. Rev. Plant Biol.* **66**: 487–511.
- Cui, H., Gobbato, E., Kracher, B., Qiu, J., Bautor, J., and Parker, J.E. (2017). A core function of EDS1 with PAD4 is to protect the salicylic acid defense sector in *Arabidopsis* immunity. *New Phytol.* **213**: 1802–1817.
- Cui, H., Qiu, J., Zhou, Y., Bhandari, D.D., Zhao, C., Bautor, J., and Parker, J.E. (2018). Antagonism of transcription factor MYC2 by EDS1/PAD4 complexes bolsters salicylic acid defense in *Arabidopsis* effector-triggered immunity. *Mol. Plant* **11**: 1053–1066.
- Dong, O.X., Tong, M., Bonardi, V., El Kasmi, F., Woloshen, V., Wünsch, L.K., Dangl, J.L., and Li, X. (2016). TNL-mediated immunity in *Arabidopsis* requires complex regulation of the redundant ADR1 gene family. *New Phytol.* **210**: 960–973.
- Engler, C., Kandzia, R., and Marillonnet, S. (2008). A one pot, one step, precision cloning method with high throughput capability. *PLoS One* **3**: e3647.
- Engler, C., Youles, M., Gruetzner, R., Ehnert, T.M., Werner, S., Jones, J.D., Patron, N.J., and Marillonnet, S. (2014). A Golden Gate modular cloning toolbox for plants. *ACS Synth. Biol.* **3**: 839–843.
- Falk, A., Feys, B.J., Frost, L.N., Jones, J.D., Daniels, M.J., and Parker, J.E. (1999). EDS1, an essential component of *R* gene-mediated disease resistance in *Arabidopsis* has homology to eukaryotic lipases. *Proc. Natl. Acad. Sci. USA* **96**: 3292–3297.
- Feys, B.J., Moisan, L.J., Newman, M.A., and Parker, J.E. (2001). Direct interaction between the *Arabidopsis* disease resistance signaling proteins, EDS1 and PAD4. *EMBO J.* **20**: 5400–5411.
- Feys, B.J., Wiermer, M., Bhat, R.A., Moisan, L.J., Medina-Escobar, N., Neu, C., Cabral, A., and Parker, J.E. (2005). *Arabidopsis* SENESCENCE-ASSOCIATED GENE101 stabilizes and signals within an ENHANCED DISEASE SUSCEPTIBILITY1 complex in plant innate immunity. *Plant Cell* **17**: 2601–2613.
- Gantner, J., Ordon, J., Ilse, T., Kretschmer, C., Gruetzner, R., Löffke, C., Dagdas, Y., Bürstenbinder, K., Marillonnet, S., and Stuttmann, J. (2018). Peripheral infrastructure vectors and an extended set of plant parts for the modular cloning system. *PLoS One* **13**: e0197185.
- García, A.V., Blanvillain-Baufumé, S., Huibers, R.P., Wiermer, M., Li, G., Gobbato, E., Rietz, S., and Parker, J.E. (2010). Balanced nuclear and cytoplasmic activities of EDS1 are required for a complete plant innate immune response. *PLoS Pathog.* **6**: e1000970.
- Gietz, R.D., and Schiestl, R.H. (2007). Frozen competent yeast cells that can be transformed with high efficiency using the LiAc/SS carrier DNA/PEG method. *Nat. Protoc.* **2**: 1–4.

- Goodin, M.M., Zaitlin, D., Naidu, R.A., and Lommel, S.A. (2008). *Nicotiana benthamiana*: Its history and future as a model for plant-pathogen interactions. *Mol. Plant Microbe Interact.* **21**: 1015–1026.
- Gouy, M., Guindon, S., and Gascuel, O. (2010). SeaView version 4: A multiplatform graphical user interface for sequence alignment and phylogenetic tree building. *Mol. Biol. Evol.* **27**: 221–224.
- Guindon, S., Dufayard, J.F., Lefort, V., Anisimova, M., Hordijk, W., and Gascuel, O. (2010). New algorithms and methods to estimate maximum-likelihood phylogenies: Assessing the performance of PhyML 3.0. *Syst. Biol.* **59**: 307–321.
- Hecker, A., Wallmeroth, N., Peter, S., Blatt, M.R., Harter, K., and Grefen, C. (2015). Binary 2in1 Vectors Improve in Planta (Co)localization and Dynamic Protein Interaction Studies. *Plant Physiol.* **168**: 776–787.
- Heidrich, K., Wirthmueller, L., Tasset, C., Pouzet, C., Deslandes, L., and Parker, J.E. (2011). Arabidopsis EDS1 connects pathogen effector recognition to cell compartment-specific immune responses. *Science* **334**: 1401–1404.
- Hofberger, J.A., Zhou, B., Tang, H., Jones, J.D., and Schranz, M.E. (2014). A novel approach for multi-domain and multi-gene family identification provides insights into evolutionary dynamics of disease resistance genes in core eudicot plants. *BMC Genomics* **15**: 966.
- Hu, G., deHart, A.K., Li, Y., Ustach, C., Handley, V., Navarre, R., Hwang, C.F., Aegerter, B.J., Williamson, V.M., and Baker, B. (2005). EDS1 in tomato is required for resistance mediated by TIR-class R genes and the receptor-like R gene *Ve*. *Plant J.* **42**: 376–391.
- Jacob, F., Vernaldi, S., and Maekawa, T. (2013). Evolution and conservation of plant NLR functions. *Front. Immunol.* **4**: 297.
- Jones, J.D., and Dangl, J.L. (2006). The plant immune system. *Nature* **444**: 323–329.
- Jones, J.D., Vance, R.E., and Dangl, J.L. (2016). Intracellular innate immune surveillance devices in plants and animals. *Science* **354**: aaf6395.
- Katoh, K., and Standley, D.M. (2013). MAFFT multiple sequence alignment software version 7: Improvements in performance and usability. *Mol. Biol. Evol.* **30**: 772–780.
- Khan, M., Subramaniam, R., and Desveaux, D. (2016). Of guards, decoys, baits and traps: Pathogen perception in plants by type III effector sensors. *Curr. Opin. Microbiol.* **29**: 49–55.
- Kim, S.H., Kwon, S.I., Saha, D., Anyanwu, N.C., and Gassmann, W. (2009). Resistance to the *Pseudomonas syringae* effector HopA1 is governed by the TIR-NBS-LRR protein RPS6 and is enhanced by mutations in SRRF1. *Plant Physiol.* **150**: 1723–1732.
- Kim, T.-H., Kunz, H.-H., Bhattacharjee, S., Hauser, F., Park, J., Engineer, C., Liu, A., Ha, T., Parker, J.E., Gassmann, W., and Schroeder, J.I. (2012). Natural variation in small molecule-induced TIR-NB-LRR signaling induces root growth arrest via EDS1- and PAD4-complexed R protein VICTR in Arabidopsis. *Plant Cell* **24**: 5177–5192.
- Krasileva, K.V., Zheng, C., Leonelli, L., Goritschnig, S., Dahlbeck, D., and Staskawicz, B.J. (2011). Global analysis of Arabidopsis/downy mildew interactions reveals prevalence of incomplete resistance and rapid evolution of pathogen recognition. *PLoS One* **6**: e28765.
- Kushalappa, A.C., Yogendra, K.N., and Karre, S. (2016). Plant innate immune response: Qualitative and quantitative resistance. *Crit. Rev. Plant Sci.* **35**: 38–55.
- Kushnirov, V.V. (2000). Rapid and reliable protein extraction from yeast. *Yeast* **16**: 857–860.
- Lapin, D., Kovacova, V., Sun, X., Dongus, J.A., Bhandari, D.D., von Born, P., Bautor, J., Guarneri, N., Rzemieniewski, J., Stuttmann, J., Beyer, A., and Parker, J.E. (2019). A coevolved EDS1-SAG101-NRG1 module mediates cell death signaling by TIR-domain immune receptors. *Plant Cell tpc.00118.2019*.
- Legay, S., Guerriero, G., André, C., Guignard, C., Cocco, E., Charton, S., Boutry, M., Rowland, O., and Hausman, J.F. (2016). MdMyb93 is a regulator of suberin deposition in russeted apple fruit skins. *New Phytol.* **212**: 977–991.
- Letunic, I., and Bork, P. (2019). Interactive Tree Of Life (iTOL) v4: Recent updates and new developments. *Nucleic Acids Res.* **47**: 256–259.
- Lipka, V., et al. (2005) Pre- and postinvasion defenses both contribute to nonhost resistance in Arabidopsis. *Science* **310**: 1180–1183.
- Liu, D., Shi, L., Han, C., Yu, J., Li, D., and Zhang, Y. (2012). Validation of reference genes for gene expression studies in virus-infected *Nicotiana benthamiana* using quantitative real-time PCR. *PLoS One* **7**: e46451.
- Logemann, E., Birkenbihl, R.P., Ülker, B., and Somssich, I.E. (2006). An improved method for preparing *Agrobacterium* cells that simplifies the Arabidopsis transformation protocol. *Plant Methods* **2**: 16.
- Macho, A.P., and Zipfel, C. (2014). Plant PRRs and the activation of innate immune signaling. *Mol. Cell* **54**: 263–272.
- Macho, A.P., and Zipfel, C. (2015). Targeting of plant pattern recognition receptor-triggered immunity by bacterial type-III secretion system effectors. *Curr. Opin. Microbiol.* **23**: 14–22.
- Maekawa, T., et al. (2011b) Coiled-coil domain-dependent homodimerization of intracellular barley immune receptors defines a minimal functional module for triggering cell death. *Cell Host Microbe* **9**: 187–199.
- Maekawa, T., Kufer, T.A., and Schulze-Lefert, P. (2011a). NLR functions in plant and animal immune systems: So far and yet so close. *Nat. Immunol.* **12**: 817–826.
- Maekawa, T., Kracher, B., Vernaldi, S., Ver Loren van Themaat, E., and Schulze-Lefert, P. (2012). Conservation of NLR-triggered immunity across plant lineages. *Proc. Natl. Acad. Sci. USA* **109**: 20119–20123.
- Meyers, B.C., Kozik, A., Griego, A., Kuang, H., and Michelmore, R.W. (2003). Genome-wide analysis of NBS-LRR-encoding genes in Arabidopsis. *Plant Cell* **15**: 809–834.
- Mindrinos, M., Katagiri, F., Yu, G.-L., and Ausubel, F.M. (1994). The *A. thaliana* disease resistance gene *RPS2* encodes a protein containing a nucleotide-binding site and leucine-rich repeats. *Cell* **78**: 1089–1099.
- Monteiro, F., and Nishimura, M.T. (2018). Structural, functional, and genomic diversity of plant NLR proteins: An evolved resource for rational engineering of plant immunity. *Annu. Rev. Phytopathol.* **56**: 243–267.
- Naim, F., Nakasugi, K., Crowhurst, R.N., Hilario, E., Zwart, A.B., Hellens, R.P., Taylor, J.M., Waterhouse, P.M., and Wood, C.C. (2012). Advanced engineering of lipid metabolism in *Nicotiana benthamiana* using a draft genome and the V2 viral silencing-suppressor protein. *PLoS One* **7**: e52717.
- Ordon, J., Gantner, J., Kemna, J., Schwalgun, L., Reschke, M., Streubel, J., Boch, J., and Stuttmann, J. (2017). Generation of chromosomal deletions in dicotyledonous plants employing a user-friendly genome editing toolkit. *Plant J.* **89**: 155–168.
- Parker, J.E., Holub, E.B., Frost, L.N., Falk, A., Gunn, N.D., and Daniels, M.J. (1996). Characterization of *eds1*, a mutation in Arabidopsis suppressing resistance to *Peronospora parasitica* specified by several different RPP genes. *Plant Cell* **8**: 2033–2046.
- Peart, J.R., Cook, G., Feys, B.J., Parker, J.E., and Baulcombe, D.C. (2002). An *EDS1* orthologue is required for *N*-mediated resistance against tobacco mosaic virus. *Plant J.* **29**: 569–579.

- Peele, H.M., Guan, N., Fogelqvist, J., and Dixelius, C. (2014). Loss and retention of resistance genes in five species of the Brassicaceae family. *BMC Plant Biol.* **14**: 298.
- Poland, J.A., Balint-Kurti, P.J., Wisser, R.J., Pratt, R.C., and Nelson, R.J. (2009). Shades of gray: The world of quantitative disease resistance. *Trends Plant Sci.* **14**: 21–29.
- Pombo, M.A., Zheng, Y., Fernandez-Pozo, N., Dunham, D.M., Fei, Z., and Martin, G.B. (2014). Transcriptomic analysis reveals tomato genes whose expression is induced specifically during effector-triggered immunity and identifies the Epk1 protein kinase which is required for the host response to three bacterial effector proteins. *Genome Biol.* **15**: 492.
- Pupko, T., Bell, R.E., Mayrose, I., Glaser, F., and Ben-Tal, N. (2002). Rate4Site: An algorithmic tool for the identification of functional regions in proteins by surface mapping of evolutionary determinants within their homologues. *Bioinformatics* **18**: S71–S77.
- Qi, T., Seong, K., Thomazella, D.P.T., Kim, J.R., Pham, J., Seo, E., Cho, M.-J., Schultink, A., and Staskawicz, B.J. (2018). NRG1 functions downstream of EDS1 to regulate TIR-NLR-mediated plant immunity in *Nicotiana benthamiana*. *Proc. Natl. Acad. Sci. USA*. **115**: E10979–E10987.
- Rietz, S., Stamm, A., Malonek, S., Wagner, S., Becker, D., Medina-Escobar, N., Vlot, A.C., Feys, B.J., Niefind, K., and Parker, J.E. (2011). Different roles of Enhanced Disease Susceptibility1 (EDS1) bound to and dissociated from Phytoalexin Deficient4 (PAD4) in *Arabidopsis* immunity. *New Phytol.* **191**: 107–119.
- Rosli, H.G., Zheng, Y., Pombo, M.A., Zhong, S., Bombarely, A., Fei, Z., Collmer, A., and Martin, G.B. (2013). Transcriptomics-based screen for genes induced by flagellin and repressed by pathogen effectors identifies a cell wall-associated kinase involved in plant immunity. *Genome Biol.* **14**: R139.
- Schön, M., Töller, A., Diezel, C., Roth, C., Westphal, L., Wiermer, M., and Somssich, I.E. (2013). Analyses of wrky18 wrky40 plants reveal critical roles of SA/EDS1 signaling and indole-glucosinolate biosynthesis for *Golovinomyces orontii* resistance and a loss-of-resistance towards *Pseudomonas syringae* pv. tomato AvrRPS4. *Mol. Plant Microbe Interact.* **26**: 758–767.
- Schultink, A., Qi, T., Lee, A., Steinbrener, A., and Staskawicz, B. (2017). Roq1 mediates recognition of the *Xanthomonas* and *Pseudomonas* effector proteins XopQ and HopQ1. *Plant J.* **92**: 787–795.
- Shen, C., Lu, A., Xie, W.J., Ruan, J., Negro, R., Egelman, E.H., Fu, T.-M., and Wu, H. (2019). Molecular mechanism for NLRP6 inflammasome assembly and activation. *Proc. Natl. Acad. Sci. USA*. **116**: 2052–2057.
- Shimada, T.L., Shimada, T., and Hara-Nishimura, I. (2010). A rapid and non-destructive screenable marker, FAST, for identifying transformed seeds of *Arabidopsis thaliana*. *Plant J.* **61**: 519–528.
- Sinapidou, E., Williams, K., Nott, L., Bahkt, S., Tör, M., Crute, I., Bittner-Eddy, P., and Beynon, J. (2004). Two TIR:NB:LRR genes are required to specify resistance to *Peronospora parasitica* isolate Cala2 in *Arabidopsis*. *Plant J.* **38**: 898–909.
- Solovyev, V.V. (2007). Statistical approaches in Eukaryotic gene prediction. In *Handbook of Statistical Genetics*. Balding, D.J., Bishop, M., and Cannings, C. eds. (New Jersey: John Wiley & Sons) pp. 97–159.
- Song, Y., DiMaio, F., Wang, R.Y., Kim, D., Miles, C., Brunette, T., Thompson, J., and Baker, D. (2013). High-resolution comparative modeling with RosettaCM. *Structure* **21**: 1735–1742.
- Spoel, S.H., and Dong, X. (2012). How do plants achieve immunity? Defence without specialized immune cells. *Nat. Rev. Immunol.* **12**: 89–100.
- Stuttman, J., Hubberten, H.M., Rietz, S., Kaur, J., Muskett, P., Guerois, R., Bednarek, P., Hoefgen, R., and Parker, J.E. (2011). Perturbation of *Arabidopsis* amino acid metabolism causes incompatibility with the adapted biotrophic pathogen *Hyaloperonospora arabidopsidis*. *Plant Cell* **23**: 2788–2803.
- Stuttman, J., Peine, N., Garcia, A.V., Wagner, C., Choudhury, S.R., Wang, Y., James, G.V., Griebel, T., Alcázar, R., Tsuda, K., Schneeberger, K., and Parker, J.E. (2016). *Arabidopsis thaliana* DM2h (R8) within the Landsberg RPP1-like resistance locus underlies three different cases of EDS1-conditioned autoimmunity. *PLoS Genet.* **12**: e1005990.
- Swiderski, M.R., Birker, D., and Jones, J.D. (2009). The TIR domain of TIR-NB-LRR resistance proteins is a signaling domain involved in cell death induction. *Mol. Plant Microbe Interact.* **22**: 157–165.
- Takken, F.L.W., and Govers, A. (2012). How to build a pathogen detector: Structural basis of NB-LRR function. *Curr. Opin. Plant Biol.* **15**: 375–384.
- Thieme, F., et al. (2005). Insights into genome plasticity and pathogenicity of the plant pathogenic bacterium *Xanthomonas campestris* pv. *vesicatoria* revealed by the complete genome sequence. *J. Bacteriol.* **187**: 7254–7266.
- Thomas, W.J., Thireault, C.A., Kimbrel, J.A., and Chang, J.H. (2009). Recombineering and stable integration of the *Pseudomonas syringae* pv. *syringae* 61 hrp/hrc cluster into the genome of the soil bacterium *Pseudomonas fluorescens* Pf0-1. *Plant J.* **60**: 919–928.
- Van de Weyer, A.-L., Monteiro, F., Furzer, O.J., Nishimura, M.T., Cevik, V., Witek, K., Jones, D.G.J., Dangl, J.L., Weigel, D., and Bemm, F. (2019). The *Arabidopsis thaliana* pan-NLRome. <https://www.biorxiv.org/content/10.1101/537001v1>.
- Venugopal, S.C., Jeong, R.-D., Mandal, M.K., Zhu, S., Chandra-Shekar, A.C., Xia, Y., Hersh, M., Stromberg, A.J., Navarre, D., Kachroo, A., and Kachroo, P. (2009). Enhanced disease susceptibility 1 and salicylic acid act redundantly to regulate resistance gene-mediated signaling. *PLoS Genet.* **5**: e1000545.
- Vlot, A.C., Dempsey, D.A., and Klessig, D.F. (2009). Salicylic acid, a multifaceted hormone to combat disease. *Annu. Rev. Phytopathol.* **47**: 177–206.
- Wagner, S., Stuttman, J., Rietz, S., Guerois, R., Brunstein, E., Bautor, J., Niefind, K., and Parker, J.E. (2013). Structural basis for signaling by exclusive EDS1 heteromeric complexes with SAG101 or PAD4 in plant innate immunity. *Cell Host Microbe* **14**: 619–630.
- Wang, J., Hu, M., Wang, J., Qi, J., Han, Z., Wang, G., and Chai, J. (2019a). Reconstitution and structure of a plant NLR resistosome conferring immunity. *Science*. **364**: 5870.
- Wang, J., Wang, J., Hu, M., Wu, S., Qi, J., Wang, G., and Chai, J. (2019b). Ligand-triggered allosteric ADP release primes a plant NLR complex. *Science* **364**.
- Waterhouse, A.M., Procter, J.B., Martin, D.M., Clamp, M., and Barton, G.J. (2009). Jalview version 2: A multiple sequence alignment editor and analysis workbench. *Bioinformatics* **25**: 1189–1191.
- Weber, E., Engler, C., Gruetzner, R., Werner, S., and Marillonnet, S. (2011). A modular cloning system for standardized assembly of multigene constructs. *PLoS One* **6**: e16765.
- Wei, H.L., Zhang, W., and Collmer, A. (2018). Modular study of the type III effector repertoire in *Pseudomonas syringae* pv. tomato DC3000 reveals a matrix of effector interplay in pathogenesis. *Cell Reports* **23**: 1630–1638.
- Wiermer, M., Feys, B.J., and Parker, J.E. (2005). Plant immunity: The EDS1 regulatory node. *Curr. Opin. Plant Biol.* **8**: 383–389.
- Williams, S.J., et al. (2014). Structural basis for assembly and function of a heterodimeric plant immune receptor. *Science* **344**: 299–303.

2474 The Plant Cell

- Wirthmueller, L., Zhang, Y., Jones, J.D., and Parker, J.E.** (2007). Nuclear accumulation of the Arabidopsis immune receptor RPS4 is necessary for triggering EDS1-dependent defense. *Curr. Biol.* **17**: 2023–2029.
- Wu, Z., Li, M., Dong, O.X., Xia, S., Liang, W., Bao, Y., Wasteneys, G., and Li, X.** (2019). Differential regulation of TNL-mediated immune signaling by redundant helper CNLs. *New Phytol.* **222**: 938–953.
- Xu, F., Zhu, C., Cevik, V., Johnson, K., Liu, Y., Sohn, K., Jones, J.D., Holub, E.B., and Li, X.** (2015). Autoimmunity conferred by chs3-2D relies on CSA1, its adjacent TNL-encoding neighbour. *Sci. Rep.* **5**: 8792.
- Yu, X., Feng, B., He, P., and Shan, L.** (2017). From chaos to harmony: Responses and signaling upon microbial pattern recognition. *Annu. Rev. Phytopathol.* **55**: 109–137.
- Zembek, P., et al.** (2018) Two strategies of *Pseudomonas syringae* to avoid recognition of the HopQ1 effector in *Nicotiana* species. *Front. Plant Sci.* **9**: 978.
- Zhu, S., Jeong, R.D., Venugopal, S.C., Lapchyk, L., Navarre, D., Kachroo, A., and Kachroo, P.** (2011). SAG101 forms a ternary complex with EDS1 and PAD4 and is required for resistance signaling against turnip crinkle virus. *PLoS Pathog.* **7**: e1002318.
- Zimmermann, L., Stephens, A., Nam, S.Z., Rau, D., Kübler, J., Lozajic, M., Gabler, F., Söding, J., Lupas, A.N., and Alva, V.** (2018). A completely reimplemented MPI bioinformatics toolkit with a new HHpred server at its core. *J. Mol. Biol.* **430**: 2237–2243.
- Zouine, M., Maza, E., Djari, A., Lauvernier, M., Frasse, P., Smouni, A., Pirrello, J., and Bouzayen, M.** (2017). TomExpress, a unified tomato RNA-Seq platform for visualization of expression data, clustering and correlation networks. *Plant J.* **92**: 727–735.

An EDS1-SAG101 Complex Is Essential for TNL-Mediated Immunity in *Nicotiana benthamiana*

Johannes Gantner, Jana Ordon, Carola Kretschmer, Raphaël Guerois and Johannes Stuttmann

Plant Cell 2019;31;2456-2474; originally published online July 2, 2019;

DOI 10.1105/tpc.19.00099

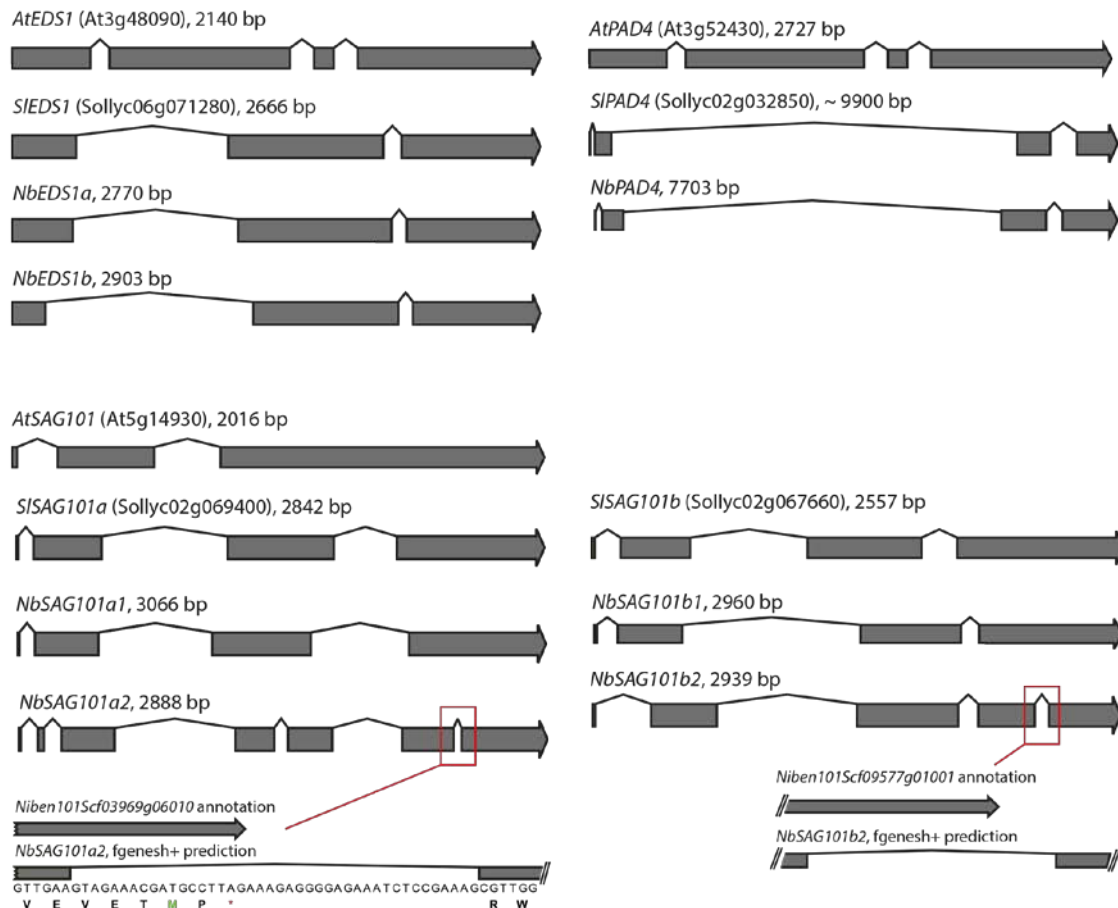
This information is current as of October 9, 2019

| | |
|---------------------------------|---|
| Supplemental Data | /content/suppl/2019/10/01/tpc.19.00099.DC2.html /content/suppl/2019/10/01/tpc.19.00099.DC3.html /content/suppl/2019/07/02/tpc.19.00099.DC1.html |
| References | This article cites 102 articles, 23 of which can be accessed free at: /content/31/10/2456.full.html#ref-list-1 |
| Permissions | https://www.copyright.com/ccc/openurl.do?sid=pd_hw1532298X&issn=1532298X&WT.mc_id=pd_hw1532298X |
| eTOCs | Sign up for eTOCs at: http://www.plantcell.org/cgi/alerts/ctmain |
| CiteTrack Alerts | Sign up for CiteTrack Alerts at: http://www.plantcell.org/cgi/alerts/ctmain |
| Subscription Information | Subscription Information for <i>The Plant Cell</i> and <i>Plant Physiology</i> is available at: http://www.aspb.org/publications/subscriptions.cfm |

3.5.2. Supplemental material to publication Gantner *et al.*, 2019

- Supplemental Figures S1 – S8 as well as Table S1-S4 are shown below
- Additional supporting information are available online:
<http://www.plantcell.org/content/31/10/2456/tab-figures-data>

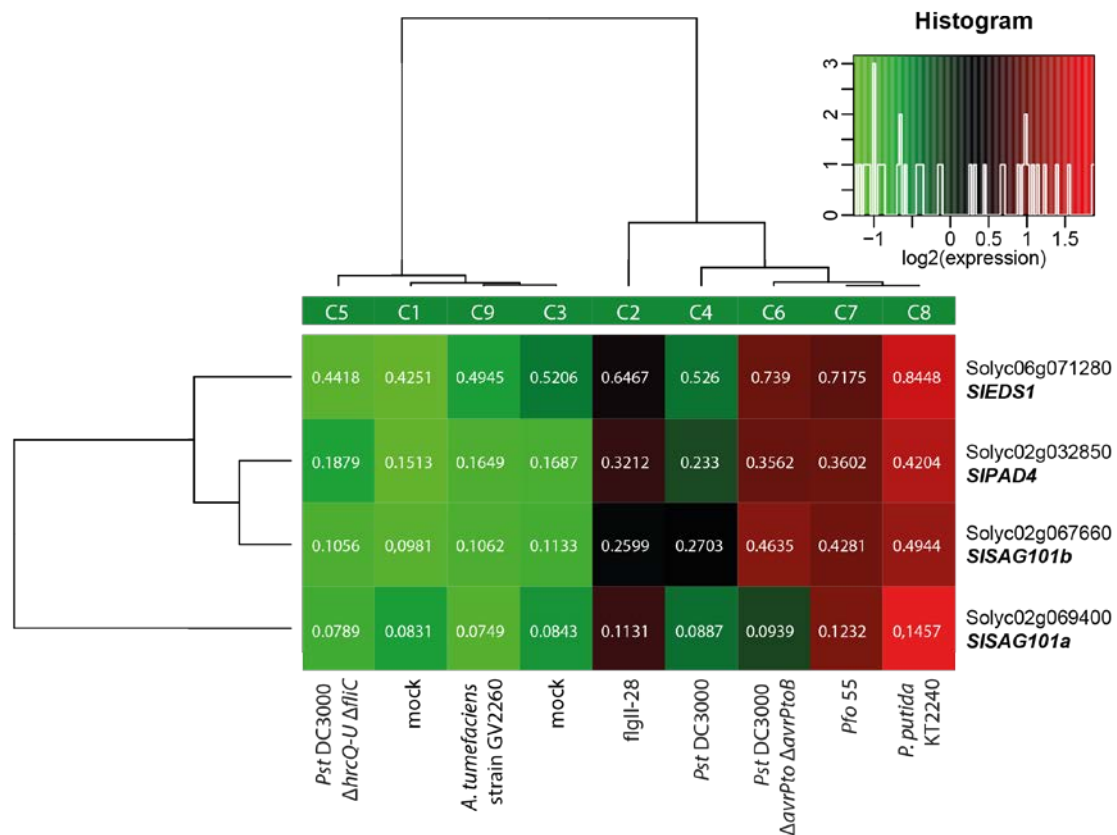
Supplemental Data. Gantner et al. (2019). Plant Cell 10.1105/tpc.19.00099.



Supplemental Figure 1: *EDS1* family gene models from Arabidopsis, tomato and *Nicotiana benthamiana*. Supports Figure 1.

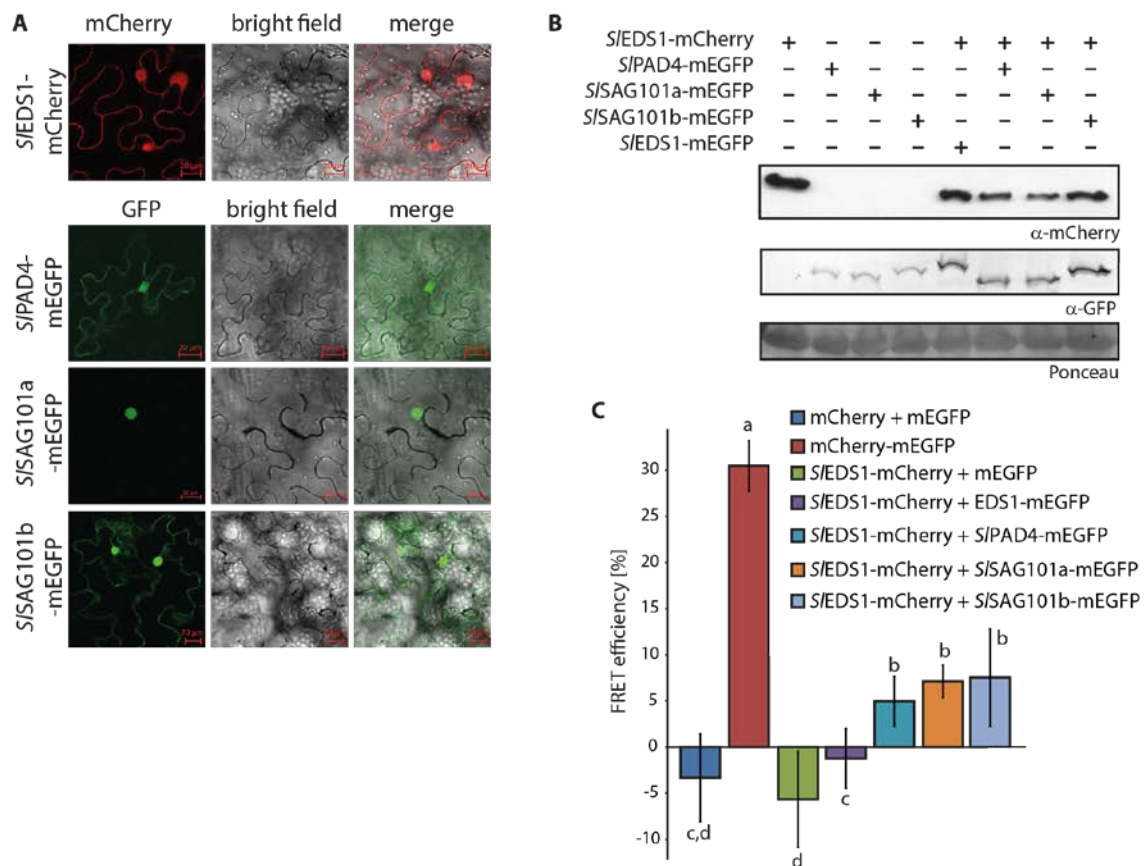
Putative *EDS1*, *PAD4* and *SAG101* homologs were detected as described in materials and methods. Gene models (*Nicotiana benthamiana*) were predicted using fgenes+ and the corresponding tomato proteins as support. The gene model depicted for *NbSAG101b1* was experimentally verified by cDNA cloning. Gene models depicted for *NbEDS1a*, *NbPAD4* and *NbSAG101a1* are supported by an alignment of public RNAseq data against the *N. benthamiana* genome (see material and methods). Inspection of alignments of RNAseq data for *NbSAG101a2/b2* did not provide support for splicing of introns marked by red boxes in the gene models. These introns are also not included in gene models of the *N. benthamiana* genome release (see insets), and contain premature STOP codons (details shown in left inset). *NbSAG101a2/b2* thus encode for truncated proteins. Sequence details including annotations are provided in Supplemental Dataset 1.

Supplemental Data. Gantner et al. (2019). Plant Cell 10.1105/tpc.19.00099.

Supplemental Figure 2: Expression of tomato *EDS1* family genes. Supports Figure 1.

A public RNAseq dataset from treatment of tomato "Rio Grande" plants with different PTI-inducers (Rosli et al., 2013) was analyzed for expression of *EDS1* family genes using the TomExpress portal (Zouine et al., 2017). Hierarchical clustering using Spearman distance (output from TomExpress) is shown. Details on treatments C1-C9 are indicated below the respective columns.

Supplemental Data. Gantner et al. (2019). Plant Cell 10.1105/tpc.19.00099.

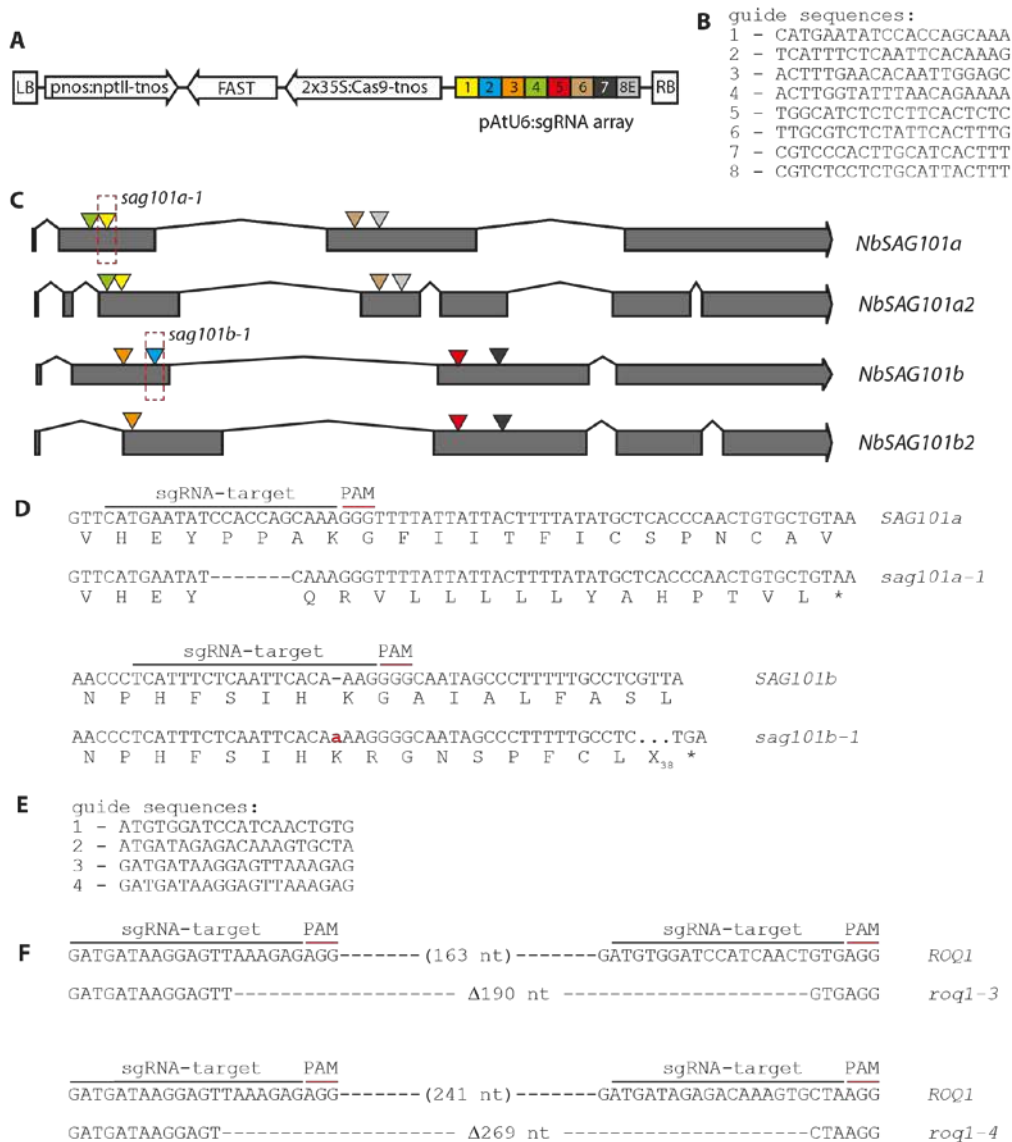


Supplemental Figure 3: Localization and complex formation of tomato EDS1 proteins. Supports Figure 2. A) Localization of tomato EDS1, PAD4 and SAG101a/b isoforms when expressed singly. Extended data supporting Figure 2A.

B) Integrity of EDS1, PAD4 and SAG101 fluorophore fusions when expressed singly or in combination. Extended data supporting Figures 2A, S3A and S3C.

C) Formation of complexes between tomato EDS1 family proteins in living cells as measured by FRET-APB (intensity-based FRET; standard deviation is shown, letters indicate statistically significant differences as determined by one way ANOVA and Fisher LSD post-hoc test, $p < 0,001$).

Supplemental Data. Gantner et al. (2019). Plant Cell 10.1105/tpc.19.00099.



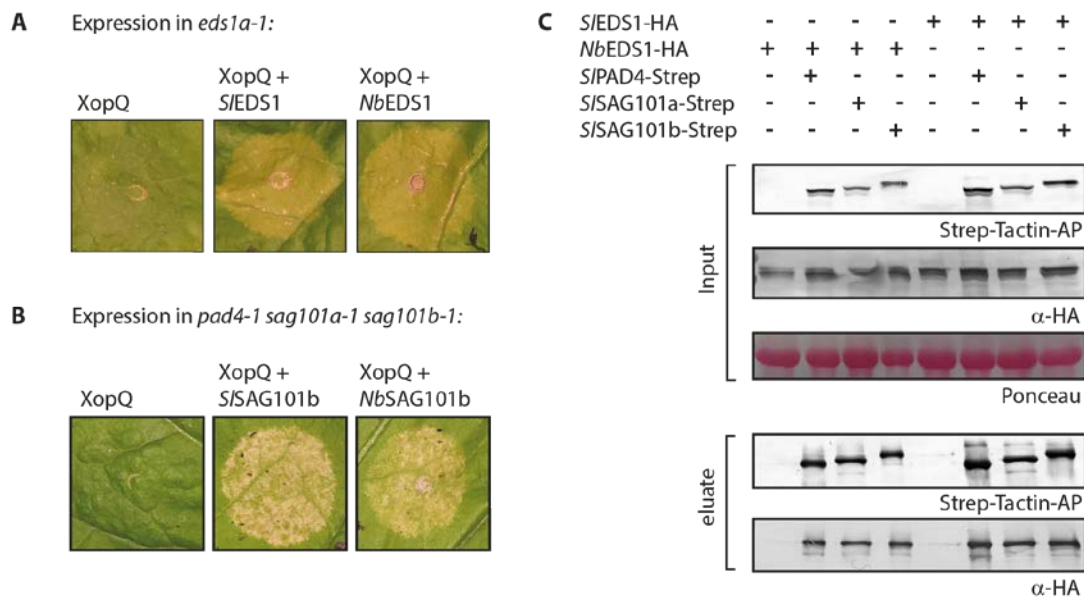
Supplemental Figure 4: Generation of mutant lines by genome editing. Supports Figure 3.

A) Scheme of the T-DNA construct used for editing *SAG101* genes in *N. benthamiana*. Construct is based on pDGE160 (Ordon et al., 2017).

B) Guide sequences incorporated in the sgRNA array of the construct shown in A).

C) Position of target sites within *SAG101* gene models. The color code corresponds to panel A).D) Details on *sag101a-1* and *sag101b-1* alleles generated by genome editing.E) Guide sequences used for editing of the *Roq1* gene. A construct similar to that in A), but based on a different pDGE recipient vector (pDGE311), was used.F) Molecular details on *roq1-3* and *roq1-4* alleles generated by genome editing.

Supplemental Data. Gantner et al. (2019). Plant Cell 10.1105/tpc.19.00099.



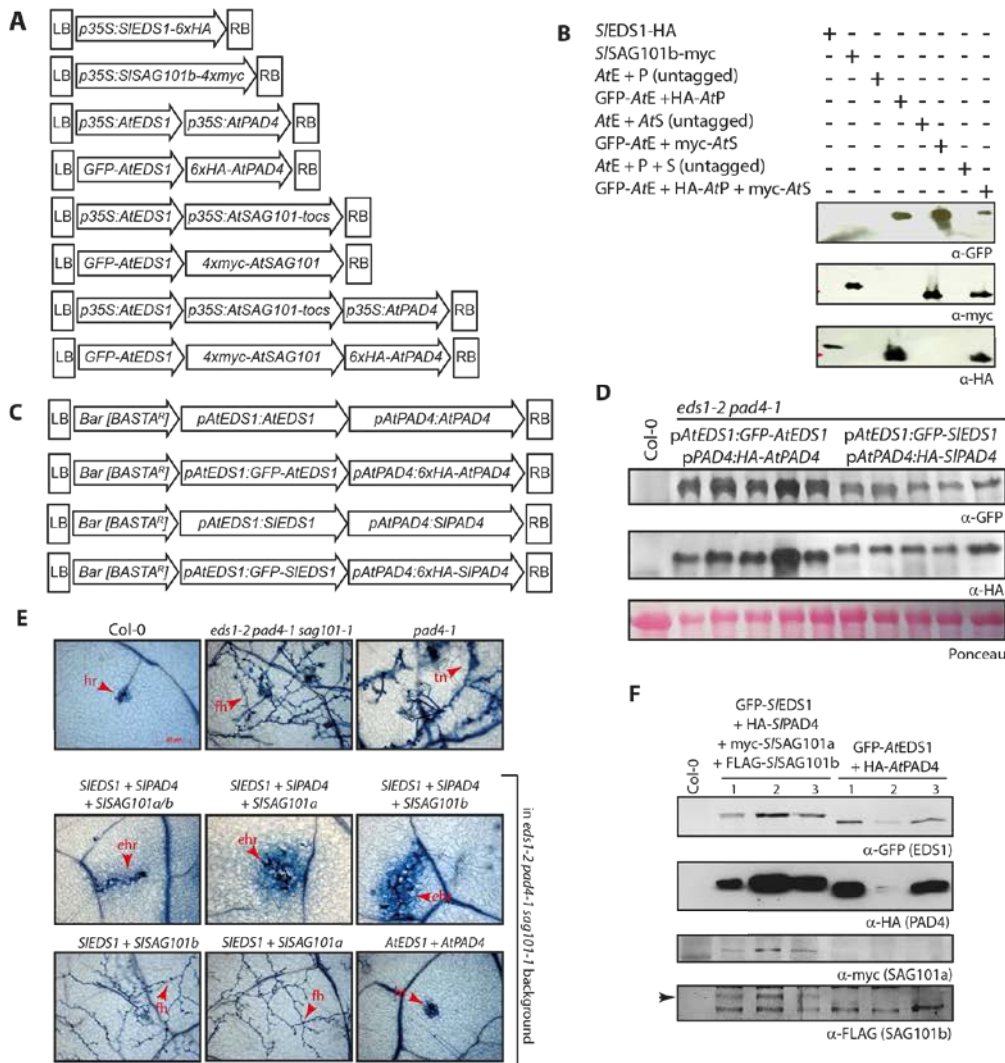
Supplemental Figure 5: Functional comparison of EDS1 and SAG101b from *N. benthamiana* and *S. lycopersicum* for XopQ-induced cell death. Supports Figure 3.

A) Restoration of XopQ-induced cell death by co-expression of *S*EDS1 and *Nb*EDS1. Indicated proteins were (co-) expressed in *eds1* mutant plants, and HR development was documented 6 dpi.

B) As in (A), but *S*SAG101b and *Nb*SAG101b were co-expressed together with XopQ in *eds1 pad4 sag101b* triple mutant plants.

C) Complex formation between *Nb*EDS1 and *S*PAD4, *S*SAG101a and *S*SAG101b. Indicated proteins were (co-) expressed in *N. benthamiana* by Agroinfiltration. Tissues were used 3 dpi for StrepII-purification.

Supplemental Data. Gantner et al. (2019). Plant Cell 10.1105/tpc.19.00099.

Supplemental Figure 6: Cross-species transfer of *EDS1*-family genes. Supports Figure 5.

A) Schematic representation of T-DNA constructs used for *Agrobacterium*-mediated transient expression of *EDS1* family genes (from *Arabidopsis* or tomato) in *N. benthamiana*. Extended data to Figure 5A.

B) Expression of *Arabidopsis* proteins in *N. benthamiana*. Extended data to Figure 5A. E – EDS1, P – PAD4, S – SAG101. Total extracts were prepared from infiltrated leaf sections 3 dpi for protein detection.

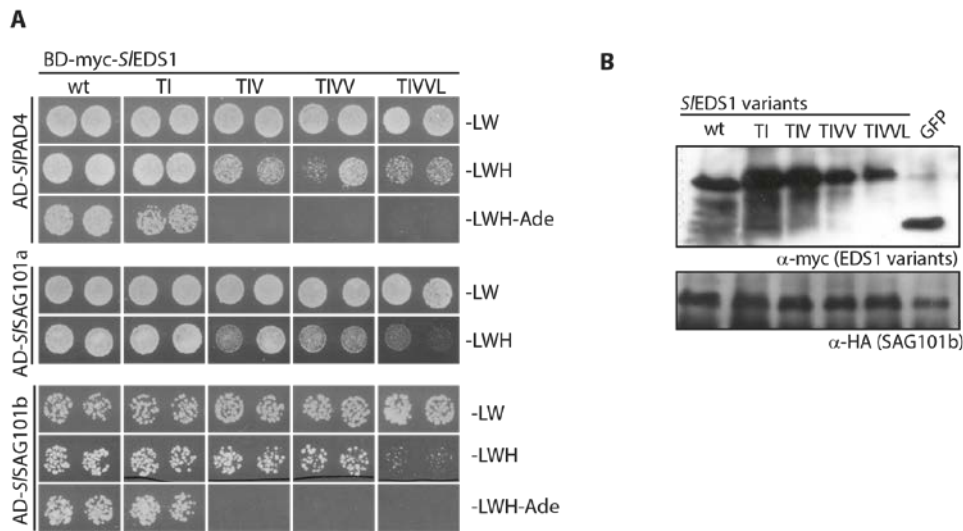
C) Schematic representation of T-DNA constructs used for *Arabidopsis* transformation.

D) Immunodetection of transgenic protein expression. Three week-old BASTA-resistant T_2 plants of individual families were pooled for protein extraction. Ponceau staining is shown as loading control.

E) Functionality of tomato *EDS1* family proteins in *Arabidopsis*. Indicated combinations of tomato genes under control of the corresponding *Arabidopsis* promoter elements were expressed (with or without an epitope tag) in the *eds1-2 pad4-1 sag101-1* triple mutant background. Constructs were of similar architecture as before (Figure S6C), but contained the FAST marker. T_1 lines from transformation of constructs without epitope tags were used for infection assays: Transformed T_1 seeds were selected by FAST seed fluorescence, three week-old plants used for infection with *Hpa* isolate Cala2, and tissues stained with Trypan Blue 7 dpi. Similarly selected plants expressing tagged proteins were used for immunodetection (Figure S6F). hr – hypersensitive response; fh – free hyphae; tn – trailing necrosis; ehr – expanded hypersensitive response.

F) Immunodetection of tomato *EDS1* family proteins in transgenic *Arabidopsis*. Each lane represents an individual T_1 plant.

Supplemental Data. Gantner et al. (2019). Plant Cell 10.1105/tpc.19.00099.

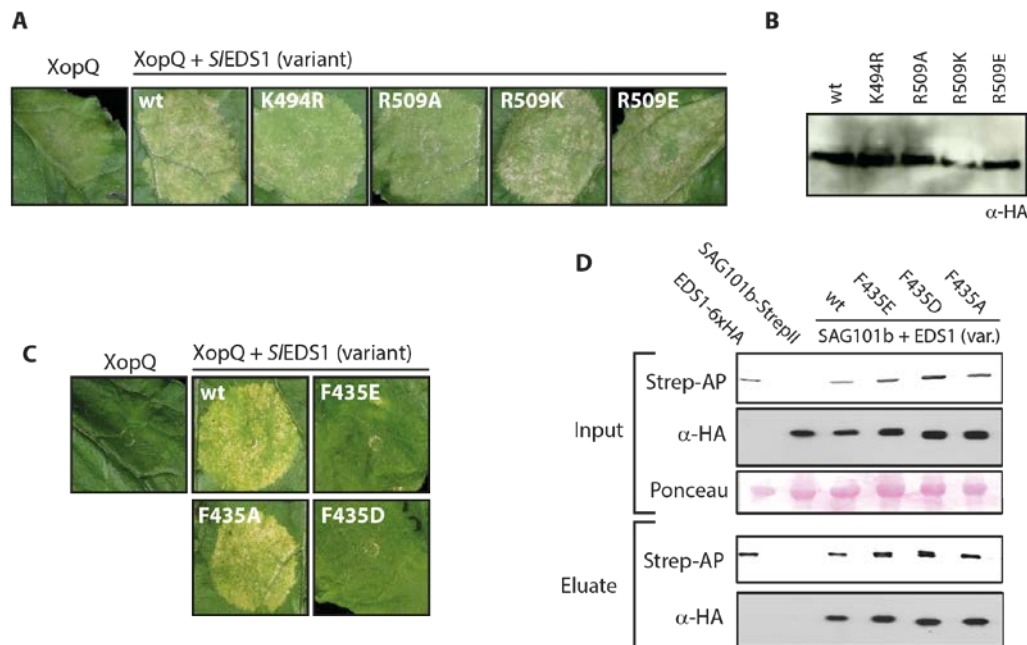


Supplemental Figure 7: Heterocomplex formation by *S/EDS1* variants in a yeast two hybrid system. Supports Figure 6.

A) Yeast two hybrid interaction assay. pGADT7 and pGBKT7 derivatives coding for the indicated protein fusions were co-transformed into yeast strain PJ69-4a. Two independent transformants were grown in dilution series on media lacking leucine and tryptophan (-LW; growth), or additionally lacking histidine (-LWH; interaction, low stringency reporter) or histidine and adenine (-LWH-Ade; interaction, high stringency reporter). Yeast plates were incubated at 30°C for 3d prior to documentation. A higher dilution is shown for the SAG101b-EDS1 interaction assay.

B) Immunodetection of fusion proteins expressed in yeast transformants from A).

Supplemental Data. Gantner et al. (2019). Plant Cell 10.1105/tpc.19.00099.



Supplemental Figure 8: Immune competence of further S/EDS1 variants. Supports Figure 7.

A) Functionality of S/EDS1 variants carrying exchanges in positively charged residues lining a cavity on the EDS1 surface. Indicated variants were co-expressed with XopQ-myc in *eds1* mutant plants, and plant reactions documented 7 dpi.

B) Immunodetection of S/EDS1 variants used in A).

C) Functionality of S/EDS1 variants carrying exchanges in the C-terminal heterocomplex interface. Indicated variants were co-expressed with XopQ-myc in *eds1* mutant plants, and plant reactions documented 7 dpi.

D) *In planta* accumulation and complex formation with SAG101b of S/EDS1 variants used in C). Indicated proteins were (co-) expressed in *N. benthamiana* by Agroinfiltration. Tissues were used 3 dpi for StrepII-purification.

Supplemental Data. Gantner et al. (2019). Plant Cell 10.1105/tpc.19.00099.

Supplemental Table 1: S/EDS1 and S/SAG101 amino acid exchanges tested for functionality by transient complementation of XopQ-induced HR formation

| Variant (EDS1) | Position | functional alteration |
|--|--|---|
| L261E [pJOG334] | N-terminal interface | none (functional) |
| V265E [pJOG335] | N-terminal interface | none (functional) |
| I268E [pJOG336] | N-terminal interface | none (functional) |
| V269E [pJOG337] | N-terminal interface | none (functional) |
| T264F I268E [pJOG341] | N-terminal interface | none (functional) |
| T264F I268E V265E [pJOG381] | N-terminal interface | partial loss-of-function |
| T264F I268E V265E V269E [pJOG382] | N-terminal interface | partial loss-of-function |
| T264F I268E V265E V269E L261E [pJOG383] | N-terminal interface | complete loss-of-function |
| P273G R275E [pJOG133] | Altering cavity composition | Protein instability |
| F64E [pJOG342] | Single, conserved residue exposed on the surface of the N-terminal domain | partial loss-of-function |
| F435E [pJOG343] | C-terminal interface | Complete loss-of-function |
| F435A [pJOG741] | C-terminal interface | functional |
| F435D [pJOG698] | C-terminal interface | Complete loss-of-function |
| V439E [pJOG696] | C-terminal interface | none (functional) |
| L442E [pJOG697] | C-terminal interface | none (functional) |
| D462N [pJOG344] | N-/C-terminal domain communication | Partial loss-of-function, reduced protein stability |
| K494R [pJOG345] R509A [pJOG346] R509E [pJOG748] R509K [pJOG749] | Residues lining an assumed cavity on the heterocomplex surface (Wagner et al., 2013), previously described in Arabidopsis (Bhandari et al., 2018). | none (functional) |
| Variant (SAG101) | Position | functional alteration |
| F17S [pJOG835] | N-terminal interface | none (functional) |
| L22S [pJOG836] | N-terminal interface | none (functional) |
| F17S L22S [pJOG852] | N-terminal interface | none (functional) |
| L13S L22S [pJOG894] | N-terminal interface | none (functional) |
| L16S L22S [pJOG895] | N-terminal interface | none (functional) |
| L13S F17S L22S [pJOG938] | N-terminal interface | Partial loss-of-function |
| L13S L16S F17S L22S [pJOG1035] | N-terminal interface | Complete loss-of-function |
| L13S L16S F17S L18S L22S [pJOG1036] | N-terminal interface | Complete loss-of-function |

Bhandari, DD, Lapin, D, Kracher, B, vonBorn, P, Bautor, J, Niefind, K, and Parker, JE. (2018). An EDS1 EP-domain surface mediating timely transcriptional reprogramming of immunity genes. bioRxiv.

Wagner, S, Stuttmann, J, Rietz, S, Guerois, R, Brunstein, E, Bautor, J, . . . Parker, JE. (2013). Structural basis for signaling by exclusive EDS1 heteromeric complexes with SAG101 or PAD4 in plant innate immunity. Cell Host Microbe 14, 619-30.

Supplemental Data. Gantner et al. (2019). Plant Cell 10.1105/tpc.19.00099.

Supplemental Table 2: Plasmids used in this study

| Plasmid type | Name | Description | Comments |
|--------------------|---------------------|--------------------------------------|--------------------------|
| Gateway Entry | pJOG13 | S/EDS1_noSTOP | |
| | pJOG43 | S/PAD4_noSTOP | |
| | pJOG371 | S/SAG101a_noSTOP | |
| | pJOG373 | S/SAG101b_noSTOP | |
| | pJOG851 | NbRoq1 | |
| | pJOG40 | S/EDS1_I268E | |
| | pJOG117 | S/EDS1_I268E/T264F | |
| | pJOG368 | S/EDS1_I268E/T264F/V265E | |
| | pJOG369 | S/EDS1_I268E/T264F/V265E/V268E | |
| | pJOG370 | S/EDS1_I268E/T264F/V265E/V268E/L261E | |
| | pJOG118 | S/EDS1_F64E | |
| | pJOG119 | S/EDS1_F435E | |
| | pJOG120 | S/EDS1_D462N | |
| | pJOG121 | S/EDS1_K494R | |
| | pJOG122 | S/EDS1_R509A | |
| | Gateway Destination | pJOG270 | p35S:Gateway-6xHA_tocs |
| pJOG327 | | p35S:Gateway-4xmyc-2xStrep_t35S | |
| pGBK_att | | Y2H: pADH1:BD-myc-Gateway | |
| pGAD_att | | Y2H: pADH1:AD-HA-Gateway | |
| Gateway Expression | pJOG333 | 35S:S/EDS1-6xHA | EDS1 variants not listed |
| | pJOG360 | 35S:NbEDS1-6xHA | |
| | pJOG384 | p35S:S/PAD4-4xmyc-2xStrep | |
| | pJOG385 | p35S:S/SAG101a-4xmyc-2xStrep | |
| | pJOG386 | p35S:S/SAG101b-4xmyc-2xStrep | |
| | pJOG | p35S:NbSAG101b-4xmyc-2xStrep | |
| | pJOG44 | BD-myc-S/EDS1 [Y2H] | EDS1 variants not listed |
| | pJOG49 | AD-HA-S/PAD4 [Y2H] | |
| | pJOG222 | AD-HA-S/SAG101a [Y2H] | |
| | pJOG379 | AD-HA-S/SAG101b [Y2H] | |
| MoClo Level 0 | pJOG113 | S/EDS1 | |
| | pJOG112 | S/EDS1_noSTOP | |
| | pJOG734 | S/EDS1_F435A | |
| | pJOG690 | S/EDS1_F435D | |
| | pJOG688 | S/EDS1_V439E | |
| | pJOG689 | S/EDS1_L442E | |
| | pJOG735 | S/EDS1_R509E | |
| | pJOG736 | S/EDS1_R509K | |
| | pJOG214 | S/SAG101a | |
| | pJOG193 | S/SAG101a_noSTOP | |
| | pJOG115 | S/PAD4 | |
| | pJOG114 | S/PAD4_noSTOP | |
| | pJOG361 | S/SAG101b | |
| | pJOG372 | S/SAG101b_noSTOP | |
| | pJOG819 | S/SAG101b_F17S | |
| | pJOG850 | S/SAG101b_F17S/L22S | |
| | pJOG919 | S/SAG101b_F17S/L22S/L13 | |

Supplemental Data. Gantner et al. (2019). Plant Cell 10.1105/tpc.19.00099.

| Plasmid type | Name | Description | Comments |
|----------------------|-----------------|--|-----------------------------|
| MoClo Level 0 | pJOG1032 | <i>S/SAG101b_F17S/L22S/L13S/L16S</i> | |
| | pJOG1033 | <i>S/SAG101b_F17S/L22S/L13S/L16S/L18S</i> | |
| | pJOG285 | <i>NbEDS1_noSTOP</i> | |
| | pJOG703 | <i>NbSAG101b</i> | |
| | pJOG738 | <i>NbSAG101b_noSTOP</i> | |
| | pJOG269 | <i>XopQ_noSTOP</i> | |
| | pJOG404 | <i>DM2h(1-279)</i> | DM2h TIR (Landsberg) |
| | pJOG899 | <i>DM2h(1-279)_noSTOP</i> | DM2h TIR (Landsberg) |
| | pJOG219 | <i>RPS4^{TIR}_noSTOP (aa 1-235)</i> | with E111K exchange |
| | pJOG872 | <i>NbRoq1</i> | |
| | pJOG28 | <i>AtEDS1</i> | |
| | pJOG29 | <i>AtPAD4</i> | |
| | pJOG694 | <i>AtSAG101</i> | |
| | pJOG944 | <i>S/SAG101bN-SAG101aC</i> | |
| | pJOG945 | <i>S/SAG101aN-SAG101bC</i> | |
| | pJOG864 | <i>pAtRPS6 [Pro+5U]</i> | |
| Level1 | pJOG197 | <i>35S:S/EDS1_tocs</i> | |
| | pJOG230 | <i>35S:S/EDS1-mEGFP_tocs</i> | |
| | pJOG233 | <i>35S:S/EDS1-mEGFP-t35S</i> | |
| | pJOG234 | <i>35S:S/EDS1-mCherry_t35S</i> | |
| | pJOG741 | <i>35S:S/EDS1-6xHA</i> | EDS1 variants not listed |
| | pJOG232 | <i>35S:S/PAD4-mEGFP-t35S</i> | |
| | pJOG231 | <i>35S:S/SAG101a-mEGFP-t35S</i> | |
| | pJOG400 | <i>35S:S/SAG101b-mEGFP-t35S</i> | |
| | pJOG835 | <i>35S:S/SAG101b- 4xmyc-2xStrep-t35S</i> | SAG101b variants not listed |
| | pJOG108 | <i>pnos:PAT-tnos [„BASTA^R“]</i> | selection marker cassette |
| | pJOG184 | <i>35S:mCherry-t35S</i> | |
| | pJOG185 | <i>35S:mEGFP-t35S</i> | |
| | pJOG189 | <i>35S:mEGFP-mCherry-t35S</i> | |
| | pJOG911 | <i>p35S:DM2h₍₁₋₂₇₉₎-6xHA-tocs</i> | |
| | pJOG469 | <i>p35S:DM2h₍₁₋₂₇₉₎-tocs</i> | |
| | pJOG320 | <i>p35S:RPS4_(1-235, E111K)-4xmyc-2xStrep-t35S</i> | |
| | pJOG873 | <i>pAtRPS6:NbRoq1-tocs</i> | |
| | pJOG873 | <i>pAtUbq10:NbRoq1-tocs</i> | |
| | pJOG604 | FAST cassette as Level 1 (Shimada et al., 2010) | |
| | pJOG272 | <i>35S:XopQ-myc-tocs</i> | |
| | pJOG62 | <i>35S:AtEDS1-tocs</i> | |
| | pJOG63 | <i>35S:AtPAD4-tnos</i> | |
| | pJOG759 | <i>35S:AtSAG101-tocs</i> | |
| | pJOG98 | <i>35S:GFP-AtEDS1_tocs</i> | |
| | pJOG99 | <i>35S:6xHA-AtPAD4_tnos</i> | |
| | pJOG760 | <i>35S:4xmyc:AtSAG101-tocs</i> | |
| | pJOG35 | <i>pAtEDS1:AtEDS1-tnos</i> | |
| | pJOG36 | <i>pAtPAD4:AtPAD4-tocs</i> | |
| | pJOG154 | <i>pAtEDS1:GFP-AtEDS1-tnos</i> | |
| | pJOG155 | <i>pAtPAD4:6xHA-AtPAD4-tocs</i> | |
| | pJOG156 | <i>pAtEDS1:S/EDS1-tnos</i> | |
| | pJOG157 | <i>pAtPAD4:S/PAD4-tocs</i> | |
| | pJOG513 | <i>pAtSAG101:S/SAG101a-t35S</i> | |
| | pJOG514 | <i>pAtSAG101:S/SAG101b-tAtug7</i> | |

Supplemental Data. Gantner et al. (2019). Plant Cell 10.1105/tpc.19.00099.

| Plasmid type | Name | Description | Comments |
|--------------|--|---|---|
| Level1 | pJOG158 | pAtEDS1:GFP-S/EDS1-tnos | |
| | pJOG159 | pAtPAD4:6xHA-S/PAD4-tocs | |
| | pJOG515 | pAtSAG101:4xmyc-S/SAG101a- t35S | |
| | pJOG516 | pAtSAG101:3xFLAG-S/SAG101b- tAtug7 | |
| | pJOG949 | 35S:S/SAG101bN:SAG101aC-4xmyc-2xStrep-t35S | |
| | pJOG950 | 35S:S/SAG101aN:SAG101bC-4xmyc-2xStrep-t35S | |
| Level2 | pJOG190 | pnos:PAT-tnos + 35S:mCherry + 35S:mEGFP | FRET (negative control) |
| | pJOG204 | pnos:PAT-tnos + 35S:mEGFP-mCherry | FRET (positive control) |
| | pJOG237 | S/EDS1-mEGFP + S/EDS1-mCherry | |
| | pJOG236 | S/PAD4-mEGFP + S/EDS1-mCherry | |
| | pJOG235 | S/SAG101a-mEGFP + S/EDS1-mCherry | FRET |
| | pJOG401 | S/SAG101b-mEGFP + S/EDS1-mCherry | |
| | pJOG238 | S/EDS1-mCherry + mEGFP | |
| | pJOG875 | FAST + p(At)RPS6-Roq1 | Arabidopsis transgenics |
| | pJOG876 | FAST + p(At)Ubq-Roq1 | |
| | pJOG651 | 35S:AtEDS1 + 35S:AtPAD4 | |
| | pJOG652 | 35S:GFP-AtEDS1 + 35S:6xHA-AtPAD4 | |
| | pJOG765 | 35S:AtEDS1 + 35S:AtSAG101 | |
| | pJOG766 | 35S:GFP-AtEDS1 + 35S:4xmyc-AtSAG101 | <i>N. benthamiana</i> expression; gene family transfer |
| | pJOG767 | 35S:AtEDS1 + 35S:AtSAG101 + 35S:AtPAD4 | |
| | pJOG768 | 35S:GFP-AtEDS1 + 35S:4xmyc-AtSAG101 + 35S:6xHA-AtPAD4 | |
| | pJOG42 | BASTA ^R + pAtEDS1:AtEDS1 + pAtPAD4:AtPAD4 | |
| | pJOG160 | BASTA ^R + pAtEDS1:GFP-AtEDS1 + pAtPAD4:6xHA-AtPAD4 | Arabidopsis transgenics; gene family transfer |
| | pJOG161 | BASTA ^R + pAtEDS1:S/EDS1 + pAtPAD4:S/PAD4 | |
| | pJOG162 | BASTA ^R + pAtEDS1:GFP-S/EDS1 + pAtPAD4:6xHA-S/PAD4 | |
| | pJOG613 | FAST + pAtEDS1:AtEDS1 + pAtPAD4:AtPAD4 | |
| | pJOG614 | FAST + pAtEDS1:GFP-AtEDS1 + pAtPAD4:6xHA-AtPAD4 | |
| | pJOG521 | FAST + pAtEDS1:S/EDS1 + pAtSAG101:S/SAG101a | |
| | pJOG522 | FAST + pAtEDS1:S/EDS1 + pAtSAG101:S/SAG101b | |
| | pJOG519 | FAST + pAtEDS1:S/EDS1 + pAtPAD4:S/PAD4 + pAtSAG101:S/SAG101a | Arabidopsis transgenics; gene family transfer II |
| pJOG520 | FAST + pAtEDS1:S/EDS1 + pAtPAD4:S/PAD4 + pAtSAG101:S/SAG101b | | |
| pJOG517 | FAST + pAtEDS1:S/EDS1 + pAtPAD4:S/PAD4 + pAtSAG101:S/SAG101a + pAtSAG101:S/SAG101b | | |
| pJOG518 | FAST + pAtEDS1:GFP-S/EDS1 + pAtPAD4:6xHA-S/PAD4 + pAtSAG101:4xmyc-S/SAG101a + pAtSAG101:3xFLAG-S/SAG101b | | |

- Gateway entry and Level 0 modules were generated by PCR and Golden Gate cloning as previously described (Engler et al., 2008; Engler et al., 2014; Gantner et al., 2018).
- In some cases, Gateway entry clones were prepared by shuttling inserts from Level 0 modules, as previously described (Gantner et al., 2018).
- Gateway destination vectors were assembled by Modular Cloning, as previously described (Gantner et al., 2018)
- Gateway expression clones were generated by LR reaction as according to manufacturer's instructions (Gateway™ LR Clonase™ II Enzyme mix, Thermo Fisher Scientific).

Supplemental Data. Gantner et al. (2019). Plant Cell 10.1105/tpc.19.00099.

- Level 1 and MoClo-based Y2H constructs were assembled from parts contained in the MoClo Plant Parts I & II kits (Engler et al., 2014; Gantner et al., 2018) by Golden Gate cloning (*Bsa*I) following standard protocols.
- Level 2 constructs were assembled by Golden Gate cloning (*Bpi*I) following standard protocols using Level 2 recipient pAGM4723 (Engler et al., 2014).

References:

- Engler, C, Kandzia, R, and Marillonnet, S.** (2008). A one pot, one step, precision cloning method with high throughput capability. PLoS ONE **3**, e3647.
- Engler, C, Youles, M, Gruetzner, R, Ehnert, TM, Werner, S, Jones, JD, . . . Marillonnet, S.** (2014). A Golden Gate Modular Cloning Toolbox for Plants. ACS synthetic biology.
- Gantner, J, Ordon, J, Ilse, T, Kretschmer, C, Gruetzner, R, Lofke, C, . . . Stuttmann, J.** (2018). Peripheral infrastructure vectors and an extended set of plant parts for the Modular Cloning system. PLoS ONE **13**, e0197185.
- Shimada, TL, Shimada, T, and Hara-Nishimura, I.** (2010). A rapid and non-destructive screenable marker, FAST, for identifying transformed seeds of *Arabidopsis thaliana*. Plant J **61**, 519-28.

Supplemental Data. Gantner et al. (2019). Plant Cell 10.1105/tpc.19.00099.

Table S3: Oligonucleotides used in this study

| Name | Sequence | Purpose | |
|-------|--|--|---|
| JS830 | ttaggtctcaaggtATGGTAAAAATTGGAGAAGG | Construction of <i>S/EDS1ns</i> Gateway entry clone (pJOG13) | |
| JS831 | TTTggtctcAaagcAGGAGTTATTTTCCTTGACAC | | |
| JG43 | TGCTGGAACTTTGTcTCTGATGGTTGGT | Removal <i>Bpil</i> site in <i>S/EDS1</i> cDNA | |
| JG44 | ACCAACCATCAGAgGACAAAGTTCCAGCA | Removal <i>Bpil</i> site in <i>S/EDS1</i> cDNA | |
| JG45 | GGCAATGTTAGAAGGcAGACAGGTAGTGT | | |
| JG46 | ACACTACCTGTCTgCCTTCTAACATTGCC | | |
| JG47 | GAGCAAGGCTGTGcCTTCGTGCAGCAGG | Removal <i>Bpil</i> site in <i>S/EDS1</i> cDNA | |
| JG48 | CCTGCTGCACGAAGgCACAGCCTTGCTC | Removal <i>Bsal</i> site in <i>S/EDS1</i> cDNA | |
| JG49 | ACAAGATATGGTCCcCATGCCCTCAGGCG | | |
| JG50 | CGCCTGAGGGCATGgGACCATATCTTGT | | |
| JS832 | ttaggtctcaaggtATGGTATCGGAGGCTTCATC | Construction of <i>S/PAD4ns</i> Gateway entry clone (pJOG43) | |
| JS833 | TTTggtctcAaagcAGGAAACTGAGGTTGGAGC | | |
| JG73 | ttagaagacaaaATGGTGTCTTGTACAACAC | Construction of <i>S/SAG101a_ns</i> Level 0 module | |
| JG74 | ttagaagacaacgaaccAGCATATCTACGAAATCCATCG | Construction of <i>S/SAG101a</i> Level 0 module in combination with JG73 | |
| JG86 | ttagaagacaaaagctcaAGCATATCTACGAAATCCATCG | | |
| JG82 | TCTCACTTTTTGGAgGACCCATCACTTC | | |
| JG83 | GAAGTGATGGGTcTCCAAAAGAGTGAGA | Removal <i>Bpil</i> site in <i>S/SAG101a</i> cDNA | |
| JG84 | TCTTGCATGTGGTgTCAGATAAAGATCCA | Removal <i>Bsal</i> site in <i>S/SAG101a</i> cDNA | |
| JG85 | TGGATCTTTATCTGAcACCACATGCAAGA | | |
| JG51 | ttagaagacaaaATGGTGAAAATTGGAGAAGG | | |
| JG52 | ttagaagacaacgaaccAGGAGTTATTTTCCTTGAC | Construction of <i>S/EDS1n_ns</i> Level 0 module | |
| JG53 | ttagaagacaaaagcccCTAAGGAGTTATTTTCCTTGAC | Construction of <i>S/EDS1n</i> Level 0 module in combination with JG51 | |
| JG54 | ttagaagacaaaATGGTATCGGAgGCTTCATCGTTCG | Construction of <i>S/PAD4_ns</i> Level 0 module | |
| JG55 | ttagaagacaacgaaccAGGAAACTGAGGTTGGAGCAGC | | |
| JG56 | ttagaagacaaaagcccTCAAGGAAACTGAGGTTGG | Construction of <i>S/PAD4</i> Level 0 module in combination with JG54 | |
| JG127 | ttagaagacaaaATGAGCCAAGTTTCCTTGTTGAG | Construction of <i>S/SAG101b</i> Level 0 module and simultaneous removal of internal <i>Bpil</i> site | |
| JG128 | ttagaagacaaaTtTCTTCTCTCCTCCATTCCTCC | | |
| JG129 | ttagaagacAGAtAACCCGTCTGGAAGTGGTAACG | | |
| JG130 | ttagaagacaaaagcCTAAGCATAACTTTGTATT | | |
| JG131 | CAGAAAGAAATGGTAtCTTCAGAAAGAGCTT | | |
| JG132 | AAGCTCTTCTGAAGAtACCATTTCTTTCTG | Removal <i>Bsal</i> site in <i>S/SAG101b</i> cDNA | |
| JG157 | ttagaagacaacgaaccAGCATAACTTTGTATT | Construction of <i>S/SAG101b_ns</i> Level 0 module in combination with JG127 | |
| JG103 | ttagaagacaaaATGCAGCCACCGCAATC | Construction of <i>XopQ_ns</i> Level 0 module and simultaneous removal of internal <i>Bpil</i> site | |
| JG104 | ttagaagacaaaGAAtACACCTTTGGCCAGC | | |
| JG105 | ttagaagacaaaTTCGATCGCCTGGCATTG | | |
| JG106 | ttagaagacaacgaaccGCGCCCGCTTGCCCTC | | |
| JG88 | gaagacaaaATGGAGACATCATCTATTTCCACTGTGGAgGAC | Construction of <i>RPS4</i> (1-235, E111K) Level 0 module and simultaneous removal of internal <i>Bpil</i> sites | |
| JG89 | ttagaagacaaaTcTcTATAGTCGTCGATAAAG | | |
| JG90 | ttagaagacaaaAgGACAGAGGTCAACCTC | | |
| JG91 | ttagaagacaaaTgTtTTCACCGCCTTCAC | | |
| JG92 | ttagaagacaaaACAGCGTTGACCGGAATAC | | |
| JG94 | ttagaagacaacgaaccAACTCCAATGATACGAGTT | | |
| JG409 | ttaggtctcaaATGTTGACTTCATCTTCCC | | Construction of <i>NbRoq1</i> Gateway entry clone (pJOG851) |
| JG410 | ttaggtctcagaccTATCTGTTTATGAGCATTTCG | | |

Supplemental Data. Gantner et al. (2019). Plant Cell 10.1105/tpc.19.00099.

| Name | Sequence | Purpose |
|-------|---|---|
| JG419 | tttgaagacaaaATGTTGACTTCATCTTCCC | Construction of <i>NbRoq1</i> Level 0 module and simultaneous removal of internal <i>Bpil</i> sites (pJOG872) |
| JG420 | tttgaagacaaGTaTCTTCTCCCTAAAGCTTAGGAA | |
| JG421 | tttgaagacAGaTACTAGAAAAACATTTGTGGGT | |
| JG422 | tttgaagacaaGTtTTCTGCAAATACAACAAGGTATGG | |
| JG423 | tttgaagacGAAaACTCTCTTTCCAACTGTTG | |
| JG424 | tttgaagacaaaagcCTATCTGTTTATGAGCATTTCG | |
| JG15 | tttgaagacTTaATGGCGtttgaagctctt | Construction of <i>AtEDS1</i> Level 0 module |
| JG16 | tttgaagacTTaagctcaggtatctgttatttc | Removal <i>Bpil</i> site in <i>AtEDS1</i> |
| JG17 | gAAAACCTCAATAGAAaTCTTCGCTCAATGA | |
| JG18 | TCATTGAGCGAAGAtTCTATTGAGTTTTc | |
| JG19 | ttaaagaacgaagaTacagggccgtacatgaaaagaggTagaccaaccg | Removal <i>Bpil</i> site in <i>AtEDS1</i> |
| JG20 | cgggttggtctAccttttcatgtacggccctgtAtcttcgttcttaa | Construction of <i>AtPAD4</i> Level 0 module |
| JG13 | tttgaagacTTaATGGACGATTGTCGATTTCGA | |
| JG14 | tttgaagacTTaagcCTAAGTCTCATTGCGTCA | |
| JG344 | tttgaagacaaaATGGAaTCTTCTTCTTCA | Construction of <i>AtSAG101</i> Level 0 module |
| JG345 | tttgaagacaaaagccctcaTTGTGACTTACCATA | Removal <i>Bpil</i> site in <i>AtSAG101</i> |
| JG346 | TGGTGACCTCTGGcCTCTTACATAGCT | |
| JG347 | AGCTATGTAAGAGgCCAGAGGTCACCA | |
| JG348 | GAACTACGGGAAGaTCTCACCCTATG | |
| JG349 | CATAGTGGTgAGAtCTCCCGTAGTTC | Removal <i>Bpil</i> site in <i>AtSAG101</i> |
| JG31 | AAACTGTTTCCAACgaaGTTCAACTTAGCCC | SDM: <i>S/EDS1_I268E</i> |
| JG32 | GGGCTAAGTTGAACttcGTTGGAAACAGTTT | SDM: <i>S/EDS1_T264F [TI]</i> |
| JG59 | ACTTACTGTTGGAAttGTTTCCAACgaaG | |
| JG60 | CttcGTTGGAAACAaaTTCCAACAGTAAGT | |
| JG151 | ACTGTTGGAAttTGaaTCCAACgaaGTTCA | SDM: <i>S/EDS1_V265E [TIV]</i> |
| JG152 | TGAACttcGTTGGAttCAaaTTCCAACAGT | SDM: <i>S/EDS1_V269E [TIVV]</i> |
| JG153 | TGaaTCCAACgaaGaaCAACTTAGCCCTTA | |
| JG154 | TAAGGGCTAAGTTGttCttcGTTGGAttCA | SDM: <i>S/EDS1_L261E [TIVVL]</i> |
| JG155 | GATGCACAACTTAgaaGTTGGAAAttGaaT | |
| JG156 | AttCAaaTTCCAACtcTAAGTTTGTGCATC | SDM: <i>S/SAG101b_F17S</i> |
| JG403 | ATTGGCAAATTTGtTcTCTGAGCTCAGATC | |
| JG404 | GATCTGAGCTCAGAgACAAATTTGCCAAT | |
| JG411 | cTCTGAGCTCAGATtcACTTCATCATTCTTG | SDM: <i>S/SAG101b_L22S [FL]</i> |
| JG412 | GATCTGAGCTCAGAgACAAATTTGCCAAT | SDM: <i>S/SAG101b_L13S [FLL]</i> |
| JG429 | TAGTGCCAAAGAAATcGGCAAATTTGTcTC | |
| JG430 | GAgACAAATTTGCCgATTCTTGCCACTA | SDM: <i>S/SAG101b_L16S [FLLL]</i> |
| JG436 | AAGAATcGGCAAATTCGTcTCTGAGCTCAG | |
| JG437 | CTGAGCTCAGAgAcgAATTTGCCgATTCTT | |
| JG438 | TcGGCAAATTCGTcTcTcGAGCTCAGATcAC | SDM: <i>S/SAG101b_L18S [FLLLL]</i> |
| JG439 | GTgaATCTGAGCTCgaAgAcgAATTTGCCgA | SDM: <i>S/EDS1_F64E</i> |
| JG61 | ACAGTAACACTTCTgaaGGAGAGAAAGAGAT | |
| JG62 | ATCTCTTCTCTCctcAGAAAGTGTACTGT | SDM: <i>S/EDS1_F435E</i> |
| JG63 | ACACCGATGATGACgaaAATGCTAATGTGAG | |
| JG64 | CTCACATTAGCATTtctGTCATCATCGGTGT | SDM: <i>S/EDS1_D462N</i> |
| JG65 | GGTATGAGCTCCCAaATAGCTTCGAGGGA | |
| JG66 | TCCCTCGAAGCTATtTGGGAGCTCATACC | |
| JG67 | ATTACAGGCACCTTcGcGAATGAAGATACTG | SDM: <i>S/EDS1_K494R</i> |
| JG68 | CAGTATCTTCATTcGcCAAGTGCCTGTAAT | SDM: <i>S/EDS1_R509A</i> |
| JG69 | GCTAGGCCTAAGGcTTATCGGTTACACA | |
| JG70 | TGTGTGAACCGATAAgcCTTAGGCCTAGC | SDM: <i>S/EDS1_F435A</i> |
| JG387 | AACACCGATGATGACgcCAATGCTAATGTG | |
| JG388 | CACATTAGCATTGgcTcATCATCGGTGTT | SDM: <i>S/EDS1_R509E</i> |
| JG394 | GCTAGGCCTAAGgagTATCGGTTACAC | |
| JG395 | GTGTGAACCGATAActcCTTAGGCCTAGC | |

Supplemental Data. Gantner et al. (2019). Plant Cell 10.1105/tpc.19.00099.

| Name | Sequence | Purpose |
|-------|--|--|
| JG396 | GCTAGGCCTAAG ^{gaa} TATCGGTTCACA | SDM: <i>S/EDS1_R509K</i> |
| JG397 | TGTGAACCGATAttCTTAGGCCTAGC | |
| JG431 | aaagaagactagcttCTTTGCAAAGATTCTTCC | Construction of Level Ons module of <i>S/SAG101bN-SAG101aC</i> chimera; in combination with JG127/JG74 |
| JG432 | tttgaagacataAGCAGAAGCTTTTCGATC | |
| JG433 | tttgaagactaGTGTTTGGCCTGAACCTCT | Construction of Level Ons module of <i>S/SAG101aN-SAG101bC</i> chimera; in combination with JG73/JG157 |
| JG434 | tttgaagacatacacAAGAGGAATGCCTTTGATC | |
| JG413 | tttgaagacaaggagTCAAGACCATTCACTTGCCTA | Construction of pAtRPS6 Level 0 module [Pro+5U] |
| JG414 | aaagaagacaacattAAAGAGAGGAGATTCTGGAAA | |

Supplemental Data. Gantner et al. (2019). Plant Cell 10.1105/tpc.19.00099.

Supplemental Table S4: Oligonucleotides used for quantitative RT-PCR analyses

| Name | Sequence [5' -> 3'] |
|------------------------|-------------------------|
| JS1128_qRT-NbPP2A_F | TCTAAGTTGCTGCCTGTGGT |
| JS1129_qRT-NbPP2A_R | TCAGGGTCTTCAGCTAGCTCT |
| JS1130_qRT-NbEF1_F | agctttacctccaagtcac |
| JS1131_qRT-NbEF1_R | agaacgcctgtcaatcttg |
| JS1612_qRT-NbEDS1a_F | TGGTACAGTTGTAGCACTTCTTT |
| JS1613_qRT-NbEDS1a_R | CAGGTTGTCATTTGGTCTTGTG |
| JS1124_qRT-NbPAD4_F | TCTACCTGAGGCAAGCTATGAAG |
| JS1125_qRT-NbPAD4_R | TGCAAGGATGGCACTATTAAGGT |
| JS1102_qRT-NbSAG101a_F | CTGGAAGCAGCTGGAGTTGA |
| JS1103_qRT-NbSAG101a_R | GTCATAATACCCAGCCTCTTCGG |
| JS1106_qRT-NbSAG101b_F | TGCCTCGTTAGTCAATCAGCT |
| JS1107_qRT-NbSAG101b_R | GATGCCACAGAACCTCCCAA |

3.5.3. Summary of publication Gantner *et al.*, 2019

EDS1 (Enhanced disease susceptibility 1) was discovered 20 years ago (Parker *et al.*, 1996). EDS1 forms heterocomplexes with PAD4 (Phytoalexin-deficient 4) and SAG101 (Senescence-associated gene 101) (Feys *et al.*, 2001; Feys *et al.*, 2005). These complexes are essential for resistance responses mediated by nucleotide-binding leucine rich-repeat-type immune receptors (NLRs) possessing an N-terminal Toll/interleukin-1 domain (TNLs) (Aarts *et al.*, 1998).

Further research revealed that PAD4 is an important complex partner in *At*, as loss of *SAG101* is compensated for by presence of *PAD4*, whereas *SAG101* only partially complements *pad4* (Feys *et al.*, 2005; Wagner *et al.*, 2013). To study EDS1-based heterocomplexes in a different species we investigated the EDS1-family proteins in *Nb*. Besides PAD4, most *Solanaceae* genomes encode for two SAG101 isoforms, both interacting with EDS1 in Y2H and *in planta*. Orthologs of tomato (*Solanum lycopersicum* (*Sl*)) and *Nb* were transiently expressed in *Nb*, delivering identical results: In contrast to *Brassicaceae*, solely SAG101b is the crucial heterocomplex partner of EDS1 in the TNL-dependent defense pathway in *Solanaceae*, whereas PAD4 does not appear to have any immune functions.

An interspecies approach displayed that the orthologous EDS1-family proteins of *At* were not able to complement an endogenous loss of the respective proteins in *Nb*. However, the tomato orthologs were sufficient to complement an endogenous deficiency of the EDS1 family proteins of *At* accession Columbia (Col-0). Intriguingly, not *S*EDS1-*S*SAG101b but rather *S*EDS1-*S*PAD4 was sufficient for complementation. Moreover, transfer of the gene coding for the TNL *Roq1* (Recognition of XopQ 1; from *Nb*) to *At* Col-0 led to plants resistant against the *Pst* strain DC3000. Interestingly, EDS1-PAD4 was needed for a defense reaction in *At* even by transferring a transgene encoding a TNL from *Nb*; a loss of *SAG101* showed no significant difference in comparison to the wt if infected with *Pst* DC3000.

Functional analysis of EDS1 and SAG101b, respectively, revealed that an N-terminal hydrophobic interaction motif (TIVVL in EDS1 and FLLLL in SAG101b) was essential for the formation of the heterocomplex and crucial for TNL-dependent defense signaling. We introduced mutations on several positions of *S*EDS1. An exchange at position F435 to glutamate abolished immune functions whereas the heterocomplex formation seemed to be unaffected. Furthermore, it was investigated which part of *S*SAG101b is important for TNL-mediated resistance, and might differ from the inactive SAG101a. We therefore constructed genes encoding for chimeric proteins of the N-terminal part of SAG101b and the C-terminal part of SAG101a (*Nb*-Ca) and *vice versa* (*Na*-Cb). The *Na*-Cb chimera was able

to partially restore XopQ induced cell death. Abolished functions of S/EDS1_F435E as well as immune competence of the Na-Cb-chimera of Sag101a clearly indicated that the C-terminal parts of the proteins are involved in the functionality of the heterocomplex.

3.6. Additional results to publication Gantner et al., 2019: Identification of candidate interactors of *S*/EDS1-based heterocomplexes by Y3H screening

One plausible hypothesis how EDS1 complexes could function in the TNL-mediated immune pathway is by recruitment of further protein interaction partners. Therefore, a yeast-three-hybrid (Y3H) library screen, using the tomato EDS1-PAD4 complex as bait, was conducted to identify candidate interactors in an unbiased approach. The different steps that were undertaken are summarized in Figure 7. In total, 18 candidate interactors were identified. In the following, the Y3H screen, as well as subsequent analyses of candidate interactors will be described.

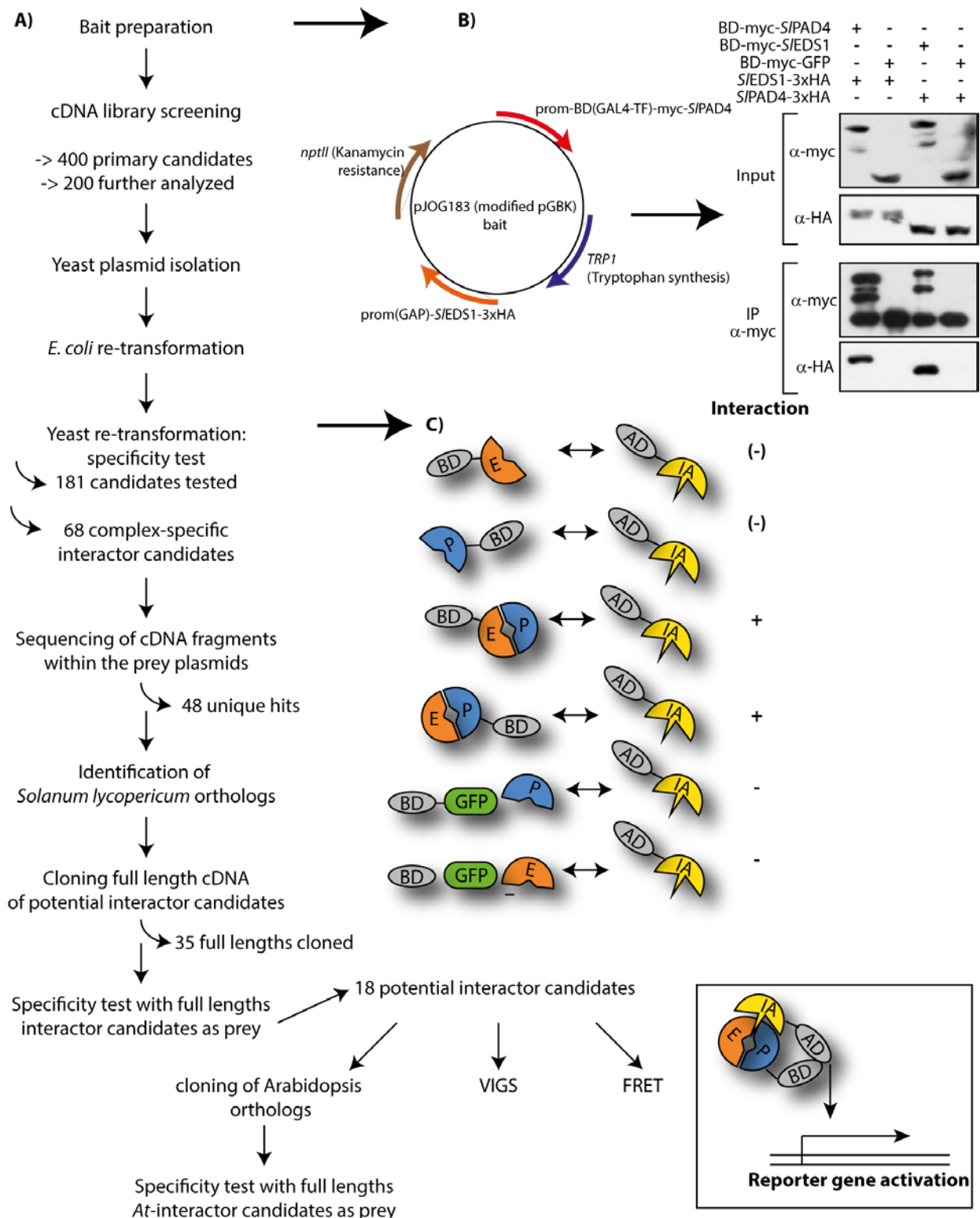


Figure 7: Flow sheet of the experimental setup to identify unknown interacting partners of the EDS1-based heterocomplex

(A) Flow sheet of the following section, starting with the Y3H library screen, a significance test, identification of the cDNA-fragments of prey, and further specificity approaches, resulting in 18 potential interactor candidates. (B) Modified bait plasmid to reconstitute the entire S/EDS1-S/PAD4 heterocomplex afterwards used for an Y3H (yeast-three-hybrid) library screen and co-immunoprecipitation in Yeast, demonstrating that the heterocomplex is build (C) Depiction of the expressed baits used for the Y3H specificity test and illustration of functional principles of an Y3H by reconstitution of a GAL4-transcription factor. E = EDS1, P = PAD4, IA = Interactor, Ad = Activation domain, BD = Binding domain, VIGS = Virus induced gene silencing, FRET = Fluorescence resonance energy transfer.

3.6.1. Modified Y2H library screen considers EDS1-based heterocomplex formation

One method to identify candidate interactors of a protein of interest is a yeast-two-hybrid (Y2H) screen. Y2H is based on the GAL4-TF, which has been separated into the DNA-binding (BD or 'bait') - and the transcription activation domain (AD or 'prey'). To test for an interaction between proteins, they are fused to either AD or BD and co-transformed into the yeast strain *Saccharomyces cerevisiae* PJ69-4a, which are unable to synthesize adenine and histidine. In case of an interaction, the GAL4-TF will be reconstituted and reporter genes will be transcribed, enabling the yeast to grow under selective conditions (James *et al.*, 1996). In this thesis *HIS3* and *ADE2* were chosen as selective markers. As bait we modified the pGBK-vector (Takara Bio, Saint-Germain-en-Laye, France) as depicted in Table 2 and Figure 8. The gene encoding for *SPAD4* was fused to the gene fragment encoding for the BD of pGBK. Additionally, a second transcription unit was added to the vector's backbone for the constitutive expression of *S/EDS1-3xHA* to allow *S/EDS1-SPAD4* heterocomplex formation. The final bait plasmid is schematically shown in Figure 7B. Due to the addition of a second transcriptional unit in the backbone of the bait plasmid, three proteins are involved in this approach, thus termed Y3H.

To test whether the heterocomplex of *S/EDS1-SPAD4* is formed in yeast, interaction assays were done. Figure 7B shows a co-immunoprecipitation of the *S/EDS1-SPAD4* heterocomplex that was utilized to validate the ability of the modified bait plasmid to express and constitute the heterocomplex in both orientations (*S/EDS1* or *SPAD4* as fusion to the BD, positive control I and II of Table 2).

Table 2: Bait plasmids used for the interaction studies in yeast

| Plasmid-Nr. | Abbreviation | Description |
|-------------|---------------------|--|
| pJOG44 | single protein I | pGBK_BD(Gal4)-myc-att- <i>S/EDS1</i> |
| pJOG46 | single protein II | pGBK_BD(Gal4)-myc-att- <i>S/PAD4</i> |
| pJOG182 | positive control I | pBGK_p(GAP)- <i>S/PAD4-3xHA</i> _BD(Gal4)-myc-att- <i>S/EDS1</i> |
| pJOG183 | positive control II | pBGK_p(GAP)- <i>S/EDS13xHA</i> _BD-myc-att- <i>S/PAD4</i> |
| pJOG194 | negative control I | pBGK_p(GAP)- <i>S/PAD4-3xHA</i> _BD(GAL4)-myc-att-GFP |
| pJOG195 | negative control II | pBGK_p(GAP)- <i>S/EDS1-3xHA</i> _BD(Gal4)-myc-att-GFP |

A cDNA library of pepper (*Capsicum annuum* (available in the Bonas lab)) was used to screen for proteins interacting with the *S/EDS1-SPAD4* heterocomplex. The library had been prepared using a mixture of infected (with the *Xcv* strain 85-10) and uninfected leaf material of pepper plants (ECW-10R and ECW-30R) (Szczyzny *et al.*, 2010).

Saccharomyces cerevisiae strain PJ69-4a was co-transformed using the LiAC/SS carrier DNA/PEG method (Gietz&Schiestl, 2007) with the plasmid positive control II (Table 2) and

the cDNA library contained in the (pGADT7) vector. Yeast transformants were plated on selective media without leucine, tryptophan, histidine, and adenine hemisulfate (-LWHA), and subsequently incubated at 30°C for three days. A lack of W and L select for co-transformation (pGBK and pGAD), while only those co-transformants expressing an AD-fusion interacting with the BD-fusion (bait) should grow on media additionally lacking Adenine (Ade) and Histidine (H). Approximately 400 co-transformants growing on selective media were replica-plated and about 200 were further analyzed. The plasmids of 181 yeast colonies were isolated with the *EZ Yeast™ Plasmid Prep Kit* (G-Bioscience, St. Louis) and transformed *via* electroporation into *E. coli* for amplification. The transformed bacteria were plated on LB media containing ampicillin to select for the presence of the respective prey plasmids, followed by re-isolation from *E. coli*. Subsequently, the prey plasmids were co-transformed with six different baits (Table 2) in order to validate the specific interaction of the cDNA-library fragments with the S/EDS1-S/PAD4 heterocomplex. As an example, eight of these yeast-transformants carrying the fished cDNA-library parts, co-expressed with one of the six control plasmids, are shown in Figure 8.

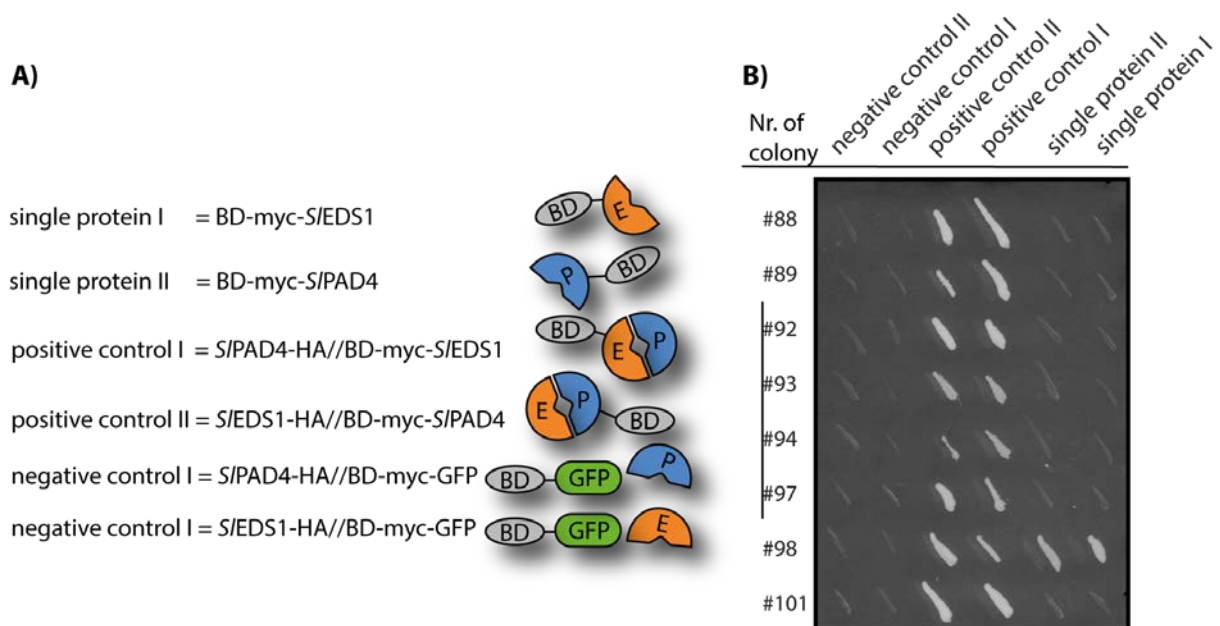


Figure 8: Example of Y3H cDNA library screen

A) Illustration of the baits which were used for the Y3H cDNA library screen. **B)** Co-transformation of yeast carrying the cDNA fragments of the pepper library fused to the AD together with six different control plasmids to validate specific interactions with the EDS1-PAD4 heterocomplex of tomato (*Solanum lycopersicum* (S)). Here, yeast co-transformants are shown replica plated with tooth sticks to the most stringent media condition (SD – LWH-Adenine hemisulfate). Interestingly, only one of the shown yeast co-transformants interacts with the single proteins, PAD4 and EDS1 as well. All other potential interactors seem to need the heterocomplex for an interaction. None of the shown co-transformants were able to interact with the negative control BD-GFP with neither EDS1 nor PAD4 (negative control I and II).

The yeast co-transformants carrying the prey plasmids and one of the indicated bait plasmids were replica plated onto the medium with the most stringent selection (without LWH and adenine hemisulfate), indicating a strong interaction. Interestingly, 90 % of all positive interacting yeast co-transformants only exhibited growth under stringent media conditions if *S/EDS1* and *SPAD4* are both co-expressed. 181 primary candidates identified from the cDNA library were tested for specificity, resulting in 68 yeast co-transformants that only grew under selective conditions if co-expressed with the positive controls (or additionally with the single proteins as well) in the re-transformation procedure (as shown in Figure 8) and were thus selected for further analysis.

3.6.2. Identification, full length cloning and validation of corresponding genes of *Solanum lycopersicum*

The prey plasmids of positive yeast clones were sequenced by Eurofins Genomics (former GATC, Ebersberg). Sequences were aligned to the cDNA of tomato using BLAST (basic local alignment search tool). The program BLASTn (nucleotide to nucleotide db) was applied and the Tomato Genome cDNA (ITAG release 2.40) was used as database (<https://solgenomics.net/tools/blast/>). Table 3 lists all potential interactors identified by BLASTn.

Table 3: Potential interactors identified by BLASTn

| Found | Description | Solyc-Identifier |
|-------|---|--------------------|
| 1 | BEL1-like homeodomain protein 1 (I) | Solyc11g068950.1.1 |
| 6 | ZZ type zinc finger domain-containing protein | Solyc03g112230.2.1 |
| 5 | Gras10 | Solyc03g025170.1.1 |
| 4 | DNA-binding bromodomain-containing protein | Solyc07g064700.2.1 |
| 2 | Kinase family protein | Solyc11g042990.1.1 |
| 1 | Heavy metal-associated domain containing protein | Solyc01g098760.2.1 |
| 1 | DnaJ (Fragment) | Solyc01g105780.2.1 |
| 1 | Unknown Protein I | Solyc11g007510.1.1 |
| 1 | Erythroid differentiation-related factor 1-like protein | Solyc06g065360.2.1 |
| 1 | Unknown Protein II | Solyc04g081420.2.1 |
| 1 | Nucleic acid binding protein | Solyc07g008490.2.1 |
| 1 | 26S protease regulatory subunit 4 | Solyc06g083620.2.1 |
| 3 | Phenylalanine ammonia-lyase | Solyc09g007900.2.1 |
| 1 | Proteasome subunit beta type | Solyc07g016200.2.1 |
| 1 | Acyl-CoA oxidase 6 | Solyc10g008110.2.1 |
| 1 | RNA helicase DEAD27 SIDEAD27 | Solyc08g076200.2.1 |
| 1 | Nuclear pore complex protein Nup155 | Solyc07g008160.2.1 |
| 1 | Calcium-dependent protein kinase 3 | Solyc01g112250.2 |
| 1 | Transcription initiation factor TFIID subunit 12 | Solyc09g009680.2.1 |
| 2 | Protein LSM14 homolog B | Solyc05g009980.2.1 |
| 1 | Auxin response factor 8-1 | Solyc03g031970.2.1 |
| 1 | Auxin response factor 8B | Solyc02g037530.2.1 |
| 1 | Phosphoglucan water dikinase | Solyc09g098040.2.1 |
| 1 | Protein VAC14 homolog | Solyc04g008010.2.1 |
| 1 | AP2 domain-containing transcription factor | Solyc10g075030.1.1 |
| 2 | Photosystem 1 reaction center protein subunit 2 | Solyc06g054260.1.1 |
| 1 | Zinc finger protein VAR3, chloroplastic | Solyc01g057780.2.1 |
| 2 | F-box/ankyrin repeat protein SKIP35 | Solyc08g015780.2.1 |
| 1 | Glutamyl-tRNA amidotransferase subunit A | Solyc11g071550.1.1 |
| 1 | DAG protein; contains Interpro domain(s) | Solyc10g007180.2.1 |
| 1 | BEL1-like homeodomain protein 1(II) | Solyc01g007070.2.1 |
| 1 | BURP domain-containing protein | Solyc05g005540.2.1 |
| 1 | Dynein light chain 1 cytoplasmic | Solyc06g071180.2.1 |
| 1 | Receptor-like protein kinase | Solyc11g065950.1.1 |
| 1 | SWI/SNF complex subunit SMARCC1 | Solyc06g060120.2.1 |
| 1 | Bell-like homeodomain protein 3 bl3 | Solyc08g081400.2.1 |
| 1 | Anaphase promoting complex subunit 6 | Solyc12g014320.1.1 |
| 1 | Poly(RC) binding protein 1 | Solyc12g055780.1.1 |
| 2 | Heterogeneous nuclear ribonucleoprotein K | Solyc12g055790.1.1 |
| 1 | Small nuclear ribonucleoprotein E | Solyc03g098470.2 |
| 1 | Calmodulin binding protein-like | Solyc12g036390.1 |
| 1 | Genomic DNA chromosome 5 BAC clone F6B | Solyc06g083660.2.1 |
| 1 | Catenin beta-1 | Solyc05g026560.2.1 |
| 1 | Actin family protein | Solyc06g043170.2.1 |
| 1 | WRKY transcription factor 17 SIWRKY17 | Solyc07g051840.2.1 |
| 1 | Pre-plastocyanin X13934 | Solyc04g082010.1.1 |
| 1 | Phospholipase D | Solyc04g82000.2.1 |
| 1 | Contains similarity to RNA-binding protein from At gi 2129727 | Solyc01g098030.2.1 |

Out of 68 sequenced prey plasmids, 49 different candidate interactors were identified. Subsequently, full length coding sequences were amplified with PCR from cDNA of *Sl* as a template and cloned *via* a GG reaction into pJOG130 (Gantner *et al.*, 2018), a Gateway entry vector. Thereafter, the experiment shown in Figure 8 was repeated with the full length cDNAs of the potential interactors. In total, the coding sequence of 35 potential interactors were cloned and tested in full length. Of those, 18 specifically interacted with the heterocomplex under the selective conditions, lacking LWH and adenine hemisulfate (data not shown).

At this point it was discovered that, in contrast to *At*, PAD4 has no function in the *Solanaceae* TNL-mediated resistance signaling. Only SAG101b was able to re-constitute an active heterocomplex with EDS1, capable of eliciting an immune response *via* the TNL pathway (Gantner *et al.*, 2019). Therefore, SAG101b was tested for its ability to specifically interact with the proteins identified as potential interacting partners from the Y3H-screen with the *S*/EDS1-*S*/PAD4 heterocomplex. The 18 potential interactor candidates were co-expressed with a new bait (pJOG778) carrying the coding sequence for the BD-*S*/SAG101b fusion protein instead of *S*/PAD4 in combination with *S*/EDS1-3xHA. All 18 candidates showed an interaction with this active heterocomplex under selective media conditions (Table 4).

Additionally, the 18 interactor candidates were aligned with BLAST to the Arabidopsis genome (TAIR) and the predicted orthologous coding sequences from *At* were cloned. It was possible to amplify the coding sequences of 17 orthologous which were shuttled to pGAD. Fused to the GAL4 AD, the orthologs were tested for interactions with BD-*At*PAD4 and BD-GFP additionally co-expressed with *At*EDS1-3xHA. Interestingly, only 5 out of 17 orthologous potential candidates were able to interact with the EDS1-PAD4 heterocomplex of *At* in Y3H (data not shown, validated by replica plating with toothpicks). Moreover, a subcellular localization of the candidate interactors of *Sl* was predicted using TargetP 1.1 (<http://www.cbs.dtu.dk/services/TargetP/>, Table 4).

Table 4: Candidates specifically interacting with the S/EDS1-S/PAD4 and SIEDS1-SISAG101b heterocomplexes, their predicted localization, and interaction of the *At*-orthologs

| Found | Description | Solyc-Identifier | predicted localization | At-Identifier | orthologue interaction |
|-------|--|--------------------|------------------------|---------------|------------------------|
| 1 | Heavy metal-associated domain containing protein | Solyc01g098760.2.1 | no prediction | At5g19090 | no |
| 2 | Protein LSM14 homolog B | Solyc05g009980.2.1 | chloroplast | At1g26110 | no |
| 1 | WRKY transcription factor 17 S/WRKY17 | Solyc07g051840.2.1 | no prediction | AT1G62300 | yes |
| 1 | BEL1-like homeodomain protein 1 (II) | Solyc11g068950.1.1 | chloroplast | AT2G35940 | yes |
| 1 | Nucleic acid binding protein | Solyc07g008490.2.1 | no prediction | At4G26000 | no |
| 1 | 26S protease regulatory subunit 4 | Solyc06g083620.2.1 | no prediction | not tested | |
| 1 | Proteasome subunit beta type | Solyc07g016200.2.1 | no prediction | not tested | |
| 1 | Genomic DNA chromosome 5 BAC | Solyc06g083660.2.1 | no prediction | AT4G28760 | no |
| 1 | Contains similarity to RNA-binding protein from <i>At</i> gi 2129727 | Solyc01g098030.2.1 | mitochondrion | AT1G53645 | yes |
| 3 | DNA-binding bromodomain-containing protein | Solyc07g064700.2.1 | mitochondrion | At5G55040 | no |
| 1 | Unknown Protein (AHRD V1) | Solyc11g007510.1.1 | no prediction | At3G52240 | no |
| 1 | Unknown Protein (AHRD V1) | Solyc04g081420.2.1 | no prediction | At1G75730 | no |
| 2 | Auxin response factor 8-1 | Solyc03g031970.2.1 | no prediction | At5G37020 | no |
| 2 | F-box/ankyrin repeat protein | Solyc08g015780.2.1 | no prediction | At2G44090 | no |
| 1 | DAG protein contains Interpro domain(s) | Solyc10g007180.2.1 | mitochondrion | At3G15000 | yes |
| 1 | BURP domain-containing protein | Solyc05g005540.2.1 | secretory pathway | At1G70370 | no |
| 1 | Dynein light chain 1 cytoplasmic | Solyc06g071180.2.1 | chloroplast | At5G20110 | no |
| 1 | Poly(RC) binding protein 1 | Solyc12g055780.1.1 | no prediction | At1G51580 | yes |
| 1 | ZZ type zinc finger domain-containing protein | Solyc03g112230.2.1 | no prediction | At4G24690 | no (but not toxic) |

Summarizing, 18 of 35 tested candidate interactors of *Sl* are able to induce a growth in Y3H, when co-expressed with the S/EDS1-S/PAD4 and S/EDS1-S/SAG101b heterocomplexes, whereas only 5 of the orthologous interact with the EDS1-PAD4 complex of *At*.

It could be shown that EDS1 localizes to the cytosol and the nucleus (Feys *et al.*, 2005). A potential interactor has to be located in the same compartments, which in consequence excluded all interacting candidates from further analyses if they are not localized in the cytoplasm or the nucleus.

3.6.3. Virus-induced gene silencing of candidate interactors

For further analysis of the biological significance of putative interactions, VIGS (virus induced gene silencing) was performed. VIGS is based on the dsRNA-induced post-transcriptional degradation of targeted plant mRNA by infection with a modified TRV (*tobacco rattle virus*), which leads to a knock-down of a gene of interest. TRV is a bipartite ssRNA virus, consisting of RNA1 and RNA2. For VIGS applications, the two parts are placed on two binary vectors, pTRV1 and pTRV2, competent for transient expression *in planta* via *Agrobacterium*-mediated transient expression (Liu *et al.*, 2012). One vector carries TRV1, which encodes the replication and movement functions, while TRV2 encodes for the coat protein and carries the variable sequence complementary to the targeted RNA (Velásquez *et al.*, 2009). The integration of the (transfer) T (transfer)-DNA of both plasmids into the plant genome (*via Agrobacterium tumefaciens*) enables the replication of the viral components and the assembly of viral particles, resulting in a systemic spread of the virus through the whole plant. *Nb* is able to recognize the assembled virus and defend against virus multiplication by

targeting the produced viral RNA for sequence-specific mRNA degradation. The variable sequence of TRV2 is thereby recognized by the plant, which induce the production of siRNAs (small interfering RNAs), resulting in targeting and degradation of the corresponding mRNA (Liu&Page, 2008).

For the construction of pTRV2 derivatives containing fragments for silencing of targeted genes, the vector pTEI31 (Gantner *et al.*, 2018) was used, allowing the direct insertion of a PCR product *via* GG cloning. Orthologous from *Nb* of the candidate interactors from *Sl* were identified per BLASTn as described in 3.6.2, but with the predicted cDNA of *Nb* (version 1.0.1) as database. cDNA fragments from *Nb* genes with lengths of 200 to 1300 bp were chosen which were located in the middle of the targeted gene (within an exon) as recommended in the literature (Liu&Page, 2008). The considered genes are listed in Table 5.

Table 5: Targeted genes for VIGS approach

| Description |
|--|
| Heavy metal-associated domain containing protein |
| WRKY transcription factor 17 |
| Nucleic acid binding protein |
| 26S protease regulatory subunit 4 |
| Proteasome subunit beta type |
| genomic DNA chromosome 5 BAC |
| Unknown Protein I |
| Unknown Protein II |
| Auxin response factor 8-1 |
| F-BOX/Ankyrin repeat protein |
| Poly(RC) binding protein 1 |
| ZZ-type zink finger domain containing protein |

TRV2-derivatives were transformed into *Agrobacterium tumefaciens* GV3101 pMP90. Strains were plate grown and resuspended in AIM (*Agrobacterium* infiltration medium; 10 mM MES pH5.4, 10 mM MgCl₂) at OD₆₀₀ = 0.4. Strains were mixed 1:1 with TRV1 and inoculated into the bottom leaves of three weeks old *Nb* wt plants using a needleless syringe. Fourteen days after inoculation, the leaves were infiltrated with *Pfl* (*Pseudomonas fluorescens*) ([EtHAN] strains expressing AvrBs3 (should not be recognized) and XopQ (EDS1-dependently recognized), as well as *Xcv*-strain 85-10 (EDS1-dependently recognized, strain contains the effector XopQ) and the *Xcv* Δ xopQ mutant (not recognized; recognition of *Xcv* is dependent on XopQ). For each gene of interest, six plants were infiltrated with *Agrobacterium* strains for reconstitution of respective TRV2-derivatives. Two leaves were infiltrated per plant and phenotypically analyzed. This experiment was repeated five times. As a positive control, *Nb eds1* was silenced. Figure 9 shows the plant reaction of the four inoculated bacteria in the *eds1* silenced *Nb* control plant, followed by the plants where putative heterocomplex interactors were silenced.

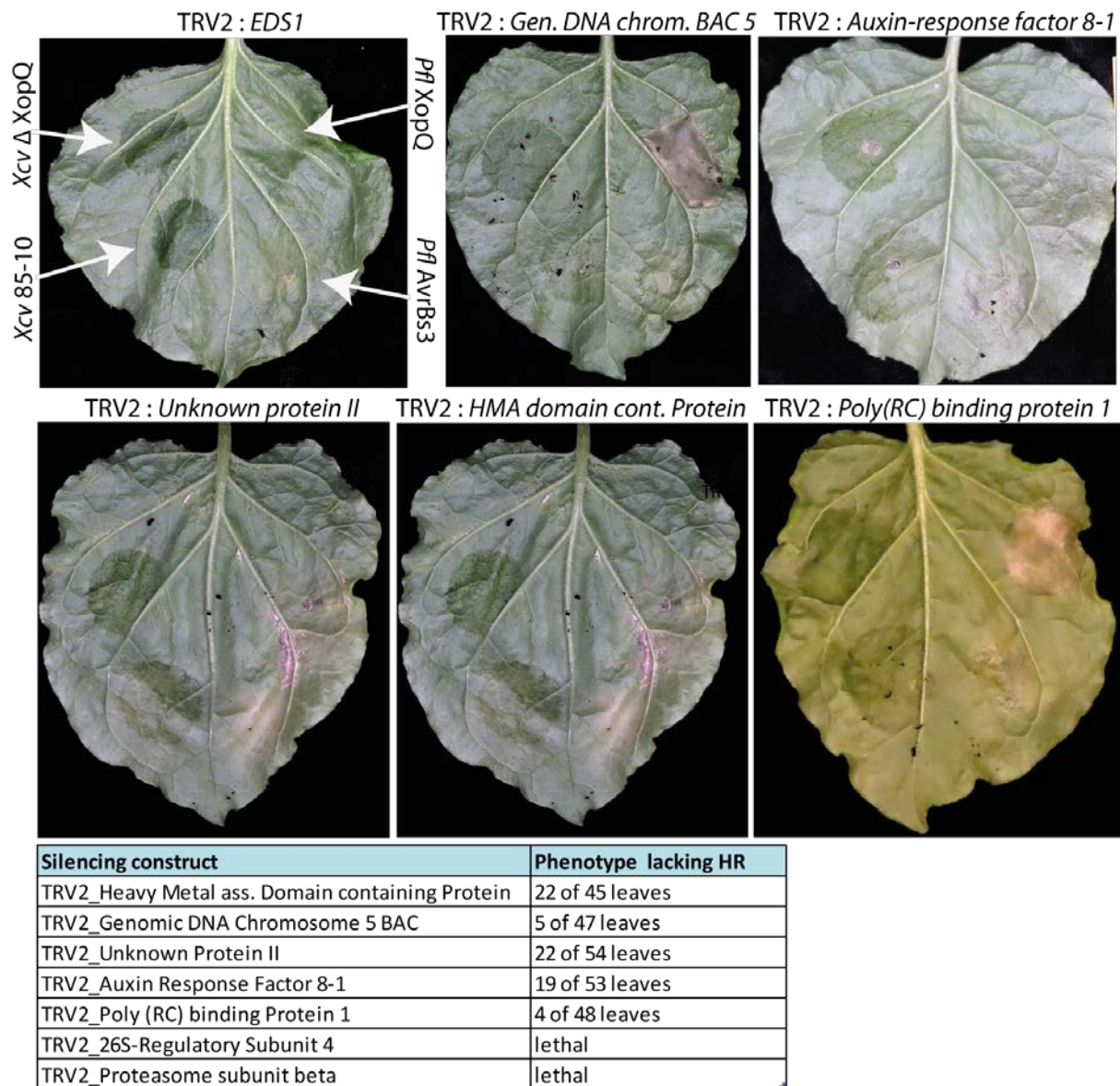


Figure 9: Phenotypic analysis of pathogen recognition in *Nb* after silencing of interacting candidate genes
 Leaves of five silenced plants are shown (as indicated) and compared to the positive control (*eds1*-silenced). All shown silenced plants behave mostly like the *eds1*-silenced control. Inoculated strains on the left side: *Xcv* (*Xanthomonas campestris* pv. *vesicatoria*) 85-10 (bottom) and *Xcv* Δ *xopQ* strain (top); on the right side: *Pfl* (*Pseudomonas fluorescens*) [EtHAn] expressing *avrBs3* (bottom) and *xopQ* (top) respectively (OD_{600} of all = 0.2).

If a potential interacting candidate would be essential for EDS1-based immune signaling, silencing of the respective candidate interactors mRNA, should lead to nearly the same plant phenotype past pathogen perception, as seen on the leaf of the *eds1*-silenced plant. Whereas *Xcv* 85-10 is recognized in untreated *Nb*, this strain is not detected in the *eds1*-silenced plant and elicits a water soaking lesion, as is would be commonly observed by an infiltration of the virulent Δ *xopQ* mutant of *Xcv* in wt plants. *XopQ* delivered by *Pfl* is recognized in *Nb* wt and show a clear HR-reaction, whereas *AvrBs3* is not detected in *Nb*. Both *Pfl*-strains were not recognized in the *eds1*-silenced control. About 40 % of plants silenced for expression of candidate interactors *Heavy Metal* ass. *Domain containing protein*,

Unknown protein II, and *Auxin Response Factor 8-1* showed reactions similar to *eds1* control plants, indicating that the TNL-immune signaling pathways could be impaired as depicted in Figure 9. About 10 % of the leaves of plants in which *Genomic DNA chromosome 5 BAC*, and *Poly(RC) Binding Protein* were silenced, showed reactions similar to the *eds1*-silenced control plants, but some leaves showed an intermediate phenotype. Whereas *Pfl XopQ* is recognized (clear cell death reaction), *Xcv 85-10* rather induces a reaction resembling water-soaked lesions (as observed for the non-recognized *Xcv ΔxopQ*). Two other potential candidate interactors could not be further analyzed by this technique, because the proteins 26S Regulatory Subunit, and Proteasome Subunit Beta-type seemed to be essential. Silenced plants died before following infection assays were possible.

3.6.3.1. In planta growth assay of plants treated with VIGS

Plants exhibited a susceptible phenotype if the genes *Heavy Metal ass. Domain containing protein*, *Unknown protein II*, and *Auxin Response Factor 8-1* were respectively silenced and treated with pathogens that are normally avirulent in the non-host plant *Nb*, as shown in Figure 9. This susceptible phenotype is always observed in the mutant plant *Nb eds1a-1* (Adlung *et al.*, 2016), indicating that those three proteins could interact with the EDS1-SAG101b heterocomplex and that an interaction could be critical for TNL-mediated immune signaling. If silencing of a candidate interactor influence TNL-dependent immune signaling, an increase in the multiplication of *Xcv 85-10* should also occur. An *in planta* growth assays was performed in plants which were silenced with TRV2-constructs that exhibited an susceptible phenotype as it was observed in *eds1*-silenced *Nb*. *eds1* and *gfp*-silenced *Nb* were used as controls. For a growth curve, *Xcv* strains 85-10 and the deletion strain *Xcv ΔxopQ* were inoculated in the bottom of leaves as described in 3.6.3, but with an $OD_{600} = 0.0004$. Leaf discs were harvested at 0 and 6 days post infection with a cork borer (5 mm in diameter) and disrupted in 10 mM $MgCl_2$ by using a bead mill. Bacterial titers were quantified *via* plating dilution series, and colonies were counted after three days. At each time point samples were taken from four independent leaves and the assays were repeated three times. Figure 10 shows the multiplication of *Xcv 85-10* in comparison to 85-10 $\Delta xopQ$ in silenced plants as indicated.

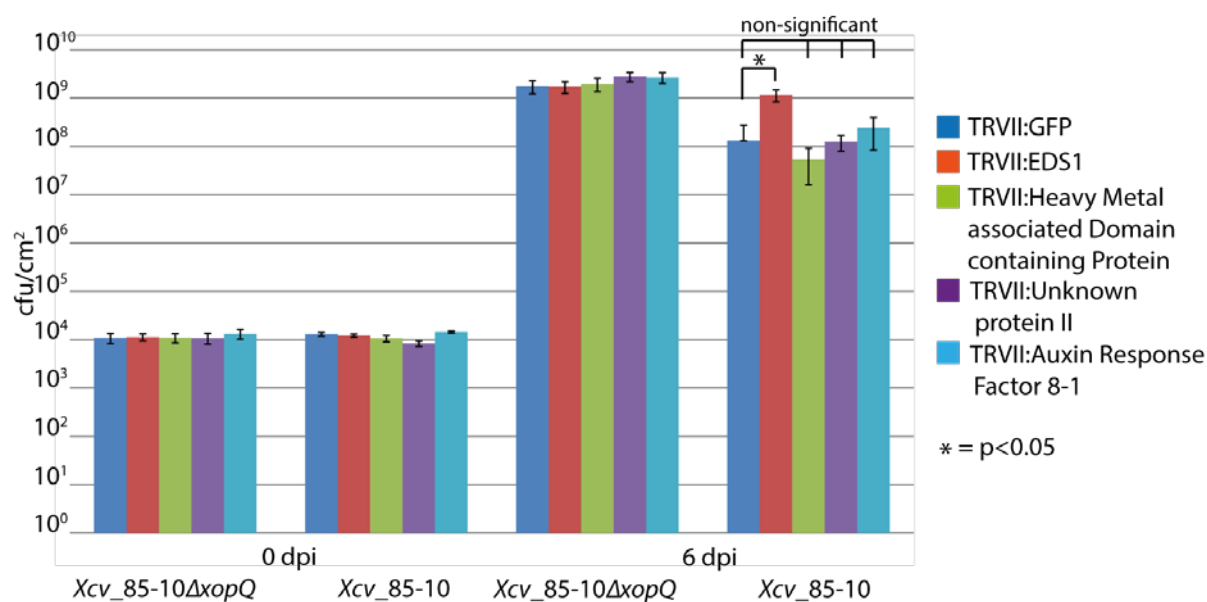


Figure 10: *In planta* growth assay of silenced interactor candidates of the phenotypical VIGS-assay

Multiplication of *Xcv* strains 85-10 and $\Delta xopQ$ were compared in VIGS-treated plants as indicated. The strains were infiltrated with an $OD_{600} = 0.0004$. Leaf material was harvested 0 and six days post infection. Dilution series were plated and bacterial titer was determined three days post plating. Four technical replicates were made per silenced plant. The assay was repeated three times. Statistical analysis were made with Student t-test ($p < 0.05$). The growth of *Xcv* 85-10 is increased in all silenced plants 6 dpi, except for the *eds1* silenced control plant, indicating that *Xcv* 85-10 is recognized in comparison to the *eds1* control plant and to the treatment with the *Xcv* deletion strain $\Delta xopQ$.

The *in planta* growth assay does not show an increase in bacterial multiplication of *Xcv* 85-10 if the expression of *Heavy Metal associated Domain containing protein*, *Unknown protein II*, *Auxin Response Factor 8-1* was silenced in comparison to the *gfp* silenced control plants. In contrast, the *eds1* silenced plants do not recognize *Xcv* 85-10, resulting in an increased multiplication which is comparable with growth rates of *Xcv* 85-10 $\Delta xopQ$. Only the multiplication rate of *Xcv* 85-10 in *eds1* silenced plants is significantly different to the *gfp* silenced plants as determined by Student's t-test ($p < 0.05$).

3.6.4. FRET-APB of candidate interactors

To further analyze promising candidate interactors, a microscopy-based approach was selected. Fluorescent proteins were fused to the proteins of interest in order to monitor subcellular localization, interaction, and movement of the respective fusion proteins. To analyze protein-protein interaction *in planta* via fluorescence the method FRET (Förster resonance energy transfer) was used. In FRET, a donor chromophore is excited with the suitable laser line. In this state, part of the emission energy can be transferred to a nearby acceptor chromophore without energy loss *via* dipole-dipole coupling (Hecker *et al.*, 2015). FRET depends on spectral overlaps of the donor and acceptor fluorophores and is most

efficient if the distance between the chromophores is smaller than 10 nm (Jares-Erijman&Jovin, 2003). In this approach the FRET-APB (acceptor photo bleaching) technique was used, in which the acceptor fluorophore is bleached. As a consequence, the donor is not able to transfer its emission energy which will be brighter, but only if the two chromophores are in close proximity (Bhat *et al.*, 2006). Improved fluorophores (mEGFP as donor, and mCherry as acceptor) within the modular cloning nomenclature were used as fusion proteins (Hecker *et al.*, 2015; Gantner *et al.*, 2018). The donor-fluorophore mEGFP was C-terminally fused to the candidate interactors. A multi-gene construct was created carrying *S/SAG101b* fused to the acceptor fluorophore mCherry (monomeric red fluorescent protein, derived from dsRED (Shaner *et al.*, 2004)), and a second transcription unit coding for *S/EDS1* with a C-terminal 3xFLAG octapeptide tag (pJOG1067). As a negative control, a multi-transcriptional unit was constructed, carrying mCherry as single transcription unit and as a second one *S/SAG101b*-3xFLAG (pJOG1069). All plasmids used for FRET-APB are illustrated in Figure 11A. The plasmids were respectively transformed to *Agrobacterium tumefaciens* GV3101 pMP90. Strains were plate grown and resuspended in AIM at $OD_{600} = 0.4$. Strains carrying the plasmids encoding for the candidate interactors were mixed 1:1 with strains either carrying pJOG1067 or pJOG1069, and inoculated into leaves of three weeks old *Nb* wt (wild-type) plants using a needleless syringe. Measured FRET-efficiencies of common controls, which were also used in the corresponding publication (Gantner *et al.*, 2019), as well as the efficiencies of the tested candidate interactors in co-expression with the heterocomplex (pJOG1067) are shown in Figure 11B, arranged in a Boxplot. Figure 11C displays the same candidate interactors but in co-expression with the negative control (pJOG1069), solely mCherry as acceptor together with *S/SAG101b*-3xFLAG. The median of the FRET-efficiencies are further listed together with the localization in co-expression with the *S/EDS1*-*S/SAG101b* heterocomplex in Figure 11D.

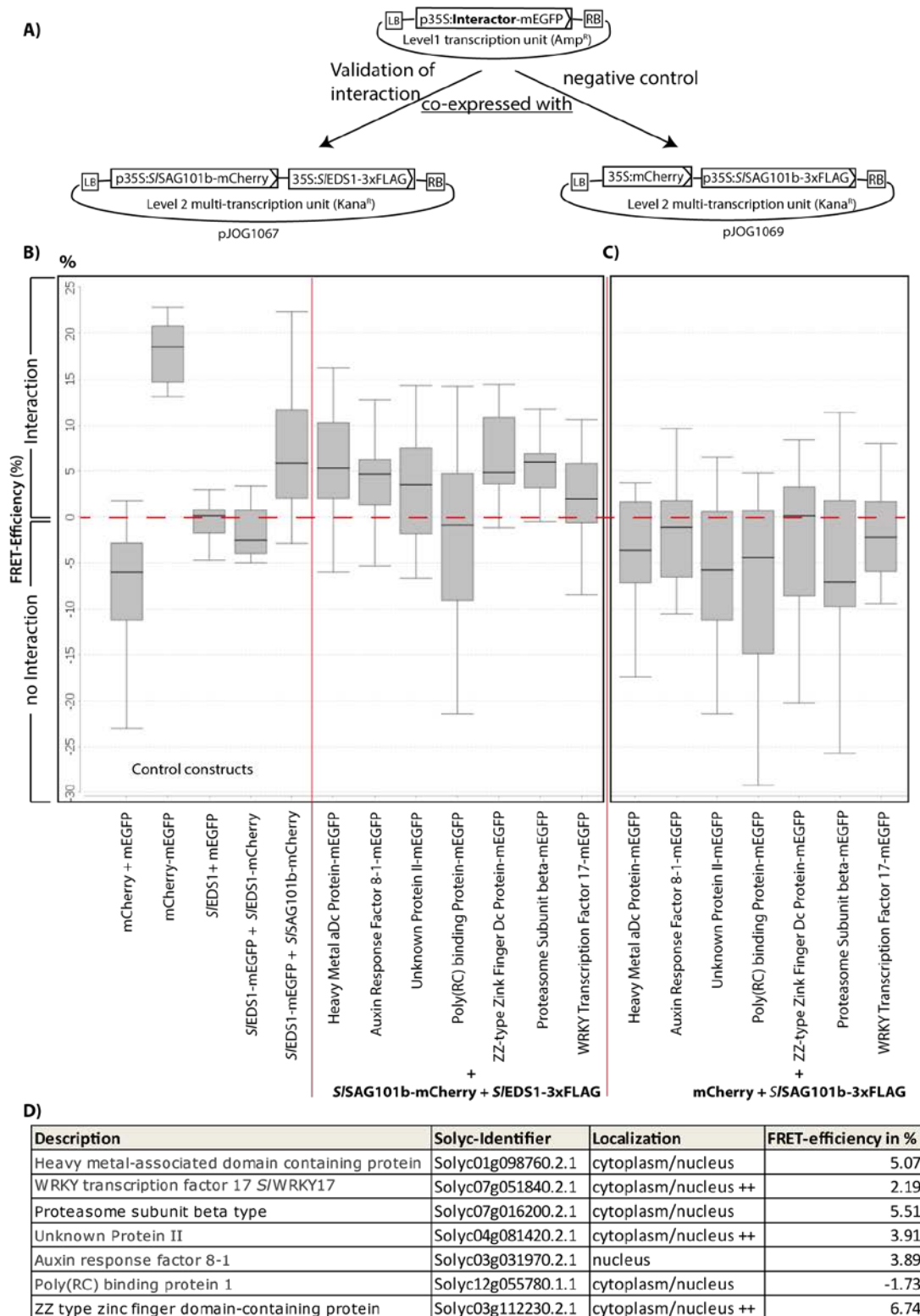


Figure 11: subcellular localization and FRET-APB of interacting candidates

(A) Transcription units coding for the potential candidate interactors are shown. Additionally, either a multigene construct carrying *p35S:SfEDS1-FLAG-tmas* (*p35S*: = 35S promoter, *tmas* = MAS-terminator) and *p35S:SfSAG101b-mCherry-t35S* (*t35S* = 35S-terminator), encoding the essential heterocomplex. As a negative control, a second construct coding for only *35S:mCherry-t35S* with an additional transcription unit *35S:SfSAG101b-FLAG-tmas* are imaged. (B) Boxplot of FRET-efficiencies of indicated controls followed by the SfEDS1-based heterocomplex or (C) of the negative controls as shown in (A), co-expressed with the candidate interactors. Black lines within the Boxplots display the median, the red dashed line the zero-point of the FRET-efficiency, and the horizontal category exhibit the FRET-efficiency in percentage (%). Except for Poly(RC) binding Protein 1, all interacting candidates showed a positive median FRET efficiency in (B) and a negative median efficiency in (C). (D) Table with tested candidate interactors, their localization, and FRET-efficiency (median).

Interestingly, only one interacting candidate, Poly(RC) binding protein, does not show a positive FRET-efficiency, if co-expressed with the S/EDS1-S/SAG101b heterocomplex, whereas all other tested interactor candidates show a positive FRET-efficiency. Furthermore, none of the tested interactor candidates exhibited a positive FRET-signal if co-expressed with the mCherry negative control as acceptor (pJOG1069). Overall, these data indicate that the putative candidate interactors with a positive FRET-efficiency are probably located in relative close proximity to the S/EDS1-S/SAG101b heterocomplex. Moreover, it could be shown that all expressed interactor candidates are located in the cytoplasm and in the nucleus (with one exception: Auxin-response factor 8-1 is only located in the nucleus). All proteins are stable synthesized which was verified by immunoblotting (data not shown).

3.6.5. Summary and Conclusion

The identification of proteins interacting with the heterocomplex might riddle the secrets of the EDS1-based heterocomplexes and could help to understand how the TNL-dependent defense pathway operates. This last part of additional results was a major project of the thesis within the first two years. More than 1100 yeast transformants were examined in a first screen (181 colonies retransformed with six controls), 35 cDNAs of candidate interactors were full length cloned, and tested again. The experimental Y3H setup pointed out that nearly all potential interactors are only able to induce a yeast growth under selective conditions if co-expressed with the entire heterocomplex, which underlines the importance of both partners of the heterocomplex, EDS1-PAD4 or EDS1-SAG101b.

Two following approaches VIGS, and FRET, identified three potential interacting proteins, Heavy metal-associated domain containing Protein, Unknown Protein II, and Auxin-response Factor 8-1, which were tested as positive candidates in both setups and will be shortly described in the following passage.

Proteins containing an HMA (heavy metal associated) domain are targets of effectors to deregulate the homeostasis of the plant cell. They are required for spatio-temporal transportation of metal ions which bind to a variety of enzymes and co-factors in a cell (Imran *et al.*, 2016). Therefore, HMA domains are integrated to NLRs to serve as bait for a pathogen arrived effector protein, mimicking the host target, which was for example shown for Pik-1 of rice (Kanzaki *et al.*, 2012; Zhai *et al.*, 2014; Maqbool *et al.*, 2015). It could be speculated that a NLR containing such an HMA domain interacts with the EDS1-based heterocomplexes to induce a defense program or to bolster an immune reaction. Another possibility might be that EDS1-based complexes interact with this protein to regulate the metal ion concentration of the cell in order to induce a defense reaction. Unknown protein II does not have any

description in literature. The orthologous protein of *At*, Transcriptional Regulator ATRX, is located in the nucleus and is involved in transcriptional regulation (arabidospis.org/(Klepikova *et al.*, 2016)). After perception of a pathogen transcriptional reprogramming takes place. A regulator of the transcription might be a possible interacting candidate. Nevertheless, the localization of Unknown Protein II is in the cytoplasm as well, in comparison to its orthologue, and might fulfill another function in the cytoplasm except for regulatory tasks in the nucleus. ARFs (Auxin response factors) play an essential role in the regulation of plant growth, development, and respond to biotic and abiotic stress (Santner&Estelle, 2009). 17 ARFs of *Sl* are identified and a comparison with ARFs of other plants within the *Solanaceae* provides a common repertoire of these proteins in *Solanaceae* (Kumar *et al.*, 2011). It is known that auxin plays a role in mediating plant defense response together with other phyto-hormones. For example, SA is able to repress the auxin signaling pathway. After pathogen perception, an accumulation of ARFs is observed (Wang *et al.*, 2007). The stabilization of these proteins might serve as a negative regulatory mechanism for immune responses, possibly *via* interaction with EDS1.

However the *in planta* growth curve, in which the respective genes were silenced, revealed no differences in bacterial growth, compared to the control. Moreover, the orthologs of all three interacting candidates of *At* did not interact with the respective EDS1-PAD4 heterocomplex in the Y3H assay. A validation of physical interaction was only detected with FRET. Further analyses will be necessary to confirm an interaction and proof a relevance in TNL-dependent immune signaling.

4. Discussion

The first two sections of this thesis are more technology- and resource-oriented: molecular cloning tools and mutant lines of *N. benthamiana* and *A. thaliana* were generated. This work is discussed in the respective publications. In the following, my work on EDS1 functions in TNL-mediated immunity will be discussed in more detail.

4.1. *N. benthamiana* as a model system for analysis of TNL-mediated immunity

The signaling cascade underlying immunity mediated by TNL-type immune receptors in *At* depends on the lipase-like protein EDS1 (Aarts *et al.*, 1998; Feys *et al.*, 2001; Feys *et al.*, 2005). EDS1 engages into mutually exclusive heterocomplexes with PAD4 or SAG101 (Wagner *et al.*, 2013). PAD4 and SAG101 are similar to EDS1 and also to each other, but the three proteins belong to distinct phylogenetic clades. Interestingly, *SAG101* is missing in genomes of plants lacking TNL-encoding genes, e.g. monocotyledons and in the genomes of *Aquilegia coerulea* or *Mimulus guttatus* eudicot genomes (Wagner *et al.*, 2013). Although this finding suggests a functional link, a relevance of SAG101 in TNL-mediated immunity was so far neglected based on analyses in the Arabidopsis model system: In Arabidopsis, SAG101-deficient plants are not impaired in resistance responses, and a minor contribution of SAG101 is revealed only in absence of PAD4 (Feys *et al.*, 2005; Wagner *et al.*, 2013). In other words, the EDS1-PAD4 complex is fully sufficient for immune responses, and EDS1-SAG101 is not required. Based on these observations, EDS1 and PAD4 were considered as the players required for pathogen resistance (Bernacki *et al.*, 2019), although this was not corroborated by experimental data from alternative plant species.

Despite a large body of genetic data supporting a contribution of EDS1 complexes to diverse biological processes (Bernacki *et al.*, 2019), the molecular functions at a mechanistic level remained unclear. Surprisingly, the crystal structure of the Arabidopsis EDS1-SAG101 complex and modeling of the EDS1-PAD4 complex did not provide new hints on the molecular function of these complexes. Since for structure-function analyses of EDS1 complexes in Arabidopsis the generation of stable transgenic lines is required, we aimed to establish *Nb* as a new model system for EDS1 structure-function analyses. The key advantage of *Nb* lies in highly efficient protein expression by *Agrobacterium*-mediated transient expression (Agroinfiltration) (Kapila *et al.*, 1997; Wydro *et al.*, 2006; Bombarely *et al.*, 2012). However, *Nb* was so far not an ideal genetic model due to its allotetraploid

genome and incomplete genome annotation. Previously, mainly virus-induced gene silencing was used for functional gene analyses in *Nb*, but this approach has important caveats (Peart *et al.*, 2002; Yu *et al.*, 2019). With reduced costs of next generation sequencing and genome editing technologies, *Nb* is now becoming increasingly important for both forward and reverse genetic analyses (Derevnina *et al.*, 2019; Schultink *et al.*, 2019). With the genetic dissection of TNL signaling pathways, this thesis made an important contribution to establish *Nb* for analysis of EDS1 functions.

4.2. Different EDS1 complexes operate in plant immunity in Arabidopsis and Solanaceae: Co-evolution within species-specific signaling networks

One prerequisite for functional analysis of a gene of interest in Agroinfiltration-based *Nb* assays will be, at least in many cases, disruption of the respective endogene. We chose to use Cas9-based RNA-guided nucleases for this purpose. As the technology had just emerged, this implicated that first adequate tools had to be developed (Ordon *et al.*, 2017).

In an initial set of stable *Nb* transformations, *eds1* and *pad4* mutant plants were generated (Ordon *et al.*, 2017). *Nb*EDS1 was previously analyzed using VIGS, and several inducers of an EDS1-dependent hypersensitive response (or cell death) had been described (Burch-Smith *et al.*, 2007; Swiderski *et al.*, 2009). The *Nb eds1* mutant line was instrumental to show that the T3E XopQ from *Xcv* 85-10 induced an EDS1-dependent cell death in *Nb* (Adlung *et al.*, 2016).

In this context, it is interesting to note that *Nb* was considered a non-host for *Xcv*, but deletion of XopQ was sufficient to render *Xcv* virulent on *Nb* (Adlung *et al.*, 2016). This questions the common notion that different mechanisms underlie non-host resistance and race-specific resistance, at least for plant species that are closely related to host species – in the case of *Xcv*, pepper and tomato isolates. This incompatible interactions between a pathogen and a plant suggests that avirulence of a pathogen isolate on “non-hosts” of the same plant family to a host is mainly caused by effector recognition, while divergent evolution of effector targets (thus rendering effectors non-functional) may underlie incompatibility on more distant plant species (Schulze-Lefert&Panstruga, 2011).

When expressed in leaf tissues after Agroinfiltration, XopQ induced chlorosis or necrosis in wt, but not *eds1*-mutant *Nb* lines (Adlung *et al.*, 2016). These findings correlated with *Xcv*-infection studies: Although *Xcv* 85-10 does not induce a strong HR in *Nb*, it did also not produce water-soaked lesions, the typical *Xcv*-induced disease symptoms. However, *Xcv* became virulent on *eds1* mutant plants, and an *Xcv* Δ xopQ mutant strain was virulent on

both wt and *eds1*-deficient *Nb* plants (Adlung *et al.*, 2016; Gantner *et al.*, 2019). These results strongly suggested recognition of XopQ by a TIR domain-containing NLR. Indeed, the respective gene, *Roq1* (*Recognition of XopQ 1*), was subsequently isolated (Schultink *et al.*, 2017), thus complementing the set of components of our experimental system.

Having identified XopQ as an inducer of EDS1-dependent immunity in *Nb*, the initially generated *eds1* and *pad4* mutant lines were tested for induction of cell death/chlorosis and also resistance to *Xcv* 85-10 bacteria (Gantner *et al.*, 2019). Surprisingly, only *eds1* mutant plants were unable to mount XopQ-induced defenses. An initial assumption was that PAD4 and SAG101 functioned redundantly in TNL-mediated immunity in *Nb*, and *SAG101* isoforms were targeted by genome editing in the background of the *pad4* mutant line.

Detailed analyses of generated mutant lines revealed that only one of these SAG101 isoforms, *NbSAG101b*, functioned in TNL-mediated immunity in *Nb*. These experiments were conducted using a *pad4 sag101a sag101b (pss)* triple mutant line and relying on transient complementation: Cell death induced by either XopQ, the TIR-domains of the TNLs *AtDM2h* or *AtRPS4* or the co-expression of the TMV Helicase protein p50 together with the tobacco TNL receptor N (Burch-Smith *et al.*, 2007) could be re-established by co-expression of SAG101b, but not SAG101a or PAD4 in this mutant line (Gantner *et al.*, 2019). These results were fully confirmed using a subsequently generated *Nb sag101b* single mutant line (Lapin *et al.*, 2019), leading to the hypothesis that TNLs in general are dependent on EDS1-SAG101b for defense signaling in *Nb* (Figure 12), whereas functions of EDS1-PAD4 and EDS1-SAG101a complexes in this species remain unknown.

Thus, the central function of EDS1 in immune signaling networks of dicotyledonous plants is conserved – but executed by EDS1 in complex with proteins of distinct phylogenetic origins in *Brassicaceae* and *Solanaceae* as shown in Figure 12. This suggests the co-evolution of these complexes within immune signaling networks of different species. Furthermore, EDS1 complexes mediating immune signaling in *Brassicaceae* (*AtEDS1-AtPAD4*) are not functional in *Solanaceae*, and *vice versa* (*SIEDS1-SISAG101b*) (Gantner *et al.*, 2019). One most plausible hypothesis is that these complexes do not form a functional module by themselves, but co-evolved with additional protein interactors that are required to complete the EDS1 signaling node.

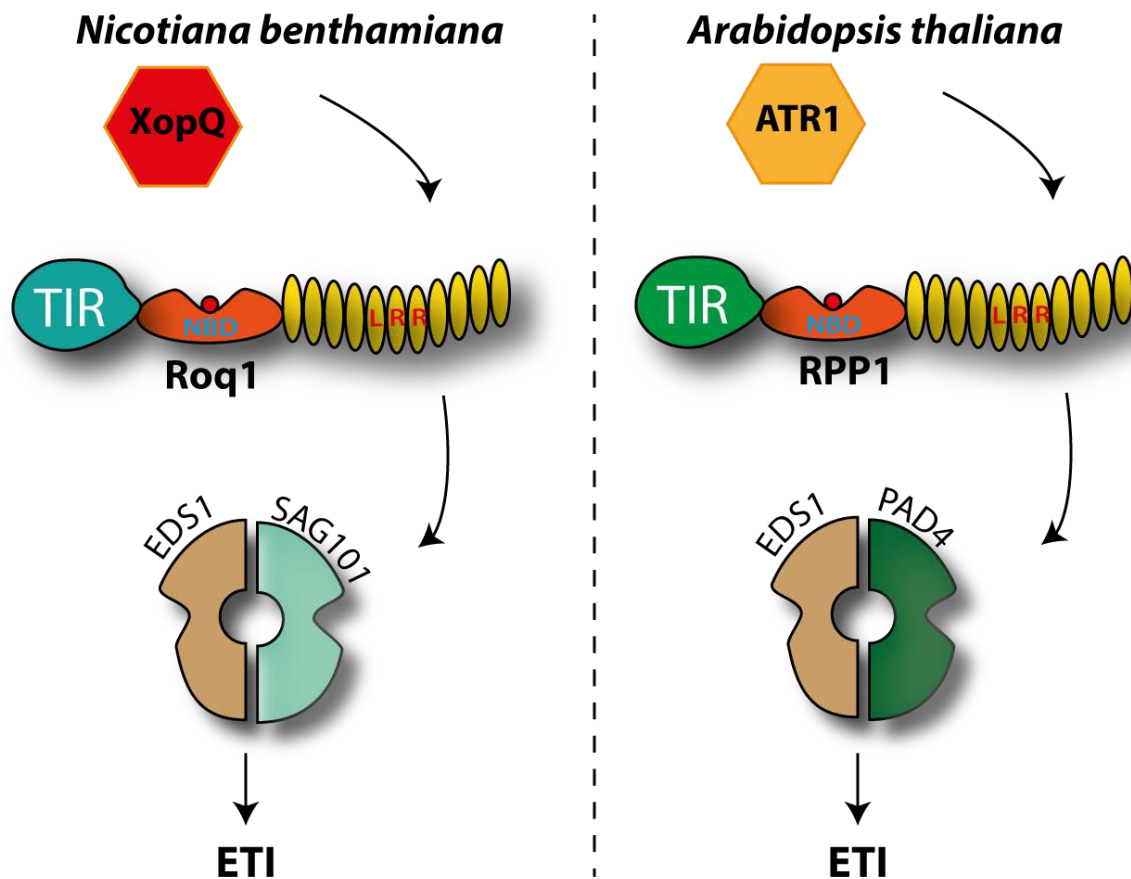


Figure 12: EDS1 recruits different interaction partners for immune signaling in *Nb* vs. *At*

Signaling cascade upon effector recognition by TIR domain-containing NLRs in *Nb* and *At*. While in *Nb*, SAG101b is needed to build a heterocomplex with EDS1 to induce an ETI after perception of XopQ, PAD4 is the more important heterocomplex partner in *At*. ATR1 (*A. thaliana* Recognized 1) is recognized by the R protein RPP1 (Recognition of Peronospora Parasitica 1) and activates the EDS1-PAD4 heterocomplex, required for ETI induction.

4.3. Identification of candidate interaction partners of EDS1- heterocomplexes in *Solanaceae*

4.3.1. A Y3H library screen employing the tomato EDS1-PAD4 complex as bait

Previous and this work indicate that EDS1 activity in TNL-mediated immunity depend on formation of EDS1-based heterocomplexes (Wagner *et al.*, 2013; Gantner *et al.*, 2019). It is, thus, reasonable to speculate that interactors required for mediating immune functions are recruited by the heterocomplex, but not single components. This aspect had not been taken into account in previous efforts to identify EDS1 interacting proteins. Therefore, a yeast-three-hybrid screen, using the EDS1-PAD4 complex from tomato as bait, was conducted in this thesis and described in 3.6.1.

A modified bait plasmid, possessing two transcriptional units for the expression of both subunits of the heterocomplex, was first constructed. Using this bait, 35 of full length cDNAs

(from tomato; the initial screen was conducted with a library prepared from pepper cDNA) were cloned and interaction tests repeated. For 18 (Table 4, section 3.6.2), interaction of the bait with the full length prey proteins could be confirmed. Interestingly, most of them interacted only with the heterocomplex (the Y3H bait), and not with the single proteins *S/EDS1* or *S/PAD4* in fusion with the GAL4 DNA-binding domain (classical Y2H bait). This indicates that only the heterocomplex itself (at least in yeast) is able to physically associate with the candidate interactors.

Since we had discovered in the meantime that, in *Solanaceae*, not the EDS1-PAD4 but the EDS1-SAG101b complex was crucial for TNL-mediated immunity, association of potential interactors with this complex was tested in similar Y3H assays. Interestingly, all 18 candidates (Table 4, section 3.6.2) that interacted with *S/EDS1-S/PAD4* also interacted with *S/EDS1-S/SAG101b*. Thus, a combined surface present in both heterocomplexes might be conserved between EDS1-PAD4 and EDS1-SAG101. Alternatively, candidate interactors might associate with EDS1 incorporated in either complex, but not EDS1 alone, e.g. due to a conformational change induced by complex formation.

The 18 remaining candidate interactors belonged to diverse protein families and did not share any conserved domain or comparable, which could represent a common EDS1 complex-binding motif. To date, a physiological relevance or function of the interactions detected by Y3H remains to be demonstrated. Indeed, three of these proteins (Table 4 section 3.6.2) are predicted to localize within chloroplasts, and are thus likely false positives that do not come in contact with EDS1 complexes inside plant cells. Yeast-based interactor screening can only be seen as a first indication for an interaction *in vivo* and must be confirmed *via* multiple approaches (Paiano *et al.*, 2019).

4.3.2. Knock-down of candidate interactor genes by virus-induced gene silencing

If association between a candidate interactor and the EDS1-based heterocomplex is essential for defense signaling, silencing of the corresponding gene is expected to lead to an altered immune response. For VIGS, only genes encoding proteins predicted to localize to the nucleus and/or the cytoplasm, thus the same compartment as EDS1 complexes, or without reliable prediction were considered. In total, genes encoding *Nb* orthologs of 12 potential interactors (Table 5, section 3.6.3) were silenced. Plants silenced for expression of five different genes showed altered responses to XopQ, similar to *eds1*-silenced control plants (section 3.6.3).

However, reduced responsiveness to XopQ was consistently observed for *eds1*-silenced plants, but only for some of the plants silenced for expression of candidate interactors. To date, it remains unclear whether this is due to fluctuations in silencing efficiencies among different plants or experimental replicates, or whether respective genes might not contribute to immune signaling. Two genes seem to be essential for plant survival as their silencing led to death of VIGS-plants before further analyses were possible. Notably, altered responses to XopQ were never observed upon silencing of five of the remaining genes (Table 5, section 3.6.3).

Silencing experiments will need to be extended by further analyses including measurements of knock-down efficiencies by quantitative Reverse-Transcriptase-PCR. Also, knock-out of respective genes by RGNs could be envisaged, but is laborious. To that end, multiple potential orthologs were detected in *Nb* genome resources for most of the remaining candidate genes. Nevertheless, varied immune responses upon silencing provide first hints that these five candidate genes might represent interesting targets for future analyses.

4.3.3. *In planta* localization and interaction studies of candidate interactors using FRET-acceptor photobleaching

To further analyze or validate interactions of candidate interactors with the S/EDS1-S/SAG101b complex *in planta*, FRET-APB was used and was described in section 3.6.4. In FRET-APB, two candidate interactors are coupled to suitable fluorophores for which the emission wavelength of a donor overlaps with the excitation spectrum of an acceptor, e.g. mEGFP and mCherry. If the two fluorophores, from interaction of the fusion partners, come into close proximity, some emission energy of the donor is transferred to the acceptor by FRET. In this case, elimination of the acceptor by photobleaching disrupts FRET, resulting in stronger light emission from the donor. Thus, emission of donor and acceptor is measured before and after acceptor photobleaching, and interaction can be detected by a gain of emission energy of the donor after bleaching. At the same time, FRET-APB allows observation of the subcellular localization of both fusion partners, and a potential interaction can be queried in either compartment by APB. However, it should be noted that a positive FRET-APB efficiency only indicates physical proximity, and not necessarily (direct) interaction, and may be very weak, as FRET efficiency decrease with the sixth power of distance between donor and acceptor (Bajar *et al.*, 2016).

The candidate interactors (Table 3, section 3.6) showed an interaction in yeast assays only if co-expressed with the EDS1-SAG101b heterocomplex, but not individual subunits. Therefore, S/EDS1-3xFLAG was co-expressed with S/SAG101b-mCherry as acceptor

complex, and interactor candidates were expressed as GFP fusions as FRET donor molecules. All tested candidates except Poly(RC) binding protein 1 resulted in positive FRET efficiencies when co-expressed with the *S/EDS1-S/SAG101b* heterocomplex, but not when co-expressed with free mCherry and *S/SAG101b-3xFLAG* as negative control. Although further interaction tests, e.g. by co-immunoprecipitation, should be conducted, these results support that the candidate interactors identified by Y3H might interact with EDS1-SAG101b inside plant cells.

For three candidate interactors identified by Y3H, namely Heavy metal-associated domain containing Protein, Unknown Protein II, and Auxin-response Factor 8-1, *in planta* interaction with EDS1-SAG101b was supported by FRET-APB analyses and silencing of respective genes by VIGS led to altered responses to XopQ (Figure 9 and Figure 11, section 3.6.3 and 3.6.4). However, enhanced growth of XopQ-translocating *Xcv* was not observed in VIGS-plants when tested (Figure 10). Also, the *Arabidopsis*-orthologs of the three candidates did not interact with the *AtEDS1-AtPAD4* heterocomplex in Y3H.

Recent analyses suggest a bifurcation of TNL-induced signaling pathways at the level of EDS1 complexes in *Arabidopsis* (Lapin *et al.*, 2019): While the EDS1-PAD4 complex is required for resistance, the EDS1-SAG101 complex appears to be required for activation of cell death programs. One hypothesis is that EDS1-PAD4 complexes might initiate resistance signaling *via* ADR1 helper NLRs, whereas EDS1-SAG101 initiates cell death *via* NRG1 (Lapin *et al.*, 2019). The *Arabidopsis* orthologs of the three candidate interactors (see above) were so far not tested for interaction with *AtEDS1-AtSAG101*. Although interactions appeared conserved in *Solanaceae*, as all 18 tested interactors could interact with both *S/EDS1-S/PAD4* and *-S/SAG101* complexes, they might be specific to EDS1-SAG101 in *Arabidopsis*, and link NRG1 to EDS1-SAG101 for cell death initiation.

In summary, the three candidate interactors Heavy metal-associated domain containing Protein, Unknown Protein II, and Auxin-response Factor 8-1, were confirmed by FRET-APB analyses and the results of the VIGS experiments hint at a physiological relevance of these interactions. They are thus attractive candidates for further analyses. One promising future experiment could be the mass-spectrometry-based identification of proteins bound to the *S/EDS1-S/SAG101b* heterocomplex after purification from plant tissues.

4.4. Rapid structure-function studies in *N. benthamiana* identified EDS1 features required for immune signaling

One rationale for the establishment of *Nb* as a new experimental system for analysis of TNL signaling was the potential for rapid analysis of a protein of interest by Agroinfiltration (Goodin *et al.*, 2008; Bombarely *et al.*, 2012; Naim *et al.*, 2012). Based on the mutant lines generated in this work, transient complementation assays for analysis of *EDS1* and *SAG101b* (from tomato or *Nb*) based on co-expression with XopQ in respective mutant backgrounds (*Nb eds1* and *Nb pss*) were established. Combined with a structural model of the *S*/*EDS1*-*S*/*SAG101b* complex (Rapahel Guerois, CEA Paris), these assays allowed rapid analysis of the function of EDS1-based heterocomplexes.

In a first set of structure-guided mutations, several amino acid (aa) exchanges were introduced within the α H helix of *S*/*EDS1* and also a hydrophobic pocket of *S*/*SAG101b*, predicted to receive this α H helix for heterocomplex formation. As observed in *At*, these exchanges disrupted formation of EDS1 complexes with PAD4 and SAG101 isoforms and abolished EDS1-SAG101b immune signaling functions. These experiments provided proof that EDS1 complex formation by tomato orthologs relies on hydrophobic interactions involving the α H helix, and also validated the transient complementation assays, based on our structural model, for analysis of EDS1-SAG101b functions.

Furthermore we could show that the EP (EDS1-PAD4)-domain of *S*/*EDS1*, which represents the C-terminal region of the protein, also contributes to immunity: Perturbation of the C-terminal interaction interface between the heterocomplex partners by the substitution of phenylalanine of *S*/*EDS1* at position 435 to glutamate or aspartate leads to a loss-of-cell-death phenotype. The corresponding substitution of F435E in *At* (F419E) also led to a LOF of *At*EDS1, stably transformed into an *eds1* mutant *At* line (Lapin *et al.*, 2019). At the same time, these exchanges did not interfere with heterocomplex formation in general. This supports the idea that heterocomplex formation is mainly driven by the N-terminal lipase-like domain, but the N-terminal domain assembly is not sufficient for defense signaling (Wagner *et al.*, 2013; Bhandari *et al.*, 2019; Gantner *et al.*, 2019), and also points towards essential functions of the C-terminal EP domain assemblies.

Further evidence for this hypothesis is provided by the construction of chimeras of *S*/*SAG101* isoforms. Chimeric proteins were constructed consisting of the N-terminal part of *S*/*SAG101a* fused to the C-terminal part of *S*/*SAG101b* or *vice versa*. Only the latter chimeric protein was able to mediate immune signaling, albeit to lesser extent than wild type SAG101b. This suggests that the main differences between *S*/*SAG101a* and *S*/*SAG101b* might reside in the C-terminal EP domain and that this domain contributes to immunity.

The EP domain is not present outside plants and does not have strong similarity to other proteins outside the EDS1-family members (Wagner *et al.*, 2013), which makes it attractive for further analysis. Interestingly, two residues (K494 and R509 of *S/EDS1*) lining a presumed cavity on the heterodimer surface of the EP domain were recently reported as required for immune signaling in *At* (K478 and R493) (Bhandari *et al.*, 2018). However, the tomato EDS1 protein carrying substitutions at these conserved positions was able to fully restore HR induction when transiently co-expressed with XopQ in *Nb eds1* tissues. One hypothesis is that these two positively charged aa (R494 and R509 in *Nb*) are not as important as in *At*. Alternatively, overexpression of *S/EDS1* might mask a minor reduction of function in *Nb*. The EDS1 proteins of *Sl* and *At* have only ~ 40 % aa similarity. Accordingly, differences in function between *AtEDS1* and *S/EDS1* are not unexpected. To that end, EDS1 orthologs engage in an immune-active heterocomplex with PAD4 or SAG101 in *Brassicaceae* and only with SAG101b in *Solanaceae*, and also appear to require different helper-NLRs for downstream signaling (Wu *et al.*, 2019).

Additional to the C-terminal F435 residue, F64, which is located in the N-terminal lipase domain, was identified as critical for immune signaling in *Nb*, without interference with complex formation. This points towards a situation in which both N- and C-terminal assemblies of EDS1-PAD4/SAG101 complexes contribute to immune signaling. It should be noted that F435 and F64 variants are the first clear non-functional mutant EDS1 alleles identified so far, despite those interfering with complex formation or protein stability. These might provide hints on docking sites of potential interactors or structural re-arrangements during activation in future analyses. Finally, the *Nb* transient complementation system allows convenient screening of novel mutant EDS1 and/or SAG101b variants (see also later sections), and will most likely be instrumental as a workhorse for elucidation of EDS1 immune functions (Gantner *et al.*, 2019).

4.5. Integration of EDS1 in immunity and hormonal networks – a central regulator of immunity and development?

Besides its essential role in TNL-mediated defense signaling, *AtEDS1* was reported to be involved in various cellular processes within the plant cell, many of which are directly or indirectly associated with biotic stress. To that end, *AtEDS1* contributes to basal immunity, the ill-defined residual resistance of plant lines to virulent pathogen isolates (Wiermer *et al.*, 2005), and to resistance mediated by CNL-type NLRs (Venugopal *et al.*, 2009; Cui *et al.*, 2016). Furthermore, *AtEDS1* is able to bolster SA production (Cui *et al.*, 2016), and may be protected by interaction with PBS3 to prevent interaction with NPR3/4, which may target

AtEDS1 for degradation (Chang *et al.*, 2019). *AtEDS1* was reported to also interact with MYC2, thereby inhibiting MYC2 transactivation activity and shifting the JA-SA balance in favor of SA (JA = antagonist of SA in *At*) (Cui *et al.*, 2018). In the context of SA production and signaling, EDS1 was reported to bind to and activate expression of *ICS1* at the chromatin (Li *et al.*, 2019), and also to interact with EDR1, a kinase with homology to mitogen-activated protein kinase kinase kinase (Neubauer *et al.*, 2019). Moreover, EDS1 was reported to interact with the DELLA protein RGL3 to fine-tune growth versus defense regulation (Li *et al.*, 2019), and to inactivate DNA repair mechanisms resulting in accumulation of DNA double strand breaks and apoptosis (Rodriguez *et al.*, 2018). Thus, EDS1 is proposed to physically interact with key regulators of three major phytohormone pathways and many additional cellular components. But how a single protein should accomplish these multiple functions remains unexplained, thus shedding some doubt on reported results which will be subsequently discussed in more detail.

EDS1 heterocomplexes inactivate components involved in DDR (DNA damage response) pathways such as *AtRAD51*, which coincidentally enhances DNA damage accumulation in case of TNL-activation (Rodriguez *et al.*, 2018). However, the increase in damaged DNA might be due to the production of ROS, which occurs during active HR, and not directly induced *via* EDS1. This is supported by the observation that an accumulation of SA does not trigger DNA damage, which is more likely a consequence of cell death induction (Rodriguez *et al.*, 2018).

Plants possess limited resources which are normally spent during development, i.e. for growth and biomass production. If a plant, for example, is attacked by a pathogen, defense programs are induced to protect the integrity of the plant. In such case, the plant redirects resources from growth to defense *via* the “growth-to-defense” switch (Huot *et al.*, 2014). Interestingly, the growth-to-defense switch is reversible and probably dependent on EDS1. It is well known that the induction of ETI suppresses pathogen growth and is frequently uncoupled from HR. Cell death induction is rather described as a quantitative overshoot of activated defense in case of late initiation of ETI in the infection cycle (Bendahmane *et al.*, 1999; Cui *et al.*, 2015). Recently published data show a direct interaction between the DELLA (proteins, which possess a domain with the five AS DELLA) protein RGL3 (Repressor of *ga1-3-Like 3*) and EDS1, which is increased after infection, probably resulting from a pathogen-mediated DELLA accumulation (Li *et al.*, 2019). This interaction can be interpreted as a feedback regulation between disease resistance and growth, because EDS1-DELLA interaction inhibits excess accumulation of SA. This was further supported by monitoring expression of the direct target gene of EDS1, *ICS1*, which is significantly reduced between 12-48 hpi in the WT but not *rgl3* deficient *At* (Li *et al.*, 2019). Research over the last decades

showed that EDS1 is essential for most if not all ETI reactions mediated by TNL-type immune receptors. EDS1 seems to be a global switch to control the power of a defense reaction involved in many pathways to judge between the reversible growth and defense or the irreversible decision to induce an HR, and therein, cell death. It would be interesting to see if the EDS1-SAG101b heterocomplex is essential for the interaction with RGL3, and thereby for the excess inhibition of SA in *Solanaceae*.

EDS1 was also described to contribute to basal resistance and some CNL-mediated responses (Wiermer *et al.*, 2005; Cui *et al.*, 2016). It is known that *Pst* DC3000 grows significantly better on the *At eds1* mutant (Wiermer *et al.*, 2005). Furthermore, *At* Col-0 recognizes *Pst* bacteria expressing AvrRpt2 via the CNL RPS2, but this recognition is impaired in plants lacking EDS1 and SA (Bent *et al.*, 1994; Venugopal *et al.*, 2009; Cui *et al.*, 2016). However, basal or CNL-mediated defense responses are not strictly dependent on EDS1. A distinct threshold of general defense responses could be required in order to induce a reaction, and this is not achieved when both SA synthesis and EDS1 are lost. This would be in line with the observation that EDS1 and SA mostly work in parallel but could be induced independently (Cui *et al.*, 2016).

The hypothesis that EDS1 and PAD4 are needed for basal plant immunity is supported by the fact that plant which lack TNLs (e.g. monocots, Lamiales (Collier *et al.*, 2011)) still possess EDS1 and PAD4. It is proposed that the proteins are co-opted for TNL-mediated immunity in eudicots. An example for EDS1-functionality in monocots was reported from overexpression of EDS1 in wheat, which leads to an increased resistance to powdery mildew (Chen *et al.*, 2018). However, EDS1 is largely unexplored in monocots, as most research was performed in *At*.

Interestingly, our work showed that there is no impairment in basal resistance observed in the *Nb eds1* mutant, indicating that EDS1 might not be involved in resistance outside the TNL-mediated immunity in this species. Further studies are needed to clarify the function of EDS1-PAD4 in different plant species and taking into account TNL immune signaling and “basal” immune responses. Our observation that *Nb*SAG101a might not have any functionality, and solely the EDS1-SAG101b heterocomplex is needed in *Solanaceae* for TNL-mediated resistance and is not important to basal immunity, is further supported by the absence of *SAG101a* in pepper, suggesting lower importance of this *SAG101* isoform. The functions of EDS1-based heterocomplexes or even of solely EDS1 might not be equal in all plants. A function in immunity outside the TNL-mediated pathway in *Nb* was not observed in this thesis. Nevertheless, in wheat or *At*, a function is proposed (Wiermer *et al.*, 2005; Venugopal *et al.*, 2009; Cui *et al.*, 2016; Chen *et al.*, 2018), and a conservation of EDS1 and

PAD4 in monocots which lack TNLs in general is a clear hint that there is a requirement of these proteins in most land plants.

Our publication (part 3.5.1) reports that *S*/EDS1 is able to build heterocomplexes with the EDS1-family proteins *S*/PAD4 and *S*/SAG101a, but these do not measurably contribute to TNL-dependent immune pathways. The conservation of PAD4, hints to an important function. Possibly, PAD and SAG101a act as a regulatory mechanism by competing with SAG101b for the EDS1 scaffold to fine-tune defense reactions. Insufficient amounts of EDS1-SAG101b might prevent induction of a defense reaction if a certain threshold is not reached. It is known that a cell death induction is the last resort in the defense mechanism (Locato&De Gara, 2018). First, the plant cell tries to stop the colonialization of an invader by changing the plant program from growth to defense which is mostly controlled by gibberellin acid (GA) and SA (Cui *et al.*, 2015; Cui *et al.*, 2016; Li *et al.*, 2019). It could be that EDS1 is only activated if the cell could not counteract the pathogen attack, thus triggering a necrosis/apoptosis reaction. This would explain the amplified expression at a later time point, 40 times 12 hours post infection (Gantner *et al.*, 2019), which might provide excess of the EDS1 binding scaffold to allow efficient formation of immune-competent EDS1-SAG101b complexes.

4.6. Activation of EDS1 in plant immune signaling most likely relies on conserved mechanisms, possibly a small molecule messenger

TNLs are mostly transferrable between far distant plant species. *E.g.*, we transferred Roq1 from *Nb* to *At* accession Col-0, which mediated resistance to usually highly pathogenic *Pst* DC3000 bacteria (Gantner *et al.*, 2019). There are many examples in which (TNL or CNL-coding) *R* genes were transferred between sexually incompatible species and maintained functionality (Wulff *et al.*, 2011), which suggests a conserved and universal mechanism.

Recent reports suggest that plant TIR domains, similar to animal TIR domains, possess enzymatic activity. It could be shown that the mammalian TIR domain-containing protein SARM1 depletes NAD⁺ (Nicotinamide adenine dinucleotide) (Essuman *et al.*, 2017), a phenomenon that was subsequently also observed for plant TNLs if the TIR domains are expressed alone *in vitro* (Horsefield *et al.*, 2019; Wan *et al.*, 2019). The *in vitro* NAD⁺-depletion by the plant TIR domains was accompanied by the production of nicotinamide, ADPR (adenosine diphosphate ribose), and v-cADPR (a cyclization variant of ADPR) (Wan *et al.*, 2019). *In planta*, the delivery of the effector HopBA1 *via Pseudomonas fluorescens* possessing a T3SS induces cell death and accumulation of v-cADPR in *At*, which is

assumed to be a breakdown product of the NADase activity of the TIR-only R protein RBA1 (Response to the bacterial type III effector protein HopBA1). As a result, v-cADPR was proposed as a biomarker of enzymatic activity of TIR domains (Wan *et al.*, 2019).

It is known that cADPR triggers calcium influx into the cytoplasm, which is necessary for an oxidative burst response and HR induction (Wu *et al.*, 1997; Grant *et al.*, 2000). If the TIR-domain alone is able to influence the homeostasis of a cell, leading to an HR, EDS1 would in turn be dispensable for the TNL pathway. Thus, such mode of HR-induction cannot explain the strict requirement of EDS1 for TNL mediated defenses. It is possible that the alteration in the ion concentration is not sufficient to induce a defense reaction, and EDS1-based heterocomplexes are additionally required to induce a defense reaction. At this point, it seems plausible that one of the products of the TIR domain enzymatic activity could be an activation signal for EDS1-based heterocomplexes. This signal seems to be a universal metabolite as, *e.g.*, the R protein *NbRoq1*, when expressed in the far distant species *At*, induces a defense reaction, which is dependent on the endogenous EDS1-based heterocomplex.

The signaling process downstream of EDS1 activation might differ among species, which is supported by our finding that the essential heterocomplex partners of EDS1 are disparate between *Brassicaceae* and *Solanaceae*. Since the EDS1-based heterocomplexes were largely uncharacterized outside of *Brassicaceae* species, this led to the initial assumption that the EDS1-PAD4 heterocomplex is most important for TNL-dependent signaling. However, recent insights gathered from studies in *Solanaceae* give cause to reconsider this conclusion and suggests that the EDS1-SAG101b heterocomplex might be the major active heterocomplex essential for TNL-mediated defense signaling outside *Brassicaceae*. A possible evolutionary scenario could be postulated: *AtPAD4* possesses a deletion within the lipase like domain in comparison to PAD4 orthologs in other plant families and is therefore more similar to SAG101 (Wagner *et al.*, 2013). Possibly, *AtPAD4* is able to fulfill more tasks than the orthologs of other dicot plant species in TNL-mediated defense signaling and SAG101 takes a backseat and might only be responsible for cell death induction, not for a bacterial growth restriction, as postulated (Lapin *et al.*, 2019). Because of the critical sequence stretch in PAD4 outside *Brassicaceae*, SAG101 might be the only heterocomplex partner essential for defense signaling in the TNL-mediated defense pathway. In contrast to the nuclear-cytosolic localized active S/SAG101b and to PAD4 in general, *AtSAG101* is only located in the nucleus (Feys *et al.*, 2005) (as well as S/SAG101a) and might not be able to fulfill the same functions.

4.7. EDS1-dependent immunity depends on plant family-specific helper-NLRs of the RPW8-type – positioning of EDS1 in networks of helper and sensor NLRs

Besides the canonical CNL- and TNL-type immune receptors, plant genomes encode NLRs containing a distinct type of CC-domain in their N-termini, which was first recognized in the (non-NLR) protein RPW8, modulating resistance to powdery mildew infection (Collier *et al.*, 2011; Jubic *et al.*, 2019). This class of NLRs is regularly referred to as RNLs, and RNLs were recently discovered to function as downstream signaling partners (helper NLRs, hNLRs) for numerous different TNL or CNL sensor NLRs in an immune signaling network (Baggs *et al.*, 2017; Jubic *et al.*, 2019). Three different classes of RNL-type hNLRs were described: The ADR1 (Activated Disease Resistance 1) class, the NRG1 (N required gene 1) class and the *Solanaceae*-specific NRCs (NB-LRR protein required for HR-associated cell death) (Jubic *et al.*, 2019).

4.7.1. EDS1-based heterocomplexes might rely on different hNLRs, depend on the heterocomplex partner

Interestingly, there is a co-occurrence between *NRG1*, *SAG101*, and TIR-NB-LRR coding genes in dicots, whereas ADR1 orthologs appear to exist in genomes of all higher plants (Collier *et al.*, 2011; Wagner *et al.*, 2013; Shao *et al.*, 2016; Qi *et al.*, 2018). In Arabidopsis, it was shown that many TNL-mediated immune responses requiring *AtEDS1-AtPAD4* function *via* ADR1 helpers, but also some CNL-dependent responses require ADR1 helpers, and other TNLs rather signal *via* NRG1 (Bonardi *et al.*, 2011; Dong *et al.*, 2016; Castel *et al.*, 2019; Wu *et al.*, 2019). Furthermore, one of the rare *At* TNL-mediated immune responses described to require rather *AtEDS1-AtSAG101* than *AtEDS1-AtPAD4*, autoimmunity induced by the *chs3-2D* allele of *CHS3* (*Chilling sensitive 3*), was found to rely mainly on NRG1s (Wu *et al.*, 2019). This might imply that EDS1-PAD4-dependent TNLs function *via* ADR1, whereas EDS1-SAG101-dependent TNL responses rely on NRG1 (Wu *et al.*, 2019).

In this context, inactivation of *NRG1a* and *NRG1b* in an *At nrg1a nrg1b* mutant line leads to only partial loss of resistance against *Pst* and several oomycete isolates. However, a transient expression of the autoimmune TIR-NLR *AtCSA1* co-expressed with the gain-of function allele *chs3-2D* (conferring a CSA1-dependent autoimmune phenotype in *At* (Xu *et al.*, 2015)), as well as the TNL/TNL-like protein pair SOC3 (Suppressors of *chs1 3*) and CHS1, are only able to induce an HR in the presence of *NbNRG1* in *Nb* (Castel *et al.*, 2019; Wu *et al.*, 2019). These findings support that NRG1 might not be essential for most TNL

signaling pathways in *At*, but would indeed be crucial for TNL-mediated defense signaling in *Nb* as predicted (Qi *et al.*, 2018) and shown in Figure 13.

4.7.2. Different plant species, different positioning of hNLRs within TNL-mediated defense pathways?

There might be distinct differences in collaboration between the helpers ADR1/NRG1 and EDS1-based heterocomplexes in *Brassicaceae* and *Solanaceae* (Figure 13). In *At*, it is postulated that at least ADR1 functions upstream of *At*EDS1, as stunting mediated by an auto-active ADR1-variant is abolished in *At pad4* mutant plants (Wu *et al.*, 2019). In contrast, the co-expression of *Nb*EDS1 together with XopQ failed to recover an immune function in *Nb nrg1* mutant, which indicates that NRG1 probably acts downstream of EDS1 in *Solanaceae* (Qi *et al.*, 2018).

Interestingly, there is no hypothesis, how defense signaling after an activation of the EDS1-based heterocomplex takes place in *At*. A positioning of *At*ADR1 upstream of *At*EDS1-*At*PAD4 (Wu *et al.*, 2019) implies that *At*ADR1 is needed for the heterocomplex activation, and is not able to induce a defense reaction as *Nb*NRG1. If *At*ADR1 would form a resistosome as it is postulated and depicted in Figure 13 (Jubic *et al.*, 2019) for *Nb*NRG1 (but not yet shown), *At*ADR1 should be able to induce a defense reaction independent of *At*EDS1-*At*PAD4. Oligomerization of ADR1 or NRG1 could not be demonstrated in *At*, whereas it was shown for NRG1 in *Nb* (Qi *et al.*, 2018; Wu *et al.*, 2019). If CC-helper-NLRs form a resistosome like the CNL ZAR1 (Wang *et al.*, 2019a), they would have to form a pentamer and oligomerization should experimentally be detectable. If a resistosome is not formed by ADR1 or NRG1 in *At*, it could be postulated that another helper-NLR might fulfill this role. How helper and sensor NLRs work together, how their activity is regulated and the precise positioning of EDS1-based heterocomplexes within the TNL-mediated defense pathway is not known. Nevertheless, sensor-NLRs like Roq1 are able to function in far distant plant species and they function together with the plant specific EDS1-heterocomplex (EDS1-PAD4 in *At*, EDS1-SAG101b in *Nb*). This indicates an essential role of EDS1-based heterocomplexes to connect sensor and helper NLR-signals.

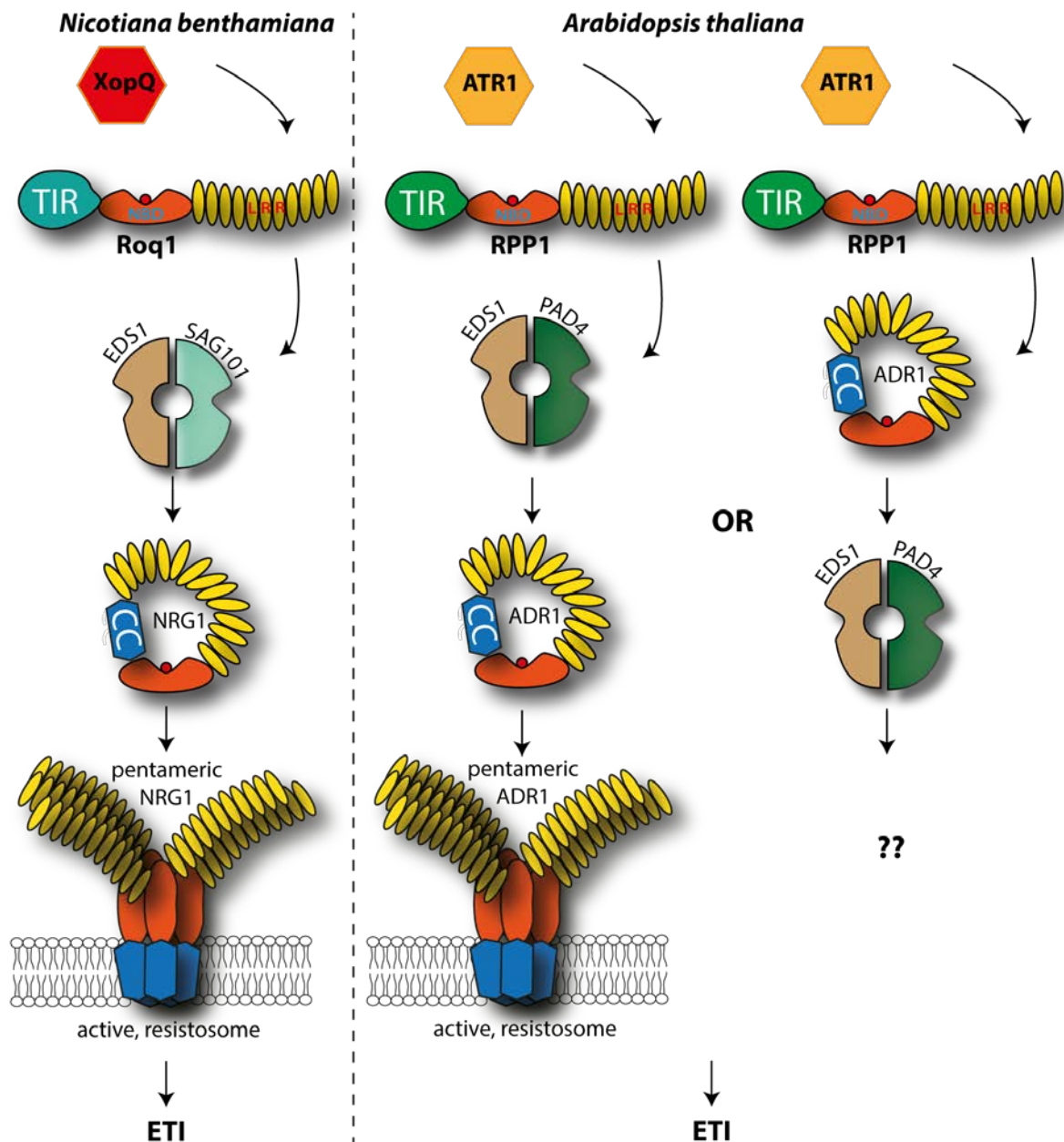


Figure 13: Model of TNL-mediated defense signaling in *Nb* versus *At*

A model of the proteins involved in the TNL signaling pathway of *Nb* (left) in comparison to *At* (right). Considering recently published data, it could be postulated for *Nb* that XopQ activates Roq1 by direct binding (Schultink *et al.*, 2017) which in turn activates with the EDS1-SAG101b heterocomplex. The active heterocomplex in turn activates the CC-helper NLR NRG1, which form a plasma membrane-associated pentamer, the so-called resistosome and thereby inducing an HR. The same model could be postulated for the signaling in *At*. As an example, the effector ATR1 (*At* recognized 1) is recognized by the TNL RPP1 (Recognition of *Peronospora parasitica* 1). In difference to *Nb*, the EDS1-PAD4 heterocomplex is mainly used, which recruits another helper-NLR, ADR1 instead of NRG1. Nevertheless, if the *At*EDS-*At*SAG101 heterocomplex is recruited, *At*NRG1 is needed for defense signaling (not shown) (Lapin *et al.*, 2019). Another model assumed that *At*ADR1 is needed for the activation of the EDS1-PAD4 heterocomplex, indicating the CC-helper NLR is located above the heterocomplex (Wu *et al.*, 2019). How signaling might progress below the EDS1-based heterocomplex activation is not known.

4.7.3. Localization and activation of hNLRs and EDS1-based heterocomplexes

The subcellular localization of the proteins involved in TNL-mediated defense responses might provide hints about their ability to interact with each other. Our localization studies

suggest that *S/SAG101b* is equally distributed between the cytosol and the nucleus (Gantner *et al.*, 2019). Additionally, it was reported that *NRG1* is not located in the nucleus (Wu *et al.*, 2019) and that *NbNRG1* can physically interact with *EDS1* in *Nb* (Qi *et al.*, 2018). In contrast, an interaction between *AtEDS1* and *AtNRG1* could not be shown (Wu *et al.*, 2019). The *AtEDS1-AtSAG101* heterocomplex localizes exclusively to the nucleus, and would therefore not reside in the same compartment as *AtNRG1* (Feys *et al.*, 2005; Wu *et al.*, 2019). However, it could be shown that *AtEDS1-AtSAG101* is able to mediate HR induction and resistance in a *Nb epss* mutant (*eds1a-1 pad4 sag101a-1 sag101b-1*) when transiently co-expressed with *AtNRG1*, but not in absence of the “fitting” Arabidopsis helper NLR (Gantner *et al.*, 2019; Lapin *et al.*, 2019). In such reconstitution assays, the heterocomplex *AtEDS1-AtSAG101* is not expected to reside in the same compartment as *AtNRG1*, arguing against direct physical interaction. It is therefore not known how the heterocomplex can activate *AtNRG1*. However, it could be speculated that a signal diffuses or gets shuttled to the cytosol from the activated *AtEDS1-AtSAG101* heterocomplex and thereby activates *AtNRG1*. The different localization of *AtEDS1-AtSAG101* and *NRG1* could explain why *AtNRG1* is needed for a reaction in *Nb*. *NbNRG1* might not need such a molecule, because *NbNRG1* is able to directly interact with the *EDS1*-based heterocomplex and induces a defense reaction (Qi *et al.*, 2018).

Interestingly, it could be shown that *NRG1* associates with the plasma membrane in *Nb*. The p-loop in *NbNRG1* is needed for this membrane association and coincidentally for its function (Jubic *et al.*, 2019). Contrary, this p-loop is dispensable in *AtADR1* or *AtNRG1* and a plasma membrane association could only be shown for *AtNRG1* (Qi *et al.*, 2018; Jubic *et al.*, 2019; Wu *et al.*, 2019). Once more, these findings indicate that there are distinct differences between the function of the helper NLRs (*At* versus *Nb*) and that *NbNRG1* could act as a resistosome. To test if the helper NLRs of the clade *ADR1* and *NRG1* act simultaneously or synergetic, a “helperless” *At* mutant was made but it could only be shown that *ADR1* and *NRG1* might have synergetic effects on basal defense compared to *adr1*, *nrg1* or wild-type *At* (Wu *et al.*, 2019). If such synergetic effects are present in ETI signaling is yet not known (Jubic *et al.*, 2019). Synergetic effects in *Nb* could be excluded as the p-loop in *NbNRG1* is required for *Roq1* dependent defense signaling and could, therefore, not be replaced by *NbADR1* (Qi *et al.*, 2018).

Along different lines, we have shown that tomato *EDS1* complexes are able to mediate immune signaling in *At*. Surprisingly, not expression of the *S/EDS1-S/SAG101b* but the *S/EDS1-S/PAD4* heterocomplex, which is not immune-competent in *Nb*, was able to complement for loss of the endogenous *EDS1* family proteins in *At eps* (*eds1 pad4 sag101*) mutant lines of accession Col-0 (Gantner *et al.*, 2019). Moreover, we showed that the R

protein *NbRoq1* is able to detect the pathogen *Pst* DC3000 in *At*. *Roq1* was stably transformed to *At*, which made the plants resistant against the highly virulent pathogen *Pst* DC3000 (Gantner *et al.*, 2019). Interestingly, *Roq1*-transformed *At* plants deficient in *pad4* and *eds1* were not able to counteract bacterial multiplication of *Pst* DC3000, respectively, but those deficient in *sag101* were as resistant as the wild type. This observation is a clear hint that R proteins may retain general functionality when transferred between families, but EDS1 recruits different heterocomplex partners after activation. PAD4 is required in *At* and SAG101b is generally required for defense reactions in *Nb*. It was shown *via* co-immunoprecipitation that *Roq1* directly interacts with XopQ/HopQ1 ((Hrp outer protein Q), the recognized R protein in *Pst* DC3000) (Schultink *et al.*, 2017). The postulated respective helper-NLR of this sensor NLR in Arabidopsis, ADR1 (Wu *et al.*, 2019), might be able to interact with the S/EDS1-S/PAD4 heterocomplex because they are located in the same compartments and an *At*-specific signal might not be needed, in comparison to the expression of *At*EDS1-*At*SAG101 in *Nb*. However, it is surprising to note that S/PAD4 which possesses the critical sequence stretch within the lipase-like domain lacking in *At*PAD4, does not interfere with the function of the protein, if expressed in *At*. This suggests that the deletion in *At*PAD4, hypothesized to render the protein more similar to SAG101, is not a prerequisite for PAD4 immune functions in *At*. Moreover, it could not be explained why S/SAG101b is incapable to induce a defense reaction together with S/EDS1 in *At*. It might be possible that the respective CC-helper NLR NRG1 is not able to interact with S/SAG101b and signaling is thus not possible, as it has been shown for *At*EDS1-*At*SAG101 which are only able to induce a defense reaction in *Nb* if the helper *At*NRG1 is co-expressed (Lapin *et al.*, 2019). Prospectively, an interaction study between S/EDS1-S/PAD4 and the CC-helper NLR *At*ADR1 or *At*NRG1 could be of interest to see which of these helpers is needed to induce the defense reaction in *At*. Another possibility to validate which CC-helper might be needed is the construction of *At nrg1* or *adr1* mutant plants in the *eps* background, which could be transformed with S/EDS1 and S/PAD4. Moreover, it might be interesting to test whether S/EDS1-S/SAG101b could gain functionality in immunity in *At* upon co-expression with S/NRG1. Summarizing, there are significant differences between the signaling cascades of TNL-mediated immunity in *Brassicaceae* and *Solanaceae* which demand further analysis.

4.7.4. Occurrence of CNL versus TNLs – detecting pathogens in the most efficient way

This study uncovered distinct differences in TNL-mediated effector recognition between *Brassicaceae* and *Solanaceae*. Interestingly, the number of TNLs varies drastically between plant species. While *At* possess between 70 -100 TNL coding genes per genome, in *Nb* only 17 TIR-domain containing NLR genes have been identified (Meyers *et al.*, 2003; Hofberger *et*

al., 2014; Peele *et al.*, 2014; Van de Weyer *et al.*, 2019). In contrast to *At*, CNLs might have a prevalent role in *Nb*. It could be postulated that TNL-mediated defense evolved in another way in *At*, because the TNLs act in the more important ETI-signaling cascade, as most of the NLRs are TNLs in *At*. The characterization of the *AtZAR1* resistosome might explain a major role of CNLs in higher plants. If all CNLs build up a funnel-shaped pentameric structure, which associates directly with the plasma membrane to act as an ion channel (Wang *et al.*, 2019a; Wang *et al.*, 2019b), some intermediate steps are not present in this pathway in comparison to TNLs. The absence of intermediate steps, such as helper NLRs, could make CNL pathways faster in response to an attack and not as susceptible to interruption of the signaling cascade in comparison to the TNL-mediated pathway. Each protein involved in such a pathway creates another potential target for a pathogen effector to inhibit the defense reaction by binding to proteins of the signaling cascade. On the other hand, a fine-tuning of pathways is important to regulate the induction of HR as late as possible. Such checkpoints are very important, and are found in almost every signaling cascade to prevent uncontrolled cell proliferation or unnecessary immune reactions. Furthermore, an increase in the proteins involved in a pathway introduces the possibility of feedback-loops to amplify a reaction if required.

4.8. An updated model for EDS1 functions in immune signaling

Considering our and other recently published data, which explore proteins involved in the TNL-mediated defense pathway, finally a new model can be postulated (Figure 14). If an effector is recognized (directly or indirectly) by a TNL, the latter is activated, and switches from a self-associated, closed, and ADP-bound to an open, ATP-bound conformation. This leads to homodimerization of at least the TIR-domains of the activated TNL, thus inducing NADase activity. Following activation, it is possible that a breakdown product of this enzymatic activity could bind to the immune-competent EDS1-based heterocomplex.

Recent experiments (J. Gantner, J. Zönnchen) suggest that a disruption of the SDH catalytic triad within the EDS1 alpha/beta hydrolase (ABH) domain of *S/EDS1* and *NbEDS1* abolishes

immune

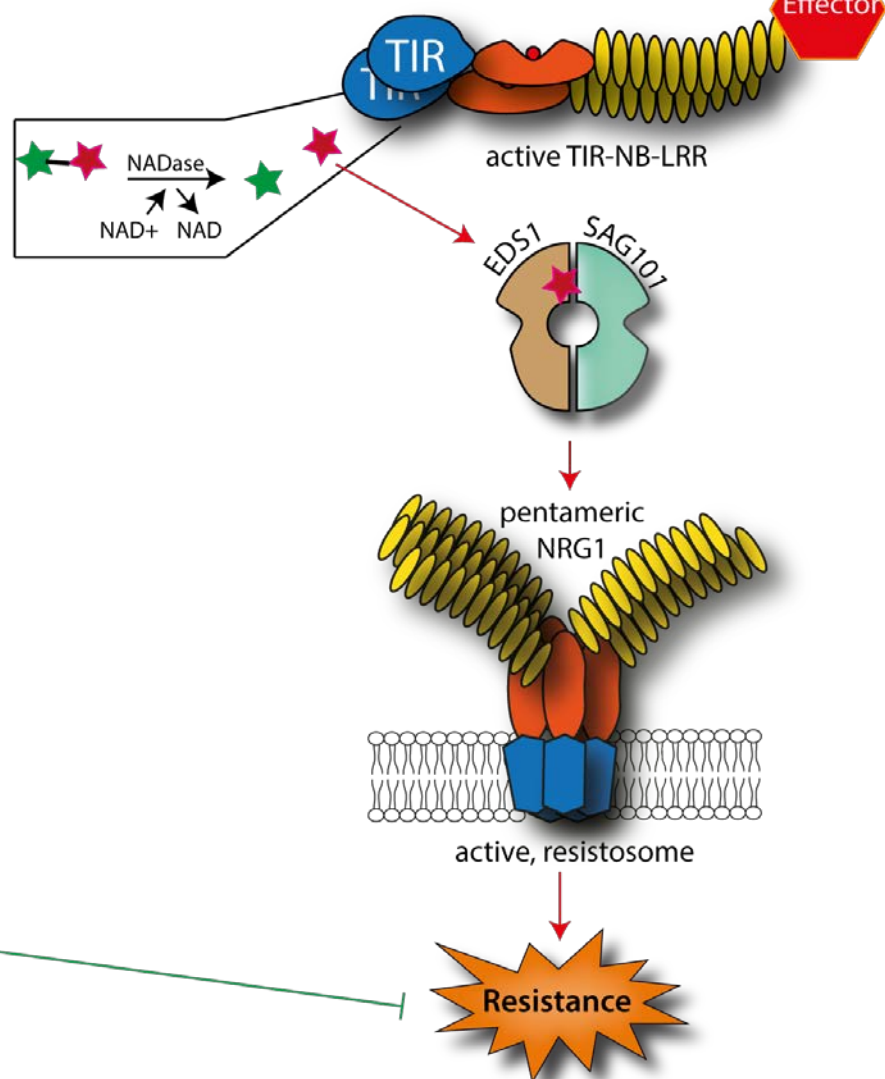
functions.

steady-state

TIR-NB-LRR



inactive

recognition of an effector**Figure 14: Model of effector activated TNL-signaling in *Solanaceae***

In the steady state TNLs are self-associated, inactive, and therefore incompetent to activate the EDS1-SAG101b heterocomplex. The CC-helper NLR NRG1 is inactive. After perception of an effector (in this model a direct perception by the LRR domain) TNLs dimerize and thereby activate a NADase. One yet uncharacterized breakdown product of this NADase deals as an activator of the EDS1-SAG101b heterocomplex. In consequence to this activation, the CC-helper NLR NRG1 is activated and might build a pentameric, plasma membrane-associated dimer, which might form a pore and deals as ion channel. This channels are able to change the homeostasis of the cell and thus activating defense mechanisms.

Interestingly, an exchange of only the serine within the SDH motif (to alanine) of S/EDS1 does not compromise immune functions. The serine residue is critical for an assumed hydrolase activity. Thus, conversion of a substrate, potentially a breakdown product of the TIR domain NADase activity, is most likely not critical for immune functions. Indeed, most severe impairment of immune functions was provoked by exchange of the aspartate residue within the SDH motif, which may be essential for binding of a respective metabolite.

Combinatorial mutations within the SD and SDH positions within S ϵ EDS1 fully abolished immune functions, and none of the variants appeared to be impaired in protein stability or interaction with SAG101b, as tested by co-IP assays (data not shown; preliminary).

Accordingly, it could be postulated that the binding of a metabolite (breakdown product of the NADase) might lead to activation of EDS1-based heterocomplexes. This is in line with several reported examples of ABH-like proteins that function as *bona fide* ligand receptors, as for example GID1 (Gibberellin insensitive dwarf 1) in the gibberellic acid (GA) response pathway (Shimada *et al.*, 2008). Similar to the function of EDS1 proposed here, GID1 is a receptor for GA, but does not appear to possess catalytic activity and is regulated solely by binding of the small molecule to the receptor (Ueguchi-Tanaka *et al.*, 2005). Upon GA binding, the N-terminal domain of GID1 changes its conformation from a flexible to a well-organized state, covering over the GA-molecule and thereby building a recognition site for DELLA proteins, a subfamily of the GRAS family of putative plant transcriptional repressors (Peng *et al.*, 1997). Upon binding, an E3-ligase is recruited which polyubiquitinylates DELLAs, thereby targeting them for degradation by the 26S proteasome, leading to expression of GA-controlled genes (Mindrebo *et al.*, 2016). This example highlights the ability of ABH-like proteins which do not require catalytic activity but serve as activation switches to enable a protein to interact with a complex partner.

A breakdown product of the NADase of the TIR-domain might interact with the SDH-triad and activate the EDS1-based heterocomplex. This activation step is a universal mechanism which seems to be equal in all plants, indicating that the produced metabolite of the NADase has to be identical. This is provided by the observation that it is possible to transfer R proteins between different species, which are able to induce a defense reaction by using the endogenous EDS1-based heterocomplex. Next, the active EDS1-based heterocomplex might induce a conformational change, thereby leading to activation of the CC-helper NRG1 (in *Nb*), which itself oligomerizes, potentially to form the pentameric resistosome. The pentamer builds a pore-like structure, which is recruited to the plasma membrane and acts as an ion channel, as described for the CNL *At*ZAR1 (Adachi *et al.*, 2019; Wang *et al.*, 2019a). The steps upon activation of the EDS1-based heterocomplex are probably not equal in all plants and only described here for *Nb*, as our preliminary experiments were made in this species and are not in line with recently published data of *At*, e.g., positioning of the respective CC-helper NLR of the *At*EDS1-*At*PAD4 heterocomplex, ADR1 in the TNL-signaling pathway (Wu *et al.*, 2019).

It is well known that the plasma membrane depolarizes after activation of ETI, indicated by higher concentrations of cytosolic calcium ions, which activate calcium-dependent protein kinases, mitogen-activated protein kinases, reactive oxygen species, phytohormone

signaling and transcriptional reprogramming (Meng&Zhang, 2013; Peng *et al.*, 2018; Adachi&Tsuda, 2019; Jubic *et al.*, 2019). One could speculate that the helper CC-NLR NRG1 builds a pentameric oligomer similar to that formed to the *AtZAR1* resistosome, and acts as a calcium channel, needed for depolarization of the plasma membrane after effector recognition as indicated in Figure 14.

Another scenario could be that a breakdown product of the enzymatic activity of the TIR-domain binds the ABH-like triad of the EDS1-SAG101b heterocomplex, which then recruits e.g. transcriptional regulators (similar to the F-Box protein TIR1 in auxin signaling) to target them for ubiquitination and subsequent degradation by the 26S proteasome. Such a transcriptional regulator could be for example a WRKY protein as described for the regulation of transcript levels of NPR1 (Mukhtar *et al.*, 2009). The Y3H-study of this thesis identified an F-Box and a WRKY-transcription factor as potential interactors of the *S*EDS1-*S*SAG101b heterocomplex, which should be noted for further interaction studies as intriguing candidates.

To verify if a breakdown product of the enzymatic active TIR domain acts as an activator of the EDS1-heterocomplex, the metabolite will need to be identified. Alternatively, undirected binding studies using *S*EDS1 as bait could be used to identify a small molecule ligand. Small molecule libraries could be probed with the purified *S*EDS1-*S*SAG101b heterocomplex versus the inactive *S*EDS1-variant (carrying mutations within the SDH triad). Alternatively, co-purification of a ligand together with the *S*EDS1-*S*SAG101b heterocomplex from plant extracts could be attempted, followed by identification of a potential ligand *via* mass spectrometry. Although extremely challenging, these will be exciting experiments to challenge this novel model for EDS1 functions as a small molecule receptor in TNL-mediated immunity.

References

- Aarts, N, Metz, M, Holub, E, Staskawicz, BJ, Daniels, MJ, and Parker, JE. (1998). Different requirements for *EDS1* and *NDR1* by disease resistance genes define at least two *R* gene-mediated signaling pathways in *Arabidopsis*. *Proc Natl Acad Sci U S A* **95**, 10306-10311.
- Adachi, H, Kamoun, S, and Maqbool, A. (2019). A resistosome-activated 'death switch'. *Nature Plants* **5**, 457.
- Adachi, H, and Tsuda, K. (2019). Convergence of cell-surface and intracellular immune receptor signalling. *New Phytologist* **221**, 1676-1678.
- Adamian, L, Naveed, H, and Liang, J. (2011). Lipid-binding surfaces of membrane proteins: evidence from evolutionary and structural analysis. *Biochim Biophys Acta* **1808**, 1092-1102.
- Adlung, N, Prochaska, H, Thieme, S, Banik, A, Bluher, D, John, P, Nagel, O, Schulze, S, Gantner, J, Delker, C, Stuttmann, J, and Bonas, U. (2016). Non-host resistance induced by the *Xanthomonas* effector XopQ is widespread within the genus *Nicotiana* and functionally depends on EDS1. *Front Plant Sci* **7**, 1796.
- Ameline-Torregrosa, C, Wang, B-B, O'Bleness, MS, Deshpande, S, Zhu, H, Roe, B, Young, ND, and Cannon, SB. (2008). Identification and characterization of nucleotide-binding site-leucine-rich repeat genes in the model plant *Medicago truncatula*. *Plant Physiol* **146**, 5-21.
- Ausubel, FM. (2005). Are innate immune signaling pathways in plants and animals conserved? *Nat Immunol* **6**, 973-979.
- Baggs, E, Dagdas, G, and Krasileva, KV (2017). NLR diversity, helpers and integrated domains: making sense of the NLR IDentity. *Curr Opin Plant Biol* **38**, 59-67.
- Bai, J, Pennill, LA, Ning, J, Lee, SW, Ramalingam, J, Webb, CA, Zhao, B, Sun, Q, Nelson, JC, Leach, E, and Hulbert, H. (2002). Diversity in nucleotide binding site-leucine-rich repeat genes in cereals *Genome Res* **12**, 1871-1884.
- Bajar, B, Wang, E, Zhang, S, Lin, M, and Chu, J. (2016). A guide to fluorescent protein FRET pairs. *Sensors*, MDPI **16**, 1488.
- Barrangou, R, and Marraffini, LAJMc. (2014). CRISPR-Cas systems: prokaryotes upgrade to adaptive immunity. *Mol Cell* **54**, 234-244.
- Bendahmane, A, Farnham, G, Moffett, P, and Baulcombe, DC. (2002). Constitutive gain-of-function mutants in a nucleotide binding site – leucine rich repeat protein encoded at the Rx locus of potato. *The Plant Journal* **32**, 195-204.
- Bendahmane, A, Kanyuka, K, and Baulcombe, DC. (1999). The Rx gene from potato controls separate virus resistance and cell death responses. *Plant Cell* **11**, 781-791.
- Bent, AF, Kunkel, BN, Dahlbeck, D, Brown, KL, Schmidt, R, Giraudat, J, Leung, J, and Staskawicz, BJ. (1994). *RPS2* of *Arabidopsis thaliana*: A leucine-rich repeat class of plant disease resistance genes. *Science* **265**, 1856-1860.
- Bentham, A, Burdett, H, Anderson, PA, Williams, SJ, and Kobe, B. (2016). Animal NLRs provide structural insights into plant NLR function. *Annals of Botany* **119**, 827-702.
- Bernacki, MJ, Czarnocka, W, Szechyńska-Hebda, M, Mittler, R, and Karpiński, S. (2019). Biotechnological Potential of LSD1, EDS1, and PAD4 in the Improvement of Crops and Industrial Plants. *Plants*, MDPI **8**, 290.
- Bernoux, M, Burdett, H, Williams, SJ, Zhang, X, Chen, C, Newell, K, Lawrence, GJ, Kobe, B, Ellis, JG, and Anderson, PA. (2016). Comparative analysis of the flax immune receptors L6 and L7 suggests an equilibrium-based switch activation model. *Plant Cell* **28**, 146-159.
- Bernoux, M, Ve, T, Williams, S, Warren, C, Hatters, D, Valkov, E, Zhang, X, Ellis, JG, Kobe, B, and Dodds, PN. (2011). Structural and functional analysis of a plant resistance protein TIR domain reveals interfaces for self-association, signaling, and autoregulation. *Cell Host Microbe* **9**, 200-211.
- Bhandari, DD, Lapin, D, Kracher, B, Bautor, J, Niefind, K, and Parker, JE. (2018). An EDS1 EP-domain surface mediating timely transcriptional reprogramming of immunity genes. *bioRxiv*, 362921.

- Bhandari, DD, Lapin, D, Kracher, B, von Born, P, Bautor, J, Niefind, K, and Parker, JE.** (2019). An EDS1 heterodimer signalling surface enforces timely reprogramming of immunity genes in *Arabidopsis*. *Nature communications* **10**, 772.
- Bhat, RA, Lahaye, T, and Panstruga, R.** (2006). The visible touch: *in planta* visualization of protein-protein interactions by fluorophore-based methods. *Plant Methods* **2**, 12.
- Bhattacharjee, S, Halane, MK, Kim, SH, and Gassmann, W.** (2011). Pathogen effectors target *Arabidopsis* EDS1 and alter its interactions with immune regulators. *Science* **334**, 1405-1408.
- Bigeard, J, Colcombet, J, and Hirt, H.** (2015). Signaling mechanisms in pattern-triggered immunity (PTI). *Molecular plant* **8**, 521-539.
- Boller, T, and Felix, G.** (2009). A renaissance of elicitors: perception of microbe-associated molecular patterns and danger signals by pattern-recognition receptors. *Annu Rev Plant Biol* **60**, 379-406.
- Bolotin, A, Quinquis, B, Sorokin, A, and Ehrlich, SD.** (2005). Clustered regularly interspaced short palindrome repeats (CRISPRs) have spacers of extrachromosomal origin. *Microbiology* **151**, 2551-2561.
- Bombarely, A, Rosli, HG, Vrebalov, J, Moffett, P, Mueller, LA, and Martin, GB.** (2012). A draft genome sequence of *Nicotiana benthamiana* to enhance molecular plant-microbe biology research. *Mol Plant Microbe Interact* **25**, 1523-1530.
- Bonardi, V, Tang, S, Stallmann, A, Roberts, M, Cherkis, K, and Dangl, JL.** (2011). Expanded functions for a family of plant intracellular immune receptors beyond specific recognition of pathogen effectors. *Proc Natl Acad Sci U S A* **108**, 16463-16468.
- Bortesi, L, and Fischer, R.** (2015). The CRISPR/Cas9 system for plant genome editing and beyond. *Biotechnol Adv* **33**, 41-52.
- Brikos, C, and O'Neill, LA.** (2008). Signalling of toll-like receptors. In *Toll-like receptors (TLRs) and innate immunity* (Springer), pp. 21-50.
- Burch-Smith, TM, Schiff, M, Caplan, JL, Tsao, J, Czymmek, K, and Dinesh-Kumar, SP.** (2007). A novel role for the TIR domain in association with pathogen-derived elicitors. *PLoS Biol* **5**, e68.
- Büttner, D.** (2016). Behind the lines-actions of bacterial type III effector proteins in plant cells. *FEMS Microbiol Rev*.
- Cai, X, Chen, J, Xu, H, Liu, S, Jiang, Q-X, Halfmann, R, and Chen, ZJ.** (2014). Prion-like polymerization underlies signal transduction in antiviral immune defense and inflammasome activation. *Cell* **156**, 1207-1222.
- Casini, A, Storch, M, Baldwin, GS, and Ellis, T.** (2015). Bricks and blueprints: methods and standards for DNA assembly. *Nat Rev Mol Cell Biol* **16**, 568-576.
- Castel, B, Ngou, PM, Cevik, V, Redkar, A, Kim, DS, Yang, Y, Ding, P, and Jones, JD.** (2019). Diverse NLR immune receptors activate defence *via* the RPW 8-NLR NRG1. *New Phytologist* **222**, 966-980.
- Cesari, S, Bernoux, M, Moncuquet, P, Kroj, T, and Dodds, PN.** (2014). A novel conserved mechanism for plant NLR protein pairs: the "integrated decoy" hypothesis. *Front Plant Sci* **5**, 606.
- Cesari, S.** (2018). Multiple strategies for pathogen perception by plant immune receptors. *New Phytol* **219**, 17-24.
- Chan, SL, Mukasa, T, Santelli, E, Low, LY, and Pascual, J.** (2010). The crystal structure of a TIR domain from *Arabidopsis thaliana* reveals a conserved helical region unique to plants. *Protein Science* **19**, 155-161.
- Chang, M, Zhao, J, Chen, H, Li, G, Chen, J, Li, M, Palmer, IA, Song, J, Alfano, JR, and Liu, F.** (2019). PBS3 protects EDS1 from proteasome-mediated degradation in plant immunity. *Molecular plant* **12**, 678-688.
- Chen, G, Wei, B, Li, G, Gong, C, Fan, R, and Zhang, X.** (2018). *TaEDS1* genes positively regulate resistance to powdery mildew in wheat. *Plant Mol Biol* **96**, 607-625.
- Chen, W-H, Qin, Z-J, Wang, J, and Zhao, G-P.** (2013). The MASTER (methylation-assisted tailorable ends rational) ligation method for seamless DNA assembly. *Nucleic Acids Res* **41**, e93-e93.

- Chinchilla, D, Zipfel, C, Robatzek, S, Kemmerling, B, Nurnberger, T, Jones, JD, Felix, G, and Boller, T.** (2007). A flagellin-induced complex of the receptor FLS2 and BAK1 initiates plant defence. *Nature* **448**, 497-500.
- Cho, SW, Kim, S, Kim, JM, and Kim, J-S.** (2013). Targeted genome engineering in human cells with the Cas9 RNA-guided endonuclease. *Nat Biotechnol* **31**, 230.
- Collier, SM, Hamel, LP, and Moffett, P.** (2011). Cell death mediated by the N-terminal domains of a unique and highly conserved class of NB-LRR protein. *Mol Plant Microbe Interact* **24**, 918-931.
- Cong, L, Ran, FA, Cox, D, Lin, S, Barretto, R, Habib, N, Hsu, PD, Wu, X, Jiang, W, Marraffini, LA, and Zhang, F.** (2013). Multiplex genome engineering using CRISPR/Cas systems. *Science* **339**, 819-823.
- Creagh, EM, and O'Neill, LA.** (2006). TLRs, NLRs and RLRs: a trinity of pathogen sensors that cooperate in innate immunity. *Trends in immunology* **27**, 352-357.
- Cui, H, Gobbato, E, Kracher, B, Qiu, J, Bautor, J, and Parker, JE.** (2016). A core function of EDS1 with PAD4 is to protect the salicylic acid defense sector in Arabidopsis immunity. *New Phytol.*
- Cui, H, Qiu, J, Zhou, Y, Bhandari, DD, Zhao, C, Bautor, J, and Parker, JE.** (2018). Antagonism of transcription factor MYC2 by EDS1/PAD4 complexes bolsters salicylic acid defense in Arabidopsis effector-triggered immunity. *Molecular plant* **11**, 1053-1066.
- Cui, H, Tsuda, K, and Parker, JE.** (2015). Effector-triggered immunity: from pathogen perception to robust defense. *Annu Rev Plant Biol* **66**, 487-511.
- Dangl, JL, Horvath, DM, and Staskawicz, BJ.** (2013). Pivoting the plant immune system from dissection to deployment. *Science* **341**, 746-751.
- Dangl, JL, and Jones, JDG.** (2001). Plant pathogens and integrated defence responses to infection. *Nature* **411**, 826-833.
- Derevnina, L, Kamoun, S, and Wu, Ch.** (2019). Dude, where is my mutant? *Nicotiana benthamiana* meets forward genetics. *New Phytologist* **221**, 607-610.
- Deslandes, L, Olivier, J, Peeters, N, Feng, DX, Khounlotham, M, Boucher, C, Somssich, L, Genin, S, and Marco, Y.** (2003). Physical interaction between RRS1-R, a protein conferring resistance to bacterial wilt, and PopP2, a type III effector targeted to the plant nucleus. *Proc Natl Acad Sci U S A* **100**, 8024-8029.
- Dinesh-Kumar, S, Tham, W-H, and Baker, BJ.** (2000). Structure–function analysis of the *tobacco mosaic virus resistance* gene N. *Proc Natl Acad Sci U S A* **97**, 14789-14794.
- Dodds, PN, Lawrence, GJ, Catanzariti, A-M, Ayliffe, MA, and Ellis, JG.** (2004). The *Melampsora lini AvrL567* avirulence genes are expressed in haustoria and their products are recognized inside plant cells. *Plant Cell* **16**, 755-768.
- Dodds, PN, Lawrence, GJ, Catanzariti, A-M, Teh, T, Wang, C-IA, Ayliffe, MA, Kobe, B, and Ellis, JG.** (2006). Direct protein interaction underlies gene-for-gene specificity and coevolution of the flax resistance genes and flax rust avirulence genes. *Proc Natl Acad Sci U S A* **103**, 8888-8893.
- Dodds, PN, and Rathjen, JP.** (2010). Plant immunity: towards an integrated view of plant-pathogen interactions. *Nat Rev Genet* **11**, 539-548.
- Dong, OX, Tong, M, Bonardi, V, El Kasm, F, Woloshen, V, Wünsch, LK, Dangl, JL, and Li, X.** (2016). TNL-mediated immunity in Arabidopsis requires complex regulation of the redundant *ADR1* gene family. *New Phytologist* **210**, 960-973.
- Dyrka, W, Lamacchia, M, Durrens, P, Kobe, B, Daskalov, A, Paoletti, M, Sherman, DJ, Saupe, SJ.** (2014). Diversity and variability of NOD-like receptors in fungi. *Genome Biology and Evolution* **6**, 3137-3158.
- Engler, C, Kandzia, R, and Marillonnet, S.** (2008). A one pot, one step, precision cloning method with high throughput capability. *PLoS ONE* **3**, e3647.
- Essuman, K, Summers, DW, Sasaki, Y, Mao, X, DiAntonio, A, and Milbrandt, J.** (2017). The SARM1 toll/interleukin-1 receptor domain possesses intrinsic NAD⁺ cleavage activity that promotes pathological axonal degeneration. *Neuron* **93**, 1334-1343. e1335.

- Falk, A, Feys, BJ, Frost, LN, Jones, JD, Daniels, MJ, and Parker, JE.** (1999). EDS1, an essential component of *R* gene-mediated disease resistance in *Arabidopsis* has homology to eukaryotic lipases. *Proc Natl Acad Sci U S A* **96**, 3292-3297.
- Faulkner, C, and Robatzek, S.** (2012). Plants and pathogens: putting infection strategies and defence mechanisms on the map. *Curr Opin Plant Biol* **15**, 699-707.
- Feys, BJ, Moisan, LJ, Newman, MA, and Parker, JE.** (2001). Direct interaction between the *Arabidopsis* disease resistance signaling proteins, EDS1 and PAD4. *EMBO Journal* **20**, 5400-5411.
- Feys, BJ, Wiermer, M, Bhat, RA, Moisan, LJ, Medina-Escobar, N, Neu, C, Cabral, A, and Parker, JE.** (2005). *Arabidopsis* SENESCENCE-ASSOCIATED GENE101 stabilizes and signals within an ENHANCED DISEASE SUSCEPTIBILITY1 complex in plant innate immunity. *Plant Cell* **17**, 2601-2613.
- Fineran, PC, and Charpentier, E.** (2012). Memory of viral infections by CRISPR-Cas adaptive immune systems: acquisition of new information. *Virology* **434**, 202-209.
- Fu, ZQ, and Dong, X.** (2013). Systemic acquired resistance: turning local infection into global defense. *Annu Rev Plant Biol* **64**, 839-863.
- Fu, ZQ, Yan, S, Saleh, A, Wang, W, Ruble, J, Oka, N, Mohan, R, Spoel, SH, Tada, Y, and Zheng, N.** (2012). NPR3 and NPR4 are receptors for the immune signal salicylic acid in plants. *Nature* **486**, 228.
- Gantner, J, Ordon, J, Ilse, T, Kretschmer, C, Gruetzner, R, Loeffke, C, Dagdas, Y, Buerstenbinder, K, Marillonnet, S, and Stuttmann, J.** (2018). Peripheral infrastructure vectors and an extended set of plant parts for the Modular Cloning system. *PLoS ONE* **13**, e0197185.
- Gantner, J, Ordon, J, Kretschmer, C, Guerois, R, and Stuttmann, J.** (2019). An EDS1-SAG101 complex is essential for TNL-mediated immunity in *Nicotiana benthamiana*. *Plant Cell*, tpc.00099.02019.
- Garcia, AV, Blanvillain-Baufume, S, Huibers, RP, Wiermer, M, Li, G, Gobbato, E, Rietz, S, and Parker, JE.** (2010). Balanced nuclear and cytoplasmic activities of EDS1 are required for a complete plant innate immune response. *PLoS Pathog* **6**, e1000970.
- Geu-Flores, F, Nour-Eldin, HH, Nielsen, MT, and Halkier, B.** (2007). USER fusion: a rapid and efficient method for simultaneous fusion and cloning of multiple PCR products. *Nucleic Acids Res* **35**, e55.
- Gibson, DG, Young, L, Chuang, RY, Venter, JC, Hutchison, CA, and Smith, HO.** (2009). Enzymatic assembly of DNA molecules up to several hundred kilobases. *Nat Methods* **6**, 343-345.
- Gietz, RD, and Schiestl, RH.** (2007). High-efficiency yeast transformation using the LiAc/SS carrier DNA/PEG method. *Nat Protoc* **2**, 31-34.
- Göhre, V, Spallek, T, Häweker, H, Mersmann, S, Mentzel, T, Boller, T, de Torres, M, Mansfield, JW, and Robatzek, S.** (2008). Plant pattern-recognition receptor FLS2 is directed for degradation by the bacterial ubiquitin ligase AvrPtoB. *Current Biology* **18**, 1824-1832.
- Goodin, MM, Zaitlin, D, Naidu, RA, and Lommel, SA.** (2008). *Nicotiana benthamiana*: its history and future as a model for plant-pathogen interactions. *Mol Plant Microbe Interact* **21**, 1015-1026.
- Grant, M, Brown, I, Adams, S, Knight, M, Ainslie, A, and Mansfield, J.** (2000). The *RPM1* plant disease resistance gene facilitates a rapid and sustained increase in cytosolic calcium that is necessary for the oxidative burst and hypersensitive cell death. *The Plant Journal* **23** (4), 441-450.
- Hartley, JL, Temple, GF, and Brasch, MA.** (2000). DNA cloning using in vitro site-specific recombination. *Genome Res* **10**, 1788-1795.
- Hecker, A, Wallmeroth, N, Peter, S, Blatt, MR, Harter, K, and Grefen, C.** (2015). Binary 2in1 vectors improve in planta (Co)localization and dynamic protein interaction studies. *Plant Physiol* **168**, 776-787.
- Heidrich, K, Wirthmueller, L, Tasset, C, Pouzet, C, Deslandes, L, and Parker, JE.** (2011). *Arabidopsis* EDS1 connects pathogen effector recognition to cell compartment-specific immune responses. *Science* **334**, 1401-1404.

- Hofberger, JA, Zhou, B, Tang, H, Jones, JD, and Schranz, ME. (2014). A novel approach for multi-domain and multi-gene family identification provides insights into evolutionary dynamics of disease resistance genes in core eudicot plants. *BMC Genomics* **15**, 966.
- Horsefield, S, Burdett, H, Zhang, X, Manik, MK, Shi, Y, Chen, J, Qi, T, Gilley, J, Lai, J-S, Rank, MX, Casey, LW, Gu, W, Ericsson, DJ, Foley, G, Hughes, RO, Bosanac, T, von Itzstein, M, Rathjen, JP, Nanson, JD, Boden, M, Dry, IB, Williams, SJ, Staskawicz, BJ, Coleman, MP, Ve, T, Dodds, PN, and Kobe, B. (2019). NAD⁺ cleavage activity by animal and plant TIR domains in cell death pathways. *Science* **365**, 793-799.
- Horvath, P, and Barrangou, R. (2010). CRISPR/Cas, the immune system of bacteria and archaea. *Science* **327**, 167-170.
- Huot, B, Yao, J, Montgomery, BL, and He, SY. (2014). Growth–defense tradeoffs in plants: a balancing act to optimize fitness. *Molecular plant* **7**, 1267-1287.
- Hwang, WY, Fu, Y, Reyon, D, Maeder, ML, Tsai, SQ, Sander, JD, Peterson, RT, Yeh, JJ, and Joung, JK. (2013). Efficient genome editing in zebrafish using a CRISPR-Cas system. *Nat Biotechnol* **31**, 227.
- Imran, QM, Falak, N, Hussain, A, Mun, B-G, Sharma, A, Lee, S-U, Kim, K-M, and Yun, B-W. (2016). Nitric oxide responsive heavy metal-associated gene *AtHMAD1* contributes to development and disease resistance in *Arabidopsis thaliana*. *Frontiers in Plant Science* **7**, 1712.
- Ishino, Y, Shinagawa, H, Makino, K, Amemura, M, and Nakata, A. (1987). Nucleotide sequence of the *iap* gene, responsible for alkaline phosphatase isozyme conversion in *Escherichia coli*, and identification of the gene product. *Journal of Bacteriology* **169**, 5429-5433.
- Jacob, F, Vernaldi, S, and Maekawa, T. (2013). Evolution and conservation of plant NLR functions. *Front Immunol* **4**, 297.
- James, P, Halladay, J, and Craig, EA. (1996). Genomic libraries and a host strain designed for highly efficient two-hybrid selection in yeast. *Genetics* **144**, 1425-1436.
- Jansen, R, Embden, JDv, Gastra, W, and Schouls, LM. (2002). Identification of genes that are associated with DNA repeats in prokaryotes. *Molecular Microbiology* **43**, 1565-1575.
- Jares-Erijman, EA, and Jovin, TM. (2003). FRET imaging. *Nat Biotechnol* **21**, 1387.
- Jia, Y, Yuan, Y, Zhang, Y, Yang, S, and Zhang, X. (2015). Extreme expansion of NBS-encoding genes in Rosaceae. *BMC Genetics* **16**, 48.
- Jinek, M, Chylinski, K, Fonfara, I, Hauer, M, Doudna, JA, and Charpentier, E. (2012). A programmable dual-RNA-guided DNA endonuclease in adaptive bacterial immunity. *Science* **337**, 816-821.
- Jinek, M, East, A, Cheng, A, Lin, S, Ma, E, and Doudna, J. (2013). RNA-programmed genome editing in human cells. *elife* **2**, e00471.
- Jones, JD, and Dangl, JL. (2006). The plant immune system. *Nature* **444**, 323-329.
- Jones, JD, Vance, RE, and Dangl, JL. (2016). Intracellular innate immune surveillance devices in plants and animals. *Science* **354**.
- Jubic, LM, Saile, S, Furzer, OJ, El Kasm, F, and Dangl, JL. (2019). Help wanted: helper NLRs and plant immune responses. *Curr Opin Plant Biol* **50**, 82-94.
- Kanzaki, H, Yoshida, K, Saitoh, H, Fujisaki, K, Hirabuchi, A, Alaux, L, Fournier, E, Tharreau, D, and Terauchi, R. (2012). Arms race co-evolution of *Magnaporthe oryzae* AVR-Pik and rice Pik genes driven by their physical interactions. *Plant Journal* **72**, 894-907.
- Kapila, J, De Rycke, R, Van Montagu, M, and Angenon, G. (1997). An *Agrobacterium*-mediated transient gene expression system for intact leaves. *Plant Science* **122**, 101-108.
- Klepikova, AV, Kasianov, AS, Gerasimov, ES, Logacheva, MD, and Penin, AA. (2016). A high resolution map of the *Arabidopsis thaliana* developmental transcriptome based on RNA-seq profiling. *The Plant Journal* **88**, 1058-1070.
- Knepper, C, Savory, EA, Day, B. (2011). The role of NDR1 in pathogen perception and plant defense signaling. *Plant Signal Behav* **6**, 1114-1116.
- Knight, T. (2003). Idempotent vector design for standard assembly of biobricks. *Artificial Intelligence Laboratory*

- Konig, H, Frank, D, Heil, R, and Coenen, C.** (2013). Synthetic genomics and synthetic biology applications between hopes and concerns. *Current genomics* **14**, 11-24.
- Koonin, EV, and Aravind, L.** (2000). The U box is a modified RING finger - a common domain in ubiquitination. *Current Biology* **25**, 223-224.
- Kourelis, J, and van der Hoorn, RA.** (2018). Defended to the nines: 25 years of resistance gene cloning identifies nine mechanisms for R protein function. *Plant Cell* **30**, 285-299.
- Krasileva, KV, Dahlbeck, D, and Staskawicz, BJ.** (2010). Activation of an Arabidopsis resistance protein is specified by the in planta association of its leucine-rich repeat domain with the cognate oomycete effector. *Plant Cell* **22**, 2444-2458.
- Kroj, T, Chanclud, E, Michel-Romiti, C, Grand, X, and Morel, J.** (2016). Integration of decoy domains derived from protein targets of pathogen effectors into plant immune receptors is widespread. *New Phytol* **210**, 618-626.
- Kumar, R, Tyagi, AK, and Sharma, AK.** (2011). Genome-wide analysis of auxin response factor (ARF) gene family from tomato and analysis of their role in flower and fruit development. *Molecular Genetics and Genomics* **285**, 245-260.
- Lampropoulos, A, Sutikovic, Z, Wenzl, C, Maegele, I, Lohmann, JU, and Forner, J.** (2013). GreenGate-A novel, versatile, and efficient cloning system for plant transgenesis *PLoS One* **8**, e83043.
- Lapin, D, Kovacova, V, Sun, X, Dongus, JA, Bhandari, DD, von Born, P, Bautor, J, Guarneri, N, Rzemieniewski, J, Stuttmann, J, Beyer, A, and Parker, JE.** (2019). A coevolved EDS1-SAG101-NRG1 module mediates cell death signaling by TIR-domain immune receptors. *Plant Cell*, tpc.00118.02019.
- Le Roux, C, Huet, G, Jauneau, A, Camborde, L, Tremousaygue, D, Kraut, A, Zhou, B, Levailant, M, Adachi, H, Yoshioka, H, Raffaele, S, Berthome, R, Coute, Y, Parker, JE, and Deslandes, L.** (2015). A receptor pair with an integrated decoy converts pathogen disabling of transcription factors to immunity. *Cell* **161**, 1074-1088.
- Leipe, DD, Koonin, EV, and Aravind, L.** (2004). STAND, a class of P-loop NTPases including animal and plant regulators of programmed cell death: multiple, complex domain architectures, unusual phyletic patterns, and evolution by horizontal gene transfer *J Mol Biol* **343**, 1-28.
- Li, J, Ding, J, Zhang, W, Zhang, Y, Tang, P, Chen, J-Q, Tian, D, and Yang, S.** (2010). Unique evolutionary pattern of numbers of gramineous NBS-LRR genes. *Molecular Genetics and Genomics* **283**, 427-438.
- Li, Y, Yang, Y, Hu, Y, Liu, H, He, M, Yang, Z, Kong, F, Liu, X, and Hou, X.** (2019). DELLA and EDS1 form a feedback regulatory module to fine-tune plant growth-defense tradeoff in Arabidopsis. *Molecular plant*.
- Lin, D, and O'Callaghan, CA.** (2018). MetClo: methylase-assisted hierarchical DNA assembly using a single type IIS restriction enzyme. *Nucleic Acids Research* **46**, e113-e113.
- Liu, D, Shi, L, Han, C, Yu, J, Li, D, and Zhang, Y.** (2012). Validation of reference genes for gene expression studies in virus-infected *Nicotiana benthamiana* using quantitative real-time PCR. *PLoS One* **7**, e46451.
- Liu, E, and Page, JEJpm.** (2008). Optimized cDNA libraries for virus-induced gene silencing (VIGS) using tobacco rattle virus. *Plant Methods* **4**, 5.
- Locato, V, and De Gara, L.** (2018). Programmed cell death in plants: An overview. in *plant programmed cell death* (Springer), pp. 1-8.
- Macho, AP, and Zipfel, C.** (2014). Plant PRRs and the activation of innate immune signaling. *Mol Cell* **54**, 263-272.
- Maekawa, T, Cheng, W, Spiridon, LN, Toller, A, Lukasik, E, Saijo, Y, Liu, P, Shen, QH, Micluta, MA, Somssich, IE, Takken, FL, Petrescu, AJ, Chai, J, and Schulze-Lefert, P.** (2011a). Coiled-coil domain-dependent homodimerization of intracellular barley immune receptors defines a minimal functional module for triggering cell death. *Cell Host Microbe* **9**, 187-199.
- Maekawa, T, Kufer, TA, and Schulze-Lefert, P.** (2011b). NLR functions in plant and animal immune systems: so far and yet so close. *Nat Immunol* **12**, 817-826.
- Makarova, KS, Grishin, NV, Shabalina, SA, Wolf, YI, and Koonin, EV.** (2006). A putative RNA-interference-based immune system in prokaryotes: computational analysis of the predicted

- enzymatic machinery, functional analogies with eukaryotic RNAi, and hypothetical mechanisms of action. *Biology direct* **1**, 7.
- Makarova, KS, Wolf, YI, Alkhnbashi, OS, Costa, F, Shah, SA, Saunders, SJ, Barrangou, R, Brouns, SJ, Charpentier, E, and Haft, D.** (2015). An updated evolutionary classification of CRISPR–Cas systems *Nature* **13**, 722.
- Mali, P, Yang, L, Esvelt, KM, Aach, J, Guell, M, DiCarlo, JE, Norville, JE, and Church, GM.** (2013). RNA-guided human genome engineering via Cas9. *Science* **339**, 823-826.
- Maqbool, A, Saitoh, H, Franceschetti, M, Stevenson, C, Uemura, A, Kanzaki, H, Kamoun, S, Terauchi, R, and Banfield, M.** (2015). Structural basis of pathogen recognition by an integrated HMA domain in a plant NLR immune receptor. *Elife* **4**, e08709.
- Matteï, PJ, Faudry, E, Job, V, Izoré, T, Attree, I, and Dessen, A.** (2011). Membrane targeting and pore formation by the type III secretion system translocon. *The FEBS journal* **278**, 414-426.
- Meng, X, and Zhang, S.** (2013). MAPK cascades in plant disease resistance signaling. *Annual review of phytopathology* **51**, 245-266.
- Meyers, BC, Kozik, A, Griego, A, Kuang, H, and Michelmore, RW.** (2003). Genome-wide analysis of NBS-LRR-encoding genes in *Arabidopsis*. *Plant Cell* **15**, 809-834.
- Mindrebo, JT, Nartey, CM, Seto, Y, Burkart, MD, and Noel, JP.** (2016). Unveiling the functional diversity of the alpha/beta hydrolase superfamily in the plant kingdom. *Curr Opin Struc Biol* **41**, 233-246.
- Miya, A, Albert, P, Shinya, T, Desaki, Y, Ichimura, K, Shirasu, K, Narusaka, Y, Kawakami, N, Kaku, H, and Shibuya, N.** (2007). CERK1, a LysM receptor kinase, is essential for chitin elicitor signaling in *Arabidopsis*. *Proc Natl Acad Sci U S A* **104**, 19613-19618.
- Mojica, FJ, Diez-Villasenor, C, Garcia-Martinez, J, and Soria, E.** (2005). Intervening sequences of regularly spaced prokaryotic repeats derive from foreign genetic elements. *J Mol Evol* **60**, 174-182.
- Mojica, FJ, García-Martínez, J, and Soria, E.** (2005). Intervening sequences of regularly spaced prokaryotic repeats derive from foreign genetic elements. *Journal of Molecular Evolution* **60**, 174-182.
- Mondragón-Palomino, M, Meyers, BC, Michelmore, RW, and Gaut, BS.** (2002). Patterns of positive selection in the complete NBS-LRR gene family of *Arabidopsis thaliana*. *Genome Res* **12**, 1305-1315.
- Monie, TP, Bryant, CE, and Gay, NJ.** (2009). Activating immunity: lessons from the TLRs and NLRs. *Trends in biochemical sciences* **34**, 553-561.
- Mou, Z, Fan, WH, and Dong, XN.** (2003). Inducers of plant systemic acquired resistance regulate NPR1 function through redox changes. *Cell* **113**, 935-944.
- Mukhtar, MS, Nishimura, MT, and Dangl, J.** (2009). NPR1 in plant defense: it's not over'til it's turned over. *Cell* **137**, 804-806.
- Naim, F, Nakasugi, K, Crowhurst, RN, Hilario, E, Zwart, AB, Hellens, RP, Taylor, JM, Waterhouse, PM, and Wood, CC.** (2012). Advanced engineering of lipid metabolism in *Nicotiana benthamiana* using a draft genome and the V2 viral silencing-suppressor protein. *PLoS ONE* **7**, e52717.
- Neubauer, MP, Serrano, IM, Rodibaugh, N, Bhandari, D, Bautor, J, Parker, JE, and Innes, RW.** (2019). *Arabidopsis* ENHANCED DISEASE RESISTANCE1 protein kinase regulates the association of ENHANCED DISEASE SUSCEPTIBILITY1 and PHYTOALEXIN DEFICIENT4 to inhibit cell death. *Molecular Plant-Microbe Interactions*.
- Ogura, T, and Wilkinson, AJ.** (2001). AAA+ superfamily ATPases: common structure–diverse function. *Genes to Cells* **6**, 575-597.
- Ordon, J, Bressan, M, Kretschmer, C, Dall’Osto, L, Marillonnet, S, Bassi, R, and Stuttmann, J.** (2019). Optimized Cas9 expression systems for highly efficient *Arabidopsis* genome editing facilitate isolation of complex alleles in a single generation. *Funct Integr Genomics*, 1-12.
- Ordon, J, Gantner, J, Kemna, J, Schwalgun, L, Reschke, M, Streubel, J, Boch, J, and Stuttmann, J.** (2017). Generation of chromosomal deletions in dicotyledonous plants employing a user-friendly genome editing toolkit. *Plant J* **89**, 155-168.

- Paiano, A, Margiotta, A, De Luca, M, and Bucci, C.** (2019). Yeast-two-Hybrid assay to identify interacting proteins. *Current Protocols in Protein Science* **95**, e70.
- Parker, JE, Holub, EB, Frost, LN, Falk, A, Gunn, ND, and Daniels, MJ.** (1996). Characterization of *eds1*, a mutation in *Arabidopsis* suppressing resistance to *Peronospora parasitica* specified by several different RPP genes. *Plant Cell* **8**, 2033-2046.
- Patron, NJ, Orzaez, D, Marillonnet, S, Warzecha, H, Matthewman, C, Youles, M, Raitskin, O, Leveau, A, Farre, G, Rogers, C, Smith, A, Hibberd, J, Webb, AA, Locke, J, Schornack, S, Ajioka, J, Baulcombe, DC, Zipfel, C, Kamoun, S, Jones, JD, Kuhn, H, Robatzek, S, Van Esse, HP, Sanders, D, Oldroyd, G, Martin, C, Field, R, O'Connor, S, Fox, S, Wulff, B, Miller, B, Breakspear, A, Radhakrishnan, G, Delaux, PM, Loque, D, Granell, A, Tissier, A, Shih, P, Brutnell, TP, Quick, WP, Rischer, H, Fraser, PD, Aharoni, A, Raines, C, South, PF, Ane, JM, Hamberger, BR, Langdale, J, Stougaard, J, Bouwmeester, H, Udvardi, M, Murray, JA, Ntoukakis, V, Schafer, P, Denby, K, Edwards, KJ, Osbourn, A, and Haseloff, J.** (2015). Standards for plant synthetic biology: a common syntax for exchange of DNA parts. *New Phytol* **208**, 13-19.
- Peart, JR, Cook, G, Feys, BJ, Parker, JE, and Baulcombe, DC.** (2002). An *EDS1* orthologue is required for N-mediated resistance against tobacco mosaic virus. *Plant J* **29**, 569-579.
- Peart, JR, Mestre, P, Lu, R, Malcuit, I, and Baulcombe, DCJCb.** (2005). NRG1, a CC-NB-LRR protein, together with N, a TIR-NB-LRR protein, mediates resistance against tobacco mosaic virus **15**, 968-973.
- Peele, HM, Guan, N, Fogelqvist, J, and Dixelius, C.** (2014). Loss and retention of resistance genes in five species of the Brassicaceae family. *BMC Plant Biol* **14**, 298.
- Peng, J, Carol, P, Richards, DE, King, KE, Cowling, RJ, Murphy, GP, and Harberd, NP.** (1997). The *Arabidopsis* GAI gene defines a signaling pathway that negatively regulates gibberellin responses. *Genes Dev* **11**, 3194-3205.
- Peng, Y, van Wersch, R, and Zhang, Y.** (2018). Convergent and divergent signaling in PAMP-triggered immunity and effector-triggered immunity. *Molecular Plant-Microbe Interactions* **31**, 403-409.
- Pollak, B, Cerda, A, Delmans, M, Álamos, S, Moyano, T, West, A, Gutiérrez, RA, Patron, N, Federici, F, and Haseloff, J.** (2018). Loop Assembly: a simple and open system for recursive fabrication of DNA circuits. *New Phytol*
- Pourcel, C, Salvignol, G, and Vergnaud, G.** (2005). CRISPR elements in *Yersinia pestis* acquire new repeats by preferential uptake of bacteriophage DNA, and provide additional tools for evolutionary studies. *Microbiology* **151**, 653-663.
- Qi, S, Pang, Y, Hu, Q, Liu, Q, Li, H, Zhou, Y, He, T, Liang, Q, Liu, Y, and Yuan, X.** (2010). Crystal structure of the *Caenorhabditis elegans* apoptosome reveals an octameric assembly of CED-4. *Cell* **141**, 446-457.
- Qi, T, Seong, K, Thomazella, DP, Kim, JR, Pham, J, Seo, E, Cho, M-J, Schultink, A, and Staskawicz, B.** (2018). NRG1 functions downstream of EDS1 to regulate TIR-NLR-mediated plant immunity in *Nicotiana benthamiana*. *Proc Natl Acad Sci U S A* **115**, E10979-E10987.
- Ravensdale, M, Nemri, A, Thrall, PH, Ellis, JG, and Dodds, PN.** (2011). Co-evolutionary interactions between host resistance and pathogen effector genes in flax rust disease. *Molecular Plant Pathology* **12**, 93-102.
- Rebatchouk, D, Daraselia, N, and Narita, JO.** (1996). NOMAD: a versatile strategy for in vitro DNA manipulation applied to promoter analysis and vector design. *Proc Natl Acad Sci U S A* **93**, 10891-10896.
- Riedl, SJ, Li, W, Chao, Y, Schwarzenbacher, R, and Shi, Y.** (2005). Structure of the apoptotic protease-activating factor 1 bound to ADP. *Nature* **434**, 926.
- Rodriguez, E, Chevalier, J, El Ghouli, H, Voldum-Clausen, K, Mundy, J, and Petersen, M.** (2018). DNA damage as a consequence of NLR activation. *PLoS Genetics* **14**, e1007235.
- Santner, A, and Estelle, M.** (2009). Recent advances and emerging trends in plant hormone signalling. *Nature* **459**, 1071.

- Sarrion-Perdigones, A, Falconi, EE, Zandalinas, SI, Juarez, P, Fernandez-del-Carmen, A, Granell, A, and Orzaez, D.** (2011). GoldenBraid: an iterative cloning system for standardized assembly of reusable genetic modules. *PLoS ONE* **6**, e21622.
- Sarrion-Perdigones, A, Vazquez-Vilar, M, Palaci, J, Castelijns, B, Forment, J, Ziarsolo, P, Blanca, J, Granell, A, and Orzaez, D.** (2013). GoldenBraid 2.0: a comprehensive DNA assembly framework for plant synthetic biology. *Plant Physiol* **162**, 1618-1631.
- Sarris, PF, Cevik, V, Dagdas, G, Jones, JD, and Krasileva, KV.** (2016). Comparative analysis of plant immune receptor architectures uncovers host proteins likely targeted by pathogens. *BMC biology* **14**, 8.
- Sarris, PF, Duxbury, Z, Huh, SU, Ma, Y, Segonzac, C, Sklenar, J, Derbyshire, P, Cevik, V, Rallapalli, G, Saucet, SB, Wirthmueller, L, Menke, FL, Sohn, KH, and Jones, JD.** (2015). A plant immune receptor detects pathogen effectors that target WRKY transcription factors. *Cell* **161**, 1089-1100.
- Sasaki, Y, Sone, T, Yoshida, S, Yahata, K, Hotta, J, Chesnut, JD, Honda, T, and Imamoto, F.** (2004). Evidence for high specificity and efficiency of multiple recombination signals in mixed DNA cloning by the Multisite Gateway system. *Journal of biotechnology* **107**, 233-243.
- Schultink, A, Qi, T, Bally, J, and Staskawicz, B.** (2019). Using forward genetics in *Nicotiana benthamiana* to uncover the immune signaling pathway mediating recognition of the *Xanthomonas perforans* effector XopJ4. *New Phytologist* **221**, 1001-1009.
- Schultink, A, Qi, T, Lee, A, Steinbrenner, AD, and Staskawicz, B.** (2017). Roq1 mediates recognition of the *Xanthomonas* and *Pseudomonas* effector proteins XopQ and HopQ1. *Plant J.*
- Schulze-Lefert, P, and Panstruga, R.** (2011). A molecular evolutionary concept connecting nonhost resistance, pathogen host range, and pathogen speciation. *Trends Plant Sci* **16**, 117-125.
- Sela, H, Spiridon, LN, PETRESCU, AJ, Akerman, M, MANDEL-GUTFREUND, Y, Nevo, E, Loutre, C, Keller, B, Schulman, AH, and Fahima, T.** (2012). Ancient diversity of splicing motifs and protein surfaces in the wild emmer wheat (*Triticum dicoccoides*) LR10 coiled coil (CC) and leucine-rich repeat (LRR) domains. *Mol Plant Pathol* **13**, 276-287.
- Shaner, NC, Campbell, RE, Steinbach, PA, Giepmans, BN, Palmer, AE, and Tsien, RY.** (2004). Improved monomeric red, orange and yellow fluorescent proteins derived from *Discosoma* sp. red fluorescent protein. *Nat Biotechnol* **22**, 1567-1572.
- Shao, Z-Q, Xue, J-Y, Wu, P, Zhang, Y-M, Wu, Y, Hang, Y-Y, Wang, B, and Chen, J-Q.** (2016). Large-scale analyses of angiosperm nucleotide-binding site-leucine-rich repeat genes reveal three anciently diverged classes with distinct evolutionary patterns. *Plant Physiol* **170**, 2095-2109.
- Shimada, A, Ueguchi-Tanaka, M, Nakatsu, T, Nakajima, M, Naoe, Y, Ohmiya, H, Kato, H, and Matsuoka, M.** (2008). Structural basis for gibberellin recognition by its receptor GID1. *Nature* **456**, 520-523.
- Sleight, SC, Bartley, BA, Lieviant, JA, and Sauro, H.** (2010). In-Fusion BioBrick assembly and re-engineering. *Nucleic Acids Res* **38**, 2624-2636.
- Stavrinos, J, McCann, HC, and Guttman, DS.** (2008). Host-pathogen interplay and the evolution of bacterial effectors. *Cellular microbiology* **10**, 285-292.
- Stuttman, J, Peine, N, Garcia, AV, Wagner, C, Choudhury, SR, Wang, Y, James, GV, Griebel, T, Alcazar, R, Tsuda, K, Schneeberger, K, and Parker, JE.** (2016). Arabidopsis thaliana DM2h (R8) within the Landsberg RPP1-like Resistance Locus Underlies Three Different Cases of EDS1-Conditioned Autoimmunity. *PLoS Genet* **12**, e1005990.
- Sueldo, DJ, Shimels, M, Spiridon, LN, Caldararu, O, Petrescu, AJ, Joosten, MH, and Tameling, W.** (2015). Random mutagenesis of the nucleotide-binding domain of NRC1 (NB-LRR Required for Hypersensitive Response-Associated Cell Death-1), a downstream signalling nucleotide-binding, leucine-rich repeat (NB-LRR) protein, identifies gain-of-function mutations in the nucleotide-binding pocket. *New Phytol* **208**, 210-223.
- Swiderski, MR, Birker, D, and Jones, JD.** (2009). The TIR domain of TIR-NB-LRR resistance proteins is a signaling domain involved in cell death induction. *Mol Plant Microbe Interact* **22**, 157-165.

- Szczesny, R, Büttner, D, Escolar, L, Schulze, S, Seiferth, A, and Bonas, U.** (2010). Suppression of the AvrBs1-specific hypersensitive response by the YopJ effector homolog AvrBsT from *Xanthomonas* depends on a SNF1-related kinase. *New Phytol* **187**, 1058-1074.
- Szybalski, W, Kim, SC, Hasan, N, and Podhajska, AJ.** (1991). Class-II restriction enzymes—a review. *Gene* **100**, 13-26.
- Takken, FL, Albrecht, M, and Tameling, WI.** (2006). Resistance proteins: molecular switches of plant defence. *Curr Opin Plant Biol* **9**, 383-390.
- Takken, FLW, and Goverse, A.** (2012). How to build a pathogen detector: structural basis of NB-LRR function. *Curr Opin Plant Biol* **15**, 375-384.
- Tameling, WI, Elzinga, SD, Darmin, PS, Vossen, JH, Takken, FL, Haring, MA, and Cornelissen, BJ.** (2002). The tomato R gene products I-2 and MI-1 are functional ATP binding proteins with ATPase activity. *Plant Cell* **14**, 2929-2939.
- Tameling, WI, Vossen, JH, Albrecht, M, Lengauer, T, Berden, JA, Haring, MA, Cornelissen, BJ, and Takken, FL.** (2006). Mutations in the NB-ARC domain of I-2 that impair ATP hydrolysis cause autoactivation. *Plant Physiol* **140**, 1233-1245.
- Tapping, RI.** (2009). Innate immune sensing and activation of cell surface Toll-like receptors. *Semin Immunol* **21**, 175-184.
- Ueguchi-Tanaka, M, Ashikari, M, Nakajima, M, Itoh, H, Katoh, E, Kobayashi, M, Chow, T-y, Yue-ie, CH, Kitano, H, and Yamaguchi, I.** (2005). GIBBERELLIN INSENSITIVE DWARF1 encodes a soluble receptor for gibberellin. *Nature* **437**, 693.
- Urbach, JM, and Ausubel, FM.** (2017). The NBS-LRR architectures of plant R-proteins and metazoan NLRs evolved in independent events. *Proc Natl Acad Sci U S A* **114**, 1063-1068.
- Van de Weyer, A-L, Monteiro, F, Furzer, OJ, Nishimura, MT, Cevik, V, Witek, K, Jones, JD, Dangl, JL, Weigel, D, and Bemm, F.** (2019). A Species-Wide Inventory of NLR Genes and Alleles in *Arabidopsis thaliana*. *Cell* **178**, 1260-1272. e1214.
- van der Biezen, EA, and Jones, JD.** (1998). The NB-ARC domain: a novel signalling motif shared by plant resistance gene products and regulators of cell death in animals. *Current Biology* **8**, R226-R228.
- Vazquez-Vilar, M, Quijano-Rubio, A, Fernandez-Del-Carmen, A, Sarrion-Perdigones, A, Ochoa-Fernandez, R, Ziarsolo, P, Blanca, J, Granell, A, and Orzaez, D.** (2017). GB3.0: a platform for plant bio-design that connects functional DNA elements with associated biological data. *Nucleic Acids Res* **45**, 2196-2209.
- Velásquez, AC, Chakravarthy, S, and Martin, GB.** (2009). Virus-induced gene silencing (VIGS) in *Nicotiana benthamiana* and tomato. *JoVE*
- Venugopal, SC, Jeong, R-D, Mandal, MK, Zhu, S, Chandra-Shekara, AC, Xia, Y, Hersh, M, Stromberg, AJ, Navarre, D, Kachroo, A, and Kachroo, P.** (2009). Enhanced disease susceptibility 1 and salicylic acid act redundantly to regulate resistance gene-mediated signaling. *Plos Genetics* **5**.
- Wagner, S, Stuttmann, J, Rietz, S, Guerois, R, Brunstein, E, Bautor, J, Niefind, K, and Parker, JE.** (2013). Structural basis for signaling by exclusive EDS1 heteromeric complexes with SAG101 or PAD4 in plant innate immunity. *Cell Host Microbe* **14**, 619-630.
- Walker, JE, Saraste, M, Runswick, MJ, and Gay, NJ.** (1982). Distantly related sequences in a- and b-subunits of ATP synthase myosin, kinases and other ATP-requiring enzymes and a common nucleotide binding fold. *EMBO J.* **1**, 945-951.
- Wan, L, Essuman, K, Anderson, RG, Sasaki, Y, Monteiro, F, Chung, E-H, Osborne Nishimura, E, DiAntonio, A, Milbrandt, J, Dangl, JL, and Nishimura, MT.** (2019). TIR domains of plant immune receptors are NAD⁺-cleaving enzymes that promote cell death. *Science* **365**, 799-803.
- Wang, D, Pajerowska-Mukhtar, K, Culler, AH, and Dong, X.** (2007). Salicylic acid inhibits pathogen growth in plants through repression of the auxin signaling pathway. *Current Biology* **17**, 1784-1790.
- Wang, G, Roux, B, Feng, F, Guy, E, Li, L, Li, N, Zhang, X, Lautier, M, Jardinaud, M-F, and Chabannes, M.** (2015). The decoy substrate of a pathogen effector and a pseudokinase specify pathogen-induced modified-self recognition and immunity in plants. *Cell host & microbe* **18**, 285-295.

- Wang, J, Hu, M, Wang, J, Qi, J, Han, Z, Wang, G, Qi, Y, Wang, H-W, Zhou, J-M, and Chai, J. (2019a). Reconstitution and structure of a plant NLR resistosome conferring immunity. *Science* **364**, eaav5870.
- Wang, J, Wang, J, Hu, M, Wu, S, Qi, J, Wang, G, Han, Z, Qi, Y, Gao, N, and Wang, H-W. (2019b). Ligand-triggered allosteric ADP release primes a plant NLR complex. *Science* **364**, eaav5868.
- Weber, E, Engler, C, Gruetzner, R, Werner, S, and Marillonnet, S. (2011). A modular cloning system for standardized assembly of multigene constructs. *PLoS ONE* **6**, e16765.
- Wiermer, M, Feys, BJ, and Parker, JE. (2005). Plant immunity: the EDS1 regulatory node. *Curr Opin Plant Biol* **8**, 383-389.
- Wildermuth, MC, Dewdney, J, Wu, G, and Ausubel, FM. (2001). Isochorismate synthase is required to synthesize salicylic acid for plant defence. *Nature* **414**, 562-565.
- Williams, SJ, Sohn, KH, Wan, L, Bernoux, M, Sarris, PF, Segonzac, C, Ve, T, Ma, Y, Saucet, SB, Ericsson, DJ, Casey, LW, Lonhienne, T, Winzor, DJ, Zhang, X, Coerdts, A, Parker, JE, Dodds, PN, Kobe, B, and Jones, JD. (2014). Structural basis for assembly and function of a heterodimeric plant immune receptor. *Science* **344**, 299-303.
- Williams, SJ, Sornaraj, P, deCourcy-Ireland, E, Menz, RI, Kobe, B, Ellis, JG, Dodds, PN, and Anderson, P. (2011). An autoactive mutant of the M flax rust resistance protein has a preference for binding ATP, whereas wild-type M protein binds ADP. *APS* **24**, 897-906.
- Wu, Y, Kuzma, J, Maréchal, E, Graeff, R, Lee, HC, Foster, R, and Chua, N-H. (1997). Abscisic acid signaling through cyclic ADP-ribose in plants. *Science* **278**, 2126-2130.
- Wu, Z, Li, M, Dong, OX, Xia, S, Liang, W, Bao, Y, Wasteneys, G, and Li, X. (2019). Differential regulation of TNL-mediated immune signaling by redundant helper CNLs. *New Phytologist* **222**, 938-953.
- Wulff, BB, Horvath, DM, and Ward, ER. (2011). Improving immunity in crops: new tactics in an old game. *Curr Opin Plant Biol* **14**, 468-476.
- Wydro, M, Kozubek, E, and Lehmann, P. (2006). Optimization of transient Agrobacterium-mediated gene expression system in leaves of *Nicotiana benthamiana*. *ACTA BIOCHIMICA POLONICA-ENGLISH EDITION* **53**, 289.
- Xu, F, Zhu, C, Cevik, V, Johnson, K, Liu, Y, Sohn, K, Jones, JD, Holub, EB, and Li, X. (2015). Autoimmunity conferred by chs3-2D relies on CSA1, its adjacent TNL-encoding neighbour. *Scientific reports* **5**, 8792.
- Yan, N, Chai, J, Lee, ES, Gu, L, Liu, Q, He, J, Wu, J-W, Kokel, D, Li, H, and Hao, Q. (2005). Structure of the CED-4–CED-9 complex provides insights into programmed cell death in *Caenorhabditis elegans*. *Nature* **437**, 831.
- Yu, G, Xian, L, Sang, Y, and Macho, AP. (2019). Cautionary notes on the use of Agrobacterium-mediated transient gene expression upon SGT1 silencing in *Nicotiana benthamiana*. *New Phytol* **222**, 14-17.
- Yu, X, Feng, B, He, P, and Shan, L. (2017). From chaos to harmony: Responses and signaling upon microbial pattern recognition. *Annu Rev Phytopathol* **55**, 109-137.
- Zhai, C, Zhang, Y, Yao, N, Lin, F, Liu, Z, Dong, Z, Wang, L, and Pan, Q. (2014). Function and interaction of the coupled genes responsible for Pik-h encoded rice blast resistance. *PLoS ONE* **9**, e98067.
- Zhang, L, Chen, S, Ruan, J, Wu, J, Tong, AB, Yin, Q, Li, Y, David, L, Lu, A, and Wang, WL. (2015). Cryo-EM structure of the activated NAIP2-NLRC4 inflammasome reveals nucleated polymerization. *Science* **350**, 404-409.
- Zhang, L, Du, L, and Poovaiah, B. (2014). Calcium signaling and biotic defense responses in plants. *Plant signaling & behavior* **9**, e973818.
- Zhu, S, Jeong, RD, Venugopal, SC, Lapchyk, L, Navarre, D, Kachroo, A, and Kachroo, P. (2011). SAG101 forms a ternary complex with EDS1 and PAD4 and is required for resistance signaling against turnip crinkle virus. *PLoS Pathog* **7**, e1002318.
- Zhu, Z, Xu, F, Zhang, Y, Cheng, YT, Wiermer, M, Li, X, and Zhang, Y. (2010). Arabidopsis resistance protein SNC1 activates immune responses through association with a transcriptional corepressor. *Proc Natl Acad Sci U S A* **107**, 13960-13965.

Lebenslauf

Angaben zur Person

Name Johannes Gantner

Anschrift

[REDACTED]

Geburtsdatum 07. Mai 1986

Geburtsort Darmstadt

Staatsangehörigkeit deutsch

Ausbildung und Akademische Qualifikation

Seit 2015 MARTIN-LUTHER-UNIVERSITÄT HALLE-WITTENBERG

Promotion an der Naturwissenschaftlichen Fakultät I;
Institut für Biologie/Pflanzengenetik

- Thema der Dissertation:
Comparative and translational analysis of immune signaling pathways in Arabidopsis and *Solanaceae*

10/2007 - 09/2013 TECHNISCHE UNIVERSITÄT DARMSTADT

Diplomstudiengang in den Naturwissenschaften im
Fachbereich Biologie

- Thema der Diplomarbeit:
Untersuchungen an den Kaliumkanälen
 $KCV_{\text{Next-to-Smith}}$ und $KCV_{\text{ATCV-1}}$
 - Abschluss: Diplom Biologie

08/1993 – 06/2006 FREIE WALDORFSCHULE DARMSTADT

- Abschluss: Abitur

Halle (Saale), den 26.06.2020

Danksagung

Ganz herzlich bedanke ich mich bei denjenigen, die in den letzten Jahren an mich geglaubt und damit einen großen Anteil am Gedeihen und an der Fertigstellung dieser Arbeit beigetragen haben.

Allen voran möchte ich mich bei Dr. Johannes Stuttmann bedanken. Durch seine innovativen Ideen und seine stetige Verfügbarkeit, Geduld und das Vertrauen in meine Person konnte diese Arbeit erst angefertigt werden. Jederzeit konnte man ein offenes Ohr und faktisch immer eine gute Idee bei praktischen und theoretischen Problemen erwarten.

Ebenfalls gilt mein Dank Prof. Dr. Ulla Bonas für die Möglichkeit meine Arbeit in Ihrer Abteilung anfertigen zu können und für die Begutachtung der Arbeit.

Als „fremder“ Doktorand, welcher sein Studium nicht in Halle absolviert hat, bin ich sehr dankbar so freundschaftlich in der AG Bonas aufgenommen worden zu sein. Speziell bei meinen ArbeitskollegInnen Dr. Tina Hoppe, Carola Kretschmer, Michael Jordan, Evelyn Löschner, Jan Kemna und Jana Ordon bedanke ich mich für die tolle Zusammenarbeit, ihr seid spitzen Freunde geworden und habt dafür gesorgt, dass der Arbeitsalltag auch mal mit ein wenig Witz und Heiterkeit versüßt wurde.

Für die Korrektur meiner Arbeit danke ich Dr. Tina Hoppe, Dr. Jessica Erickson, Christian Heise, Jana Ordon, Dr. Eric Kröber und Dr. Corina Mathew!

Von Herzen danke ich meinem Medi-Freundeskreis und allen BewohnerInnen der Marienstraße 27a, die mit ihrer Liebe, Tatendrang und Geselligkeit dafür gesorgt haben, dass ich diese Stadt, meine neue Heimat, eigentlich gar nicht mehr verlassen möchte.

Meinen Eltern Evelyn und Hans danke ich von Herzen für ihre liebevolle, uneingeschränkte Unterstützung meines Lebensweges, ich bin stolz solch tolle Eltern zu haben und es tut unglaublich gut zu wissen, dass ihr immer für mich da seid! Meinen Brüdern Gösta und Florian danke ich für die teils fachlichen Diskussionen und andererseits für die emotionale Unterstützung vor allem an so einigen Wochenenden in meiner alten Heimat Darmstadt, schön dass es euch zwei gibt und dass wir so prima zusammenhalten!

Eidesstattliche Erklärung

Hiermit erkläre ich, dass ich die vorliegende wissenschaftliche Arbeit selbstständig und ohne fremde Hilfe verfasst habe. Ich erkläre weiterhin, dass andere als die von mir angegebenen Quellen und Hilfsmittel nicht benutzt und die den benutzten Werken wörtlich oder inhaltlich entnommenen Stellen als solche kenntlich gemacht wurden.

Mit dieser Arbeit bewerbe ich mich erstmals um die Erlangung des Doktorgrades.

Halle (Saale), den 26.06.2020

Johannes Gantner